IMMUNE BIOMARKERS IN BREAST CANCER PATHOLOGY SPECIMENS: CHARACTERIZATION AND CLINICAL IMPLICATIONS

by

Samantha Burugu

B.Sc., University of Ottawa, 2012

M.Sc., McGill University, 2015

A THESIS SUBMITTED IN PARTIAL FULFILLMENT OF

THE REQUIREMENTS FOR THE DEGREE OF

DOCTOR OF PHILOSOPHY

in

THE FACULTY OF GRADUATE AND POSTDOCTORAL STUDIES

(Pathology and Laboratory Medicine)

THE UNIVERSITY OF BRITISH COLUMBIA

(Vancouver)

June 2019

The following individuals certify that they have read, and recommend to the Faculty of Graduate and Postdoctoral Studies for acceptance, the dissertation entitled:

Immune biomarkers in breast cancer pathology specimens: Characterization and clinical implications

submitted by Samantha Burugu in partial fulfillment of the requirements for

the degree of Doctor of Philosophy

in Pathology and Laboratory Medicine

Examining Committee:

Torsten O. Nielsen
Supervisor

John J. Spinelli
Supervisory Committee Member

Peter C.V. Black
University Examiner

Kenneth W. Harder
University Examiner

Additional Supervisory Committee Members:

Kevin L. Bennewith
Supervisory Committee Member

Nickolas Myles
Supervisory Committee Member

Brad H. Nelson
Supervisory Committee Member

Abstract

Immunotherapy is dramatically changing the landscape of cancer treatment and is becoming incorporated into the standard of care for some tumor types. Until recently, breast cancer has not been generally considered particularly immunogenic. However, breast cancer is a heterogeneous disease and increasing evidence suggests that patients with basal-like breast cancer, an aggressive subtype lacking targeted therapy options, may be amenable to immunotherapy.

My research goals have included the investigation and clinical characterization of two emerging targetable immune checkpoint biomarkers: lymphocyte-activation gene 3 (LAG-3) and the T-cell Immunoglobulin and Mucin domain-containing molecule 3 (TIM-3), by applying immunohistochemistry to a well-annotated tissue microarray cohort of 3,992 breast cancers. As an additional research goal, I evaluated a novel *in situ* multiplex biomarker assessment method (Nanostring-based digital spatial profiling-DSP) for its compatibility with breast cancer tissue microarrays, to generate immune profiles from patient surgical specimens.

I report that the expression of LAG-3 or TIM-3 on intra-epithelial tumor-infiltrating lymphocytes (iTILs) was observed in a minority of cases (11%) in the whole cohort, but was significantly enriched in basal-like breast cancers (33% and 28% of basal-like breast cancers being infiltrated with LAG-3+ and TIM-3+iTILs, respectively). Furthermore, I found that LAG-3+iTILs and TIM-3+iTILs were present in breast cancers co-infiltrated with established immunotherapy targets (program cell death-1/PD-1 and its ligand, PD-L1). In multivariate analyses, LAG-3+iTILs or TIM-3+iTILs were independent favorable prognostic factors in breast cancer patients. In the last part of the thesis, I profiled the tumor immune microenvironment of two basal-like-enriched breast cancer cohorts, quantifying the expression of 31 immuno-oncology biomarkers using DSP. I then validated the digital counts for CD8 and PD1 by

comparing with immunohistochemistry, and CD45 digital counts by comparing with hematoxylin & eosin-stained stromal TILs counts. Lastly, I identified a 4-biomarker signature indicative of a pre-existing immunity in breast cancer patients.

The body of work presented here may help guide the selection of breast cancer patients for clinical trial evaluation of emerging immunotherapy agents. Furthermore, I show that digital spatial profiling technology can efficiently and quantitatively profile immune expression on breast cancer patient specimens using only a tiny fraction from precious tumor samples.

Lay Summary

Immune checkpoint inhibitors are drugs that restore patients' own immune system to fight cancer and have revolutionized cancer treatment. However, in most cancers (including breast cancer), the success of current immunotherapy targets has been limited to few patients for reasons that are still unknown, so new drugs for new targets are being investigated. Using breast tumor samples from more than 3,000 patients, I found that two emerging targets for immunotherapy (LAG-3 and TIM-3) were particularly enriched in patients with an aggressive breast cancer subtype called basal-like, providing the largest evidence yet about the presence of LAG-3 and TIM-3 in breast cancer. Furthermore, using a novel technology that identifies multiple immune populations in a patient's tumor, I identified 4 key immune populations that might help to select patients amenable to immune-modulating therapies. The work presented here can inform the prioritization and design of clinical trials for immune therapies in breast cancer.

Preface

Portions of **Chapter 1** are modified versions based on two publications:

Sections **1.2** (Immune system in cancer and all subsections), **1.3.2.1** (CTLA-4) and **1.3.2.2** (PD-1/PD-L1) are based on a published review:

> **Burugu S**, Asleh-Aburaya K, Nielsen TO. *Immune infiltrates in the breast cancer microenvironment: detection, characterization and clinical implication*. Breast Cancer. 2017 Jan;24(1):3-15. doi: 10.1007/s12282-016-0698-z. Epub 2016 May 2. Review. PubMed PMID: 27138387.

Co-author Asleh-Aburaya K and I were responsible for writing the manuscript under the supervision of Dr. Nielsen. The content in the sections described in this thesis chapter was originally written by me, with the exceptions of the sections describing the prognostic value of immune biomarkers (which are modified versions of sections initially written by Asleh-Aburaya K).

Section **1.3.3.1** (LAG-3) and section **1.3.3.2** (TIM-3) are based on a published review:

> **Burugu S**, Dancsok AR, Nielsen TO. *Emerging targets in cancer immunotherapy*. Semin Cancer Biol. 2018 Oct;52(Pt 2):39-52. doi: 10.1016/j.semcancer.2017.10.001. Epub 2017 Oct 5. Review. PubMed PMID: 28987965.

Co-author Dancsok AR and I equally contributed to the entire manuscript writeup under the supervision of Dr. Nielsen. Section **1.3.3.1** was written by me and Section **1.3.3.2**.in this thesis is a modified section originally drafted by co-author Dancsok AR.

Versions of **Chapter 2** and **Chapter 3** have been published:

Burugu S, Gao D, Leung S, Chia SK, Nielsen TO. *LAG-3+ tumor infiltrating lymphocytes in breast cancer: clinical correlates and association with PD-1/PD-L1+ tumors.* Ann Oncol. 2017 Dec 1;28(12):2977-2984. doi: 10.1093/annonc/mdx557. PubMed PMID: 29045526.

Burugu S, Gao D, Leung S, Chia SK, Nielsen TO. *TIM-3 expression in breast cancer*. *Oncoimmunology*. 2018 Aug 23;7(11):e1502128. doi:10.1080/2162402X.2018.1502128. eCollection 2018. PubMed PMID: 30377566

For both publications, I was responsible for drafting the manuscript, preparing the figures and tables and addressing comments from reviewers. I optimized LAG-3 and TIM-3 antibody immunohistochemistry staining conditions and performed the initial statistical analyses. Scoring of the immunohistochemically-stained breast cancer tissue microarrays was performed by Dr. Dongxia Gao. I coordinated the scoring system for the immune biomarkers. Samuel Leung conducted the final statistical analyses and helped in addressing comments from reviewers. Dr. Stephen Chia was involved in the manuscript writeup and addressing comments from reviewers. The experimental design for both studies, manuscript writeup and addressing comments from reviewers were supervised by Dr. Torsten Nielsen.

Chapter 4 is unpublished material and part of a manuscript in preparation:
Staining of the two breast cancer tissue microarrays by the digital spatial profiling was performed by Yang Liang and JingJing Gong at the Nanostring headquarter in Seattle, US after the Nielsen lab was selected for a technology access program grant. I coordinated the fluorescent markers included for visualization and for the selection of the regions of interest to be analyzed by digital spatial profiling. I prepared the data to send to a biostatistician (Xing Ren) at Nanostring who conducted the unsupervised hierarchical cluster analyses. All additional analyses

were conducted by me. Early results were selected for a poster presentation at the British Columbia Cancer Summit held in Vancouver on November 23, 2018.

Chapter 5 is unpublished material written by myself

All human research studies performed in the thesis were conducted under the human ethics approval of the UBC Research Ethics Board: Certificate number: H17-01385 Immune biomarkers in breast cancer.

Table of Contents

List of Tables

List of Figures

List of Abbreviations

BCSS	Breast cancer-specific survival
BRCA	Breast cancer gene
CDK4/6	Cyclin-dependent kinase 4/6
CEACAM-1	Carcinoembryonic antigen-related cell adhesion molecule 1
CEF	Cyclophosphamide-Epirubicin-5'Fluorouracil
CK5/6	Cytokeratin 5/6
CMF	Cyclophosphamide-Methotrexate-5'Fluorouracil
CTLA4	Cytotoxic T lymphocyte-associated antigen 4
DAB	3,3'-diaminobenzidine
EGFR	Epidermal growth factor receptor 1
ER	Estrogen receptor
FOXP3	Forkhead box P3
GZMB	Granzyme B
H&E sTILs	Hematoxylin and eosin-stained stromal tumor-infiltrating lymphocytes
HER2	Human epidermal growth factor receptor 2
IFNγ	Interferon gamma
IHC	Immunohistochemistry
iTILs	Intra-epithelial tumor-infiltrating lymphocytes
LAG3	Lymphocyte-activation gene 3
LPBC	Lymphocyte-predominant breast cancer
MDSC	Myeloid-derived suppressor cells

MHC	Major histocompatibility complex
PAM50	Prediction analysis of microarray 50
pCR	Pathologic complete response
PD1	Programmed cell-death 1
PDL1	Programmed cell-death ligand 1
PR	Progesterone receptor
PTEN	Phosphatase and tensin homolog
RECIST	Response evaluation criteria in solid tumors
ROI	Region of interest
sTILs	Stromal tumor-infiltrating lymphocytes
TAM	Tumor-associated macrophages
TIM3	T-cell Immunoglobulin and Mucin domain-containing molecule 3
TNBC	Triple negative breast cancer
TNFα	Tumor necrosis factor alpha
VISTA	V-domain Ig suppressor of T cell activation

Acknowledgements

I would like to express my utmost gratitude to an incredible supervisor, Dr. Torsten Nielsen, who introduced me to the immuno-oncology field. For your willingness to actively listen to my ideas and share your knowledge, for your encouragement and insightful advices throughout my PhD, un très grand merci!

I would like to thank my supervisory committee (Drs. David Huntsman, Brad Nelson, John Spinelli, Nickolas Myles and Kevin Bennewith) for their guidance and helpful comments. To my GPEC family (Christine Chow, Angela Cheng, Karama Asleh and Jenny Wang), I can't thank you enough for all the support inside and outside the lab and to my fellow Nielsen lab mates (Dongxia Gao, Amanda Dancsok, Samuel Leung, Jamie Yu, Angela Goytain, Alvin Qiu and Neal Poulin), thank you for creating such as great work environment. In particular, Doris for your significant contributions in my thesis and great baby advice; Sam for helping me learn statistics in an easy way and always being available to answer to my not-so-quick questions.

This thesis could not have been completed without the generous funding support from the Fonds de Recherche du Quebec en Santé and the UBC Faculty of Medicine Graduate award.

Special and heartfelt thanks to my husband, Emmanuel, for always believe in me, encouraging me to pursue a PhD and for giving me the gift of becoming a mother. To my mother, family and friends, thank you for your unconditional support throughout my degree.

To Eugenie and Rose

Chapter 1: Introduction

1.1 Breast cancer

Breast cancer is the most common cancer diagnosed among Canadian women. According to the Canadian Cancer Society, breast cancer accounted for 25% of cancer newly diagnosed among women in 2017. Campaigns for early breast cancer detection and evolution of treatments led to high survival rates for breast cancer patients. 87% of Canadian women diagnosed with early breast cancer survive at least 5 years (Canadian Cancer Society). However, the survival rates dramatically decrease in patients who present or progress to metastatic breast cancer to 22% of chance for survival after 5 years. In the past 2 decades, molecular profile studies revealed breast cancer as not a single disease but an agglomeration of multiple diseases.

1.1.1 Heterogeneity of breast cancers

Different molecular features have been used to classify breast cancers including gene or protein expression, DNA aberrations, and miRNA profiles[1-6]. The seminal molecular study that profiled >8,000 genes of breast cancer patients using cDNA microarrays identified 4 distinct intrinsic breast cancer subtypes based on gene expression patterns[1]. These were: Luminal-like, basal-like, Erb-B2+ and normal-like.

Gene expression patterns that distinguished the intrinsic subtypes included expression of transcription factors such as the estrogen receptor for luminal-like breast cancers, expression of genes associated with basal epithelial cells for basal-like breast cancers and over-expression of *ERBB2* gene (coding for human epidermal growth factor receptor 2 protein or HER2) for Erb-B2+ breast cancers [1]. Breast cancer intrinsic subtypes, as established in this study, were validated in subsequent studies and refined into the 4 major molecular subtypes : Luminal A, Luminal B,

HER2-enriched (HER2E) and basal-like [3,4,7-9] **(Table 1.1).** These four subtypes are distinct and display different clinical outcomes and response to therapy; a finding that has been repeatedly recapitulated using different gene expression platforms and different independent clinical datasets.[10-14]

Another major breast cancer study further classified into 10 different subtypes termed integrative clusters by analyzing various molecular features such as aberrations in DNA copy number and gene expression[2]. The study showed that luminal A and luminal B breast cancer intrinsic subtypes can be further divided into 8 different integrative clusters. The prognosis varies greatly among the 10 integrative clusters but shows similarity with breast cancer intrinsic subtypes[2,15,16].

In clinical practice, partly due to high costs of molecular assays, immunohistochemistry surrogates are used to identify the intrinsic subtypes[10,17,18]**(Table 1.1)**: For **luminal A**: estrogen receptor (ER) and/or progesterone receptor (PR) positivity, low levels of Ki67, and HER2 negative; for **luminal B**: ER and/or PR positive, high levels of Ki67 and/or HER2+ by immunohistochemistry or fluorescent in situ hybridization; for **HER2E**: ER and PR negative and HER2+[19] and for **basal-like**: ER, PR and HER2 negative and sometimes referred to an improved definition that adds CK5/6+ and/or EGFR+ to the triple negative phenotype[20]. Among these breast cancer subtypes, the triple negative immunohistochemistry phenotype (TNBC) is the most distinct and identifies, by gene expression, a heterogeneous group of breast cancers of which approximatively 50-75% are of basal-like subtype [21-24].

1.1.2 Evolution of breast cancer treatments

1.1.2.1 Chemotherapy

The efficacy of chemotherapy in treating breast cancer has been shown since the establishment of the first chemotherapy regimen made of cyclophosphamide, methotrexate and 5'fluorouracil (CMF)[25,26] . This combination is composed of a DNA-damaging alkylating agent (cyclophosphamide) and 2 antimetabolites: an inhibitor of folic acid synthesis (methotrexate) and a nucleoside analogue (5'-fluorouracil). Chemotherapy regimens have evolved and improved breast cancer patients outcomes in both neoadjuvant and adjuvant settings with a current backbone composed of anthracyclines and taxanes[26]. Anthracyclines are anti-tumor nucleic acid intercalating agent and taxanes have anti-mitotic activity.

Breast cancer intrinsic subtypes respond differently to CMF, and basal-like breast cancers are more responsive to CMF[14,27,28] . Anthracyclines appear to be particularly efficacious in the treatment of HER2E breast cancers in part due to alterations in the topoisomerase 2 gene present in the same chromosomal location as *ERBB2* gene (and thus often co-amplified) [14,29-31].

More recent chemotherapy agents are used to treat metastatic breast cancer and include additional antimetabolites/nucleoside analogues (capecitabine, gemcitabine) and DNA-crosslinking agents (platinum-based therapies) with clinical responses dependent on breast cancer stage and subtype[13,32,33].

1.1.2.2 Targeted therapy

Molecular profiling of breast cancers led to personalized therapies with direct effects on the prognosis of patients. ER expression in Luminal A and B breast cancer intrinsic subtypes is a predictive biomarker of response to anti-ER compounds such as letrozole and tamoxifen[34]. Similarly, HER2E breast cancers are treated with anti-HER2 therapies such as trastuzumab[35]. In contrast, the majority of basal-like breast cancers do not have proven targeted therapy options partly due to the heterogeneity of the subtype [22,23,36]. Only BRCA-mutated basal-like/triple negative breast cancers (accounting for about 15% of triple negative breast cancers)[37] have been shown to respond to poly(ADP-ribose) polymerase inhibitors, agents that target the DNA damage repair system through synthetic lethality, which led to recent US health authority approvals[38,39]. However, accumulating evidence suggests that basal-like breast cancers might be the most amenable breast cancer subtype to immune-modulating therapies.

1.2 Immune system and cancer

The potential of anti-tumor immunity has been known for centuries, owing to pioneers such as Paul Ehrlich who introduced the immune surveillance concept in the 1900s[40] – a concept that has been reinvigorated in recent years, with the rise of immunotherapy, and relies on the interplay between cancer cells and the tumor immune microenvironment in opposing tumor development and progression. The cancer-immunity interaction is described as a 3-phase process: Elimination, Equilibrium and Escape **(Figure 1.1)** [41-43]

The elimination phase begins when transformed or cancer cells are recognized by the immune system. The immune response that proceeds is mediated by collective actions of the innate and the adaptive immune system. The latter includes cytotoxic T cells that target cancer cells expressing various types of antigens[44]. The actions of the innate immune system are mostly

antigen-independent with some exceptions including antibody-dependent cellular cytotoxicity and antibody-dependent cellular phagocytosis which provide a link between the innate and adaptive immune system.

The immunogenicity of the tumor is shaped during the equilibrium phase. It is at this phase that highly immunogenic cancer clones are successfully eliminated by the immune system leaving cancer clones with low immunogenic potential to grow unchecked by the immune system. A recent study reports the occurrence of immune-editing in metastatic sites[45]. It is believed that all cancers go through cancer immune-editing, and only become clinically detectable at the escape phase.

The tumor immune microenvironment includes polymorphonuclear cells, macrophages, T cells, natural killer cells, dendritic cells and B cells. These components vary in frequency and composition across different types of cancers. For instance, melanoma, renal cell, lung and colorectal carcinomas are known to have more extensive immune infiltrates in overall comparison to other types of cancers, such as breast or prostate carcinomas[46] . This difference in immune infiltrates has been partly attributed to the degree of mutational burden observed prominently for example in melanoma[47,48]. Genetic instability and high mutation rates lead to increased production of neo-epitopes that induce a polyphenotypic immune response and generate a chronically inflamed tumor microenvironment [47,49].

Basal-like breast cancers are associated with genetic instability (via copy number alterations) and a relatively high mutational burden (partly due to mutations in p53 and deficiencies in DNA repair pathways) that make them the most immunogenic of all breast cancer intrinsic subtypes[2,50]

The presence of important cell populations of the innate and adaptive immune system has been reported in breast cancer [51]. While the cells of the adaptive immune system have been the major focus in breast cancer, innate immune cells are frequently found in tumor specimens.

1.2.1 Innate immunity

Innate immunity constitutes a heterogeneous family and is the first immune response to an insult such as cellular transformation[52]. Following recognition of the insult, innate immune cells mediate their actions through distinct mechanisms such as phagocytosis for neutrophils and macrophages, cellular cytotoxicity for natural killer cells and γδ T cells, and antigen presentation for dendritic cells and macrophages. Only innate immune cells of myeloid origin with reported immunosuppressive activity are presented below.

1.2.1.1 Tumor-associated neutrophils

Neutrophils are primarily known for their major role in the clearance of micro-organisms at sites of infection. In cancer, cytokines secreted in the tumor microenvironment such as IL-8 help in the recruitment and replenishment of these short-lived cells[53]. In preclinical studies tumor-associated neutrophils have been shown to be immunosuppressive by reducing T cell proliferation in breast cancer mouse models[54,55]. The role of tumor-associated neutrophils in breast cancer patients is still unclear.

Myeloid-derived suppressor cells (MDSCs), a heterogeneous population of immature myeloid cells with immunosuppressive activity constitute a phenotypically – but not histologically – distinct subset of neutrophils[56,57] . MDSCs are observed in the tumor microenvironment of different types of cancer (including breast cancer), and have perhaps best been characterized in mouse models[58,59] . Their phenotype varies but common markers used to recognize human MDSCs by flow cytometry include at least a CD11b+CD33+ phenotype[60].

Importantly, the presence of MDSCs in breast cancer patient tumors correlates with late-stage disease and poor prognosis[61].

1.2.1.2 Macrophages

Tumor-associated macrophages (TAM) found in cancer specimens are divided into two main categories, namely classically-activated M1 and alternatively-activated M2 macrophages, based on the main biological processes in which they participate. TAMs with an M1 phenotype are associated with a pro-inflammatory microenvironment and production of type I cytokines including TNFα and nitric oxide synthase. M1 macrophages appear to be involved in anti-tumor immune reactions but lack a unique biomarker to identify them by immunohistochemistry in clinical biopsy specimens[62].

In contrast, the M2 phenotype is associated with an immunosuppressive microenvironment, producing cytokines such as IL-4 and IL-10. M2 macrophages have a role in establishing an immune environment that is permissive to tumor growth and spread; biomarkers such as CD163 have been used to identify this population[63]. By using CD68 as a pan-marker that can identify both M1 and M2 macrophages, and CD163 as a more specific marker for M2 macrophages, several studies have implicated a role for M2 macrophages in breast cancer patients as both high CD68 and CD163 counts are associated with poor outcome[63-66].

The interaction between TAMs and breast cancer cells might also be tumor subtype dependent, because in vitro data shows that co-culture of TAMs with estrogen receptor positive/luminal breast cancer cell lines generates M1 phenotype TAMs, whereas an M2 phenotype is generated when macrophages are co-cultured in the presence of triple negative/basal breast cancer cell lines[67].

Recent studies have shown that the immunosuppressive activity of TAMs can also be mediated by the expression of an immune checkpoint receptor called Programmed cell Death-Ligand 1 (PD-L1) that leads to inhibition of cytotoxic tumor-infiltrating lymphocytes[68] . PD-L1 expression is in turn driven by the secretion of IFNγ by activated T cells, representing a negative feedback loop that highlights the importance of cross-talk between T lymphocytes and macrophages within the tumor immune microenvironment[68,69].

1.2.2 Adaptive immunity

1.2.2.1 Tumor-infiltrating lymphocytes in breast cancer

In breast cancer, TILs composed primarily of B and T cells are observed in about 80% of patients and vary greatly by breast cancer subtypes[70,71]. In addition, tertiary lymphoid structures that include B cells can be identified in formalin-fixed paraffin-embedded breast tumor whole sections, particularly those taken from the interface been carcinoma and adjacent normal tissues[72,73]. Measurement of TILs is typically done on standard hematoxylin and eosin (H&E)-stained slides made from core biopsies or surgical excision specimens from breast cancer patients **(Figure 1.2)**. Even though research results from biomarker-assessed TILs on tissue microarray cores vs. whole sections are concordant (in terms of associations with clinicopathological parameters and prognosis), and 4 micron thick whole sections still only represent a minuscule fraction of the total tumor specimen, the international TIL working group recommends that TIL assessment be done on whole sections to better capture the spatial distribution of TILs on H&E slides[74].

In a seminal study investigating the prognostic value of TILs in breast cancer, the scoring of H&E TILs was assessed irrespective of their localization in the tumor and was categorized by density[75]. In an effort to further its clinical implementation, an international TIL working group

has set recommendations to standardize the assessment process for this biomarker[74]. Stromal TILs (sTILs) are defined as the percentage of the stromal area infiltrated by TILs that are not in direct contact with carcinoma cells, whereas intraepithelial TILs (iTILs) are defined as the percentage of the tumor area occupied by TILs within tumor nests in direct contact with carcinoma cells[74] **(Figure. 1.2)**. Although there is a positive correlation between sTIL and iTIL scores, only H&E sTILs are recommended to be assessed for prognostic or predictive analyses due to the higher analytical reproducibility of sTIL scoring among different pathologists[74,76].

The prognostic and predictive values of H&E TILs in breast cancer vary by subtype as reported in numerous studies[70]. The role of H&E TILs as a prognostic marker has been evaluated in several large studies that consistently show that among patients with triple negative breast cancer, 10% increments in H&E TILs are associated with an improved clinical outcome, especially for the endpoint of relapse-free survival[77-81].

H&E TILs as a predictive factor have been evaluated in breast cancer neoadjuvant and adjuvant settings in multiple studies[81-83]. In neoadjuvant settings, a recent study analyzing breast cancers pooled from 6 randomized neoadjuvant clinical trials reported increasing H&E TIL concentration is a predictive factor for pathologic complete response in all breast cancers (irrespective of subtype)[78]. In contrast, in the adjuvant setting, a correlation between presence of high levels of H&E TILs (≥ 60%, a cut-off sometimes used to define lymphocyte-predominant breast cancers) and response to particular adjuvant chemotherapy agents or anti-HER2 agents has been shown[82,84]; however discrepant results have also been reported [83]. This suggests that the predictive value of H&E TILs might be immune cell-type specific.

1.2.2.2 B cells

In comparison to T lymphocytes, the role of B cells in the context of breast cancer has not been studied as comprehensively. Although B cells have an established primary role in antibody production, they express MHC class II proteins that enable them to present antigens to CD4+ T cells; therefore, they do play a role in modulating T cell mediated anti-tumor activity [85]. Several markers can be used to identify B cells by immunohistochemistry on formalin-fixed paraffin-embedded tumor tissues, but most studies have used CD20[51,71,86,87].

In the context of breast cancer, few studies have assessed the specific role of B cells in patient tumors[86-89]. One large study looked at the density of CD20+ B cells by immunohistochemistry using tissue microarrays representing 1470 breast carcinomas[86]. Results showed that the presence of CD20+ B cells was significantly associated with high grade tumors, hormone receptor negativity, basal-like subtypes and improved survival in the ER negative subtypes – associations very similar to those reported for most T-cell markers.

Moreover, the presence of antibody-secreting plasma cells in breast tumors and its prognostic implications have been reported[90]. Plasma cells are morphologically distinct from other B cells and can be visualized on hematoxylin and eosin-stained slides[90]. Immunohistochemical biomarkers have been used to identify plasma cells in breast tumors and include CD138 and immunoglobulin kappa C[87]. The prognostic value of plasma cells is still unsettled and depends on biomarkers used to identify plasma cells with some studies pointing to a favorable prognostic factor[91,92] while others reporting the opposite[87,90].

Evidence suggests there is also a T-cell independent immunosuppressive role for a subset of B cells, through their secretion of immunosuppressive cytokines such as IL-10 and TGFβ. These B cells are sometimes referred as tumor-evoked B cells in breast cancer[93], and promote

lung metastases in a breast cancer mouse model by converting helper T cells into regulatory T cells[93]. In one study, B-cell gene signatures were shown to improve progression- and metastasis-free survival in breast cancer, with a more pronounced effect in the basal-like subtype[94].

Overall, these studies emphasize the potential importance of the role played by B-cells in tumor immune responses, but more studies investigating the role of these important TILs are needed.

1.2.2.3 T cells

1.2.2.3.1 CD8+ TILs

The elimination of cancer cells by the immune system is in part mediated by CD8+ cytotoxic T lymphocytes. After recognition of their specific epitopes presented on MHC class I molecules expressed antigen-presenting cells and by cancer cells, CD8+ T cells release perforin and granzymes leading to cancer cell death. The presence of infiltrating CD8+ T cells measurable by immunohistochemistry in breast carcinomas has been reported in several studies[87,95,96].

The location of CD8+ TILs in the tumor is assessed in the same manner as H&E evident lymphocyte counts, with CD8+ iTILs defined as CD8+ lymphocytes in direct contact with carcinoma cells or as CD8+ sTILs when they are located outside of carcinoma cells nests. CD8+ TIL counts are usually reported as absolute numbers. CD8+ tumor infiltrating lymphocytes (iTILs and sTILs) are observed mostly in the HER2-enriched and basal-like / triple negative breast cancer subtypes, which are known to be associated with increased levels of genomic instability[2,95-97]. Genomic instability can lead to increased production of neo-antigens that can be recognized by these CD8+ T cells, possibly explaining their high prevalence in these subtypes[98].

The localization of CD8+ T cells in the tumor can affect their function, as CD8+ T cells need to be in direct contact with cancer cells to kill them. Stromal factors such as abundant collagen have been identified in stromal gene signatures of breast cancer (using laser capture microdissection) and can play a role in limiting T cell infiltration within tumors[99].

Results from several studies evaluating CD8+ TILs as a prognostic marker reported that high levels of CD8+ TILs are associated with better clinical outcomes. A large study that included 12 439 tumors combining patients from 4 different cohorts showed that CD8+ TILs were associated with a significantly reduced relative risk of death from breast cancer[97] . Moreover, the presence of stromal and intraepithelial CD8+ TILs was associated with significantly higher survival when compared with tumors not containing CD8+ TILs. Importantly, a subgroup analysis showed that this prognostic effect was observed in ER negative and in HER2 enriched tumors, but was not observed in ER+ (luminal subtype) cases[97]. Consistent with these findings, a retrospective analysis done on 1334 primary breast cancer tissue samples demonstrated a significant favorable association of CD8+TILs with breast cancer specific survival in patients with ER negative cancers and their component HER2 enriched and basal-like intrinsic molecular phenotypes [95].

While there is therefore strong evidence supporting the prognostic effect of CD8+ TILs in breast cancer, a predictive utility for CD8+ TILs in the adjuvant setting has been demonstrated for the value of adding anthracycline chemotherapy to other chemotherapeutic agents[97,100]. A prospective-retrospective analysis of the National Epirubicin Adjuvant Trial (NEAT) showed that the presence of CD8+ iTILs among ER negative tumors was associated with a higher benefit in the anthracycline containing arm (epirubicin added to cyclophosphamide-methotrexate-5'fluorouracil(E-CMF)) compared to tumors negative for CD8+ iTILs. A significant interaction

was observed between the presence of CD8+ iTILs and the relative benefit of adding anthracyclines, at least among the ER negative breast tumors; patients receiving the control arm of non-anthracycline chemotherapy (CMF alone) did not show improved outcomes among cases with CD8+ iTILs [97].

Furthermore, I worked on a study that showed a significant interaction between low levels of CD8+sTILs and improved progression-free survival in metastatic breast cancer patients receiving trastuzumab, an antibody-based anti-HER2 agent[101]. The study was conducted on clinical trial material from patients enrolled in the MA.31 Phase III clinical trial that randomized metastatic breast cancer patients to receive adjuvant trastuzumab or lapatinib (small molecule-based anti HER2 agent) in combination with taxane chemotherapy[101] . Results from this study suggest that low levels of pre-existing CD8+ TILs could favor an enhanced anti-tumor immunity promoted by an antibody-based therapy in metastatic settings.

Several studies have reported that higher levels of CD8+TILs correlate with higher pCR rates after neoadjuvant chemotherapy[102-104] ; however, all of these studies were retrospective analyses of non-randomized studies. Therefore, high level of evidence studies of the type required to prove the clinical utility of CD8+ TILs for predicting response to chemotherapy are still lacking.

1.2.2.3.2 CD4+ T cells

CD4+ T cells recognized MHC class II expressed on antigen-presenting cells and are divided into many subsets based on their specific functions and include Th1, Th2, regulatory T cells and follicular helper T cells[105]. By secreting IFNγ, Th1 CD4+ T cells are essential for the activation of CD8+ cytotoxic T cells, and have been shown to correlate with favorable survival

in breast cancer[106]. A different primary function is ascribed to Th2 CD4+ T cells, which secrete humoral immunity-related cytokines such as IL-4 and IL-6 [105]; their role in breast cancer is less clear.

The function of regulatory T cells is to dampen the immune system so as to limit excessive immune responses that can cause collateral damage to normal tissue. By immunohistochemistry, these cells are most readily identified via the expression of a nuclear factor called Forkhead box P3 (FOXP3). FOXP3+ TILs are associated with high risk clinicopathological factors such as high grade and ER negativity[95,107 108-110]. Some studies report significantly increased survival within ER negative subtypes that have high FOXP3+ TILs, specifically for triple negative and basal breast cancers[95,107,111].

The CD8/FOXP3 ratio is a parameter that indicates an activated immune microenvironment in the tumor and reflects the interplay between activating cytotoxic immune responses through CD8+ and downregulating it through FOXP3+ T cells. A higher CD8/FOXP3 ratio was shown to be significantly associated with better survival in ER negative tumors[110]. However, it should be noted that the analysis of FOXP3 lacks independent prognostic significance in multivariate analyses[95,107] and many of the studies that examined the prognostic value of FOXP3 have a limited power to derive conclusions regarding its clinical utility. Accordingly, the role of FOXP3 as a prognostic marker in breast cancer needs to be further established in large prospective-retrospective clinical trial study designs. While it may seem intuitive that high levels of immunosuppressive FOXP3 TILs would reflect a pro-tumoral immunosuppressive microenvironmental change, their presence actually represents a natural secondary consequence of an active immune response and using a ratio of CD8/FOXP3 may

therefore not be an appropriate parameter for representing the clinical implications of the underlying biology.

Follicular helper T cells (Tfh) are another subset of CD4+ lymphocytes which function as mediators of B cell activation in germinal centers[112,113] . Tfh cells, measured by IHC or by gene expression, are present in breast cancer immune infiltrates and are linked to a better prognosis, especially within HER2+ cases [106]. One study showed that high expression of CXCL13 (an important chemokine responsible for T and B cell homing in germinal centers) by Tfh in breast cancer is associated with higher levels of pathological complete response to anthracycline-based treatment regimens, and with better subsequent disease-free survival[106].

1.3 Cancer immunotherapy: A new strategy in breast cancer treatment

Immunotherapy can be described as any therapy that promote directly or indirectly the immune system. In cancer, immunotherapy agents can be broadly classified by their basic mechanism of action: immune augmentation or immune restoration.

1.3.1 Immune augmentation

Immune augmentation strategies in cancer involve treatments that directly or indirectly establish and enhance anti-tumor immune responses. A few of these strategies are presented below.

1.3.1.1 Direct effects

Immune augmentation can be established by altering anti-tumor immunity through different methods such as therapeutic vaccination, adoptive T cell therapy and with chimeric antigen T cell receptors.

Therapeutic cancer vaccines are vaccines that induce immunity against targeted-cancer antigens. Cancers can produce a plethora of antigens with different degrees of immunogenicity

that may be targeted by strategies under active investigation including viral-based and dendritic cell-based vaccines such as sipuleucel-T[114,115]. Although not exclusively based on dendritic cells, sipuleucel-T is a health authority-approved therapeutic cancer vaccine that is intended for the treatment of hormone-refractory prostate cancers by targeting the prostatic acid phosphatase[116]. In breast cancer, the most promising therapeutic cancer vaccines have been those targeting shared tumor-associated antigens such as HER2, with results yet to be published for the HER2 peptide E75 vaccine being evaluated in a phase III clinical trial (NCT01479244)[117].

In adoptive T cell therapy, autologous TILs are activated in a milieu containing fragments from patient's own tumor[118]. This technique leads to the selection and expansion of tumor-specific T cells which are then transferred back into the patients and has been used mostly in melanoma patients where it appears to reliably work[118].

Another immune augmentation strategy is manufacturing T cells with chimeric antigen T cell receptors (CAR T cells) which is now approved by health authorities in the United States for treatment of some forms of lymphomas[119] . With recombinant DNA, the antigen receptors for CAR T cells are engineered to target receptors expressed on cancer cells (such as CD20 or CD19 for B cell lymphoma) in addition to carrying additional immune modulating regions in their cytosolic tails[119]. Adoptive cell therapy holds promise for otherwise poorly-immunogenic tumors such as ER+ breast cancers and can be used in combination with immune restoration strategies discussed below [120,121].

1.3.1.2 Indirect effects

Particular conventional chemotherapy agents are known to elicit an anti-tumor immune response by creating a process termed immunogenic cell death in dying cancer cells. Immunogenic cell death elicits the presence of damage-associate molecular patterns in dying

cancer cells such as exposure of cell surface calreticulin and release of HMGB1, promotes antigen cross-presentation by dendritic cells in addition to the release of antigens[122,123]. Cyclophosphamide and anthracyclines are among the conventional breast cancer chemotherapy agents working via this mechanism of action[122] . Additionally, particular chemotherapy agents such as cyclophosphamide and gemcitabine preferentially suppress T regulatory and myeloid-derived suppressor cells to a much greater extent than cytotoxic and helper T-cells, enhancing antitumor immune responses[124].

In addition to chemotherapy agents, radiation is thought to augment anti-tumor immunity through the release of antigens in irradiated tumors that also lead to elimination of non-irradiated tumors, a process termed the "abscopal effect"[125,126]. However, additional factors such as selection of combination treatment agents and radiation dosage modulate the induced- immune response[125,127].

Antibody-dependent cellular cytotoxicity, antibody-dependent cellular phagocytosis, and complement-dependent cytotoxicity are immune-mediated effects of some antibody-based targeted therapies such as trastuzumab [101,128-130]. Antibody-dependent cellular cytotoxicity and phagocytosis appear to be more frequent than complement-dependent cytotoxicity and is mediated by immune populations with receptors for the Fc portion of the antibody[131]. These cells include macrophages that engulf antibody-coated cells in antibody-dependent cellular phagocytosis and Natural Killer cells that become activated following binding to their respective Fc receptors[132,133].

1.3.2 Immune restoration via immune checkpoint receptor inhibition

Immune restoration is characterized by strategies that reinvigorate a patient's own anti-tumor immunity *in situ* such as by targeting immune checkpoint receptors **(Figure 1.3).**

Following activation of a T cell, the expression of various inhibitory receptors, termed immune checkpoints, is induced as part of a normal feedback circuitry as another way to avoid excessive immune responses and limit damage to normal tissue. The term 'exhaustion' is also used to describe effector T cells exhibiting reduced proliferation and decreased production of IFNγ in the context of a chronic antigen stimulation, a characteristic of the tumor microenvironment [134]. In cancer, such pathways appear upregulated, as part of cancer immuno-evasion that characterizes the Escape phase. Fortunately, these repressive pathways themselves are targeted by checkpoint inhibitor drugs.

1.3.2.1 CTLA-4

CTLA-4 is a receptor expressed on T cell membranes that acts through binding to CD80/86 expressed on dendritic cells, blocking T cell activation signal 2 and thereby leading to T cell anergy, a normal biological negative feedback process. Dendritic cell interactions with T cells that may yield CTLA-4/CD80 binding events occur mostly within peripheral lymphoid organs such as lymph nodes, and for this reason CTLA-4+ TILs are not often observed on primary tumor specimens[135]. Few immune gene signature studies have evaluated CTLA4 mRNA expression in breast cancer, although recent conference presentations describe increased expression correlating with reduced survival[136,137].

The approach of CTLA-4 blockade and its clinical success in melanoma therapy pioneered the field of immune checkpoint inhibition[138-140], leading to even more recent advances on other targetable immune checkpoints such as PD-1[141]. However, a breast cancer clinical trial examining tremelimumab (a human monoclonal anti-CTLA-4 antibody) in addition to exemestane in metastatic ER+ breast cancer patients did not achieve any partial or complete responses, while exposing patients to some potential serious side effects of anti-CTLA-4 therapy

(**Table 1.2)** [142]. Accordingly, the selection of breast cancer patients for clinical trials that would benefit from anti-CTLA-4 agents needs to be done carefully, and specifically investigated among the particular subgroups of breast cancer patients most likely to benefit from immune restoration strategies (who are unlikely to be ER+ populations due to their low immunogenicity).

1.3.2.2 PD-1/PD-L1

PD-1 is a cellular receptor expressed on antigen-experienced T cells[143]. Binding to its ligands – PD-L1 or PD-L2, which are expressed normally on antigen-presenting cells and aberrantly on tumor cells – leads to inhibition of effector functions[144].

PD-1 inhibition of effector functions results from targeting CD28, the co-stimulatory T cell receptor, for dephosphorylation[145]. Inhibitors targeting the PD-1/PD-L1 pathway have exhibited durable responses in multiple clinical trials leading to various health authorities' approval for treatment of certain cancers such as melanoma, non-small cell lung cancer and bladder cancer[146].

PD-1/PD-L1 inhibitors have also been evaluated in several breast cancer clinical trials including a recent phase III clinical trial (IMpassion 130) that randomized 902 advanced triple negative breast cancer patients to receive PD-L1 inhibitor (atezolizumab) with chemotherapy, or chemotherapy alone [147-149](**Table 1.2).** Accumulating reports from these trials show that clinical responses are mostly limited to patients receiving immune checkpoint inhibitors as first-line treatment and/or with immunogenic tumors characterized by PD-L1 expression [148,150-152]. In the IMpassion 130 clinical trial, 40.9% of randomized patients were PD-L1 positive. PD-L1+ breast cancer patients randomized to the atezolizumab+chemo arm had a significant longer median progression-free survival (7.5 months vs 5 months, hazard ratio:0.62, 95%CI 0.49-0.78) and overall survival (25 months vs 15.5 months, hazard ratio: 0.62, 95%CI 0.45-0.86) in comparison

to PD-L1+ patients treated with chemotherapy alone[148]. PD-L1 assessment in clinical trials as a potential predictive marker is the subject of controversy and has not reached a high level of analytical validity due to several factors such as heterogeneity of PD-L1 expression, variable cut-offs for PD-L1 positivity and the variety of PD-L1 monoclonal antibodies in diagnostic use[153].

It is important to highlight that while tumors with a positive PD-L1 expression can clinically benefit from PD-1 or PD-L1 checkpoint inhibitor monotherapy, other tumors with negative or minimal expression for PD-L1 might need the combination of other agents with anti-PD-1 to elicit the immune system to fight against their tumors. An intriguing hypothesis is that the combination of immune modulating conventional chemotherapy agents or radiotherapy with checkpoint inhibitors could have special value in patients with a low immune response that exhibit low base-line levels of TILs and minimal expression of PD-L1. In support of such hypotheses, a pilot study assessing the interaction of the immune system with the combination of tumor cryoablation plus ipilimumab interestingly found that the combination of these two very different treatment approaches leads to activation of the immune system, as marked by increased production of plasma IFNγ and proliferation of T-cells [154]. Since this combination therapy has been shown to be associated with upregulation of IFNγ, it could lead to a higher expression of PD-L1[66,67] and thus could benefit patients with little to no pre-existing immune response (based on the levels of TILs and PD-1/PD-L1 expression). More studies are needed to define the best dosage therapy and target population of patients most likely to benefit from combinations of immunotherapy with conventional therapies.

1.3.3 Beyond CTLA-4 and PD-1/PD-L1

Following the success of CTLA4 and PD1/PDL1 inhibitors, additional immune checkpoint targets have recently emerged and made their way into early phase clinical trials[155]. These include LAG-3 and TIM-3.

1.3.3.1 LAG-3

Lymphocyte Activation Gene 3 (LAG-3) is an exhaustion marker with immunosuppressive activity expressed on activated T cells [156]. Major histocompatibility complex class II (MHC-II) is a ligand for LAG-3; additional ligands (e.g., L-selectin and galectin-3) have also been identified[156]. Regulatory T cells (Tregs) expressing LAG-3 have enhanced suppressive activity, whereas cytotoxic CD8+ T cells expressing LAG-3 have reduced proliferation rates and effector cytokine production in cancer and autoimmune diabetes[157-159]. A splice variant of LAG-3 cleaved by metalloproteinases and secreted in the cellular microenvironment has immune-activating properties when bound to MHC-II on antigen presenting cells[160].

LAG-3+ tumor-infiltrating lymphocytes (TILs) have been reported in melanoma, colon, pancreatic, breast, lung, hematopoietic, and head and neck cancer patients[161-167], in association with aggressive clinical features. Antibody-based LAG-3 blockade in multiple cancer mouse models restores CD8+ effector T cells and diminishes Treg populations, an effect enhanced when combined with anti-PD-1[168,169]. A recent study in a metastatic ovarian cancer mouse model showed that LAG-3 blockade leads to upregulation of other immune checkpoints (PD-1, CTLA-4, and TIM-3), and combination therapy targeting LAG-3, PD-1, and CTLA-4 increases functional cytotoxic T cell levels while reducing Tregs and myeloid-derived suppressor cells[170].

Multiple early phase clinical trials are testing antagonistic LAG-3 agents in combination with anti-PD-1 and/or anti-CTLA-4 therapy (>15 phase I or II clinical trials on clinicaltrials.gov-

February 2019). In view of the activating properties of soluble secreted LAG-3, a soluble agonist LAG-3 antibody (IMP321) was tested in advanced solid malignancies as a single agent[171], and demonstrated sufficient tolerability and efficacy to warrant advancement to phase II (NCT02614833).

1.3.3.2 TIM-3

T-cell Immunoglobulin- and Mucin-domain-containing molecule 3 (TIM-3) is an immune-inhibitory molecule first identified on CD4+ Th1 (helper) T-cells and CD8+ Tc1 (cytotoxic) T-cells[172], then later on Th17 T-cells,[173] regulatory T-cells[174,175], and innate immune cells[176-178]. TIM-3 is activated primarily by its widely-expressed ligand, galectin-9[179], leading to effector T-cell death through calcium influx, cellular aggregation, and apoptosis[180]. When TIM-3 signaling is active, interferon-producing T-cells become exhausted, resulting in Th1 suppression and immune tolerance[180-182]. TIM-3 expression is commonly observed during chronic infection, as a characteristic marker of exhausted T cells.[183-187].

In cancer, tumor-infiltrating lymphocytes expressing TIM-3 have been observed in melanoma[188,189], non-Hodgkin's lymphoma[190], lung[174], gastric[191], and other cancers[192-195]. In these studies, TIM-3 is co-expressed with PD-1 and associated with effector T-cell exhaustion and dysfunction. This phenomenon is also observed in mouse models of solid[196] and hematologic[197] cancers, where TIM3+PD1+CD8+ T-cells exhibit an exhausted phenotype characterized by reduced proliferation and defective production of IL-2, TNFα, and IFN-γ. In contrast, TIM-3 positive Treg display increased expression of effector molecules and are more immunosuppressive than their TIM-3 negative counterparts[198,199].

Inhibition of TIM-3 alone tends to have little effect on tumor growth in pre-clinical mouse models, despite some evidence supporting a reversal of immune cell exhaustion[188,196,200-

[202]. However, combined targeting of PD-1 and TIM-3 leads to a substantial reduction in tumor growth – better than either pathway alone – in numerous preclinical in vivo models[188,196,197,202], supporting the concept that malignant cells become resistant to PD-1 checkpoint blockade by activating another immune checkpoint. Indeed, mouse models partially responsive to PD-L1 inhibition upregulated TIM-3 expression in resistant tumors[194,203], and addition of TIM-3 blockade was successful in overcoming that resistance. Upregulation of TIM-3 has also been observed in patients receiving PD-L1 monotherapy, suggesting it may represent a form of adaptive resistance to this therapy [203]. At least seven early phase clinical trials are underway that attempt to combine anti PD-L1/PD-1 therapy with agents targeting TIM-3 (NCT03489343, NCT02817633, NCT03680508, NCT03311412, NCT03099109, NCT03744468, NCT03066648).

1.4 Rationale for thesis and research objectives

As an increasing number of immune targets for cancer immunotherapy are being discovered in pre-clinical animal studies, the characterization of immune infiltrates in patient tumors and the investigation of these immunotherapy targets are crucial for clinical trial study design and assay development studies that may lead to clinical implementation of immune targets as potential prognostic or predictive biomarkers.

At the start of my thesis, immuno-oncology research in breast cancer was still in its infancy and early phase immune checkpoint inhibitor clinical trials in breast cancer were just opening. The main goal of my research was to investigate the presence and prognostic implications of clinically relevant immune infiltrates in well-annotated breast cancer pathology specimens.

My hypothesis is that immunotherapy targets will be expressed on infiltrating immune cells in a specific subset of breast cancers, detectable in breast cancer pathology specimens.

Furthermore, these biomarkers will have prognostic implications and may serve as a guide for breast cancers amenable to emerging immunotherapy strategies.

Specifically, my thesis is based on the following 2 aims:

1. *Development and prognostic analyses of emerging immune checkpoint biomarkers by immunohistochemistry in an annotated breast cancer cohort, with subsequent validation using a larger breast cancer cohort.*

For this aim, my hypothesis is that emerging immunotherapy targets would be enriched in estrogen receptor negative breast cancer patients and their presence will be associated with unfavorable survival.

I reviewed the literature to identify emerging immune checkpoint biomarkers beyond PD-1/ PD-L1 that were being evaluated in clinical trials. I then organized evaluation of these candidates by immunohistochemistry on an initial breast cancer patient cohort consisting of 330 breast tumor excision specimens built into tissue microarrays and linked to clinical outcome. This cohort serves as a training set to screen for biomarkers compatible for immunohistochemistry assessment on formalin-fixed paraffin-embedded tumor tissues. In addition, I used the training set for cut-point determination for positivity and to generate hypotheses to be validated on an independent larger cohort. The latter consists of a tissue microarray series spread over 17 blocks, representing 3,992 breast cancer patients linked to clinical outcome and extensive biomarker data. Prior to the analyses on this larger cohort, my results on the training cohort set of 330 breast cancer patients and the specific hypotheses I generated were reviewed by the breast cancer outcomes unit at the BC Cancer Agency for approval to access the valuable large cohort.

2. *Development of a new in situ multiplex methodology for immune profiling of breast cancer patients*

My hypothesis for this second aim is that a signature composed of immune and tumor biomarkers would discriminate between immune-enriched and immune-desert profiles of breast cancer tumors.

Immune infiltrates present in tumors represent multiple important immune cell types which likely mediate different activities within the tumor microenvironment that could promote or inhibit responses to immune-modulating therapies. Assessing and visualizing the presence of multiple biomarkers within a tissue remains a technical challenge. For this aim, I set out to evaluate a novel immunohistochemical multiplex technology called digital spatial profiling by Nanostring, capable of generating quantitative assessment of 31 targets in tumor tissues. I tested the feasibility of the digital spatial profiling technology using two different breast cancer tissue microarray cohorts.

The results generated in the first aim are presented in **Chapter 2** and **Chapter 3** whereas **Chapter 4** presents the results of the Nanostring-based digital spatial profiling platform tested on two initial cohort-based sets. **Chapter 5** summarizes the body of work presented in the thesis and provides perspectives for the future in breast cancer immunotherapy.

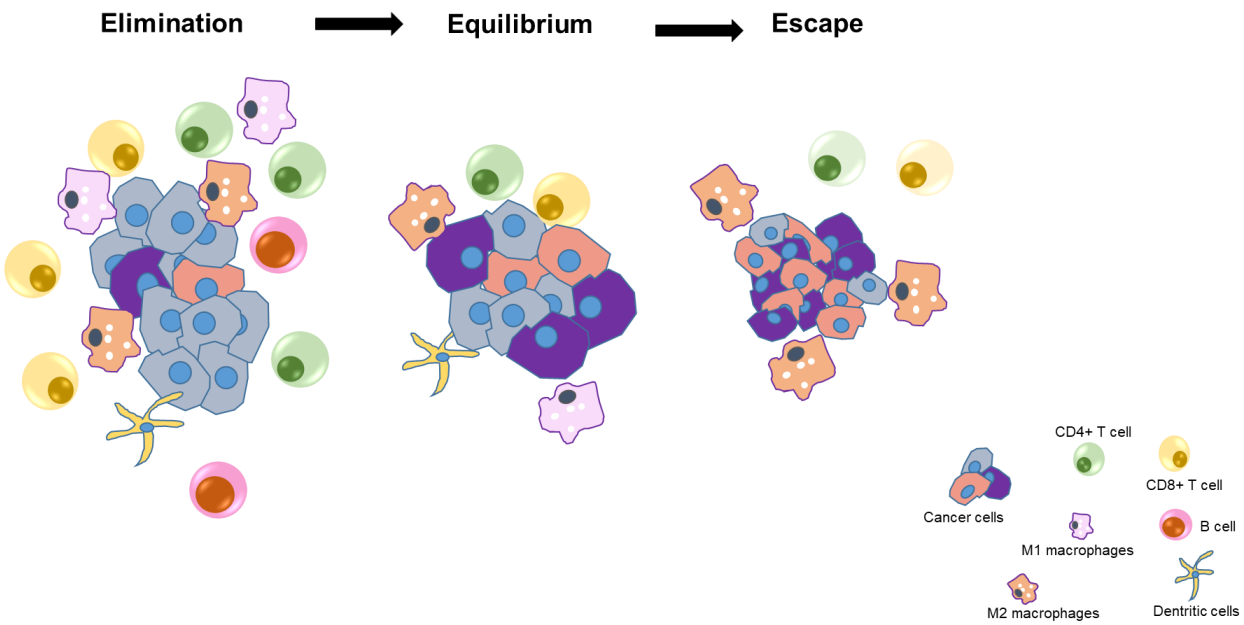

Figure 1.1 Cancer-immune interaction
Simplified illustration depicting the 3 phases of cancer-immune interaction: Elimination, Equilibrium and Escape. The dynamic tumor immune microenvironment is depicted by the changes in the composition of cancer clones and immune populations at each phase.

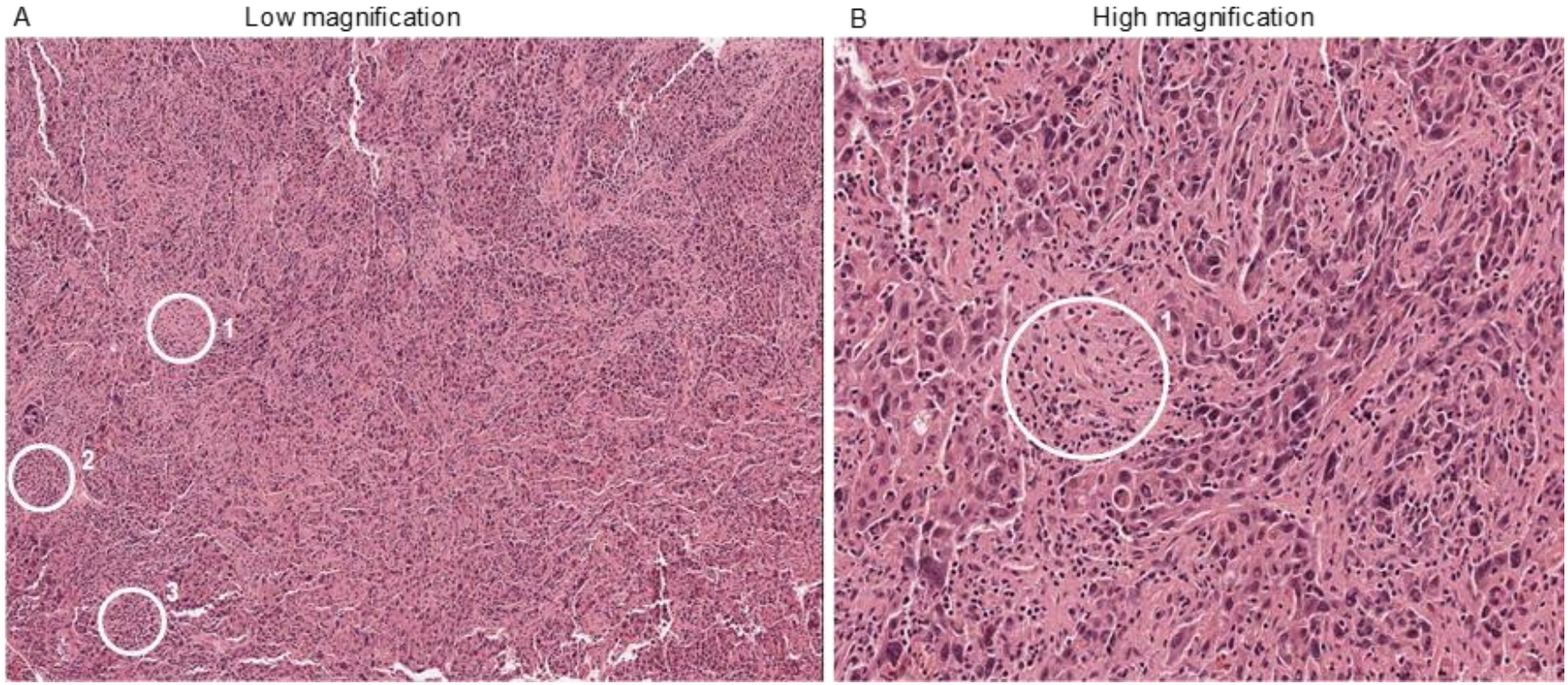

Figure 1.2 Assessment of tumor-infiltrating lymphocytes in the breast cancer microenvironment.
Hematoxylin and Eosin-stained section of a breast cancer specimen displaying the immune infiltrates in the tumor stroma compartments used for scoring TILs (representative scoreable areas are indicated by white circles) as per recommendations of the international TILs Working Group[74]. **A,** low magnification view of the tumor used to identify areas where stromal TIL count can be assessed. **B,** High magnification view of one stromal area included in the scoring, estimated at 20% sTILs. Reproduced with permission.

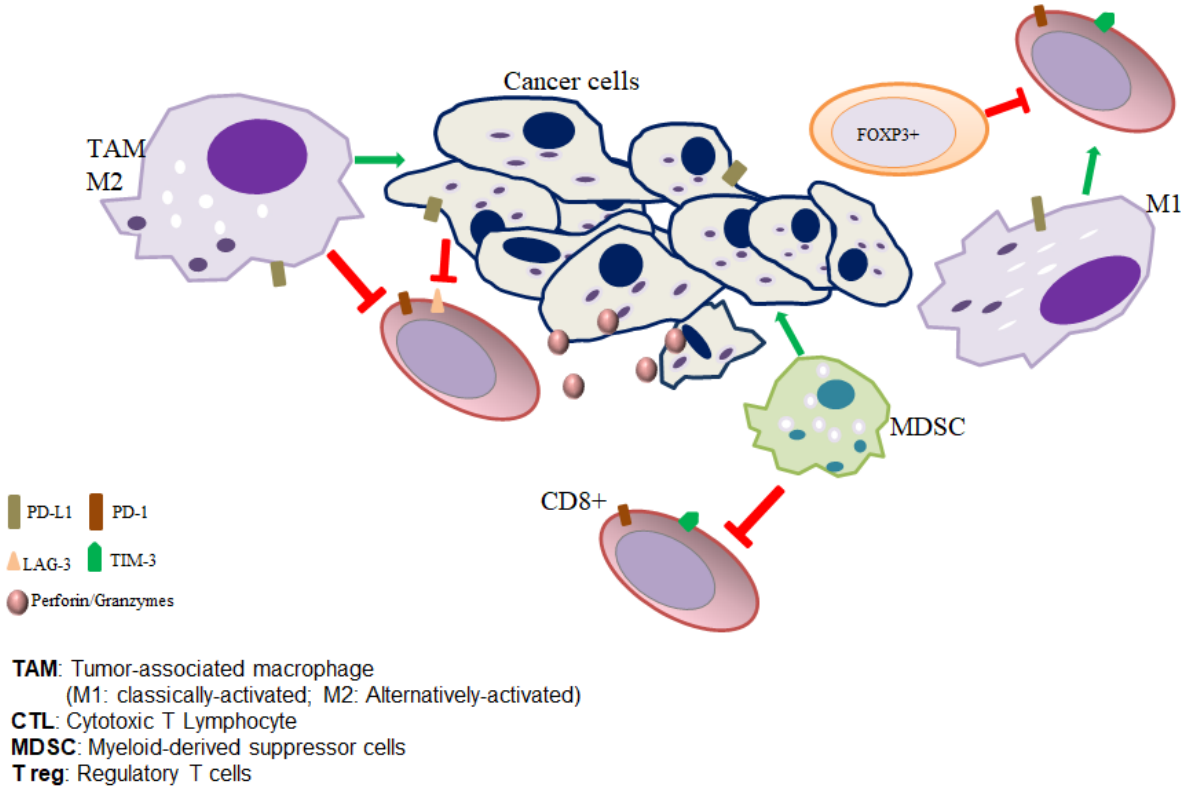

Figure 1.3 Immune regulation in the breast cancer microenvironment

Different populations of immune cells are observed in breast cancer specimens and are associated with both anti- and pro-tumorigenic effects. Immune checkpoint inhibitor-expressing immune cells are identified by the presence of PD-1, LAG-3 and TIM-3 on the cell

surface. Green arrows indicate interactions leading to activation whereas red arrows indicate inhibitory interactions. Reproduced with permission.

Table 1.1 Description of breast cancer clinical intrinsic subtypes.

	Luminal A	Luminal B	HER2E	Basal-like
Frequency (%)	70-80		10-15	10-15
Clinical IHC surrogate	ER+, PR+ Ki67 (<14%) HER2–	ER+, PR+ Ki67 (≥14%) (Luminal/HER2+)	ER–, PR– HER2+	ER–, PR–, HER2–, CK5/6+ and/or EGFR+ TNBC (ER–, PR–, HER2–)
Therapy options	Hormonal therapy +/- chemotherapy or radiotherapy	Hormonal therapy, chemotherapy, radiotherapy	Anti-HER2, Chemotherapy	Chemotherapy, PARP inhibitors for BRCA-mutated
Prognosis	Good	Intermediate	Intermediate	Worse
Immunogenicity	Low	Intermediate	Intermediate	High

Table 1.2 Breast cancer immunotherapy clinical trials

Target	Agent (company)	Study	Phase	Population	Reported results
PD-1	Pembrolizumab (Merck)	**KEYNOTE-028** (single agent) Rugo HS et al., *Clin Can Res*, 2018	Ib	Advanced ER+/HER2- (N=25)	ORR: 12% (3 PR)
		KEYNOTE-086 (single agent) Adams S et al.,*Ann Oncol*, 2018	II	Metastatic triple negative breast cancer (N=254)	Cohort A: previously treated, TNBC unselected (N=170) : ORR=5.3% (2 CR, 7 PR) Cohort B: previously untreated, TNBC PD-L1+ (N=84): ORR= 21.4% (4 CR, 14 PR)
		KEYNOTE-012 (single agent) Nanda R. et al., *J Clin Oncol*, 2016	Ib	Selected PD-L1+ metastatic triple-negative breast cancer (N=27)	ORR=18.5 % (1CR, 4 PR)
		ENHANCE-1/KEYNOTE-150 (in combination with eribulin) Tolaney SM et al., *Canc res, 2018*.P6-13 abstr	Ib/II	Advanced triple-negative breast cancer (N=106)	ORR: 26.4% (3 CR, 25 PR)
		KEYNOTE-173 (in combination with various chemotherapy agents) Schmid P et al., *J Clin Oncol*, 556 (2017). abstr.	Ib	Advanced triple-negative breast cancer (N=20)	pCR: Cohort A treated with pembro followed by pembro+nab-paclitaxel followed by pembro+doxorubin/cyclophosphamide: 60% Cohort B treated with pembro followed by pembro+ nab-paclitaxel + carboplatin and by pembro+ doxorubin/cyclophosphamide: 90%
		I-SPY 2 (in combination with paclitaxel or paclitaxel alone followed by doxorubicin/cyclo-phosphamide) Nanda R et al., *J Clin Oncol,* 506 (2017).abstr.	II	Primary breast cancer (N=249)	pCR: TNBC: 60% pembro arm vs 20% control HR+/HER2-: 34% pembro vs 13% control
PD-L1	Avelumab (Pfizer and EMD serono)	**JAVELIN** (single agent) Dirix LY. et al, *Breast Cancer Res Treat,* 2018	Ib	Metastatic breast cancer (N=153)	ORR=4.8% (1 CR, 7 PR)
	Atezolizumab (Roche)	**IMPassion 130** (in combination with nab-paclitaxel vs nab-paclitaxel alone) Schmid P et al., *N Engl J Med,* 2018	III	Advanced triple-negative breast cancer (N=902; randomized 1:1)	Primary endpoints in atezo+nab-pacli: Median PFS: 7.2 months vs 5.5 months, p=0.002 Median OS : 21.3 months vs 17.6 months p=0.08
	Durvalumab (Imfizi)	**Yale study** Pusztai L et al., *J Clin Oncol,* 572 (2017). abstr	I/II	Primary triple-negative breast cancer (N=7)	pCR: 71.4%
CTLA-4	Tremelimumab (Astrazeneca)	**Vonderheide RH et al**.,*Clin Cancer Res,* 2010, (In combination with exemestane	I	Metastatic ER+/HER2- breast cancer (N=26)	ORR=0 11 SD (42%)

ORR: objective response rate by RECIST 1.1 criteria; CR: complete response, PR: partial response
pCR: Pathologic complete response

Chapter 2: LAG-3+ tumor infiltrating lymphocytes in breast cancer: clinical correlates and association with PD-1/PD-L1+ tumors

SYNOPSIS

Novel immune checkpoint blockade strategies are being evaluated in clinical trials and early phase studies are now including strategies targeting the lymphocyte activation gene 3 (LAG-3) checkpoint, alone or in combination with PD-1/PD-L1 blockade. In this chapter, I investigated LAG-3 expression and its prognostic value in a large series of breast cancer patients, and correlated LAG-3 expression with key biomarkers including PD-1 and PD-L1. LAG-3 expression was evaluated by immunohistochemistry on two tissue microarray series incorporating 4322 breast cancer primary excision specimens (N=330 in the training and N= 3,992 in the validation set) linked to detailed clinico-pathological, biomarker and long term clinical outcome data. PD-1 and PD-L1 expression were also evaluated by immunohistochemistry.

After locking down interpretation cutoffs on the training set, LAG-3+ intra-epithelial tumor-infiltrating lymphocytes (iTILs) were found in 11% of cases in the validation set. In both sets, LAG-3+iTILs were significantly associated with negative prognostic factors: young age, large tumor size, high proliferation, HER2E and basal-like breast cancer subtypes. In multivariate analyses, breast cancer patients with LAG-3+iTILs had a significantly improved breast cancer-specific survival (BCSS) (HR: 0.71,95%CI 0.56-0.90), particularly among ER– patients (HR: 0.50,95%CI 0.36-0.69). Furthermore, we found that 53% of PD-L1+ and 61% of PD-1+ cases are also positive for LAG-3+iTILs, supporting potential immune checkpoint blockade combination strategies as a treatment option for breast cancer patients.

2.1 Introduction

Although breast cancer is not generally considered an especially immunogenic malignancy in comparison to melanoma and lung cancer[47], recent studies show that some tumors, especially estrogen receptor (ER) negative breast cancers, do elicit an immune response [70]. Immune checkpoint inhibitors targeting cytotoxic T-lymphocyte-associated protein 4(CTLA-4), the programmed cell death receptor 1(PD-1) and/or its ligand (PD-L1) have shown clinical efficacy, especially in melanoma and lung cancer [138,204]. In breast cancer, results from early phase trials have suggested checkpoint inhibitor efficacy may be primarily seen in triple negative cases [205]. While the immuno-oncology field is moving at a fast pace, large scale studies of immune checkpoint expression in breast cancer series are as yet few. The lymphocyte activation gene 3 (LAG-3) represents one example of a new immune checkpoint target.

LAG-3 is a cellular receptor expressed by activated T lymphocytes and is associated with T cell exhaustion [156]. LAG-3 is commonly upregulated with PD-1; pre-clinical data suggests that LAG-3 blockade releases T cells effector functions and synergizes with other immune checkpoint inhibitors such as anti-PD-1[168]. Thus, LAG-3 represents an interesting target for immunotherapy and there are a number of ongoing early phase clinical trials testing anti-LAG-3 therapeutic antibodies in different types of cancer. Our objective was to assess the prognostic value of LAG-3 and its association with PD-1 and PD-L1 immune checkpoints in a large, well-characterized cohort of breast cancer specimens.

2.2 Materials and methods

2.2.1 Study cohorts

The initial set (a training set used to finalize staining and scoring methodology) consisted of 330 invasive breast cancer cases from University of British Columbia hospitals diagnosed between 1989 and 2002 [206]. The validation set, previously described in detail [107], consisted of 3,992 female patients diagnosed with invasive breast cancer at centres of the British Columbia Cancer Agency across the province between 1986 and 1992 and for which formalin-fixed paraffin-embedded primary breast tumor excision specimens were collected from a central estrogen receptor testing laboratory. None of these patients received neoadjuvant treatment. A further description of the study cohorts is provided in **Section 3.2.1** of **Chapter 3**.

Basic clinical and pathological parameters of the study populations are summarized in **Table 2.1 and 2.2**. The median follow-up time is 12.6 years for both sets. Access to the samples and corresponding de-identified clinico-pathologic, treatment and outcome data was approved by the Clinical Research Ethics Board of the University of British Columbia and by the BC Cancer Agency Breast Cancer Outcomes Unit.

2.2.2 Immunohistochemistry

Formalin-fixed paraffin-embedded primary excision specimens were used to build tissue microarrays, represented as 0.6mm cores as previously described [206,207]. Biomarkers previously stained by immunohistochemistry on the validation tissue microarray include ER, PR, HER2, Ki67, EGFR, CK5/6, and CD8 [96]. Immunohistochemistry for LAG-3 and PD-1 was performed using a Ventana Ultra automated stainer in accordance with manufacturer's protocol using the following antibodies and concentrations: LAG-3 (Clone 17B4, dilution 1:100, Abcam, see **Appendix A**), PD-1 (Clone NAT105, dispenser, Roche). PD-L1 staining was performed at the

Deeley Research Centre (Victoria, Canada) using clone SP142, dilution 1:100 (Spring Bioscience) (see **Figure 2.1** for representative staining of LAG-3, PD-1, and PD-L1). Breast cancer intrinsic subtypes from both cohorts were previously determined by immunohistochemical methods that were originally developed against gene expression gold standards [208]. Briefly, Luminal A was defined as ER+ (≥1%) or PR+ (≥1%), HER2– and low Ki67, Luminal B as ER+ (or PR+) and HER2+ or high Ki67 (≥14%); HER2E as HER2+ and ER– and PR–; Basal-like as HER2–/ER–/PR– with EGFR+ or CK5/6+.

2.2.3 LAG-3, PD-1 and PD-L1 scoring

Biomarkers were evaluated and reported following REMARK guidelines [209]. TMA slides were digitally scanned and visually scored by an experienced pathologist blinded to clinical information. Scoring and quantification of LAG-3 and PD-1 were carried out as previously described for other lymphocyte biomarkers [107]. In brief, stromal lymphocytes were defined as lymphocytes not in direct contact with the breast carcinoma nest whereas intra-epithelial lymphocytes were located within the carcinoma nest. Scores of lymphocyte biomarkers were reported as absolute counts, and any positive expression (≥1 TILs per TMA core) was used for dichotomization into positive and negative cases. PD-L1 scoring is a matter of controversy in the current literature; in this study we used the method of McDermott DF et al., [210] whereby expression was assessed as the percentage of carcinoma cells with membranous expression; any cores with ≥1% of PD-L1+ carcinoma cells were considered positive. We found only 24 cases out of 2918 cases with PD-L1+ immune cells and they were discarded for further analyses. Cutoffs determined using the training set were locked down for analysis on the validation set.

Overall stromal tumor-infiltrating lymphocytes were assessed following the methods established by the international TIL working group[74] on scanned images of hematoxylin and

eosin-stained tissue microarray slides and were only available on the training set at the time of the publication of this chapter.

2.2.4 Statistical Analysis

Statistical analyses were carried out using IBM SPSS (version 24.0) and R (version 3.3.2) software. Breast cancer-specific survival (BCSS) was the primary outcome, defined as the time from date of diagnosis to date of death attributed to breast cancer. Patients who died from another cause or were alive at the end of follow-up were censored. Relapse-free survival (RFS) analyses were also performed, defined as time from date of diagnosis to date of any type of breast cancer relapse (local, regional, distant, or contralateral). In addition, patients were censored if they had not died from breast cancer or if they had not relapsed at the end of follow-up time for relapse-free survival analyses. Univariate associations between LAG-3 and survival were examined using Kaplan-Meier survival curves and log-rank test. Cox proportional hazards regression was used to estimate hazard ratios for LAG-3 adjusted for the following clinicopathological parameters: age (<50 vs ≥50), tumor grade (grade 3 vs grade 1,2), tumor size (>2cm vs ≤2 cm), lymphovascular invasion status and nodal status). Findings observed on the initial set, to be tested on the validation set, were prespecified in a formal written statistical plan, presented at the BC Cancer Agency Breast Cancer Outcomes Unit. Additionally, for analyses of lymphocytes biomarker relationships, due to low numbers of positive cases in the initial set, a training and validation approach was used by splitting the validation set in half. Findings to be validated on the other half of the set were prespecified in a written statistical plan prior to the analyses (see **Appendix B**). All statistical tests performed were two-sided at α=0.05.

2.3 Results

2.3.1 Selection of LAG-3+TILs cutoffs on the training set

278 (84%) of breast cancer cases in the training set were interpretable for LAG-3 **(Table 2.1).** As relatively few cases had LAG-3+TILs in 0.3mm^2 cores, any cases that had ≥1 lymphocyte expressing LAG-3 were deemed as positive. We found stromal lymphocytes expressing LAG-3 in 15% and intra-epithelial lymphocytes expressing LAG-3 in 14% of cases. Both LAG-3+sTILs and iTILs were significantly associated with negative prognostic factors including high grade tumor, ER negativity and high Ki67 proliferation **(Table 2.1)**. Following our previous publications on lymphocyte biomarkers [96,107], we set on LAG-3+iTILs≥1 per 0.3mm^2 core as our primary analysis for the validation set to allow comparison among lymphocyte biomarkers.

2.3.2 LAG-3+iTILs are enriched in ER negative subtypes and associated with improved survival

2,921 (73%) cases were interpretable for LAG-3 staining on the validation set. LAG-3+iTILs≥1 per 0.3mm^2 core were observed in 11% of breast cancer patients with a distribution range of 0-45 (**Table 2.2**). The presence of LAG-3+iTILs was significantly associated with younger age, large tumor size, ER/PR negativity, and high Ki67 proliferation index (**Table 2.2**; interaction test by subtype shown in **Table 2.3**). ER negative tumor subtypes more commonly contained LAG-3+iTILs, present in 33% of basal-like and 27% of HER2E samples (versus 3% and 11% in luminal A and luminal B tumor subtypes respectively).

In the whole cohort and in the ER+ breast cancer subset (81% of cases), the presence of LAG-3+iTILs was not significantly associated with survival in univariate analyses (**Figure 2.2**A-B). In contrast, ER negative breast cancer patients with LAG3+iTILs had significantly improved

breast cancer-specific survival and relapse-free survival, an association present in both HER2E and basal-like subtypes (**Figure 2.2C-E, Figure 2.3**). In multivariate analyses that adjusted for breast cancer-specific clinicopathalogical factors, LAG-3+iTILs were a significant favorable prognostic factor in the whole cohort and among ER negative breast cancer patients (**Table 2.4A**). Due to the correlation between the other immune checkpoints markers, the presence of LAG-3+iTILs is not an independent prognostic factor in a multivariate analysis that include CD8, PD-1 and PD-L1 as covariates (**Table 2.4B**); only the presence of PD-1+iTILs represented a significant prognostic factor for improved breast cancer-specific survival in this model.

2.3.3 LAG-3+iTILs are strongly associated with PD-L1/PD-1+ tumors

Expression of immune checkpoint markers is regulated in a time-dependent manner and can lead to cells expressing multiple immune checkpoint markers such as LAG-3 and PD-1[156]. We investigated the association between tumors containing LAG-3+TILs, PD-1+TILs, and carcinoma cells expressing PD-L1.

As expected, immune checkpoint markers were significantly associated with each other **(Table 2.5)** and with total H&E stromal TIL levels (**Table 2.6**). 53% of PD-L1+tumors and 61% of tumors with PD-1+TILs were also positive for LAG-3+iTILs on equivalent-sized tissue microarray cores, whereas only 38% of tumors with CD8+iTILs were co-infiltrated with LAG-3+TILs. The percentage of PD-L1+tumors infiltrated with PD-1+TILs was similar to that of LAG-3+TILs but only ~20% of tumors with CD8+iTILs had carcinoma cells positive for PD-L1 (**Table 2.5**). Scatter plots relating the investigated biomarkers are presented in **Figure 2.4**

2.3.4 Exploratory survival analyses of concurrent tumor infiltration with LAG-3+ and CD8+T cells

Given that LAG-3 can be expressed on different lymphocyte subsets (CD8 or CD4)[168], we investigated the association between the presence of cytotoxic CD8+iTILs and the prognostic value of LAG-3+iTILs. In the absence of CD8+iTILs, with relatively few cases positive for LAG-3, we found that the presence of LAG-3+iTILs was no longer associated with survival among ER negative breast cancer patients **(Figure 2.5A**). In contrast, concurrent infiltration of LAG-3+iTILs and CD8+iTILs was significantly associated with improved survival, suggesting an important role of CD8+TILs expressing LAG-3 in breast cancer. Furthermore, we observed similar findings with concurrent infiltration of PD-1+iTILs and CD8+iTILs **(Figure 2.5B**; LAG-3 and PD-1 co-infiltration shown in **Figure 2.6**). Surprisingly, in ER negative breast cancer patients with no detectable CD8+iTILs per 0.3mm^2 core, the presence of PD-L1+ carcinoma cells was associated with a trend for poor BCSS, whereas patients with both CD8+iTILs and PD-L1+ carcinoma cells had significantly improved BCSS **(Figure 2.5C**).

2.4 Discussion

In a large set of breast cancer patients, we report on the presence of an immune checkpoint biomarker targetable with new drugs. We found that LAG-3+TILs can be scored quantitatively by immunohistochemistry on tissue microarrays with consistent results supporting its analytical validity as a biomarker. By this methodology, LAG-3+TILs were observed in a limited subset of patients (11%) that mostly fall into the HER2E and basal-like breast cancer subtypes and is a favorable prognostic factor in ER negative breast cancers. The presence of

immune infiltrates most prominently in ER negative breast cancers, detectable with lymphocyte biomarker assays, is now supported by a large body of evidence [70].

In contrast, LAG-3+iTILs were not prognostic in ER+ patients. This finding may not be surprising as ER+ breast cancers appear generally to be less immunogenic and have lower levels of TILs than ER negative patients [70]. In the FinHER trial, the presence of TILs was not associated with survival in early stage ER+/HER2– breast cancer patients [80], and in a combined analysis of two French Phase III clinical trials TILs were only prognostic in triple negative and HER2 positive patients [83].

High pretreatment serum levels of soluble LAG-3 have been associated with improved survival among ER+ breast cancer patients [211]. Soluble LAG-3 represents a splice variant with activating functions when bound to major histocompatibility complex II protein expressed on dendritic cells [134]. By contrast, our study measured the expression of LAG-3 on TILs in breast carcinoma tissues, and agrees with a recently published smaller study that found a subset of triple negative breast cancers had concurrent infiltration of LAG-3+/PD-1+ TILs and that this was associated with a (non-significant) trend for improved survival [163].

In pre-clinical studies, LAG-3 expressing CD8+TILs are exhausted and do not function properly, whereas LAG-3 expressing CD4+ regulatory T cells exhibit an enhanced immune suppressive function, supporting a hypothesis that the presence of LAG-3+TILs in cancer patients should lead to poor survival. Instead, our results suggest that the presence of LAG-3 expressing TILs may in fact indicate that there is an ongoing cancer-immune interaction, a phenotype that is described as an inflamed tumor [212] and usually implies an improved prognosis. Indeed, we found that >50% of breast cancers that are PD-L1+ or are infiltrated with PD-1+TILs have concurrent infiltration of LAG-3+TILs.

In the training set where H&E sTILs counts were available, we found that high levels of H&E sTILs (>50%, a level termed "lymphocyte predominant breast cancer" or LPBC) correlated with increased co-infiltration of LAG-3+/PD-1+ TILs. H&E sTILs are prognostic in ER- breast cancers and can be predictive of response to trastuzumab in HER2+ patients [80,213]; emerging evidence also suggests TIL count may predict response to anti-CTLA4 (ipilimumab) and anti-PD-1(pembrolizumab) [214,215]. TIL counts performed on H&E sections have the advantage of being applicable to existing slide sets or incident cases without requiring new immunohistochemical assays. However, this method necessarily combines all lymphocytes – including activating, suppressing and anergic populations, as well as NK and B cells. Theoretically, direct assessment of LAG-3 should be more likely to predict response to LAG-3-targeted checkpoint inhibitors; our study is a first step in defining an assessment method and a description of expression patterns over a large number of cases with detailed follow-up. The tissue microarray format limits the capacity to directly compare with standardized H&E TIL scores [74], and an assessment of the predictive capacity of LAG-3 in breast cancer will of course require application to randomized clinical trials.

The clinical activity of immune checkpoint inhibitors as single agents in breast cancer appears limited based on recent and varying results. In the KEYNOTE-012 trial of 32 women with advanced triple negative breast cancer (TNBC) and ≥1% PD-L1 expression treated with pembrolizumab (a PD-1 inhibitor), the response rate was 18.5% [205], with the median duration of response not yet reached at study publication. In a more recent presentation of 115 metastatic TNBC patients treated with atezolizumab (a PD-L1 inhibitor), a 10% overall response rate was seen irrespective of PD-L1 status, with most of this activity in the 1st line setting[216]. The median progression free survival was 1.4 months, but in those patients who achieved a response, the

median duration of response was 21.1 months. Of note, in the exploratory biomarker analyses, there was a suggestion for better clinical outcomes in those tumors with higher levels of CD8+ T cell infiltrates. Lastly in a phase Ib study of previously taxane / anthracycline-treated, advanced breast cancer (*N*=168) treated with avelumab (a PD-L1 inhibitor), the response rate was only 4.8% in the overall population, and 8.6% in the TNBC cohort[217].

It seems clear that the majority of advanced breast cancers do not achieve a response to single agent immune checkpoint inhibition, although in the minority that do, the response appears relatively durable – as has been seen in other malignancies treated with these agents. The results of our study suggest considering stratification of patients in these clinical trials for both PD-1/PD-L1 status and LAG-3 status. As the field is now studying combinations of immune checkpoint inhibitors, our results raise the question whether the cohort of tumors with co-expression of PD-1/PD-L1 and LAG-3+iTILs should be excluded from these trials as the natural history of this cohort is relatively favorable. However, this could be due to the effects of adjuvant therapy that may have reinvigorated a de *novo* immune response.

Although this study has major strengths, such as the use of analytically validated antibodies and multiple, large, well-annotated sets of breast cancer specimens, it also has some limitations. While long term follow-up is a strength, the study cohort does date from a time prior to use of HER2 targeted therapies or taxanes, which may affect generalization to contemporary patients. The breast cancer specimens used in the study were retrospectively collected and assembled into TMAs and as such, the area of the tumor analyzed reflects only a minute sampling of the original tumor tissue. In addition, co-infiltration of immune subsets (LAG-3+, PD-1+, CD8+) had to be inferred from results of individually-stained tissue sections and therefore cannot directly assess co-expression of immune checkpoints on the same cell.

In conclusion, LAG-3 is an immune checkpoint marker targeted by emerging treatments and is most commonly expressed among ER- breast cancer patients – including in one third of basal-like breast cancers, an aggressive subtype where checkpoint inhibitors have great promise and potential. Although our study does not directly measure biomarker expression in the metastatic setting, the strong association between tumors positive for PD-1/PD-L1+ and LAG-3+ biomarkers suggests a potential for the combination of therapies targeting these immune checkpoint markers, a concept currently being evaluated in clinical trials in metastatic disease [218].

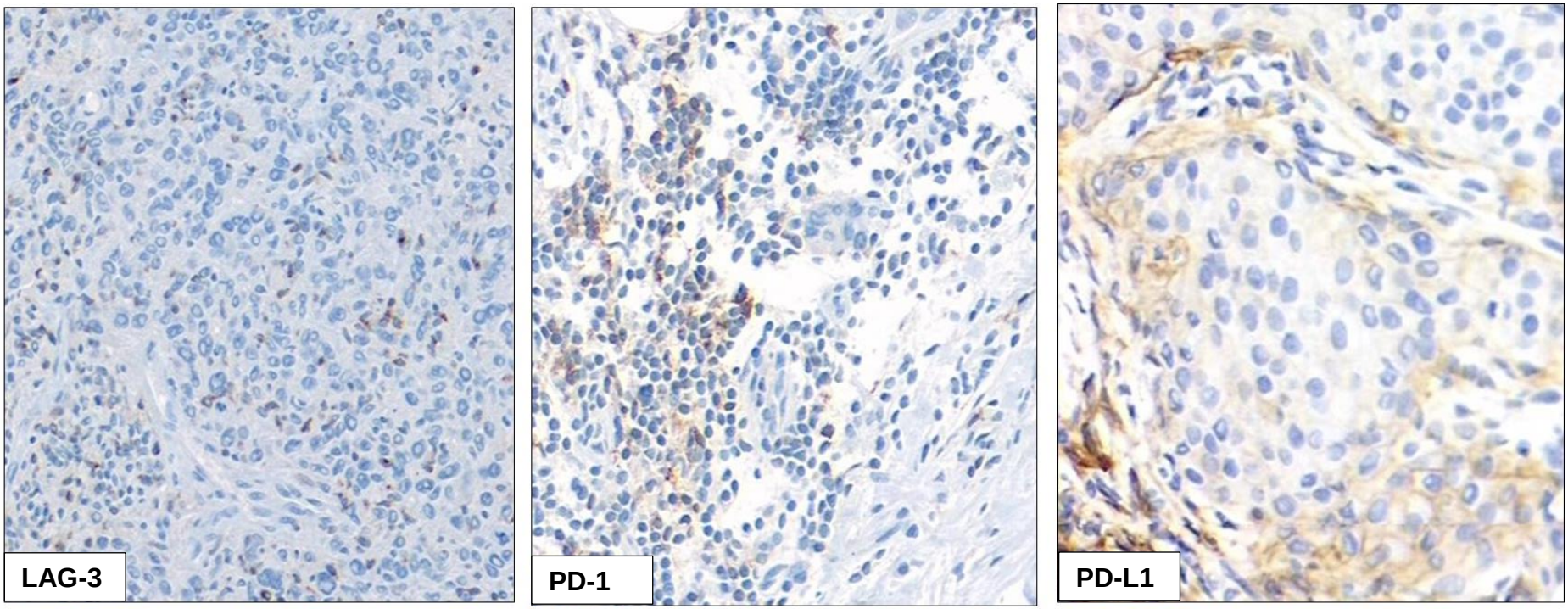

Figure 2.1 Representative immunohistochemical staining of LAG-3, PD-1, and PD-L1 in breast tumor tissue microarray cores
Brown staining on intra-epithelial and stromal tumor-infiltrating lymphocytes can be observed for LAG-3 and PD-1 micrographs whereas PD-L1 staining can mainly be observed on carcinoma cell membranes. Micrographs were taken under X20 objective magnification.

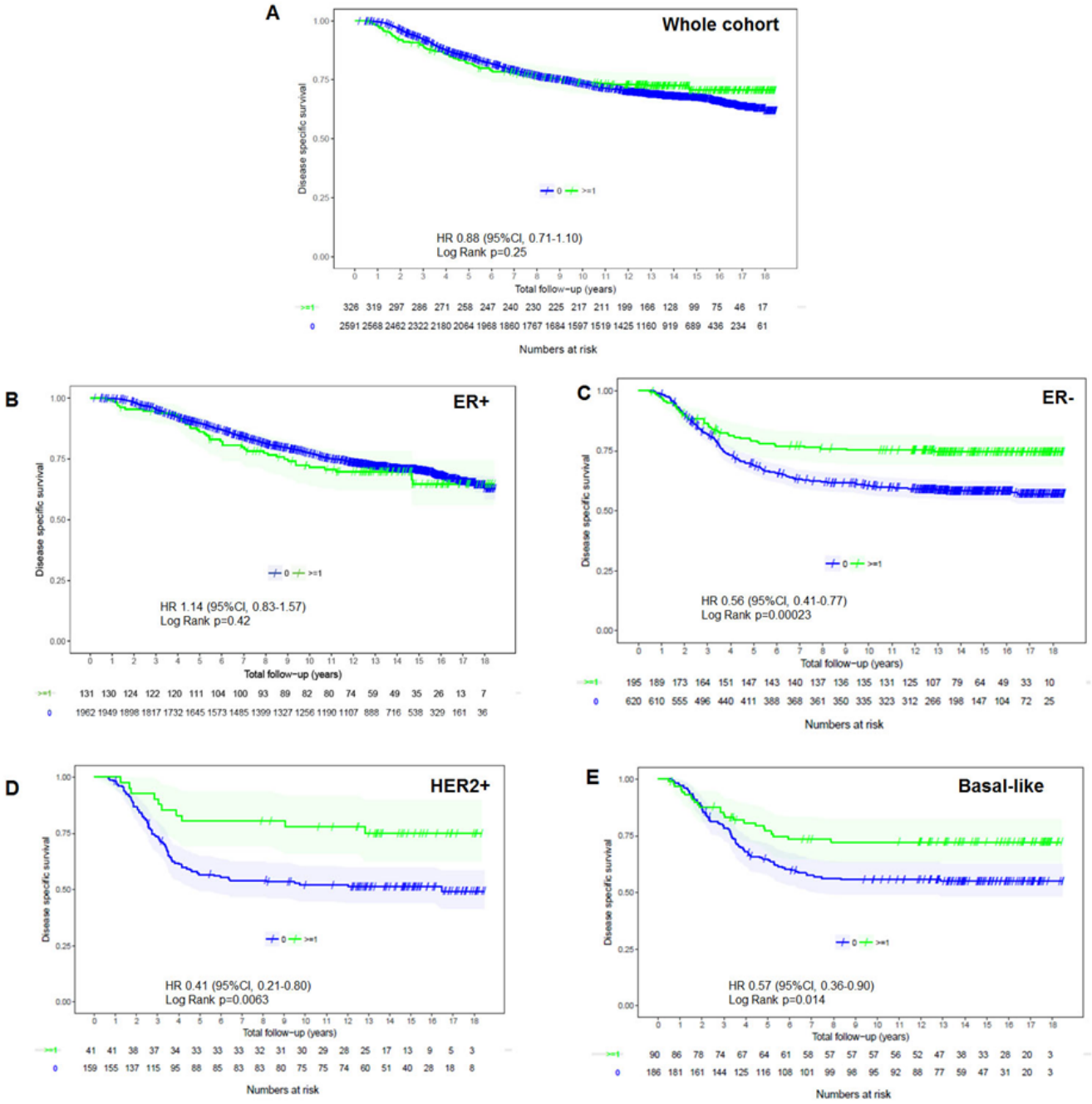

Figure 2.2 LAG-3+iTILs association with breast cancer-specific survival.
(A) whole cohort, **(B)** ER+, **(C)** ER–, **(D)** HER2E and **(E)** Basal-like.

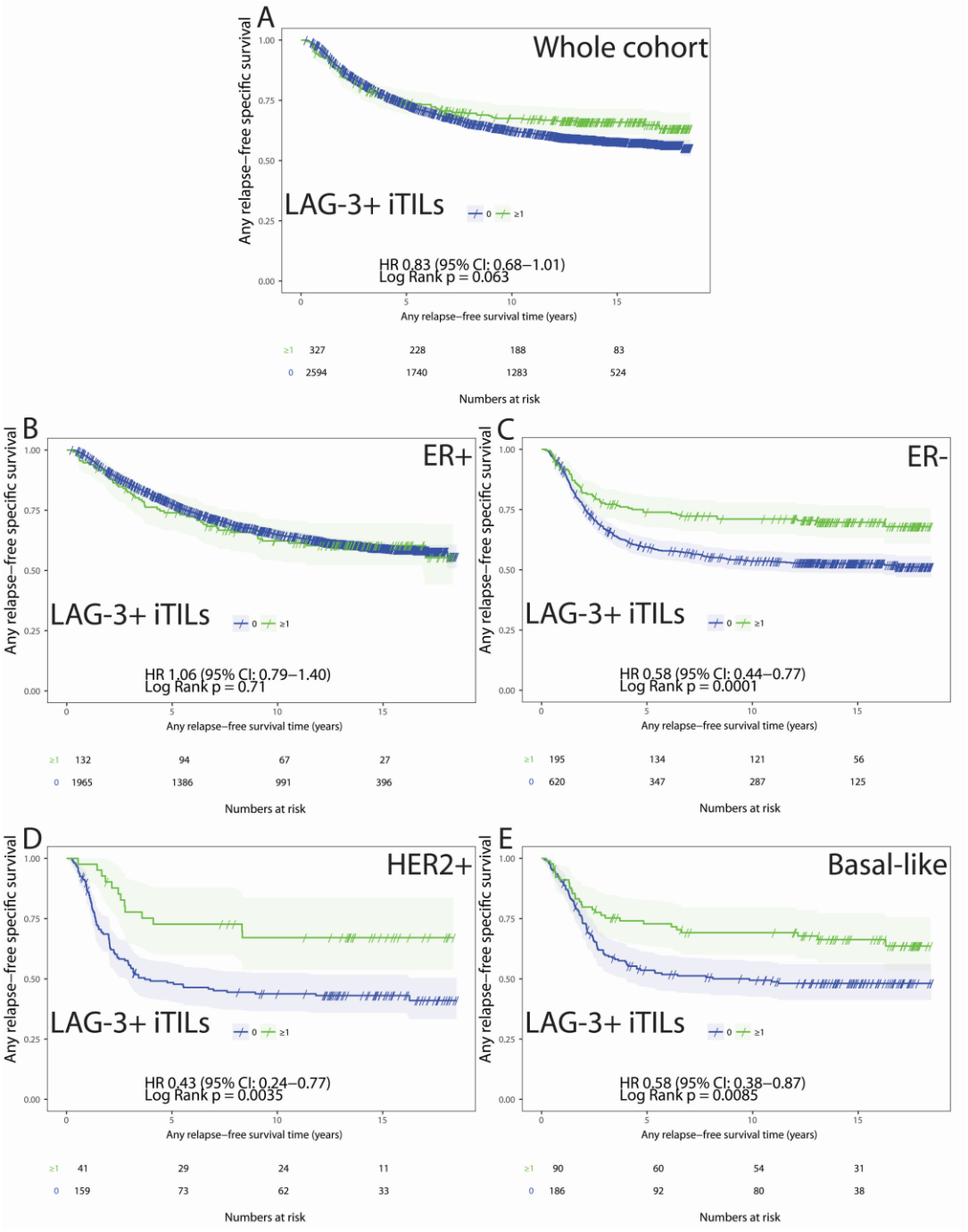

Figure 2.3 Association with relapse-free survival for LAG-3+ intra-epithelial tumor-infiltrating lymphocytes.
Association with relapse-free survival for LAG-3+iTILs. **(A)** Whole cohort, **(B)** ER+, **(C)** ER–, **(D)** HER2E and **(E)** Basal-like.

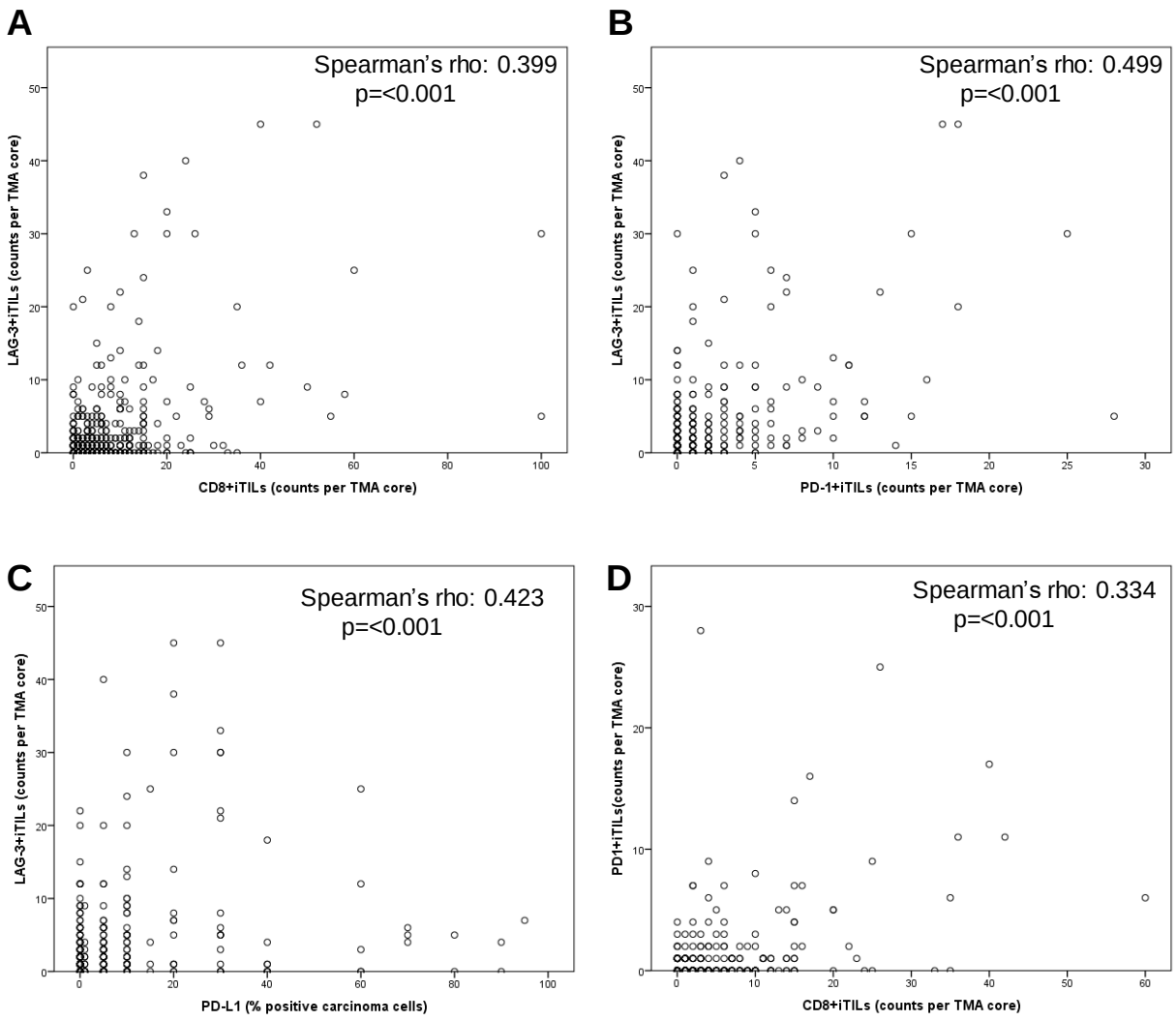

Figure 2.4 Correlation between LAG-3, PD-1, PD-L1 and CD8 scores.
Scatter plots with spearman's rho correlation coefficient and p values for each pair of immune markers. **A**, LAG-3+iTILs and CD8+iTILs; **B**, LAG-3+iTILs and PD-1+iTILs; **C**, LAG-3+iTILs and PD-L1+ carcinoma cells; **D**, PD-1+iTILs and CD8+iTILs

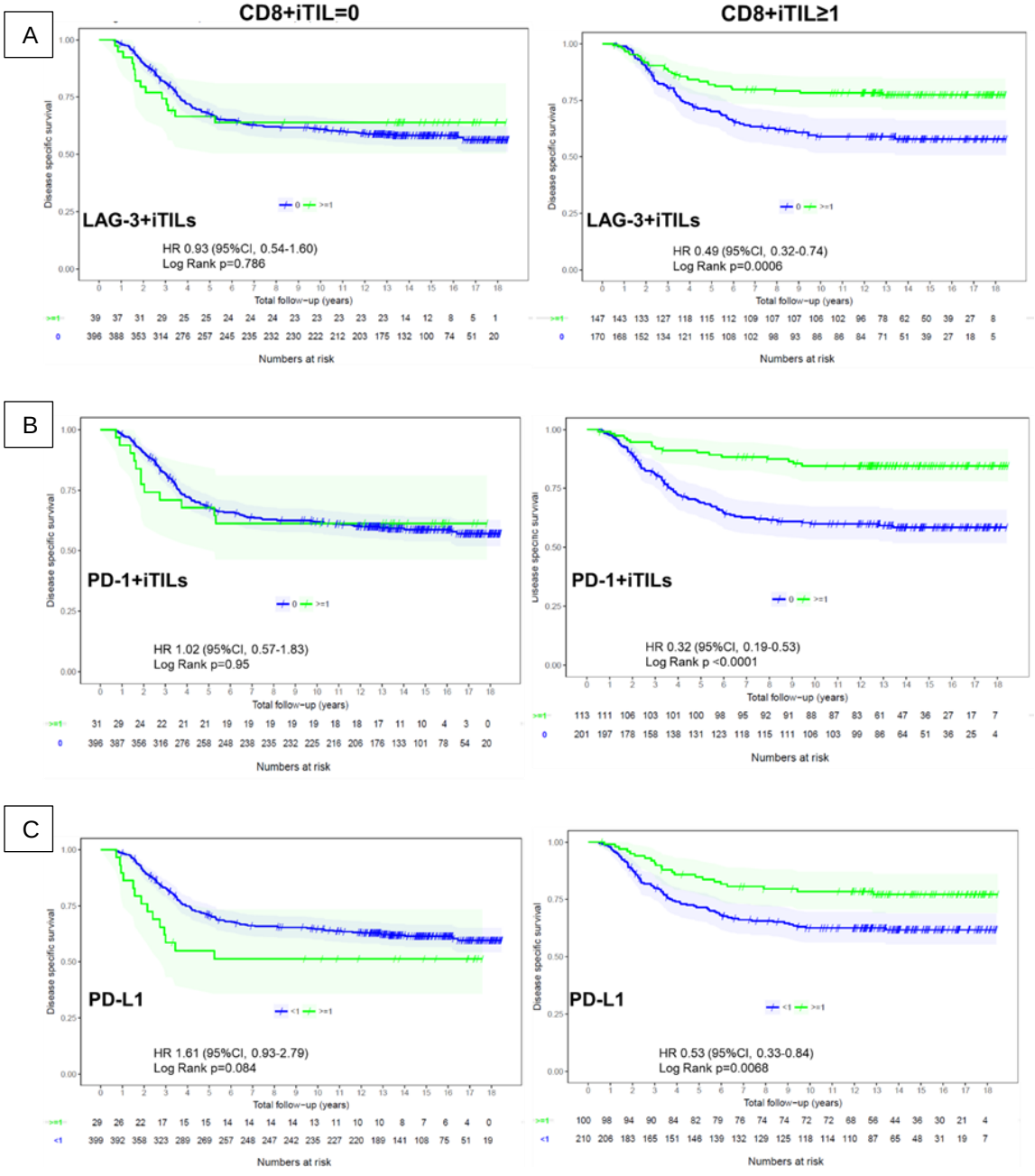

Figure 2.5 Association between CD8+iTILs and the prognostic value of immune checkpoint markers.

Breast cancer-specific survival Kaplan-Meier curves of patients in the whole validation set stratified by the presence of immune checkpoint markers **(A)** LAG-3, **(B)** PD-1, **(C)** PD-L1 in the absence (Left panel) or presence (Right panel) of concurrent CD8+iTILs.

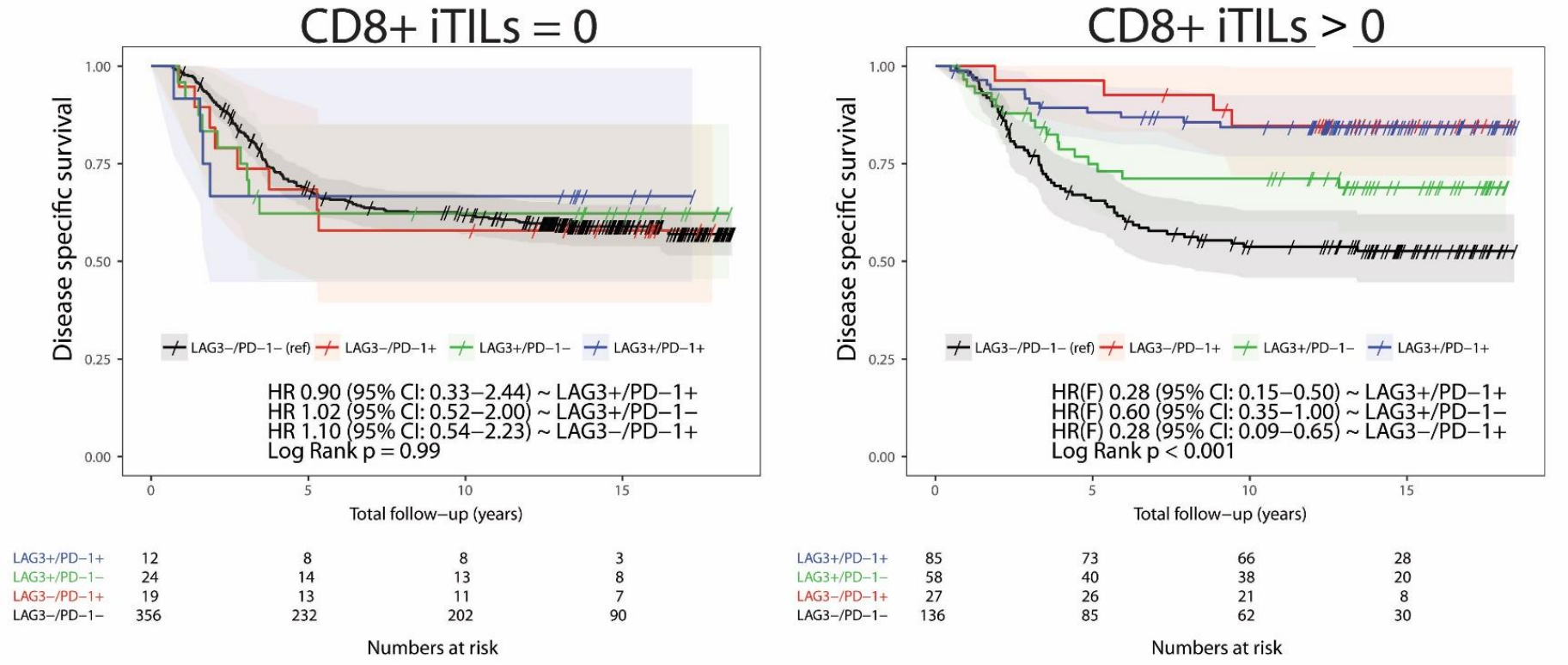

Figure 2.6 Association with breast cancer-specific survival for LAG-3+/PD-1+ intra-epithelial tumor-infiltrating lymphocytes in the presence or absence of CD8+ intra-epithelial tumor-infiltrating lymphocytes among ER negative patients.

Table 2.1 Association of LAG-3+intra-epithelial and stromal tumor-infiltrating lymphocytes with clinicopathological parameters in the training set

	Training set (*N*=278)					
Parameters	**Negative** *N*=240	**LAG-3+iTILs ≥1** *N*=38 (14%)	***P* value***	**Negative** *N* =235	**LAG-3+sTILs ≥1** *N* =43 (15%)	***P* value***
Age at diagnosis (year)			0.47			0.61
<50	90	17(16%)		89	18 (17%)	
≥50	150	21(12%)		146	25 (15%)	
Tumor size (cm)			0.05			0.24
≤2	143	16 (10%)		138	21 (13%)	
>2	97	22 (19%)		97	22 (18%)	
Grade			<0.001			<0.001
1&2	157	6 (4%)		155	8 (5%)	
3	81	32 (28%)		78	35 (31%)	
Unknown	2	-				
ER			<0.001			<0.001
Negative	36	23 (39%)		37	22 (37%)	
Positive	202	15 (7%)		196	21 (10%)	
Unknown	2	-		5	-	
PR			<0.001			<0.001
Negative	66	26		66	26 (28%)	
Positive	171	12		166	17 (9%)	
Unknown	3	-		3	-	
Ki67			<0.001			<0.001
<14%	149	8		144	13 (8%)	
≥14%	86	30		86	30 (26%)	
Unknown	5	-		5	-	
Subtypes			<0.001			<0.001
Luminal A	135	6 (4%)		131	10 (7%)	
Luminal B	56	7 (11%)		53	10 (16%)	
HER2E	7	4 (36%)		7	4 (36%)	
Basal-like	14	11 (44%)		16	9 (36%)	
NOS	3	0		3	0	
Unknown	25	10		25	10	

*****Fisher's exact tests were computed for 2x2 association. Association between subtypes and TIM-3+TILs was analyzed by Chi square test

Table 2.2 Association of LAG-3+ intra-epithelial tumor-infiltrating lymphocytes and clinicopathological parameters.

	Validation set (*N* =2921)		
Parameters	**Negative**	**LAG-3+iTILs ≥1**	
	N=2594	*N*=327 (11%)	*P* value*
Age at diagnosis (years)			<0.001
<50	719	131(15%)	
≥50	1875	196 (9%)	
Tumor size (cm)			<0.001
≤2	1371	139 (9%)	
>2	1211	186 (13%)	
Grade			<0.001
1&2	1206	60 (5%)	
3	1283	255 (17%)	
Unknown	105	12	
Ki67			<0.001
negative	1386	66 (4%)	
positive (≥14%)	989	237 (19%)	
Unknown	219	24	
ER			<0.001
Negative	620	195 (24%)	
Positive (>1%)	1965	132 (6%)	
Unknown	9	0	
PR			<0.001
Negative	1094	234 (18%)	
Positive (>1%)	1354	84 (6%)	
Unknown	146	9	
Subtypes			<0.001
Luminal A	1144	38 (3%)	
Luminal B	744	95 (11%)	
HER2E	159	41 (20%)	
Basal-like	186	90 (33%)	
NOS	-	-	
Unknown	224	13	

*Chi square p value

Table 2.3 Differences in survival by LAG-3 expression and breast cancer subtypes, as assessed by interaction test

Survival endpoint	Interaction test *P* value*
Breast cancer-specific survival	0.002
Relapse free survival	0.004

*interaction test was conducted using the likelihood ratio test to assess the interaction between a cox regression model with and without the LAG-3 x breast cancer subtype (luminal vs non-luminal) interaction term.

Table 2.4 Multivariate analyses of LAG-3+iTILs in the whole cohort and among ER- patients for breast cancer-specific survival.
A), only clinico-pathological parameters and LAG-3+iTILs as covariates, and B), clinico-pathological parameters and all immune biomarkers as co-variates.

A)

Whole cohort (# of events/n: 805/2702**)**				**Among ER- (# of events/n:** 283/764**)**	
		Hazard Ratio for BCSS (95% CI)	**LRT *P*-value**	**Hazard Ratio for BCSS (95% CI)**	**LRT *P*-value**
Age at diagnosis (Reference group:<50)	≥50	1.00 (0.87-1.16)	0.96	1.04 (0.82-1.32)	0.75
Tumor grade (Reference group: grade 1-2)	Grade 3	1.83 (1.57-2.13)	<0.0001	1.96 (1.42-2.72)	<0.0001
Tumor size (Reference group: ≤2cm)	>2	1.70 (1.47-1.97)	<0.0001	1.54 (1.19-200)	<0.0001
Lymphovascular invasion status (Reference group: negative)	Positive	1.32 (1.12-1.56)	0.0007	1.45 (1.09-1.93)	0.01
Nodal status (Reference group: negative)	Positive	2.00 (1.69-2.35)	<0.0001	2.21 (1.68-2.91)	<0.0001
LAG-3+iTILs (Reference group: 0)	≥1	0.71 (0.56-0.90)	0.003	0.50 (0.36-0.69)	<0.0001

B)

Whole cohort (# of events/n: 697/2384**)**				**Among ER- (# of events/n:** 224/634**)**	
		Hazard Ratio for BCSS (95% CI)	**LRT *P*-value**	**Hazard Ratio for BCSS (95% CI)**	**LRT *P*-value**
Age at diagnosis (Reference group:<50)	≥50	0.99 (0.85-1.16)	0.92	0.97 (0.75-1.27)	0.85
Tumor grade (Reference group: grade 1-2)	Grade 3	1.89 (1.61-2.23)	<0.0001	2.10 (1.45-3.05)	<0.0001
Tumor size (Reference group: ≤2cm)	>2	1.61 (1.38-1.89)	<0.0001	1.43 (1.08-1.91)	0.012
Lymphovascular invasion status (Reference group: negative)	Positive	1.36 (1.14-1.63)	0.00063	1.41 (1.02-1.95)	0.035
Nodal status (Reference group: negative)	Positive	1.95 (1.63-2.32)	<0.0001	2.20 (1.61-3.01)	<0.0001
CD8+iTILs (Reference group: 0)	≥1	0.98 (0.83-1.16)	0.84	1.04 (0.76-1.42)	0.81
PD-1+iTILs (Reference group: 0)	≥1	0.65 (0.47-0.91)	0.0082	0.50 (0.32-0.80)	0.002
PD-L1 (Reference group: <1)	≥1%	0.80 (0.58-1.10)	0.16	0.81 (0.52-1.28)	0.36
LAG-3+iTILs (Reference group: 0)	≥1	0.95 (0.71-1.28)	0.75	0.73 (0.49-1.09)	0.12

BCSS: Breast cancer-specific survival, LRT: Likelihood ratio test

Table 2.5 Associations among immune response biomarkers in breast cancer patients

Immune markers	**LAG3+iTILs=0**	**LAG-3+iTILs Positive (≥1)**	***P*-value *(χ2)***
PD-L1*			
Negative	2306	189 (7.6%)	<0.0001
Positive (≥1%)	109	**125 (53.4%)**	
PD-1+iTILs*			
Negative	2382	170 (6.6%)	<0.0001
Positive (≥1)	97	**147 (60.7%)**	
CD8+iTILs*			
Negative	1775	69 (4%)	<0.0001
Positive (≥1)	693	245 (26%)	
	PD-1+iTILs=0	**PD-1+iTILs Positive (≥1)**	
PD-L1			
Negative	2332	151 (6.1%)	<0.0001
Positive (≥1%)	141	**89 (38.6%)**	
CD8+iTILs			
Negative	1785	63 (3.4 %)	<0.0001
Positive (≥1)	762	178 (18.9 %)	
	PD-L1=0	**PD-L1 Positive (≥1%)**	
CD8+iTILs			
Negative	1793	62 (3.3%)	<0.0001
Positive (≥1)	763	174 (18.6%)	

*Frequency in the whole cohort: **PD-L1 ≥1%**= 241/2918 (8.3%); **PD-1+iTILs ≥1** = 246/2908 (8.5%); **CD8+iTILs ≥1**=1089/3403 (32%)

Table 2.6 Association of hematoxylin and eosin-stained (H&E) stromal TILs with PD-1+, LAG-3+, and PD-1+/LAG-3+ concurrent infiltration.

	H&E sTILs categories*			
	Low (<10% sTILs)	**Intermediate (≥10%- 50% sTILs)**	**High (LPBC) (>50% sTILs)**	**Total**
	n (%)	**n (%)**	**n (%)**	
PD-1+iTILs(≥1)	34/225 (15%)	24/59 (41%)	9/10 (90%)	n=67
LAG-3+iTILs(≥1)	11/205 (5%)	23/57 (40%)	4/9 (44%)	n=38
PD1+/LAG3+**	8/197 (4%)	14/54 (26%)	4/9 (44%)	n=26

Abbreviations: sTILs: stromal tumor infiltrating lymphocytes; LPBC: lymphocyte predominant breast cancer.
* sTILs were assessed on the training set by the method of Salgado R et al.[74]
**Concurrent infiltration of PD-1+iTILs and LAG-3+iTILs in TMA cores.

Chapter 3: TIM-3 expression in breast cancer

SYNOPSIS

Upregulation of additional immune checkpoint markers is one mechanism of resistance to current inhibitors that might be amenable to targeting with newer agents. T-cell Immunoglobulin and Mucin domain-containing molecule 3 (TIM-3) is an immune checkpoint receptor that is an emerging target for cancer immunotherapy. In this chapter, I investigated TIM-3 immunohistochemical expression in 3,992 breast cancer specimens assembled into tissue microarrays, linked to detailed outcome, clinico-pathological parameters and biomarkers including CD8, PD-1, PD-L1 and LAG-3.

We found that breast cancer patients with TIM-3+ intra-epithelial tumor-infiltrating lymphocytes (iTILs) (≥1) represented a minority of cases (11%), with a predilection for basal-like breast cancers (among which 28% had TIM-3+iTILs). The presence of TIM-3+iTILs highly correlated with hematoxylin and eosin-stained stromal TILs and with other immune checkpoint markers (PD-1+iTILs, LAG-3+iTILs and PD-L1+ tumors). In prognostic analyses, early breast cancer patients with TIM-3+iTILs had significantly improved breast cancer-specific survival. In multivariate analyses, the presence of TIM-3+iTILs was an independent favorable prognostic factor in the whole cohort as well as among ER negative patients. This study supports TIM-3 as a target for breast cancer immunotherapy.

3.1 Introduction

The presence of small round dark mononuclear cells characteristic of tumor-infiltrating lymphocytes (TILs) on hematoxylin and eosin (H&E) - stained breast cancer specimens has garnered increased attention with the emergence of immune checkpoint inhibitors and has led to a

re-examination of the role of the immune system in breast tumors. Accumulating evidence shows that the presence of an immune response in breast cancers correlates with estrogen receptor negative (ER-) subtypes (i.e. the HER2 and basal-like intrinsic subtypes) among whom there is an association with favorable outcomes [79-81]. In contrast, the more common ER+ breast cancer subtypes rarely display such heightened immune responses, which when present are associated with unfavorable prognosis[78,219,220].

Immune checkpoint inhibitors targeting cytotoxic T-Lymphocyte-associated antigen 4 (CTLA-4), programmed cell death-1 (PD-1) or its ligand (PDL-1) perform best in immunogenic cancers such as melanoma and non-small cell lung cancer[138,221], but responses have recently been reported in triple negative / basal-like breast cancers[205,222,223] (for reviews see refs. [224,225]). However, even among such potentially immunogenic cancers, immune checkpoint inhibitors benefit only a relatively small number of patients[138,224,226-230]. As resistance may be due to the activation of alternative checkpoint pathways, additional immune checkpoint targets have become a subject of active research, including the T-cell Immunoglobulin and Mucin-domain- containing molecule 3 (TIM-3)[155].

TIM-3 is an immune receptor discovered in 2002 that is expressed on a variety of immune cells including dendritic cells, macrophages, and T cells[172,231,232]. TIM-3 mediates its suppressive activity on immune cells via its ligands that include phosphatidylserine, CEACAM-1 and the widely expressed ligand galectin-9 [180,233]. TIM-3 is expressed on activated T cells and its signaling on cytotoxic T cells leads to an exhausted phenotype, characterized by a reduction in proliferation, decreased production of effector cytokines and apoptosis of effector T cells[234]. In addition, TIM-3+ TILs can co-express PD-1, with blockade of both receptors leading to a more pronounced tumor regression than either agent alone, at least in pre-clinical studies [188,196].

Multiple studies have now reported on the presence of TIM-3+TILs in human tumors[194,235-238]. However, in breast cancer, TIM-3+TILs have been evaluated by immunohistochemistry in a limited number of patients, with one recent study reporting positive associations with lymph node metastases[239,240]. The objective of our study is to evaluate the expression of TIM-3 on TILs in a large series of breast cancers powered for multivariate correlation with clinico-pathological parameters, survival, and other important immune biomarkers.

3.2 Material and methods

3.2.1 Study cohorts

The study cohorts were the same as in **Chapter 2**. The initial set consisting of 330 breast cancer patients was used to finalize biomarker staining and interpretation conditions for an initial analysis of TIM-3. These patients were diagnosed with invasive breast cancer at University of British Columbia hospitals between 1989 and 2002 and have been previously described[206]. A detailed description of the validation set consisting of 3,992 breast cancer patients has been previously published[107,241]. In brief, newly diagnosed invasive breast cancers from centres across the province of British Columbia performing breast cancer excision surgery, referred to the British Columbia cancer agency between 1986 and 1992 and for which both blocks from a central estrogen receptor testing laboratory and detailed de-identified clinico-pathologic, treatment and outcome data collected by the British Columbia cancer agency breast cancer outcomes unit were available were assembled into 17 single core tissue microarray blocks. None of these patients (training and validation cohorts) received neoadjuvant treatment**.** The median follow-up for both cohorts is 12.6 years. The Clinical Research Ethics Board of the University of British Columbia and the British

Columbia Cancer Agency Breast Cancer Outcomes Unit approved the access to the samples and corresponding de-identified outcome data.

3.2.2 Immunohistochemistry and scoring

Tissue microarrays (TMAs) were built from formalin-fixed paraffin-embedded primary excision specimens from patients in the training and validation cohorts and represented as 0.6mm cores across 3 blocks for the training cohort and 17 blocks for the validation cohort. These TMAs have been previously stained and scored for multiple biomarkers including ER, PR, HER2, Ki67, EGFR, CK5/6, CD8, LAG-3, PD-1 and PD-L1[242]. Breast cancer intrinsic subtypes were previously determined from both cohorts by immunohistochemistry (IHC) benchmarked against a gene expression gold standard (the PAM50 intrinsic subtype classifier) [208] . Briefly, ER+ (≥1%) or PR+ (≥1%), HER2– (including IHC 2+ cases that were HER2– by fluorescence in situ hybridization) and low (<14%) Ki67 were defined as Luminal A; hormone receptor positive cases which were also either HER2+ or had high Ki67 were defined as Luminal B; HER2+/ER–/PR– cases were defined as HER2E, and triple negative cases that were positive for EGFR+ or CK5/6+ were defined as basal-like.

Overall stromal TILs were scored on H&E-scanned images of the TMA cores using the assessment recommendations of the International TILs Working Group[74], whereby stromal TILs are scored as the percentage of intertumoral stromal surface area (i.e. excluding areas occupied by carcinoma cells) containing mononuclear lymphocytic infiltrates.

TIM-3 immunohistochemistry was conducted with anti-TIM-3 rabbit monoclonal antibody clone D5D5R from Cell Signaling (Cat# 45208) as employed in other publications [231,239,243,244], here using a Ventana Ultra automated stainer (Ventana Medical Systems) in concordance with manufacturer's protocol. In brief, slides underwent antigen retrieval with Standard Cell

Conditioning 1 reagent (Ventana Medical Systems) followed by 60 minutes of primary antibody incubation (applied at 1:50 dilution) with no heat, and visualized using a chromoMap DAB detection kit (Ventana Medical Systems). Membranous staining in tonsil tissue served as a positive control in each staining run. TIM-3+ lymphocytes scores were reported as absolute counts per TMA core for intra-epithelial or stromal locations. TIM-3+ intra-epithelial lymphocytes (TIM-3+iTILs) were defined as TIM-3+ lymphocytes located within carcinoma nests whereas TIM-3+ stromal lymphocytes (TIM-3+sTILs) were those not in direct contact with the carcinoma nest.

3.2.3 Statistical analysis

IBM SPSS software (version 24.0) and R (version 3.3.2) were used to conduct all the statistical analyses. TIM-3+ iTILs scores were dichotomized ≥1 (as positive) vs. 0 (as negative). In addition, TIM-3 expression on other immune cells (non-lymphocytes) was assessed, but as only 1% of cases were positive on the training set this staining pattern was not further analyzed.

For prognostic analyses, the primary end-point, breast cancer-specific survival, was defined as the time from date of diagnosis to date of death attributed to breast cancer. Patients were censored at death from another cause or if alive at end of follow-up. Relapse-free survival and overall survival were secondary end-points. Relapse-free survival was defined as time from date of diagnosis to date of any type of breast cancer relapse (local, regional, distant, or contralateral) and overall survival as time from date of diagnosis to date of death, irrespective of the cause of death. In addition, patients were censored if they had not died from breast cancer or if they had not relapsed at the end of follow-up time for relapse-free survival analyses. Correlation with survival was conducted using Kaplan-Meier curves, log-rank test and Cox regression models. Proportional hazard assumptions were assessed by visual examinations of Kaplan-Meier plots. In the case where the proportional hazard assumption was violated (for the basal-like subgroup, beyond 5 years), the

follow-up time and hazard ratios were modified accordingly in the multivariate Cox regression model. The effect size was adjusted in multivariate Cox regression models by taking into account significant clinicopathological parameters (age, tumor grade, tumor size, lymphovascular invasion and nodal status).

Clinico-pathological and prognostic associations for TIM-3+iTILs were analyzed first on the training cohort (n=330) and further tested on the validation cohort (n=3,992) in a pre-specified formal written statistical plan, presented at the British Columbia Cancer Agency Breast Cancer Outcomes Unit. Furthermore, half of the validation cohort served for a training and a validation approach specifically for correlations and combinatorial analyses among immune biomarkers (TIM-3, PD-L1, PD-1, LAG-3, CD8) due to the low number of positive cases observed in the training set. In addition, 40% of cases in the validation cohort were considered TIM-3+sTIL positive based on a ≥1 positive TIL cut-point. A cut-point of ≥2 positive TILs for TIM-3+sTILs, representing 20% of cases, was selected following testing of various cut-points (≥1, ≥2) based on the distribution on half of the validation cohort set in prognostic analyses. In these cases, a pre-specified written statistical plan for validation on the other half of the set was presented prior to statistical analyses (see **Appendix C**). Prognostic analyses of co-infiltrated immune checkpoint markers were nevertheless considered exploratory. All statistical tests performed were two-sided at α=0.05.

3.3 Results

3.3.1 Distribution of TIM-3+TILs in breast cancers

To define staining conditions and interpretation, we conducted an initial evaluation of TIM-3 staining and correlation with clinico-pathological parameters on a tissue microarray

consisting of 330 breast cancer patients (representing a training set). We observed 12% of breast cancer cases with TIM-3+ intratumoral tumor infiltrating lymphocytes (≥1 iTIL per 0.6 mm diameter core) whereas stromal TIM-3+sTILs (≥1) were present in 48% of cases (Results for TIM-3+iTILs shown in **Table 3.1**). We then proceeded with TIM-3 staining on a TMA comprising an independent cohort of 3,992 breast cancer cases, of which 3,148 cases were interpretable for TIM-3 immunohistochemistry staining **(Figure 3.1**). The results were consistent with the training set as 11% of cases had ≥1 TIM-3+ iTILs and 40% of cases had ≥1 TIM-3+ sTILs (**Figure 3.2**). TIM-3 expression on macrophages was only observed in 1% of cases and was not analyzed further.

As there were a large number of cases with TIM-3+sTILs, a cut-off for dichotomization of ≥2 sTIL/0.6 mm core, a level reached in 20% of breast cancers, was selected based on analyses of Kaplan Meier curves of different TIM-3+sTILs cut points (as described in Methods: Statistics). However, TIM-3+iTILs were selected as the primary analysis parameter, to allow comparison with previously published immune biomarkers in this breast cancer cohort[96,242] .

3.3.2 The presence of TIM-3+iTILs in breast cancer is associated with unfavorable clinico-pathological factors

Consistent with the results in the initial cohort of 330 patients, breast cancer cases with TIM-3+iTILs in the validation cohort were significantly associated with younger age at presentation, higher grade, hormone receptor (ER/PR) negativity, and high Ki67 proliferation index [defined as ≥14%] (**Table 3.2**). In addition, the presence of TIM-3+iTILs was much more common in the basal-like subtype relative to other subtypes (28% in basal-like vs 6% in luminal A). The results for TIM-3+sTILs reflected similar associations with clinico-pathological parameters to TIM-3+iTILs findings (**Table 3.3**).

3.3.3 TIM-3+iTILs correlate with the presence of other immune checkpoint markers (LAG-3, PD-1, PD-L1) and overall H&E sTILs

Because this large cohort had been previously assessed for key immune biomarkers including PD-1, PD-L1 and LAG-3, we were able to analyze their correlations with TIM-3. In addition, we scored overall H&E stromal TILs to allow a parallel evaluation with immune checkpoint markers.

We found that breast tumors with TIM-3+iTILs were highly significantly associated with the presence of additional immune checkpoint markers **(Table 3.4).** Indeed, nearly half of breast cancers that were positive for PD-L1 or PD-1+iTILs or LAG-3+iTILs were also infiltrated with TIM-3+iTILs in the same 0.6 mm TMA core. However, only 3% (91/2736 interpretable cases) expressed all three immune checkpoint markers (TIM-3+/PD-1+/LAG-3+) **(Table 3.4)** when assessed by this method. No particularly unique association pattern was observed between the presence of TIM-3+iTILs and any of the other individual immune checkpoint markers tested, suggesting that the TIM-3 checkpoint expression on TILs occurs in tumors containing T cells positive for other exhausted markers. Furthermore, we found that all immune checkpoint markers correlated positively ($p<0.001$) with H&E sTILs (**Figure 3.3**). In this cohort, less than 1% of cases were categorized as lymphocyte-predominant breast cancer (LPBC, defined as ≥50% H&E sTILs).

3.3.4 TIM-3+iTILs are associated with good prognosis in early breast cancer

In univariate analyses, the presence of TIM-3+iTILs in early breast tumors was associated with improved breast cancer-specific survival (BCSS) in the whole cohort (HR: 0.76, 95%CI 0.61-0.96, Log Rank p=0.02) **(Figure 3.4)**. When breast cancer subtypes were stratified in the analysis, only HER2+ and basal-like breast cancer patients with TIM-3+iTILs displayed

significantly improved BCSS (HER2+: HR: 0.27, 95%CI 0.10-0.72, Log Rank p=0.005; Basal-like: HR: 0.48, 95%CI 0.29-0.78, Log Rank p=0.003) **(Figure 3.4**). These results were similar using overall survival and relapse-free survival secondary endpoints (**Figure 3.5** for overall survival; **Figure 3.6** for relapse-free survival). In contrast, the presence of TIM-3+sTILs had a trend for favorable prognosis for BCSS and relapse-free survival and reached significance in the whole cohort for overall survival (**Figure 3.7** for BCSS; **Figure 3.8** for overall survival and **Figure 3.9** for relapse-free survival).

In multivariate analyses that included H&E sTILs as a covariate, the presence of TIM-3+iTILs remained a favorable prognostic factor in the whole cohort and among ER- breast cancer patients **(Table 3.5 –** Whole cohort: HR: 0.64, 95%CI 0.48-0.85, p=0.001; ER-: HR: 0.58, 95%CI 0.39-0.86, p=0.004, Basal-like: HR: 0.58, 95%CI 0.32-1.03, p=0.052). Similar findings were observed for TIM-3+sTILs albeit not reaching significance for basal-like breast cancer patients (**Table 3.6**). We also found that ER- breast cancer patients with tumors that were co-infiltrated with TIM-3+, PD-1+ and LAG-3+ TILs had a significant improved breast cancer specific survival, in univariate and multivariate analyses, relative to patients with a single positive, dual positive, or complete absence of these three immune checkpoint markers (**Figure 3.10, Table 3.7**).

3.4 Discussion

We report the first study of TIM-3 expression in a large (>1000 case) series of early breast cancers. TIM-3 expression in this cohort was restricted to tumor-infiltrating lymphocytes and was present in about 12% of cases when 0.6 mm cores were evaluated for expression on intra-epithelial TILs, or 20% of cases when assessed on stromal TILs. The presence of TIM-3+iTILs was

associated with younger age, high grade and high Ki67 proliferation index and was enriched in the basal-like breast cancer subtype. Moreover, TIM-3+iTILs highly correlated with co-infiltration of additional immune checkpoint markers PD-L1 (on carcinoma cells), PD-1 and LAG-3+ (on TILs). In prognostic analyses, early breast cancer patients with TIM-3+ iTILs had significantly improved survival for all assessed endpoints, as compared to patients whose tumors lacked TIM-3+iTILs. In multivariate analyses, the prognostic effect was maintained in the whole cohort as well as among ER- and basal-like breast cancer patients.

Studies from our group and from others have been consistent in finding that the presence of immune checkpoint markers on intra-epithelial TILs in breast tumors is an uncommon event, and mostly restricted to ER- breast cancers[163,239,242]. However, TILs positive for immune checkpoint markers are able to discriminate breast cancer patients with favorable survival, consistent with an active anticancer immune microenvironment. Indeed, we found that breast tumors infiltrated with TIM-3+iTILs highly correlate with tumors positive for other checkpoint markers (PD-1, PD-L1 and LAG-3). Results are consistent with other reported studies and imply that the expression of multiple different immune checkpoints can occur during tumor progression, reflecting an ongoing battle between cancer cells and the immune system[212,245]. In our cohort, coexpression of TIM-3 with PD-1 and LAG-3 is associated with a particularly favorable prognosis, perhaps reflecting an underlying robust immune recognition of the cancer cells that is difficult for the tumor to evade. Furthermore, other studies have reported TIM-3 expression on carcinoma cells to be associated with poor prognosis (for meta-analysis see ref. [246]), which we did not observe in our large breast cancer cohort. These apparently conflicting results may be due to the different types of tumor and possible confounding by stage or other factors, as the smaller studies in other tumors were not powered for multivariate analyses.

Strengths of our study include the use of a large cohort of early breast cancer patients, treated consistently according to provincial guidelines, linked to detailed long-term outcome data and assessed using a training and validation approach to biomarker interpretation. Some limitations include, first, the necessity in such a large series to rely on TMA cores, representing a 0.28 mm^2 surface area sampling of a tumor for assessment of the tumor immune microenvironment. Second, infiltration of TILs bearing multiple immune biomarkers could only be inferred from single stains and therefore does not directly identify co-expression on the same lymphocyte. Third, breast cancer patients in the cohort received what would now be considered older treatments (predating trastuzumab, taxanes and aromatase inhibitors) which may affect extrapolation of some of the observed prognostic and predictive associations to more contemporary treatment regimens.

Accumulating evidence suggests resistance to anti- CTLA-4 or anti- PD-1/PD-L1 inhibitors can occur in otherwise immunogenic cancers through compensatory upregulation of additional immune checkpoints[170,245]. TIM-3 has recently emerged as a target for cancer immunotherapy following pre-clinical studies suggesting its non-redundant functions in comparison to the better-characterized checkpoint markers PD-1/PD-L1, and efficacious treatment synergy when TIM-3 is targeted in combination with anti-PD1/PDL1 antibodies[188,196,197,202]. Although ER- breast cancer, in particular basal and triple negative breast cancer, is considered the most immunogenic subtype, reports from immune checkpoint inhibitor clinical trials are not as encouraging. Early reports suggest metastatic breast cancer patients may benefit most from PD-1/PD-L1 blockade monotherapy in the first-line setting, or in combination with chemotherapy agents for second or third-line therapy with an objective response rate ranging from 10%-40% [205,222,223] (for review, see ref. [224]). The findings from our study imply that TIM-3 inhibitors could potentially help to treat PD-1 refractory or metastatic tumors. Currently, four early phase clinical

trials testing the efficacy of anti- TIM-3 in combination with anti- PD-1/PDL1 in advanced tumors have opened [NCT03066648, NCT02608268, NCT02817633, and NCT03099109]. Our data support that this appears to be a relevant combinatorial strategy to assess in breast cancer, particularly in patients with non-BRCA mutated basal-like tumors, an aggressive subtype for which targeted therapies are not currently available.

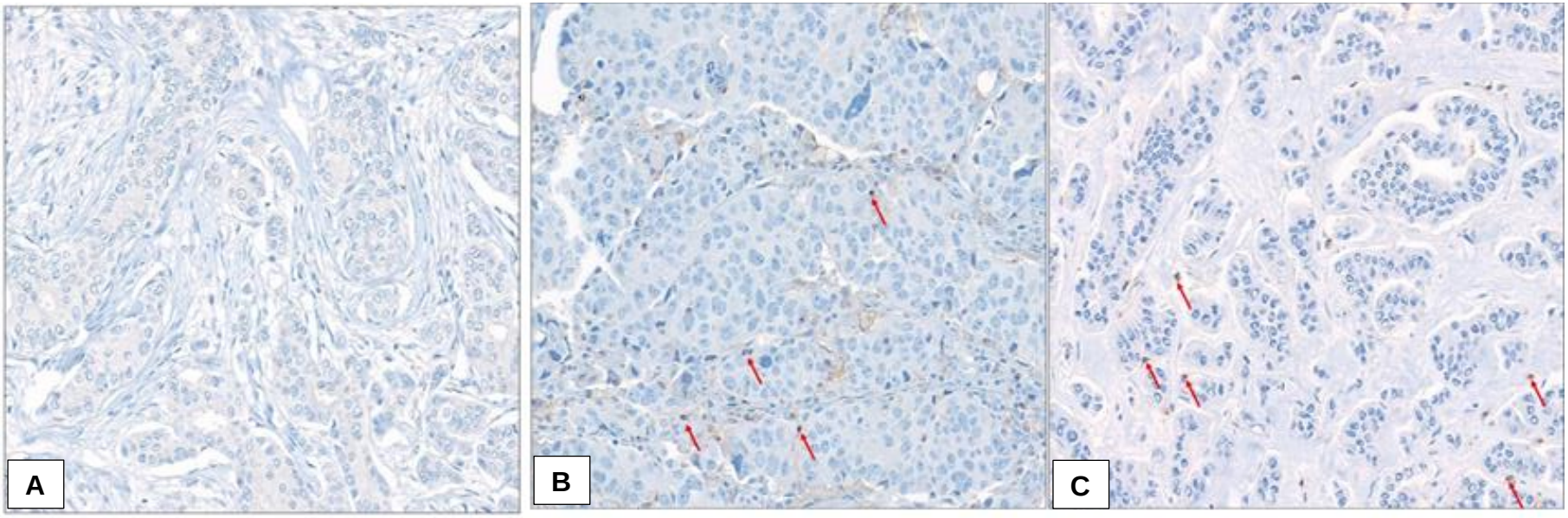

Figure 3.1TIM-3 staining in breast cancer patients
Representative images of TIM-3 immunohistochemistry staining on formalin-fixed paraffin-embedded breast cancer tissue microarray cores**. (A)** TIM-3 negative staining; **(B)** TIM-3+ intra-epithelial tumor-infiltrating lymphocytes; **(C)** TIM-3+ stromal tumor-infiltrating lymphocytes. Red arrows indicate positive TIM-3+ intra-epithelial (in **B**) or stromal (in **C**) tumor-infiltrating lymphocytes.

A

TIM-3+iTILs	Number of cases
0	2816
1	196
2	67
3	27
4	16
5	8
6	4
7	2
8	5
10	1
11	1
12	1
14	1
17	1
25	1
60	1

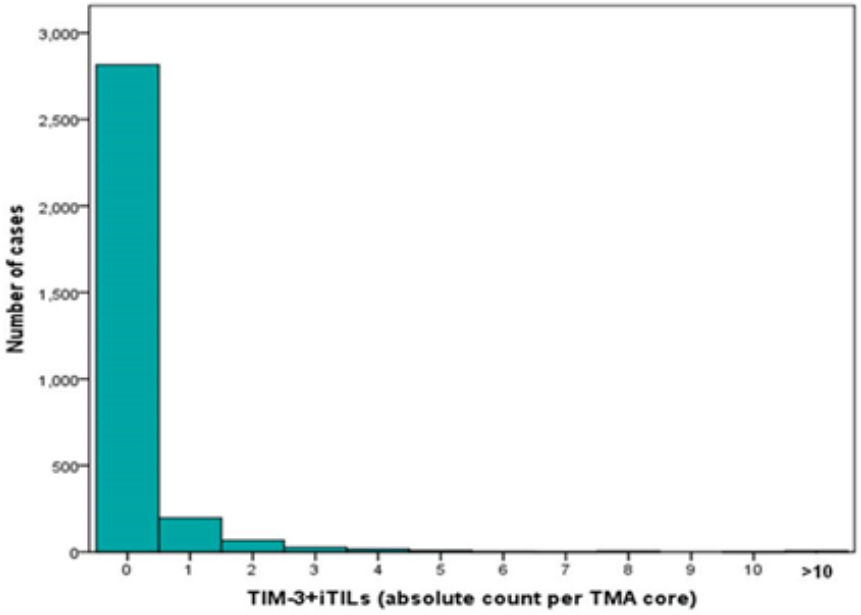

B

TIM-3+sTILs	Number of cases
0	1873
1	643
2	339
3	134
4	62
5	29
6	24
7	11
8	11
9	2
10	9
12	2
15	2
16	1
18	1
19	1
28	2
30	1
35	1

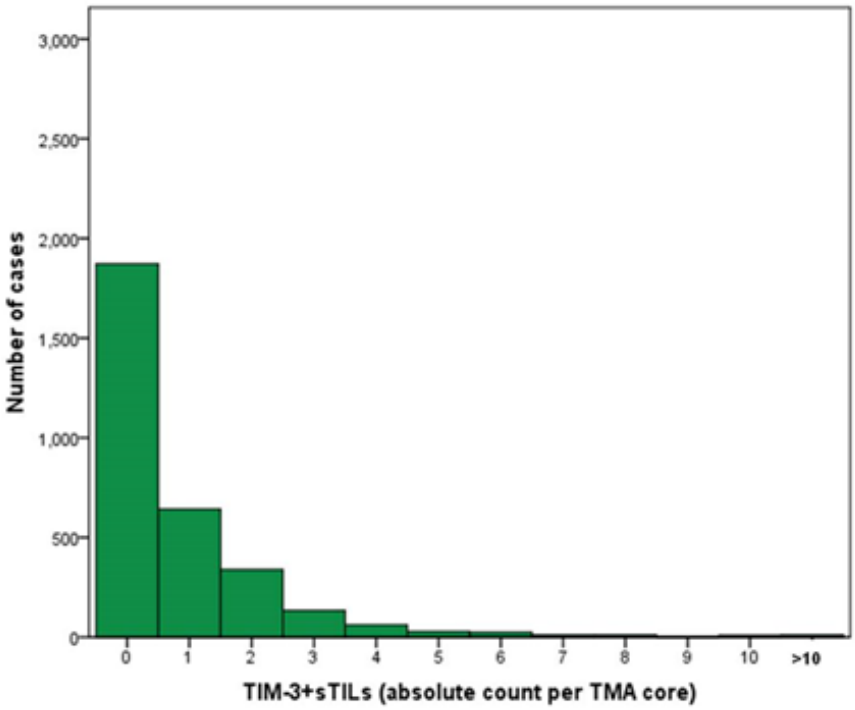

Figure 3.2 Distribution of TIM-3+ tumor-infiltrating lymphocytes in the whole (validation) cohort

Histograms illustrating the absolute count per TMA core for TIM-3+ intra-epithelial TILs **(A)** and stromal TILs **(B).** Scores were available for 3,148 cores for which immunohistochemistry staining was interpretable.

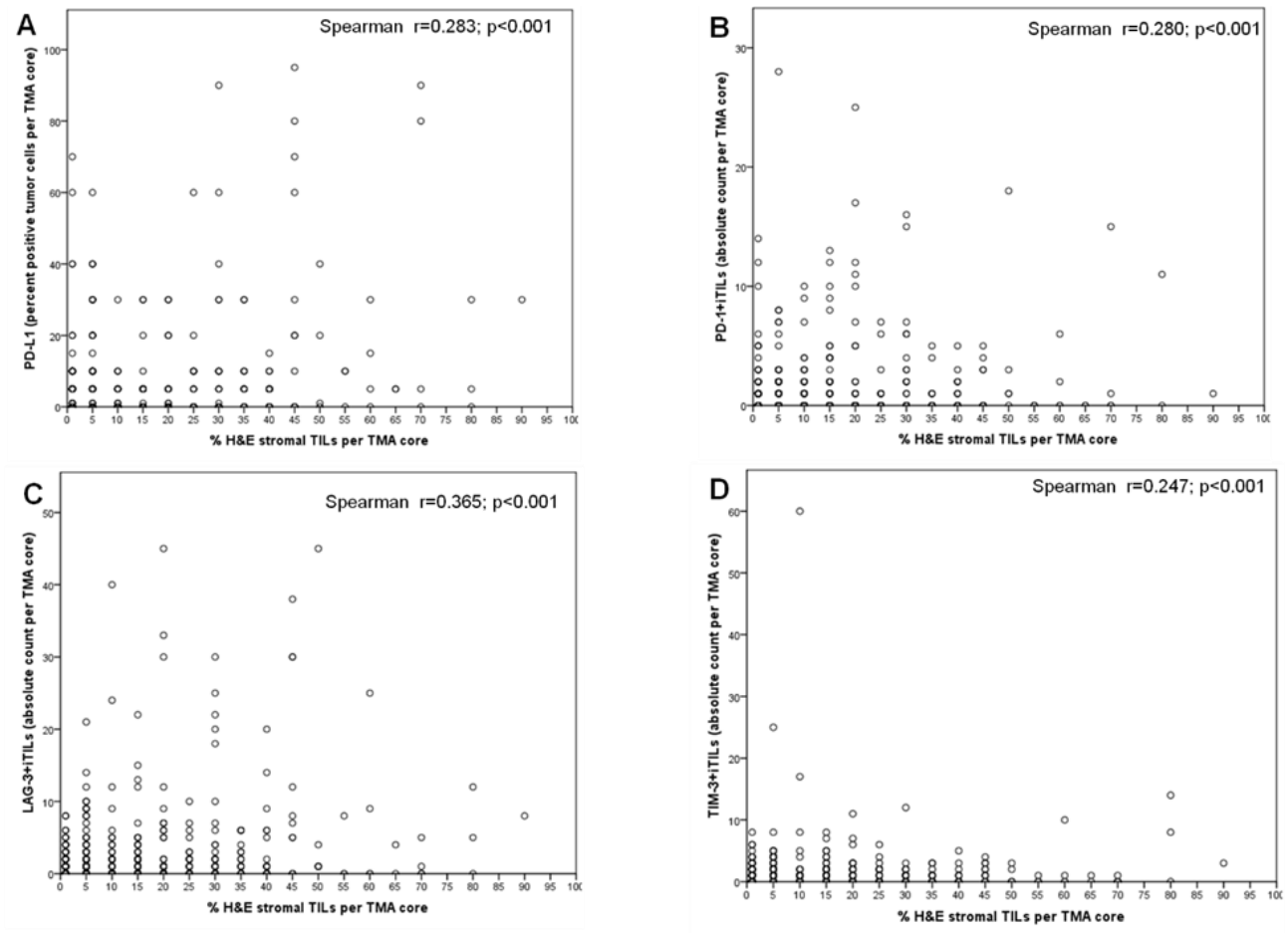

Figure 3.3 H&E sTIL correlation with immune biomarkers.
Scatter plots depicting the correlation between the percentage of H&E sTILs on the x-axis and immune biomarker scores (**A,** PD-L1; **B**, PD-1+iTILs; **C**, LAG-3+iTILs; **D**, TIM-3+iTILs) per TMA core on the y-axis, with the corresponding Spearman rho and p values.

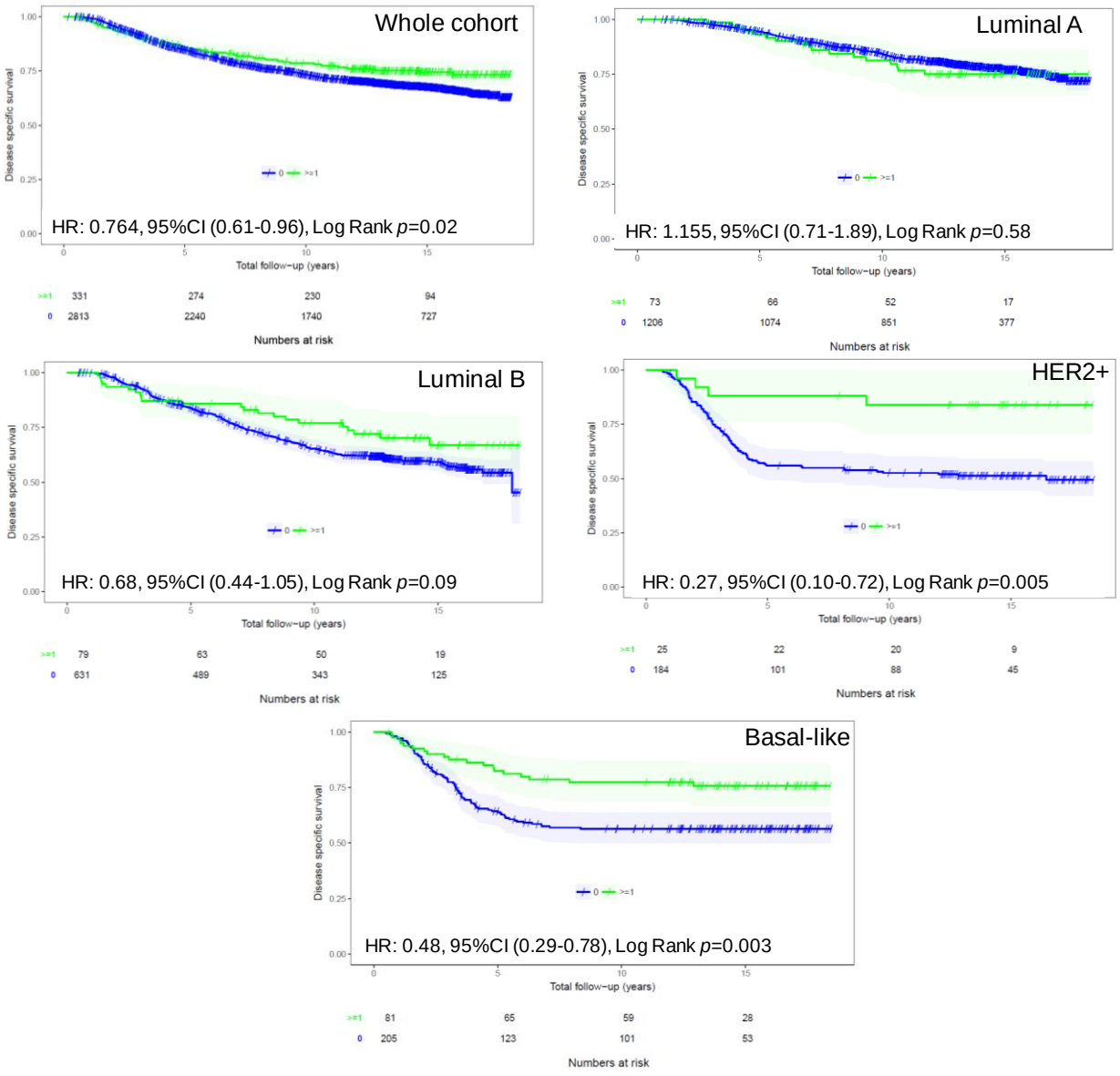

Figure 3.4 TIM-3+intra-epithelial tumor-infiltrating lymphocytes association with breast cancer-specific survival in the whole (validation) cohort and by breast cancer subtype. Kaplan Meier curves of breast cancer-specific survival in breast cancer patients stratified by the presence or absence of TIM-3+iTILs. Kaplan-Meier curves in **(A)** the whole cohort, **(B)** Luminal A cases, **(C)** Luminal B, **(D)** HER2+ and **(E)** basal-like cases are shown with their corresponding numbers of patients, events and log rank *p* values. The number of patients still at risk at the end of each 5 years of follow-up is shown at the bottom of each panel.

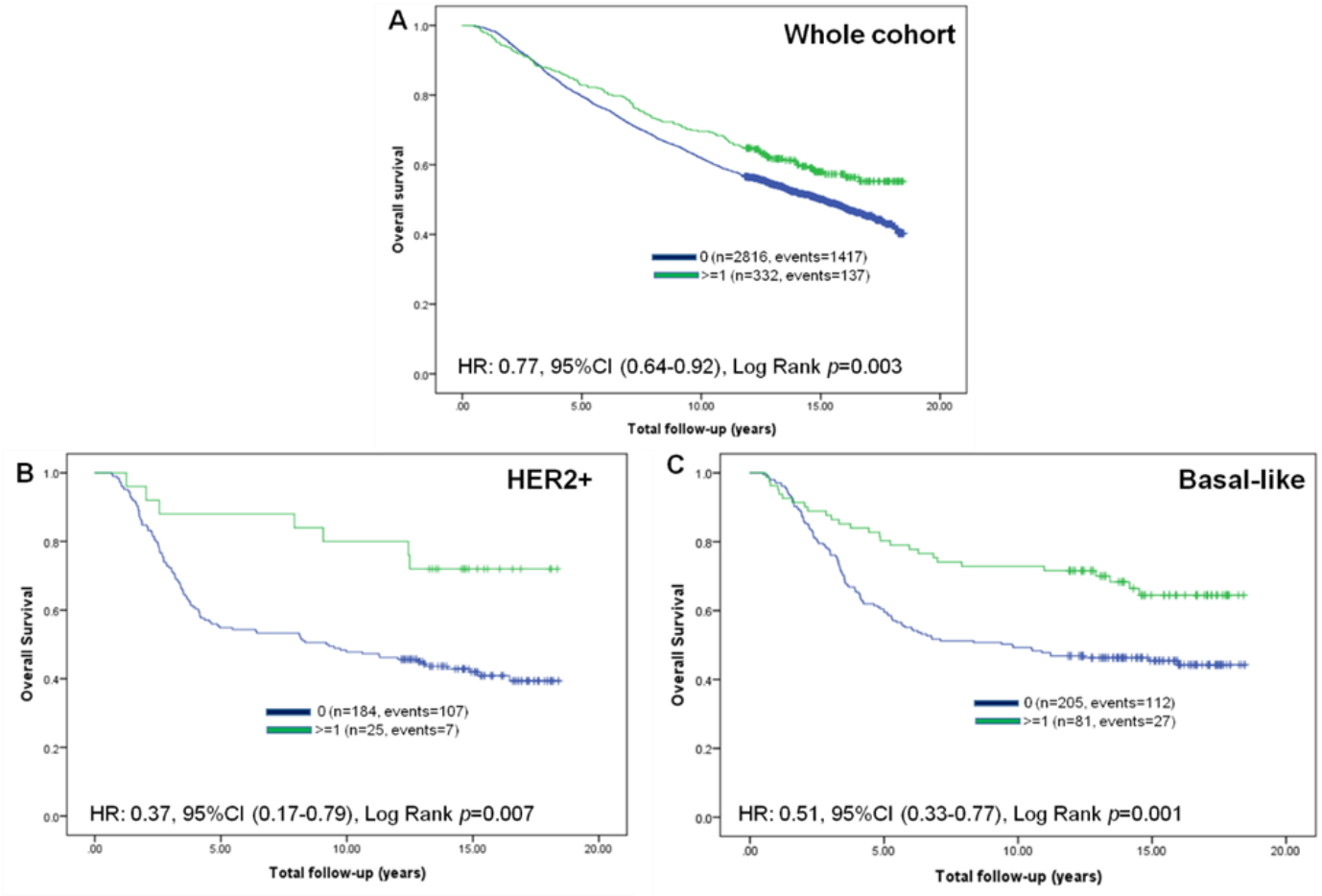

Figure 3.5 Overall survival for TIM-3+intra-epithelial tumor-infiltrating lymphocytes in the whole cohort, in HER2+ and basal-like breast cancer subtypes.
Kaplan Meier curves (KM) of overall survival in breast cancer patients stratified by the presence or absence of TIM-3+iTILs. KM curves in the whole cohort **(A),** HER2+ **(B)** and basal-like **(C)** are shown with corresponding number of patients, events and log rank p values.

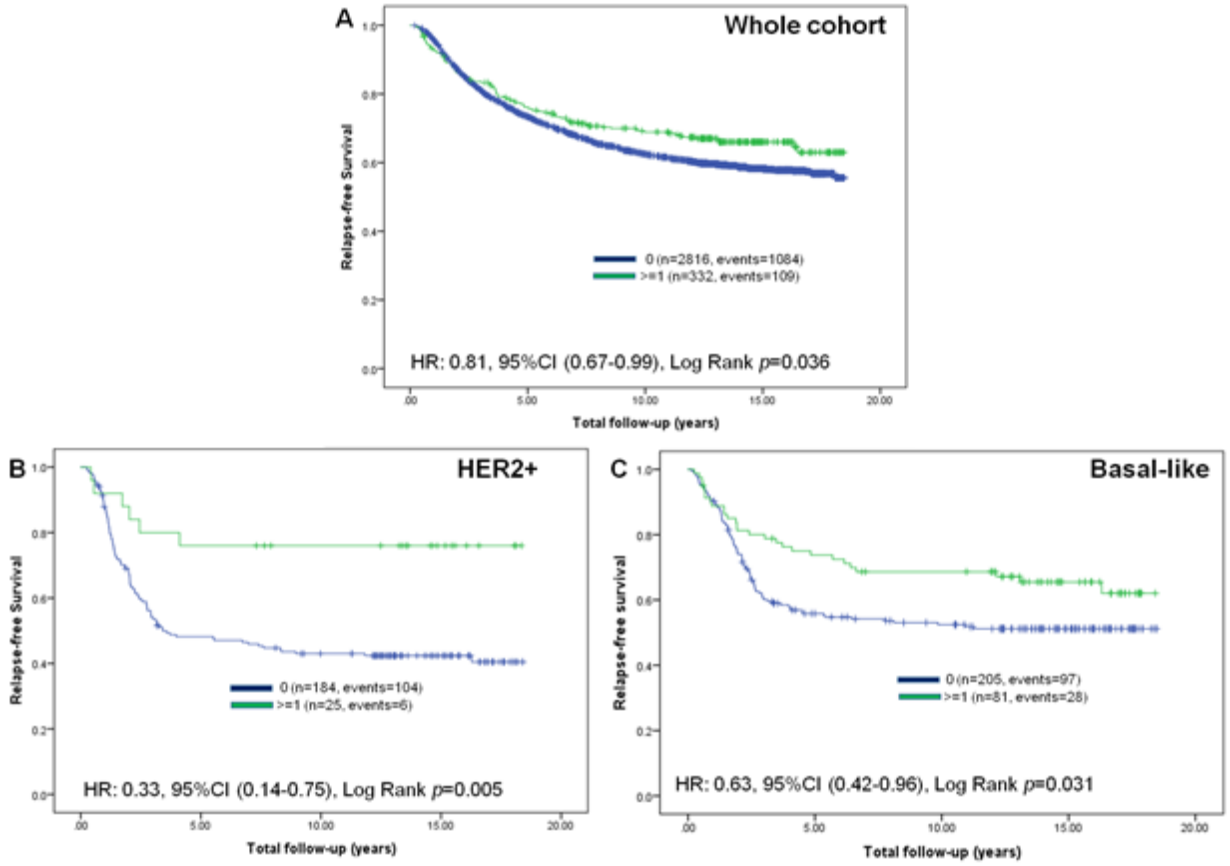

Figure 3.6 Relapse-free survival for TIM-3+ intra-epithelial tumor-infiltrating lymphocytes in the whole cohort, in HER2+ and basal-like breast cancer subtypes.
Kaplan Meier (KM) curves of relapse-free survival in breast cancer patients stratified by the presence or absence of TIM-3+iTILs. KM curves in the whole cohort **(A)**, HER2+ **(B)** and basal-like **(C)** are shown with corresponding number of patients, events and log rank *p* values.

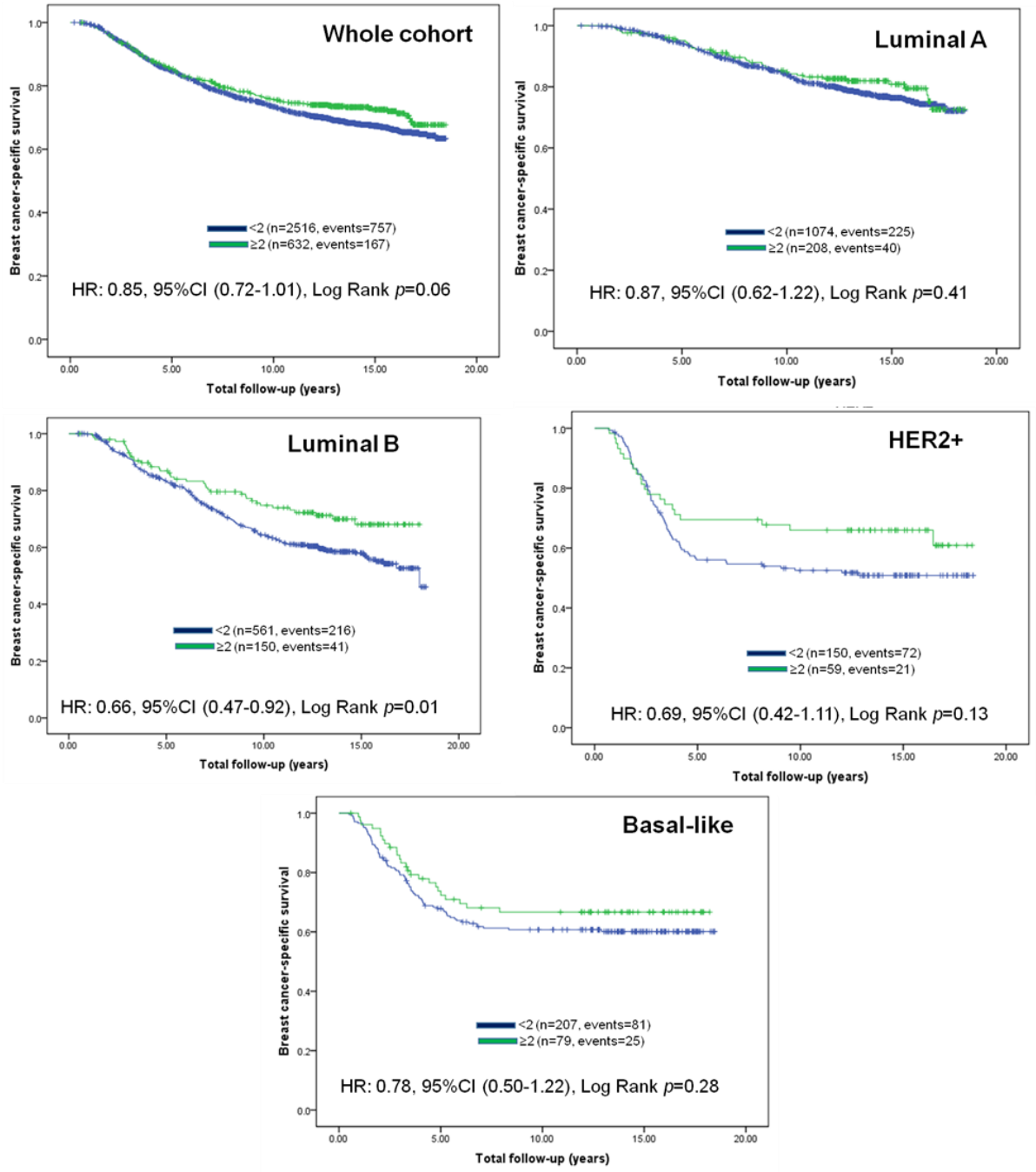

Figure 3.7 TIM-3+ stromal tumor-infiltrating lymphocytes association with breast cancer-specific survival in the whole cohort and by breast cancer subtype.
Kaplan Meier curves of breast cancer-specific survival in breast cancer patients stratified by the presence or absence of TIM-3+sTILs. KM curves in **(A)** the whole cohort, **(B)** Luminal A cases, **(C)** Luminal B, **(D)** HER2+ and **(E)** basal-like cases are shown with their corresponding numbers of patients, events, hazard ratios and log rank *p* values.

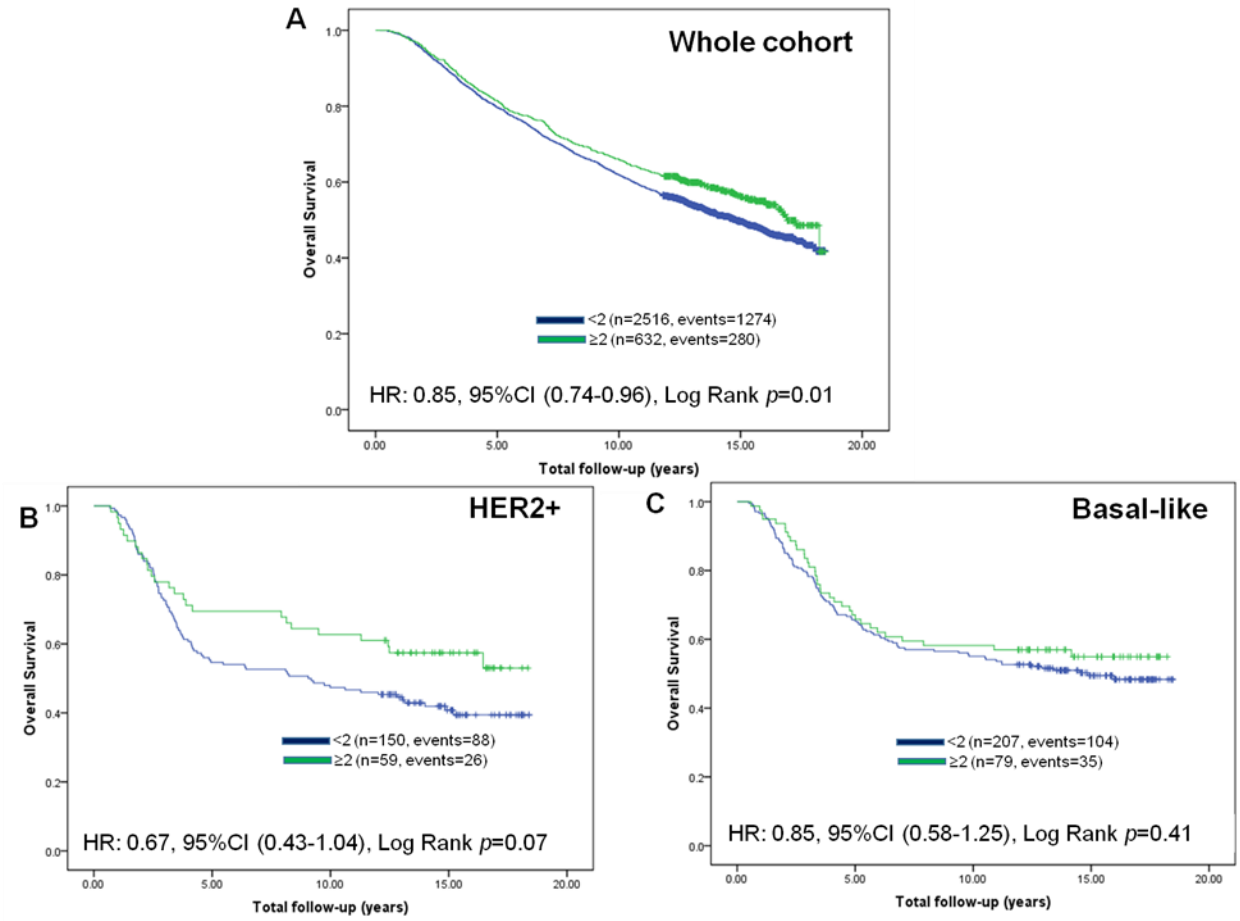

Figure 3.8 Overall survival for TIM-3+ stromal tumor-infiltrating lymphocytes in the whole cohort, in HER2+ and basal-like breast cancer subtypes.
Kaplan Meier curves (KM) of overall survival in breast cancer patients stratified by the presence or absence of TIM-3+sTILs. KM curves in the whole cohort **(A)**, HER2+ **(B)** and basal-like **(C)** are shown with corresponding numbers of patients, events, hazard ratios and log rank *p* values.

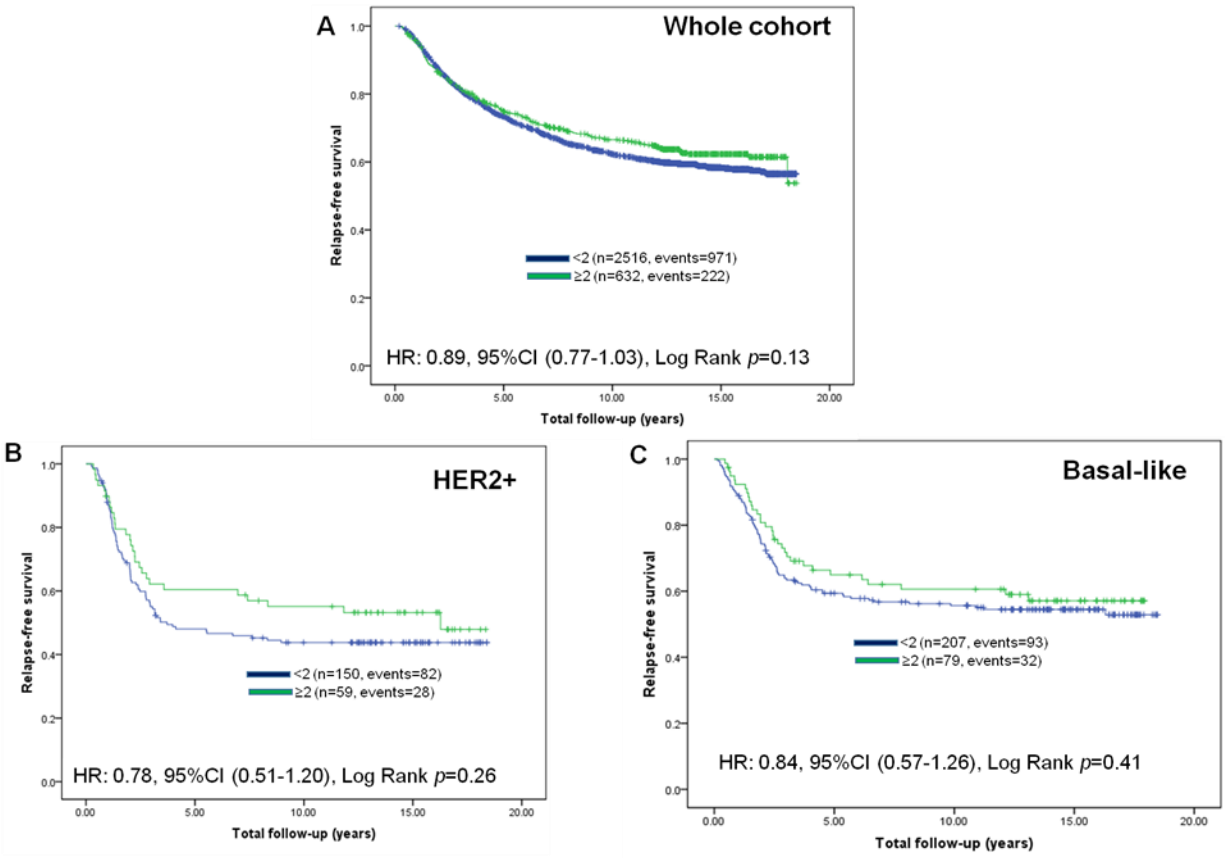

Figure 3.9 Relapse-free survival for TIM-3+ stromal tumor-infiltrating lymphocytes in the whole cohort, in HER2+ and basal-like breast cancer subtypes.
Kaplan Meier (KM) curves of relapse-free survival in breast cancer patients stratified by the presence or absence of TIM-3+sTILs. KM curves in the whole cohort **(A)**, HER2+ **(B)** and basal-like **(C)** are shown with corresponding numbers of patients, events, hazard ratios and log rank *p* values.

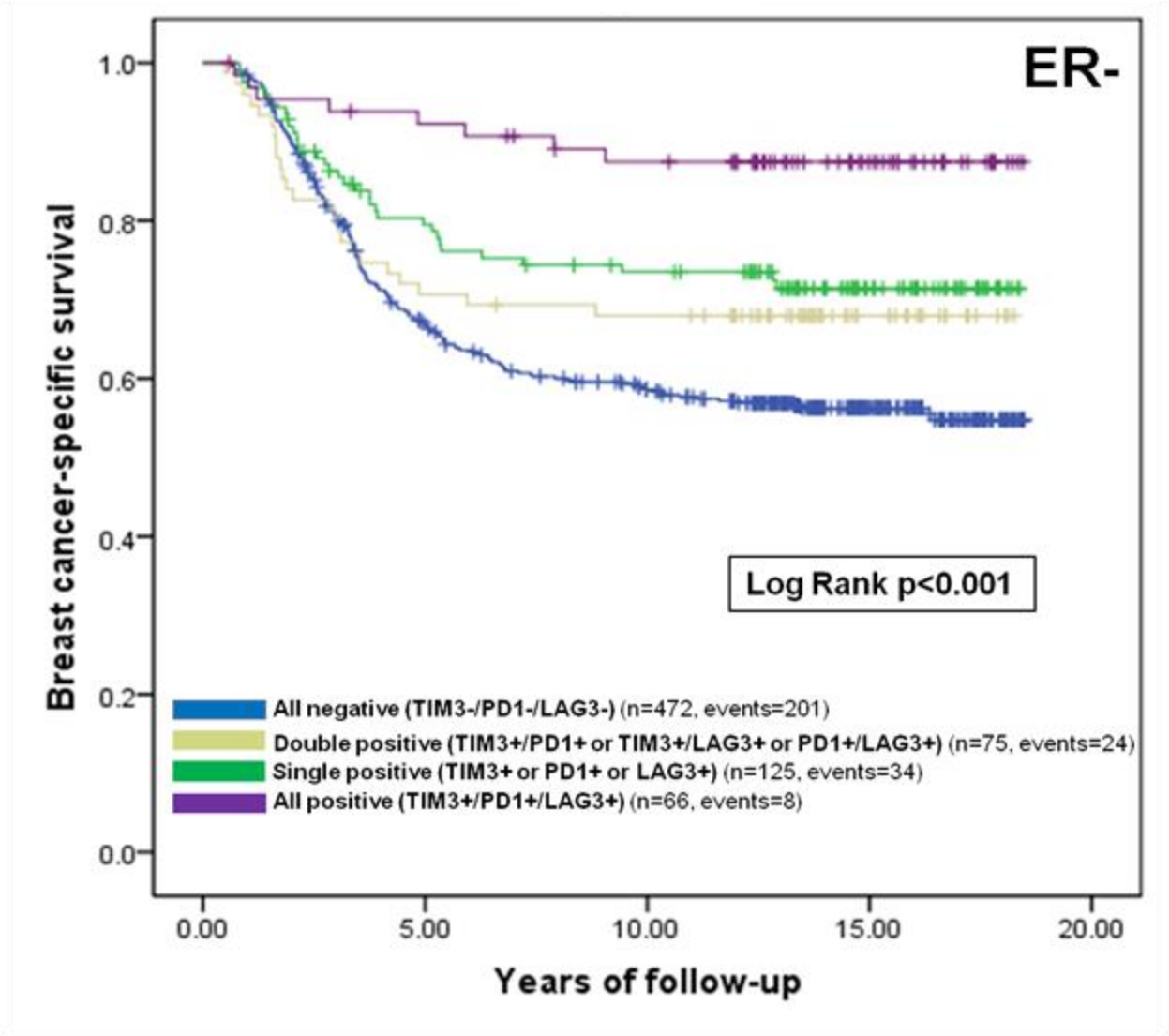

Figure 3.10 Prognostic value of TIM-3, PD-1 and LAG-3+iTILs co-infiltration among ER negative breast cancer patients.

Kaplan Meier curve of breast cancer-specific survival among ER- breast cancer patients stratified by the presence or absence of one or more immune checkpoint markers is shown with corresponding number of patients, events and a log rank p value. *Blue*: All negative (TIM3-/PD1-/LAG3-), *green*: Single positive (TIM3+ or PD1+ or LAG3+), *grey*: Double positive (TIM3+/PD1+ or TIM3+/LAG3+ or PD1+/LAG3+), *purple*: All positive (TIM3+/PD1+/LAG3+).

Table 3.1 Association of TIM-3+ iTILs with clinico-pathological parameters on the initial training cohort.

Initial training cohort (n=330; interpretable staining n=234)			
Parameters	**Negative**	**TIM-3+iTILs (≥1)**	
	n=206	**n=28** (12%)	*P* value*
Age at diagnosis (years)			0.22
<50	71	13 (15%)	
≥50	135	15 (10%)	
Tumor size (cm)			0.31
≤2	118	13 (10%)	
>2	88	15 (15%)	
Grade			0.004
1&2	122	8 (6%)	
3	83	19 (19%)	
Missing	1	1	
Ki67			0.006
Negative (<14%)	121	9 (7%)	
Positive (≥14%)	82	19 (19%)	
Missing	3	0	
ER			<0.001
Negative	40	15 (27%)	
Positive (>1%)	166	13 (7%)	
Subtypes			<0.001
Luminal A	104	8 (7%)	
Luminal B	49	6 (11%)	
HER2E	8	3 (27%)	
Basal-like	18	7 (28%)	
Unknown	27	4	

* Chi-square p value

Table 3.2 TIM-3+ intra-epithelial tumor-infiltrating lymphocytes association with clinico-pathological parameters in breast cancer

Parameters	Negative ***N*=2816**	TIM-3+iTILs ≥1 ***N*=332** (11%)	***P*-value*** ***(χ2)***
Age at diagnosis (years)			0.003
<50	787	119 (13%)	
≥50	2029	213 (10%)	
Tumor size (cm)			0.331
≤2	1467	163 (10%)	
>2	1334	166 (11%)	
Grade			<0.001
1&2	1286	96 (7%)	
3	1414	219 (13%)	
Unknown	116	12	
Ki67			<0.001
Negative (<14%)	1469	100 (6%)	
Positive (≥14%)	1085	209 (16%)	
Unknown	262	23	
ER			<0.001
Negative	716	159 (18%)	
Positive (>1%)	2091	172 (8%)	
Unknown	9	1	
Subtypes			<0.001
Luminal A	1209	73 (6%)	
Luminal B	631	80(11%)	
HER2E	184	25 (12%)	
Basal-like	205	81 (28%)	
Triple negative, non-basal	182	40 (18%)	
Unknown	240	17	

***** Chi-square test

Table 3.3 Association of TIM-3+ stromal tumor-infiltrating lymphocytes with clinico-pathological parameters.

Validation set (*N* =3,148)			
Parameters	**Low (<2)**	**TIM-3+sTILs (≥2)**	
	***N*=2516**	***N*=632** (20%)	*P* value*
Age at diagnosis (years)			<0.001
<50	683	223 (25%)	
≥50	1833	409 (18%)	
Tumor size (cm)			0.370
≤2	1313	317 (19%)	
>2	1189	311 (21%)	
Missing	14	4	
Grade			0.009
1&2	1133	249 (18%)	
3	1276	357 (22%)	
Missing	107	26	
Ki67			<0.001
Negative (<14%)	1307	262 (17%)	
Positive (≥14%)	982	312 (24%)	
Missing	227	58	
ER			<0.001
Negative	649	226 (26%)	
Positive (>1%)	1858	405 (18%)	
Missing	9	1	
Subtypes			<0.001
Luminal A	1074	208 (16%)	
Luminal B	561	150 (21%)	
HER2E	150	59 (28%)	
Basal-like	207	79 (28%)	
Triple negative, non-basal	172	50 (23%)	
Unknown	352	86	

* Chi-square p value

Table 3.4 Association of TIM-3+ intra-epithelial tumor-infiltrating lymphocytes with other immune biomarkers in breast cancer

Immune biomarkers	TIM-3+iTILs=0 (n=2816)	TIM-3+iTILs ≥1 (n=332)	*P*-value (χ^2)
PD-L1*			
Negative	2374	215 (8%)	<0.0001
Positive (≥1%)	133	**97 (42%)**	
PD-1+iTILs*			
Negative	2388	198 (8%)	<0.0001
Positive (≥1)	127	**113 (47%)**	
LAG-3+iTILs*			<0.0001
Negative	2344	169 (7%)	
Positive (≥1)	175	**146 (45%)**	
CD8+iTILs*			
Negative	1881	111 (6%)	<0.0001
Positive (≥1)	778	**213 (22%)**	

*Frequency in the whole cohort: **PD-L1 ≥ 1%**= 241/2918 (8.3%); **PD-1+iTILs ≥1** = 246/2908 (8.5%); **LAG-3+iTILs**= 327/2921 (11%), from Burugu S et al.[242] **CD8+iTILs ≥1**=1089/3403 (32%) from Liu S et al.[96]

Table 3.5 Multivariate analyses of TIM-3+ intra-epithelial tumor-infiltrating lymphocytes in the whole cohort, among estrogen receptor negative and in basal-like patients for breast cancer-specific survival including H&E sTILs as a covariate.

Whole cohort (# of events/n: 705/2379)			
		Hazard Ratio for BCSS (95% CI)	***LRT P*-value**
Age at diagnosis (Reference group:<50)	≥50	1.06 (0.86-1.30)	0.61
Tumor grade (Reference group: grade 1-2)	Grade 3	1.49 (1.26-1.77)	<0.001
Tumor size (Reference group: ≤2cm)	>2	1.63 (1.39-1.91)	<0.001
Lymphovascular invasion status (Reference group: negative)	Positive	1.33 (1.11-1.60)	0.002
Nodal status (Reference group: negative)	Positive	2.29 (1.86-2.82)	<0.001
Adjuvant systemic therapy (Reference group: no AST)	TAM only Chemo only TAM+chemo	0.73 (0.57-0.93) 0.74 (0.56-0.99) 0.69 (0.49-0.97)	0.05
Breast cancer subtypes (Reference group: Luminal A)	Luminal B/Ki67 Luminal/HER2+ HER2+ Basal-like	1.81 (1.50-2.19) 2.16 (1.64-2.84) 2.54 (1.93-3.35) 2.28 (1.74-2.99)	<0.001
H&E sTILs (10% increments)		0.98 (0.98-0.99)	<0.001
TIM-3+iTILs (Reference group: 0)	≥1	0.64 (0.48-0.85)	0.001
Among ER-* (# of events/n: 255/705)			
		Hazard Ratio for BCSS (95% CI)	**LRT *P*-value**
Age at diagnosis (Reference group:>50)	≥50	0.90 (0.66-1.23)	0.50
Tumor grade (Reference group: grade 1-2)	Grade 3	1.91 (1.35-2.70)	<0.001
Tumor size (Reference group: ≤2cm)	>2	1.62 (1.23-2.12)	0.001

Lymphovascular invasion status (Reference group: negative)	Positive	1.32 (0.99-1.77)	0.06
Nodal status (Reference group: negative)	Positive	2.44 (1.76-3.38)	<0.001
Adjuvant systemic therapy (Reference group: no AST)	TAM only Chemo only TAM+chemo	0.89 (0.59-1.34) 0.81 (0.55-1.19) 1.02 (0.59-1.75)	0.64
H&E sTILs (10% increments)		0.98(0.97-0.99)	0.002
TIM-3+iTILs (Reference group: 0)	≥1	0.58 (0.39-0.86)	0.004

Among basal-like (# of events/n: 94/263)			
		Hazard Ratio for BCSS (95% CI)	***LRT P*-value**
Age at diagnosis (Reference group:<50)	≥50	0.86 (0.50-1.46)	0.57
Tumor grade (Reference group: grade 1-2)	Grade 3	1.39 (0.72-2.71)	0.31
Tumor size (Reference group: ≤2cm)	>2	1.40 (0.91-2.16)	0.13
Lymphovascular invasion status (Reference group: negative)	Positive	1.31 (0.82-2.10)	0.26
Nodal status (Reference group: negative)	Positive	2.01 (1.19-3.38)	0.008
Adjuvant systemic therapy (Reference group: no AST)	TAM only Chemo only TAM+chemo	1.65 (0.80-3.42) 1.21 (0.65-2.25) 1.40 (0.47-4.19)	0.60
H&E sTILs (10% increments)		0.97 (0.95-0.99)	0.002
TIM-3+iTILs (Reference group: 0)	≥1	0.58 (0.32-1.03)	0.052

* including HER2 positive and negative

Table 3.6 Multivariate analyses of TIM-3+stromal tumor-infiltrating lymphocytes in the whole cohort, among estrogen receptor negative and in basal-like patients for breast cancer-specific survival.

Whole cohort (# of events/n: 705/2379)			
		Hazard Ratio for BCSS (95% CI)	***LRT P*-value**
Age at diagnosis (Reference group:>50)	≥50	1.05 (0.85-1.29)	0.66
Tumor grade (Reference group: grade 1-2)	Grade 3	1.48 (1.25-1.74)	<0.001
Tumor size (Reference group: ≤2cm)	>2	1.63 (1.39-1.91)	<0.001
Lymphovascular invasion status (Reference group: negative)	Positive	1.34 (1.11-1.60)	0.001
Nodal status (Reference group: negative)	Positive	2.29 (1.86-2.81)	<0.001
Adjuvant systemic therapy (Reference group: no AST)	TAM only Chemo only TAM+chemo	0.73 (0.58-0.93) 0.75 (0.57-1.00) 0.69 (0.49-0.98)	0.06
Breast cancer subtypes (Reference group: Luminal A)	Luminal B/Ki67 Luminal/HER2+ HER2+ Basal-like	1.80 (1.49-2.18) 2.21 (1.68-2.90) 2.58 (1.96-3.41) 2.15 (1.64-2.80)	<0.001
H&E sTILs (10% increments)		0.98 (0.97-0.99)	<0.001
TIM-3+sTILs (Reference group: <2)	≥2	0.79 (0.65-0.96)	0.017
Among ER- (# of events/n: 255/705)			
		Hazard Ratio for BCSS (95% CI)	**LRT *P*-value**
Age at diagnosis (Reference group:>50)	≥50	0.93 (0.68-1.27)	0.63
Tumor grade (Reference group: grade 1-2)	Grade 3	1.87 (1.32-2.64)	<0.001
Tumor size (Reference group: ≤2cm)	>2	1.57 (1.20-2.06)	0.001

Lymphovascular invasion status (Reference group: negative)	Positive	1.38 (1.03-1.85)	0.029
Nodal status (Reference group: negative)	Positive	2.40 (1.73-3.32)	<0.001
Adjuvant systemic therapy (Reference group: no AST)	TAM only Chemo only TAM+chemo	0.93 (0.62-1.40) 0.84 (0.57-1.23) 1.05 (0.61-1.81)	0.73
H&E sTILs (10% increments)		0.98 (0.97-0.99)	<0.001
TIM-3+sTILs (Reference group: <2)	≥2	0.73 (0.53-1.00)	0.047

Among basal-like (# of events/n: 94/263)			
		Hazard Ratio for BCSS (95% CI)	***LRT P*-value**
Age at diagnosis (Reference group:<50)	≥50	0.86 (0.50-1.46)	0.57
Tumor grade (Reference group: grade 1-2)	Grade 3	1.40 (0.72-2.71)	0.30
Tumor size (Reference group: ≤2cm)	>2	1.36 (0.88-2.11)	0.16
Lymphovascular invasion status (Reference group: negative)	Positive	1.41 (0.88-2.25)	0.15
Nodal status (Reference group: negative)	Positive	2.06 (1.22-3.48)	0.006
Adjuvant systemic therapy (Reference group: no AST)	TAM only Chemo only TAM+chemo	1.65 (0.79-3.43) 1.20 (0.64-2.24) 1.17 (0.39-3.50)	0.63
H&E sTILs (10% increments)		0.97 (0.95-0.99)	<0.001
TIM-3+sTILs (Reference group: <2)	≥2	1.05 (0.61-1.78)	0.87

Table 3.7 Multivariate analyses of TIM-3/PD-1/LAG-3+iTILs among ER negative breast cancer patients for breast cancer-specific survival.

Among ER- (# of events/n: 249/686)			
		Hazard Ratio for BCSS (95% CI)	***P*-value***
Age at diagnosis (Reference group:<50)	≥50	0.89 (0.64-1.24)	0.49
Tumor grade (Reference group: grade 1-2)	Grade 3	2.22 (1.56-3.16)	<0.001
Tumor size (Reference group: ≤2cm)	>2	1.50 (1.14-1.98)	0.004
Lymphovascular invasion status (Reference group: negative)	Positive	1.355 (0.998-1.840)	0.052
Nodal status (Reference group: negative)	Positive	2.654 (1.887-3.731)	<0.001
Adjuvant systemic therapy (Reference group: no AST)	TAM only Chemo only TAM+chemo	0.851 (0.566-1.279) 0.739 (0.495-1.103) 1.193 (0.683-2.084)	0.436
TIM-3/PD-1/LAG-3+ iTILs (Reference group: TIM3-/PD1-/LAG3-)	TIM3-/PD1+/LAG3-	0.499 (0.251-0.989)	0.046
	TIM3-/PD1-/LAG3+	0.498 (0.289-0.861)	0.012
	TIM3-/PD1+/LAG3+	0.586 (0.299-1.148)	0.119
	TIM3+/PD1-/LAG3-	0.615 (0.314-1.203)	0.155
	TIM3+/PD1+/LAG3-	0.348 (0.086-1.410)	0.139
	TIM3+/PD1-/LAG3+	0.959 (0.519-1.772)	0.893
	TIM3+/PD1+/LAG3+	0.165 (0.073-0.375)	<0.001

***Wald-test

Chapter 4: Quantitative *in situ* multiplex immune profiling of breast cancer patients using digital spatial profiling technology

SYNOPSIS:

Predictive biomarkers of immunotherapies are the focus of intensive research that has dramatically increased in a short amount of time. Immune biomarkers presented in **Chapter 2 and 3** represent only some of the immunotherapy targets that have advanced from pre-clinical to clinical phase. Studies show that more than one biomarker will likely be required to identify immunotherapy-responsive tumors. The tumor immune microenvironment is complex and requires a multiplex detection system to distinguish the various immune cell populations. In this chapter, I profiled the tumor immune microenvironment of two breast cancer cohorts (a total of 59 breast cancers enriched for the basal-like subtype) using a novel multiplex technology by Nanostring called Digital Spatial Profiling (DSP). DSP enables the characterization and expression profiling of breast cancer tumors, in my work using a 31-marker immuno-oncology panel. I then validated DSP digital counts for CD8 and PD1 by immunohistochemistry, and CD45 digital counts by assessing hematoxylin and eosin-stained stromal tumor-infiltrating lymphocyte counts. Furthermore, I was able to identify a profile of patients with favorable prognosis. Lastly, I identified a 4-biomarker signature that was indicative of a pre-existing intratumoral immune response. A proposal to evaluate the capacity of the 4-biomarker signature to predict response to immune-modulating chemotherapy is presented at the end of the chapter.

4.1 Introduction

Immunotherapy has drastically changed the cancer treatment landscape, including now in breast cancer. Clinical trials evaluating immune checkpoint inhibitors in breast cancer have mostly targeted patients with basal-like triple negative breast cancers as it represents the most immunogenic subtype [as reviewed by Wein et al.[147]]. A recent phase III clinical trial (IMpassion130) of a PD-L1-targeted immune checkpoint inhibitor reported improved progression-free survival in treatment-naive metastatic basal-like breast cancer patients[148]. Predictive biomarkers of response to immune checkpoint inhibitors are needed (to avoid unnecessary toxicities and high costs) but the identity of these biomarkers is still a subject for debate. Genomic characteristics of tumors that are associated with response include the presence of high microsatellite instability (MSI-H), mismatch-repair deficiency (dMMR), a high mutational burden, and copy number alterations[247-249]. However, MSI-H/dMMR tumors are rare, especially in breast cancer (~2% of breast cancers[250]) and no standardized means of measurement nor cut-offs for mutational burden are yet firmly established.

Tumors heavily-infiltrated with immune cells are more likely to respond to immune checkpoint inhibitors as demonstrated in earlier studies[212,215,251] [reviewed by Chen DS and Mellman I[212]]. Anti-tumor immunity is mainly mediated by T cells, which represent a heterogeneous population that includes effector, exhausted and regulator phenotypes[252]. In addition, other immune cells play key roles in anti-tumor immunity such as Natural Killer cells and macrophages[52,252]. The concurrent infiltration of the various immune cell populations in a patient's tumor, as well as their intratumoral localization pattern, may be associated with impeded or improved responses to immunotherapies. Nonetheless, to analyze multiple immune biomarkers concurrently in a patient's tumor tissue represents a technical challenge; methods that

have been tried include sequential staining of multiple antibodies or digital segmentation of tumors for image analyses[253,254].

In my study, I employed a novel quantitative spatially-resolved multiplexed antibody-based method called digital spatial profiling (DSP) using NanoString's GeoMx™ technology. This method allows for simultaneous quantitative measurement of an immuno-oncology panel (representing 31 biomarkers) in user-defined areas of formalin-fixed paraffin-embedded breast tumor tissues. The 31 biomarkers included immune cell type identification markers (CD14, CD19, CD3, CD4, CD45, CD45RO, CD56, CD68, CD8A, FOXP3, GZMB, CD20, PD1, PD-L1, VISTA), tissue and cancer biomarkers (Pan-cytokeratins, PTEN, β-catenin, Ki67, Bcl-2) and other immune-related biomarkers (B7-H3, STAT3,Beta-2 microglobulin, CD44) . We surveyed the expression of the 31 biomarkers in two basal-like enriched tissue microarray cohorts representing a total of 59 breast cancer patients.

4.2 Material and methods

4.2.1 Study cohort

Tumor excision specimens from two British Columbia breast cancer patient cohorts (herein referred to as Cohort A and Cohort B) were built into two tissue microarrays comprised of 0.6mm duplicated cores. Cohort A consisted of 39 patients diagnosed with invasive breast cancer in the period of 2008-2011, details of which have already been published in the context of a study from our laboratory of basal biomarker expression in ER negative and weakly ER positive cases[255] . Breast cancer patients from cohort B (N=20) were diagnosed between 2013-2015, with clinical triple negative breast cancer (ER–/PR–/HER2–) and treated accordingly. None of the patients (from Cohort A or B) received neoadjuvant therapy, so the samples under

investigation represent primary tumor tissue that was not exposed to radiation, chemotherapy or endocrine therapy. Clinicopathological parameters for Cohort A and B are summarized in **Table 4.1**. Identification of breast cancer subtypes in Cohort A was done using PAM50 gene expression profiling as a gold standard breast cancer subtyping assay as previously published[255]. Clinical outcome data were available for cohort A with a median follow-up time of 48 months (cohort B cases are too recent to have mature outcome data). The clinical research ethics board of the University of British Columbia and BC Cancer Agency approved access to clinical outcome and de-identified data.

4.2.2 Digital spatial profiling

Breast cancer tissue microarrays were subjected to digital spatial profiling using Nanostring GeoMx™ technology as recently published[256,257](See schematic in **Figure 4.1).** In brief, tissue microarrays were incubated with a cocktail of antibodies that included fluorescent visualization markers and an immuno-oncology biomarker panel. To select regions of interest, fluorescent visualization markers consisted of CD45 for immune cells, Pan-cytokeratins for carcinoma cells and DAPI as a nuclear stain. Each TMA core served as a defined region of interest. The immuno-oncology biomarker panel consisted of 31 antibodies (**see Figure 4.1)** linked with UV-cleavable DNA oligos that can be quantified on the Nanostring nCounter platform. Biomarker expression counts were normalized using Nanostring internal spike-in controls for hybridization (called ERCC). Biomarker expression counts from duplicated cores were averaged for each patient prior to further analyses. There were 3 cases in Cohort A and 1 case in Cohort B for which biomarker expression counts were interpretable in only one of the 2 cores.

DSP counts were divided by the geometric mean values of isotype controls to generate the signal to noise ratio for each biomarker.

4.2.3 Immunohistochemistry and scoring

Anti-CD8 mouse monoclonal antibody (clone 28/144B) and anti-PD1 rabbit monoclonal antibody (clone EPR4877) were applied to the Cohort B TMA according to manufacturer's protocol, at the Deeley Research Centre (Victoria, BC). A pathologist blinded to clinical and DSP data scored CD8+ and PD1+ lymphocytes using a previously published scoring system developed in our laboratory[242]. In brief, absolute counts of CD8+ or PD1+ lymphocytes were reported based on their localization in the tumor. Intra-epithelial tumor-infiltrating lymphocytes (iTILs) were defined as CD8+ or PD1+ lymphocytes in direct contact with carcinoma nests whereas stromal tumor-infiltrating lymphocytes (sTILs) were outside of carcinoma nests. To allow comparison with CD8 and PD1 DSP digital counts, iTIL and sTIL counts were combined to generate a total count of CD8+ or PD1+TILs for each tissue microarray core. H&E sTILs were scored on both TMA cohorts as described in **Chapter 3** based on an internationally-standardized scoring system our lab contributed to developing[74,258].

4.2.4 Statistical analysis

Unsupervised hierarchical clustering was performed on DSP biomarker expression normalized counts for each patient using ComplexHeatmap on R/Bioconductor and provided by Nanostring. Associations with clinicopathological parameters and outcome were performed in IBM SPSS software version 25. Kaplan-Meier curve estimates were built for breast cancer-specific survival, defined as the time between invasive breast cancer diagnosis and time of death attributed to breast cancer. Breast cancer patients alive at last follow-up or that had died of other causes were censored.

An intraclass correlation was calculated to assess core to core agreement of biomarker expression digital counts between two duplicated cores. Chi-square tests compared the statistical significance of the pathological parameter associations among the DSP immune expression profiles. Biomarker correlation analyses (for CD8, PD1 IHC vs DSP counts and H&E sTILs vs CD45 DSP counts) were assessed by Spearman Rho. A one-way analysis of variance (ANOVA) test was conducted to identify biomarkers differentially expressed between the three levels of H&E sTILs (low:<10%, intermediate: ≥10-<50% and high or lymphocyte-predominant breast cancer: ≥50%). To reduce Type I errors across multiple tests generated in ANOVA, a Bonferroni-correction was used to set a cut-off of 0.001 for significant p-values. Post-hoc multiple comparisons using Tukey Honest Significant Difference (HSD) test were used to assess significant differences in pairwise group comparisons. A multiple regression analysis in Cohort A (due to a larger sample size compared to Cohort B) was used to build a predictive model for identifying immune-enriched breast tumors based on the 4-biomarker signature. For this analysis, H&E sTILs counts were entered as the variable to predict. The predictive model generated, for each patient, a continuous immune score based on the 4-biomarker signature. High values of this score represented immune-enriched breast tumors.

4.3 Results

4.3.1 Overview of DSP digital counts of the 31 biomarkers

A single tissue microarray slide for each cohort (represented by duplicated cores) was stained and analyzed by using the Nanostring Digital Spatial Profiler (**Figure 4.1).** Tissue microarray cores representing 37 out of 39 cases from Cohort A and all 20 cases from Cohort B were interpretable by DSP. DSP digital counts were obtained for all the biomarkers included in

the immuno-oncology panel **(Appendix Table B.1**). All counts were normalized using hybridization technical controls as described in Material and methods. For cases with interpretable digital spatial profiling counts on duplicated cores (N=34 in Cohort A and N=19 in Cohort B), there was a good to excellent core-to-core agreement (intraclass correlation greater than 0.75) in the 31 biomarker expression counts for the majority of cases (68% for cohort A and 58% for cohort B) with only a few cases (less than16% in both cohorts) having poor (intra class correlation <0.5) core-to-core agreement **(Figure 4.2).**

In both cohorts, DSP digital counts for tissue microarray cores were highly variable ranging from less than 100 counts for biomarkers including antibody isotype controls and FOXP3 to high values of more than 80,000 counts for biomarkers such as Pan-cytokeratin and β-catenin **(Figure 4.3**, bottom tables). DSP digital counts for mouse isotype control was significantly higher in Cohort B in comparison to Cohort A and a similar trend for the rabbit isotype control (p=0.07) was observed, suggesting a possible experimental variation **(Figure 4.4A**). However, there was no significant difference in digital counts for reference biomarkers (Histone H3 and Ribosome S6), indicating that cellularity was comparable between the tissue microarray cores **(Figure 4.4B**). For further DSP analyses, a signal to noise ratio normalization was applied to DSP counts using isotype controls counts to remove non-biological background variance **(Appendix Table B.2**).

4.3.2 Validation of CD8 and PD1 DSP counts by immunohistochemistry and correlations with tumor infiltrating lymphocyte counts

To validate the biomarker digital counts generated by the digital spatial profiling, we analyzed immunohistochemistry scores assessed visually by a pathologist for CD8 and PD1 previously stained on the Cohort B tissue microarray. Based on our established, published cut-

points[96,242], CD8+ iTILs (≥1) were present in 55% of cases whereas PD1+iTILs (≥1) were observed in 50% of cases. CD8 and PD1 immunohistochemistry continuous scores significantly ($p<0.001$) correlated with the CD8 and PD1 DSP counts performed on sections from the same tissue microarray (Spearman rho r=0.674 for CD8 and r=0.838 for PD1: **Figure 4.5A; B)**. We found that there were 8 cases (40%) with PD1+ lymphocytes that were only detected by DSP, although the PD1 digital counts for these specific cases were in the lower range of distribution of PD1 DSP counts **(Figure 4.5B**). Similar findings were observed for differences between CD8 DSP counts and immunohistochemistry scores.

As H&E sTILs scores were available for both cohorts, we also analyzed the Spearman rank correlation between visual counting of lymphocytes with CD45 DSP counts (a general marker for lymphocytes) (**Figure 4.5C-D**). H&E sTILs scores and CD45 DSP counts significantly correlated ($p<0.001$) with each other, supporting that the level of immune cells detected by CD45 using DSP directly reflects the number of morphologically-characterized lymphocytes visually identifiable in a core.

4.3.3 Distinct breast cancer immune expression profiles are illustrated by DSP

Normalized counts of the 31 biomarker DSP immuno-oncology panel were subjected to an unsupervised hierarchical clustering analysis for each cohort (**Figure 4.6**). Cohort A (n=37) was clustered into 4 groups whereas Cohort B (n=20) partitioned into 3 groups (**Figure 4.6**). The level of immune infiltration based on the immune biomarkers' expression counts varied greatly between these groups. In Cohort A, breast cancer patients in Groups A2 and A3 showed the highest immune infiltration including high levels of CD45, CD3 and CD20 counts in comparison to patients represented in Group A1 and A4 (**Figure 4.6A**). However, patients in Group A2 had the most immune-enriched tumors among all the groups (**Figure 4.6A**). In Cohort

B, Group B2 included breast cancer patients with high levels of CD45, CD45RO, CD8, and CD20 counts whereas patients in Groups B1 and B3 had low to intermediate level of immune infiltration in their basal-like tumors (**Figure 4.6B**).

As expected, pan-cytokeratin counts were elevated in patients with low immune infiltration in their tumors for both cohorts (i.e., in groups A1/A4 compared to groups A2/A3 for cohort A and in groups B1/B3 compared to group B2 for cohort B, **Figure 4.6**) although it did not reach statistical significance. Similar non-significant trends were observed for additional non-immune biomarkers elevated in immune-desert breast tumors including p-AKT and beta-catenin in Cohort B **(Figure 4.6B)**. Moreover, counts for B7-H3, an emerging immune checkpoint molecule[259], appeared to be inversely correlated with immune infiltration in Cohort A **(Figure 4.6A).**

No significant associations with any of the clinicopathological parameters tested were found, likely due to the limited sample size in each cohort (**Tables 4.2 and 4.3**). However, in survival analyses (on Cohort A), improved breast cancer-specific survival was associated with immune-enriched DSP profiles (**Figure 4.7**). All the patients with death attributed to breast cancer in this 7-year follow-up were among the DSP profile groups with low tumor-immune infiltration, namely A1 and A4. Due to the absence of events in the immune-enriched DSP profiles, hazard ratios could not be computed.

4.3.4 Identification of a set of biomarkers most associated with immune-enriched profiles in both cohorts

To determine which were the key biomarkers included within the DSP immuno-oncology panel that would discriminate between immune-enriched and immune-desert breast tumors, I

conducted a one-way analysis of variance among patients stratified by the different levels of H&E sTILs shown in **Table 4.2** and **4.3**.

After performing log transformation of the DSP counts for all 31 biomarkers as per standard procedure to allow one-way analysis of variance tests statistics to be calculated, I found 8 biomarkers out of 31 with significant Bonferroni-corrected p-values showing a difference in expression between patients with different levels of H&E sTILs in Cohort A. These were: CD20, CD45RO, CD3, PD1, CD4, CD45, CD8 and CD19 **(Table 4.4).**

In Cohort B, only 4 out of 31 biomarkers were differentially expressed among patients with different levels of H&E sTILs and all 4 biomarkers (CD20, CD3, PD1 and CD45) were also shared with Cohort A **(Table 4.4)**. Post-hoc pairwise comparison analyses using Tukey honest significant difference test indicated which H&E sTILs groups had significant differences in expression of the selected biomarkers **(Table 4.4).** The B-lymphocyte biomarker CD20 had the highest fold change in expression between patients with lymphocyte-predominant breast cancers and patients with low levels of H&E sTILs. There was a more than 100-fold difference for Cohort A and a nearly 50-fold difference in expression for Cohort B **(Table 4.4).** I settled on the 4 immune biomarkers (CD20, CD3, PD1 and CD45) differentially expressed in both cohorts as a potential candidate protein biomarker-signature for immunogenic breast cancers.

The 4 biomarker-signature was entered in a multiple regression analysis to build a predictive model for immune-enriched breast tumors **(**see methods section for details-**Table 4.5**). The equation yielded in the predictive model showed a higher coefficient factor for PD1 DSP counts in comparison to the other 3 biomarkers (1.412 for PD1 vs 0.035 for CD3 counts), suggesting a significant contribution of PD1 counts to predict immune-enriched tumors. In

contrast, as CD45 expression is not restricted to lymphocytes, a negative coefficient factor was associated with CD45 DSP counts in the predictive model.

In both cohorts, this predictive model yielded a good to excellent area under the receiver operating characteristic curve (AUC=0.829 for Cohort A and AUC= 1.00 for Cohort B), indicating that this model accurately identified immune-enriched breast tumors **(Table 4.5)**. In cohort A, the 4-biomarker signature (treated as a continuous variable) correlated with improved breast cancer-specific survival albeit not reaching statistical significance (HR: 0.65 , 95% CI:0.35-1.09, Wald test p= 0.10).

4.4 Discussion

Using the digital spatial profiling technology, I was able to profile 31 protein biomarkers for their expression in 59 breast cancer patient surgical samples using just two TMA slides. Digital counts obtained by DSP on tissue microarray cores show a good core-to-core agreement between duplicated cores and exhibited a high dynamic range from biomarkers with low counts such as FOXP3 to highly abundant proteins such as cytokeratins. Digital counts from isotype controls showed variation between cohort A and cohort B whereas cellularity remained similar between the two cohorts. Furthermore, I directly validated CD8 and PD1 DSP digital counts by single stain immunohistochemistry and indirectly validated CD45 DSP digital counts by assessing H&E sTIL scores. The immune biomarker expression profiles illustrated by DSP were significantly associated with survival in one cohort. Our discovery-based study identified a signature of 4 key biomarkers (CD20, CD3, PD1 and CD45) that best discriminate immune-enriched from immune-cold breast tumors in the tested study cohorts. This represents the first

study to investigate immune expression profile in breast cancer tissue microarrays using the digital spatial profiling Nanostring-based technology.

In situ detection of multiple biomarkers in tumor tissues can also be done by fluorescent multiplex IHC or by mass cytometry. One of the most commonly used fluorescent multiplex IHC methods compatible with autostainers is the Opal system by Perkin Elmer. The Opal system offers the visualization of up to six target biomarkers in tumor tissues and is a preferred tool for proteins of low abundance as it has increased sensitivity due to tyramide-based signal amplification[260]. However, some of the disadvantages of this technique include: 1) the need for signal amplification which does not provide the relative abundance of the target in the tissue; 2) a requirement for particular planning of sequential staining of compatible antibodies in a panel, which is a laborious task and limits the number of targets that can be detected and 3) this technique requires building and training algorithms for multispectral image analysis[253,261-264].

Multiplex detection by mass spectrometry such as mass cytometry or multiplex-ion beam imaging techniques can identify more biomarkers than conventional multiplex IHC and offers quantitative measurement but still requires training for digital image analysis and can be time-consuming [254,260]. In contrast, the 31 biomarker expression DSP digital counts were generated automatically without signal amplification steps and without an image analysis training step. Thus, the Nanostring-based digital spatial profiling technology offers a way to quickly and directly profile the tumor immune microenvironment and select key biomarkers for in-depth analyses. Indeed, DSP was recently used in two different studies to profile immune biomarker expression in tumor biopsies from melanoma patients receiving immune checkpoint inhibitors (a combination of anti-CTLA4+ anti-PD1 agents or single anti-PD1 agent) and few immune

biomarkers were found to correlate with response in the neoadjuvant setting and with increased relapse-free survival in the adjuvant setting[256,257].

In addition to identifying discrete breast cancer immune profiles, I was also able to associate the DSP-derived immune expression profiles with clinical outcome in an exploratory analysis. In Cohort A, the groups of patients with high tumor immune infiltration (A2 and A3) were associated with significantly improved breast cancer-specific survival.

Using one-way analysis of variance statistics, I narrowed the DSP immuno-oncology panel down to 8 biomarkers that discriminated the groups into high-vs low immune infiltrations. These 8 biomarkers include a general lymphocyte marker (CD45) and more specifically encompass immune cell populations including T cells (CD3, CD4, CD8), B cells (CD19, CD20), exhaustion-immune checkpoint states (PD1), and memory state (CD45RO). In Cohort B, the immuno-oncology panel was narrowed down to 4 immune biomarkers that associated with those cancer patients with the highest tumor immune infiltration (grouped in lymphocyte-predominant breast cancers group), all 4 of which were also incorporated within the 8-biomarker signature from Cohort A. These 4 common biomarkers are CD20, CD3, PD1, and CD45. Furthermore, I identified a predictive model to identify immune-enriched breast tumors based on the 4-biomarker signature.

As this 4-biomarker signature illustrates, evaluating one immune biomarker at a time leaves out important information that may have clinical utility (prognostic or predictive value). Indeed, studies on predictive biomarkers of response to immune checkpoint inhibitors show the need for assessing more than one biomarker[215,249,265] [Reviewed by Gibney et al.[266]]. DSP digital counts from non-immune biomarkers such as beta-catenin and p-AKT appeared to positively correlate with breast tumors with low immune infiltration (although it did not reach statistical

significance in the two small cohorts). Beta-catenin has been reported to be associated with immune-desert tumors [Reviewed by Spranger S et al.,[267]] which further shows the importance of assessing tumor intrinsic properties in multiplex panels as in the DSP.

Assessing H&E sTIL scores evaluates all the immune populations included in the 4-biomarker signature, namely B cells, and T cells in different activation states. In my study, H&E sTIL scores correlate significantly with CD45 DSP counts. However, using this method, the information of the individual contribution of each immune cell type to the overall immune population is not evaluated. As this discovery-based study shows, biomarkers such as CD20, on an average, have the highest DSP counts in tumor immune-enriched breast cancer patients. This can be interpreted as B cells being the largest contributor to the total lymphocyte population within the tumor, since DSP digital counts are directly reflective of the number of CD20 molecules present. However, this should be taken with caution as the abundance of each antibody-targeted molecule per cell might be due to a difference in sensitivity of detection of certain epitopes (e.g. the CD20 epitope targeted in the panel could be particularly highly accessible in formalin-fixed paraffin-embedded tissues and/or could have an especially high affinity for its antibody).

Immuno-oncology biomarker studies have largely focused on T cells[265,268], as PD-1 (expressed on T cells) represents the target for the regulator-approved immunotherapy drugs in greatest clinical use. In contrast, studies on the presence of B cells in breast cancer have been mostly prognostic[86,88,89] with one study suggesting B cells are predictive of response to anthracyclines, an immune-modulating chemotherapy agent[100]. Certainly, B cells have pleiotropic functions within tumors, including antigen presentation, which can enable a de novo immune response within the tumor microenvironment[269].

Although the study I describe in **Chapter 4** successfully identified immune expression profiles from breast cancer patient specimens that have potential clinical relevance, I have to acknowledge several limitations: 1) As it is a first study applying this novel technology to breast cancer tissue microarray materials, the sample size was limited which can affect the variability of DSP profiles if analyzed in a larger cohort; 2) DSP profiles in each cohort were selected in a data-driven fashion based on the visual clusters generated by unsupervised hierarchical analysis and data-driven model-building and thus, conclusions drawn from the biomarkers and panels identified from this approach will require further validation on independent materials; and 3) due to the limited sample size, the whole tissue microarray core was selected as a region of interest without discriminating intraepithelial from stromal immune infiltration which prevented the ability to assess the importance of biomarker localization in the tissue.

As the number of clinically relevant immune biomarkers discovered is likely to continue rising, multiplex detection systems such as DSP will be needed to perform future studies. Moreover, as Chapter 4 illustrates, DSP can generate a substantial amount of protein measurements using only tissue microarray cores, therefore sparing precious patient tumor tissues. This first study on breast cancer tissue microarrays supports DSP as a technology that could be used to survey the immune context in tissue samples representing tumors responding versus non-responding to immune-modulating therapies. A proposal to use DSP to evaluate the capacity of immune biomarkers to predict response to immune-modulating chemotherapy in breast cancer is presented at the end of this chapter with a future goal of applying the technology on breast cancer immune checkpoint inhibitor clinical trials.

4.5 Proposal to apply the Nanostring digital spatial profiling technology to clinical trials material

Assessing the predictive value of immune biomarkers for response to anthracyclines, an immune-modulating chemotherapy, in the MA.5 clinical trial

Tumor immunogenicity or the ability of cancer cells to produce antigens recognized by the body's immune system is a major biological feature underlying the success of immunotherapy[270,271]. A growing body of evidence suggests that some chemotherapy drugs, such as anthracyclines, are immune-modulating as their effects include promotion of immune activation, inhibition of immunosuppressive cells, and/or release of antigens from tumors in a process termed immunogenic cell death[122,272,273].

Pre-existing immunity in breast cancer patients treated with neoadjuvant anthracycline-containing chemotherapy is associated with pathologic complete response in hormone-receptor negative subtypes[100]. However, in the adjuvant setting, the predictive value of a pre-existing anti-tumor immune response is not clear. Some studies report solely a prognostic value for high levels of H&E stained tumor-infiltrating lymphocytes in hormone-receptor negative breast cancer patients treated with anthracycline-containing chemotherapy; others report a predictive value[81,83]. The Canadian Cancer Trials Group (CCTG) MA.5 clinical trial randomized premenopausal node-positive breast cancer patients to receive adjuvant Cyclophosphamide-Methotrexate-5'Fluorouracil (CMF) or Cyclophosphamide-Epirubicin-5'Fluorouracil (CEF: anthracycline substitution) and therefore provides an opportunity to evaluate the value of pre-existing immunity in breast cancer patients to predict benefit from adjuvant anthracyclines, an immune-modulating chemotherapy.

Problem: H&E stromal tumor-infiltrating lymphocytes represent a heterogeneous population of immune cells and lack precision as a biomarker, highlighting a need to test more advanced, specific biomarkers. However, individually testing the large number of biomarkers required to identify immune populations and activation phenotypes in formalin-fixed paraffin-embedded tissues would consume a considerable amount of precious Phase III trial material.

We propose to evaluate the predictive value of immune biomarkers of response to immune modulating chemotherapy in patients from the MA.5 clinical trial by undertaking digital spatial profiling (DSP) using NanoString's new GeoMx technology, a method for which we have generated relevant preliminary data on breast cancer tissue microarrays.

4.5.1 Hypothesis:

Breast cancer patients with pre-existing immune-enriched tumors assessed by the 4-biomarker signature will benefit from adjuvant anthracycline-containing chemotherapy (CEF) more than from CMF.

Our study objectives are:

1. Assess the predictive value of the 4-immune biomarker signature of response to anthracycline-containing chemotherapy regimens
2. Characterize the pre-existing tumor immune microenvironment of a large set of breast cancer patients using a 56 antibody multiplexed immuno-oncology panel on the DSP Nanostring platform.

4.5.2 Materials and methods:

For this study, we will use the existing TMAs built from surgical excision tumor specimens from the patients in MA.5. Our laboratory has experience using the MA.5 TMAs which comprise 4 blocks representing a total of 511 cases with duplicated cores. One 4μm FFPE

unstained TMA section will be required for this study, which will be performed using a Nanostring Digital Spatial Profiler instrument being installed on site. The DSP immuno-oncology panel will be purchased from Nanostring and current iteration of this panel includes 56 biomarkers **(Table 4.6).**

Fluorescent visualization markers for selection of regions of interest will include a tumor marker (Pan-cytokeratins), a lymphocyte marker (CD45) and DAPI as a nuclear stain. To allow the assessment of intraepithelial vs stromal immune infiltration, a pan-cytokeratin and CD45 mask will be used to select two regions of interest (ROIs) per TMA core per patient to be analyzed by DSP (a total of 2044 ROIs). Pan-cytokeratin positive/CD45 negative will be defined as intraepithelial regions whereas stromal regions will be identified as pan-cytokeratin negative/CD45 positive. Analysis of biomarker expression counts in each ROI will be conducted in our lab using the Nanostring DSP platform. Internal spike-in hybridization controls and a signal to noise ratio will be applied for data normalization prior to statistical analyses.

4.5.3 Statistical design:

MA.5 randomized 710 node-positive premenopausal breast cancer patients to receive adjuvant anthracycline-containing chemotherapy (CEF, n=351) versus CMF (n=359). The 10-year follow-up trial results showed superiority of CEF over CMF for the primary endpoint, relapse-free survival (HR=1.31; 95%CI, 1.06 to 1.61; stratified log-rank, p=0.007)[274]. The MA.5 TMA consists of 511 breast cancer patients representing 72% of the clinical trial's population. We hypothesize that there will be a significant interaction observed between MA.5 study arm (CEF vs CMF) and a pre-existing antitumor immune response for the trial's primary endpoint, relapse-free survival.

Drawing from our recently-completed discovery-based study on breast cohort TMAs, we will evaluate the predictive value of the 4-biomarker signature (CD20, CD3, PD1 and CD45) in the intraepithelial region as our primary hypothesis.

Precisely, the level of immune infiltration in breast tumors will be based on the score generated by the 4-biomarker predictive model as presented in the initial cohort-based study.

The Canadian cancer trials group statisticians following a formal pre-specified written statistical plan will conduct all clinical analyses. The initial analyses will include a) a table of patient characteristics (age, nodal status, tumor stage, intrinsic subtypes previously defined by PAM50[14], according to 4-biomarker signature (as a continuous variable); b) a distribution of the 4-biomarker signature by treatment regimen (CEF vs CMF) to assess any improper balances between patients in CEF and in CMF treatment arms .

If there are no significant imbalances, Kaplan-Meier estimates in univariate analyses and multivariate cox regression analyses will use relapse-free survival as a primary endpoint and overall survival as secondary endpoint stratified by the 4-biomarker signature. Our analyses will first focus on the CEF arm alone as CMF can potentially have an immune modulating effect that could lower our power to see an effect of pre-existing immunity in response to CEF. Benefit of CEF will be estimated for all patients stratified by the 4-biomarker signature. As a secondary analysis, we will analyze benefit of CEF vs CMF for all patients stratified by the 4-biomarker signature. A treatment x 4-biomarker immune signature interaction term will be calculated using the likelihood ratio test to assess benefit of CEF vs CMF in all patients stratified by the 4-biomarker signature. Prognostic and unsupervised hierarchical clustering analyses using the full DSP 56 immune biomarker panel will be conducted as exploratory analyses.

A finalized specific statistical plan will be discussed with the Canadian cancer trials group statisticians following initial gathering and processing of DSP results and reassessment of study power based on the biomarker distribution and number of cases with interpretable data.

4.5.4 Significance of research:

This study proposes to evaluate, quantitatively, the complex tumor immune microenvironment of breast cancer patient surgical specimens using the cores on existing tissue microarrays via novel digital spatial profiling technology. As a result, large amounts of protein-level biomarker data will be generated from tiny amounts of precious clinical trial material.

Furthermore, we will assess the predictive value of a pre-existing antitumor immune response signature for benefit from anthracycline-containing chemotherapy. This could support hypotheses that particular chemotherapy regimens act in part via the immune system. Biomarker results could potentially help to better identify those breast cancer patients most amenable to immune-modulating anthracycline chemotherapies vs. those who might be spared their sometimes severe side effects.

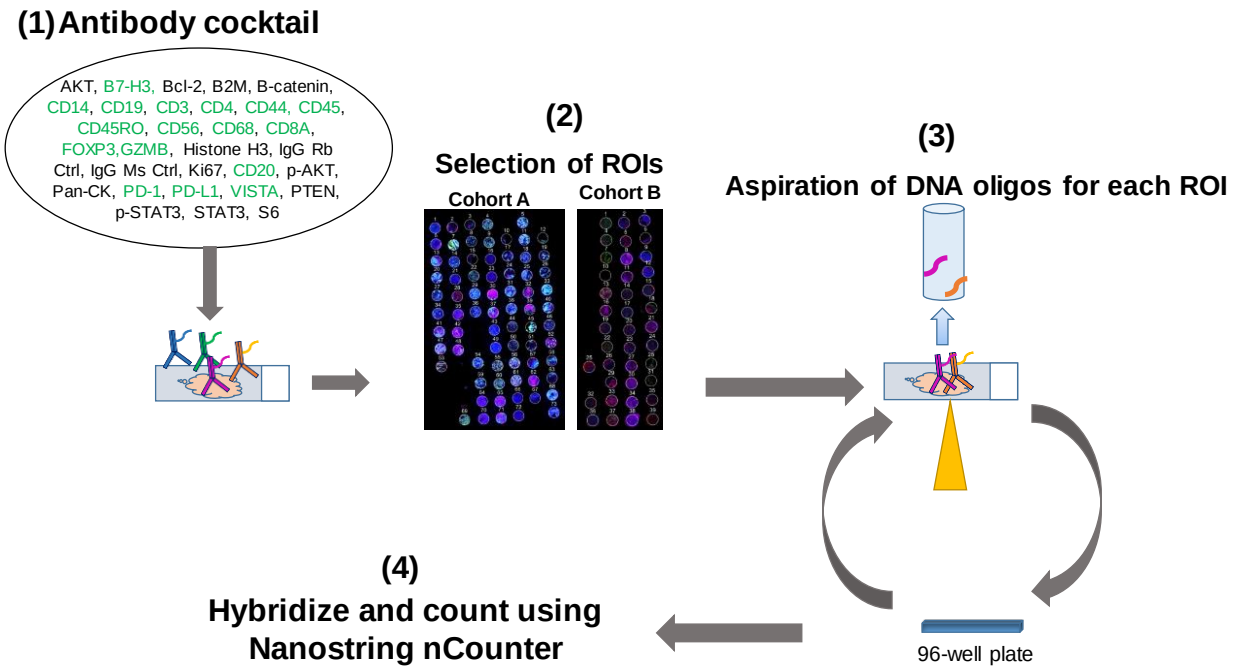

Figure 4.1 Schematic of DSP analysis process on Cohort A and B TMAs
(1) An antibody cocktail is applied to formalin-fixed paraffin-embedded tumor tissue from a 4 micron section of a tissue microarray. Green-highlighted biomarkers in the antibody cocktail represent immune cell populations. **(2)** The slide is visualized using 3 fluorescent markers included in the antibody cocktail (Pan-CK in green, CD45 in red and a nuclear stain in blue) and is used to select the regions of interest (ROIs). 37/39 cases were interpretable for Cohort A. All 20 cases were interpretable for Cohort B. **(3)** DNA oligos attached to each antibody are cleaved by UV in the selected ROI and aspirated oligos are dispensed into a 96-well plate. The process repeats for each ROI. **(4)** 96-well plate is put into the Nanostring nCounter for hybridization to corresponding capture/reporter probes and digital counts for each antibody-targeted biomarker are generated.

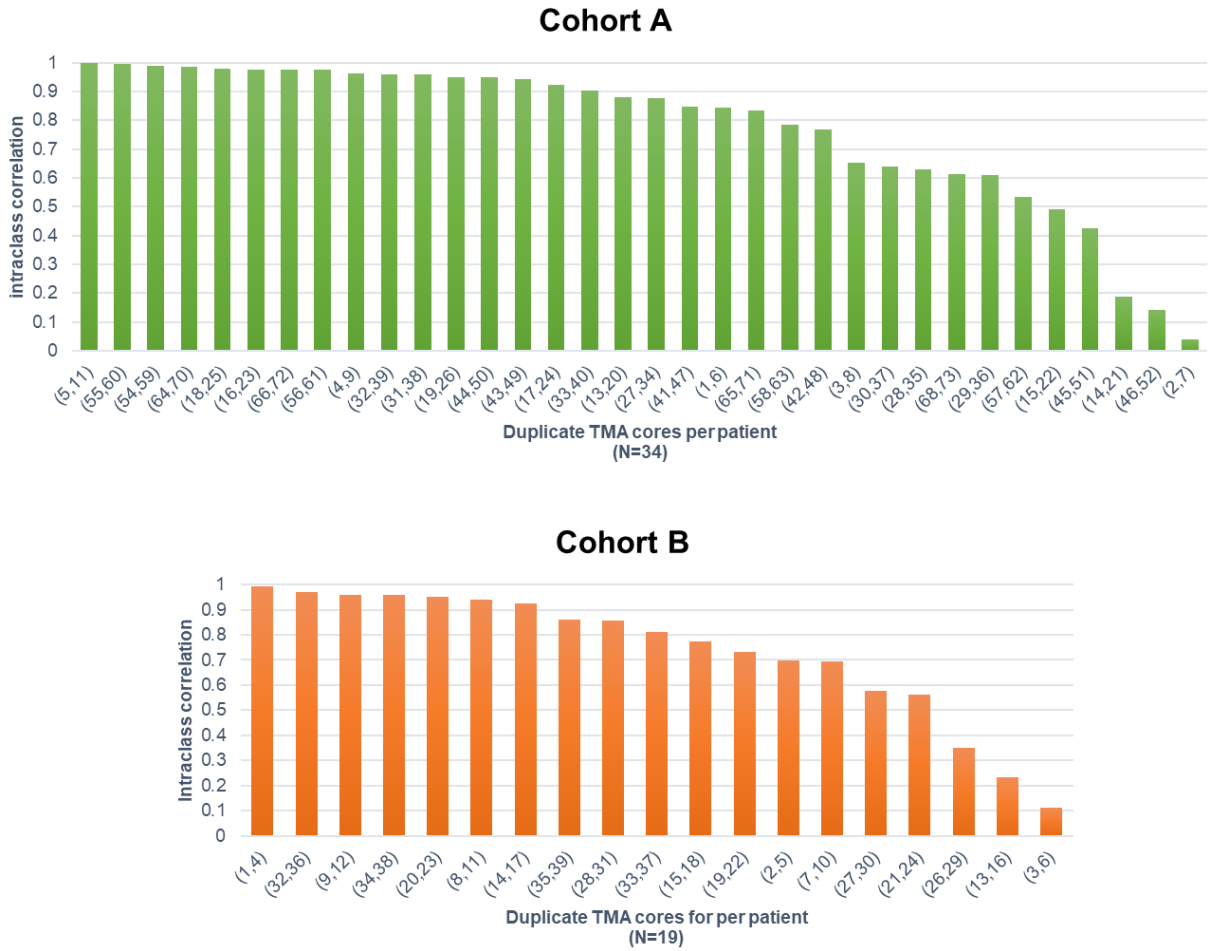

Figure 4.2 Core-to-core agreement on DSP measurements for biomarker expression counts
Graphs depicting the intraclass correlation coefficient computed for the 31 biomarkers expression counts measured in each pair of duplicated tissue microarray cores for each patient in Cohort A (top) and Cohort B (bottom) . Numbers shown in each brackets represent the tissue microarray core number of duplicates.

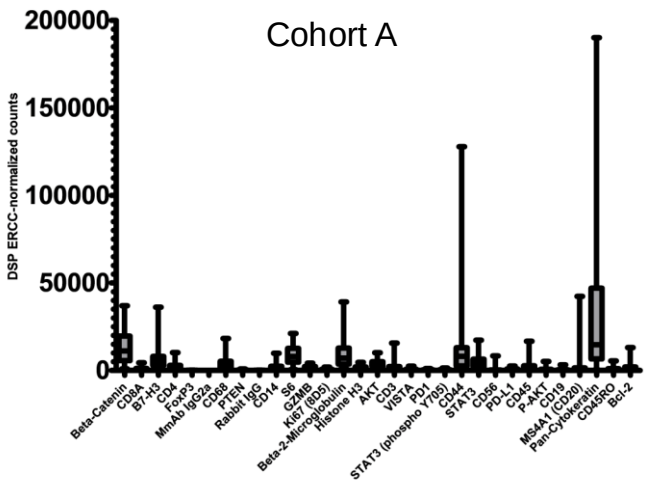

Biomarkers	DSP Median counts (IQR)
Isotype control (MmAb IgG2a)	23.6 (18.52-37.77)
Isotype control (Rabbit IgG)	79.875 (54.49-105.38)
FoxP3	91.82 (68.84-121.80)
PTEN	123.015 (73.38-194.75)
PD1	124.27 (86.16-362.48)
CD56	137.375 (92.37-285.9)
CD19	168.08 (105.74-307.53)
Ki67 (8D5)	271.96 (95.26-603.61)
CD8A	298.28 (168.15-1138.33)
MS4A1 (CD20)	333.925 (151.42-1493.90)
P-AKT	338.425 (214.67-614.11)
CD45RO	348.25 (215.25-1004.68)
VISTA	355.9 (203.30-619.90)
STAT3 (phospho Y705)	355.935 (247.84-437.17)
PD-L1	573.65 (372.64-872.15)
CD14	809.535 (440.75-2347.20)
CD45	913.495 (319.685-2699.61)
CD3	925 (319.47-2215.36)
Bcl-2	954.315 (404.63-1979.34)
CD4	1139.925 (756.9275-2915.35)
Histone H3	1513.36 (844.12-2028.49)
GZMB	1657.76 (1137.10-2239.16)
CD68	2319.255 (1549.41-5268.29)
AKT	2987.03 (2429.42-5024.98)
STAT3	3903.315 (2125.84-6451.03)
B7-H3	6098.21 (2922.57-8006.96)
Beta-2-Microglobulin	7039.69 (3666.08-12815.53)
S6	7937.145 (4715.26-12607.94)
CD44	8037.58 (2564.268-13026.063)
Beta-Catenin	11158.325 (5652.61-19637.51)
Pan-Cytokeratin	14633.85 (6563.62-47021.17)

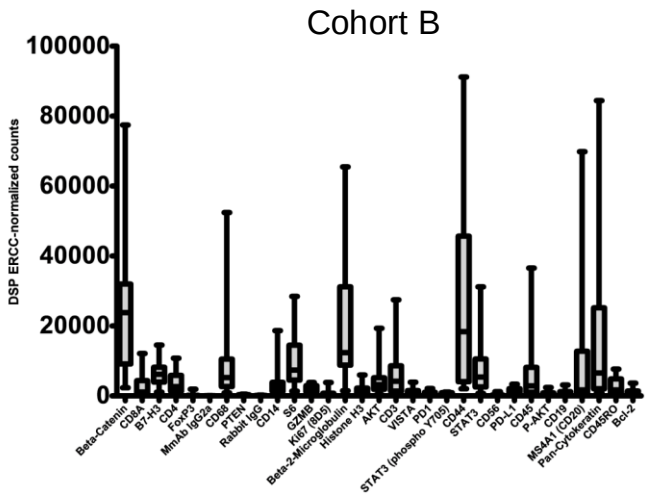

Biomarkers	DSP median counts (IQR)
Isotype control (MmAb IgG2a)	39.02 (27.27-57.63)
Isotype control (Rabbit IgG)	99.04 (72.23-147.39)
FoxP3	137.195 (99.44-182.66)
CD56	191.1975 (106.31-269.41)
PTEN	227.1475 (120.93-345.72)
CD19	368.065 (245.93-1215.64)
PD1	424.33 (155.24-1043.17)
Ki67 (8D5)	462.435 (261.59-768.73)
STAT3 (phospho Y705)	463.4825 (387.84-924.83)
P-AKT	475.7425 (252.11-866.13)
Bcl-2	680.4025 (493.19-1407.99)
VISTA	1102.2875 (368.004-1524.83)
CD8A	1102.8175 (386.21-4356.30)
Histone H3	1352.465 (884.72-2235.29)
PD-L1	1354.3925 (658.86-2095.70)
CD45RO	1705.95 (739.14-4862.07)
MS4A1 (CD20)	1722.54 (344.03-12775.21)
GZMB	1835.7125 (1104.14-2954.58)
CD14	2394.425 (1320.66-3899.49)
CD4	2656.915 (1355.98-5860.52)
CD45	2865.3675 (1043.37-8159.49)
AKT	3202.11 (1908.44-5211.51)
CD3	4185.355 (1363.36-8613.94)
CD68	5233.1575 (2670.011-10507.74)
STAT3	5399.105 (2553.42-10550.49)
B7-H3	6173.6875 (3948.85-8189.63)
Pan-Cytokeratin	6546.0125 (2048.50-25208.05)
S6	7390.95 (4503.15-14487.43)
Beta-2-Microglobulin	12374.7 (8797.75-31184.22)
CD44	18356.725 (4056.70-45684.72)
Beta-Catenin	23799.375 (9154.74-31999.41)

Figure 4.3 Distribution of DSP digital counts.
Top, boxplots illustrating DSP digital normalized counts (minimum-maximum) obtained for each DSP target in each cohort. **Bottom,** tables representing median counts and interquartile range for each DSP target in each cohort.

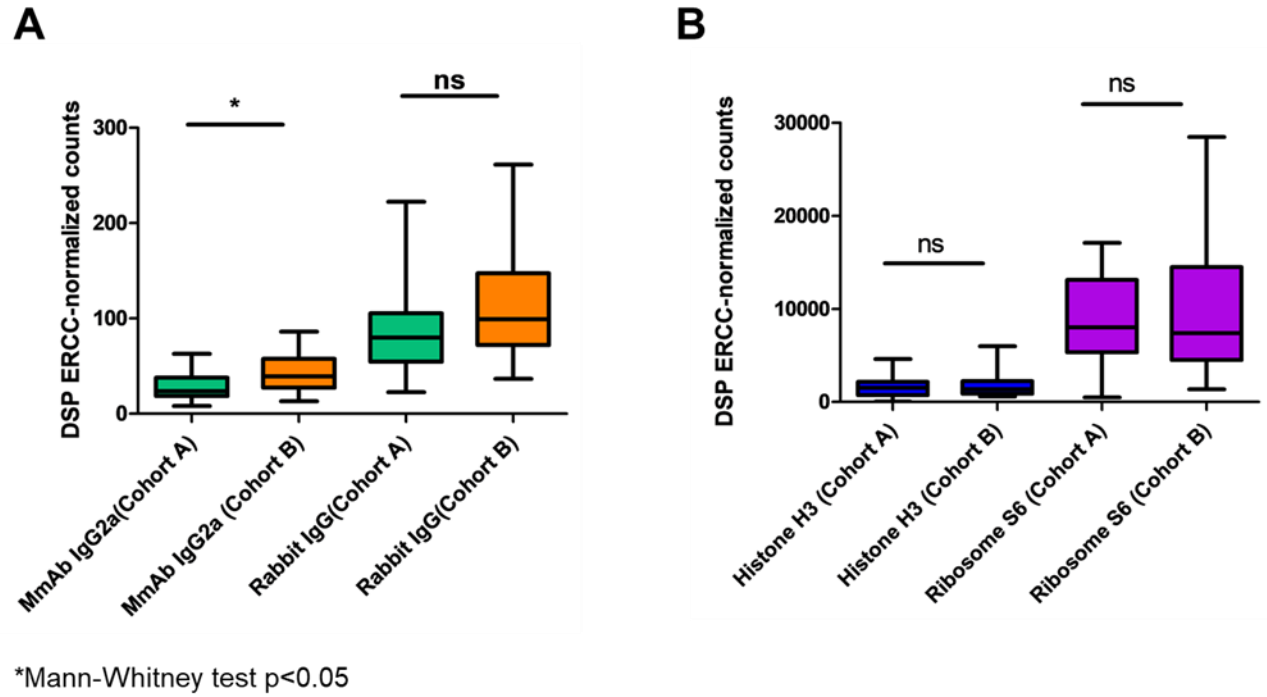

Figure 4.4 Comparison of background variance and sample cellularity between Cohort A and Cohort B.

A, boxplots depicting DSP normalized counts for each isotype antibody control (Mouse and Rabbit) in each cohort and used to evaluate background variance. **B,** boxplots illustrating DSP normalized counts for 2 reference protein biomarkers (Histone H3 and Ribosome S6) used to evaluate sample cellularity. A Mann-Whitney test was used to assess significant difference in DSP counts for isotype controls or reference proteins between Cohort A and Cohort B.
ns: non-significant *p* value

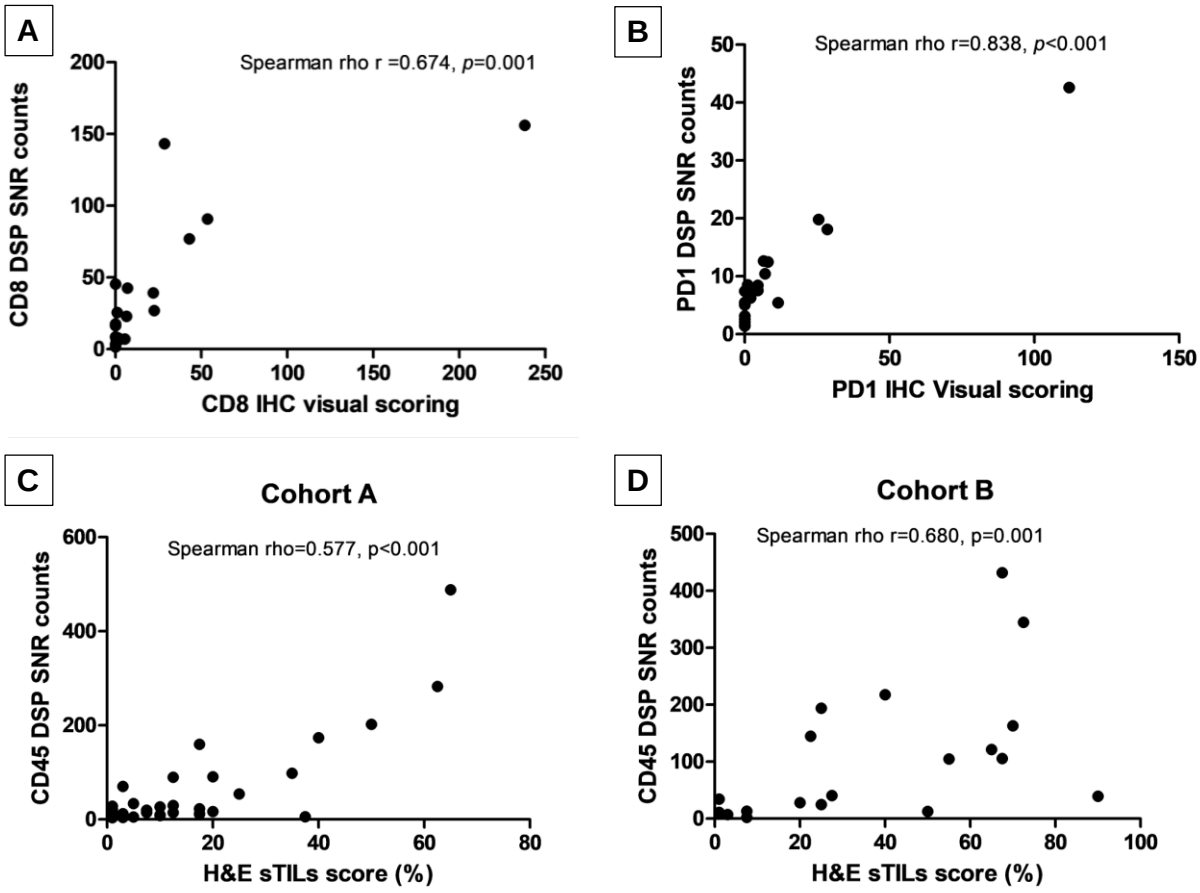

Figure 4.5 Validation of digital spatial profiling counts by immunohistochemistry and H&E staining.
Correlation between CD8 **(A)**, PD1 **(B)** digital spatial profiling counts and immunohistochemistry scores. **(C, D)** Correlation analysis between stromal tumor-infiltrating lymphocytes (sTILs) scored on H&E-stained slides and CD45 DSP counts in Cohort A and B. Spearman rho correlation coefficient and p values are displayed for each correlation analysis

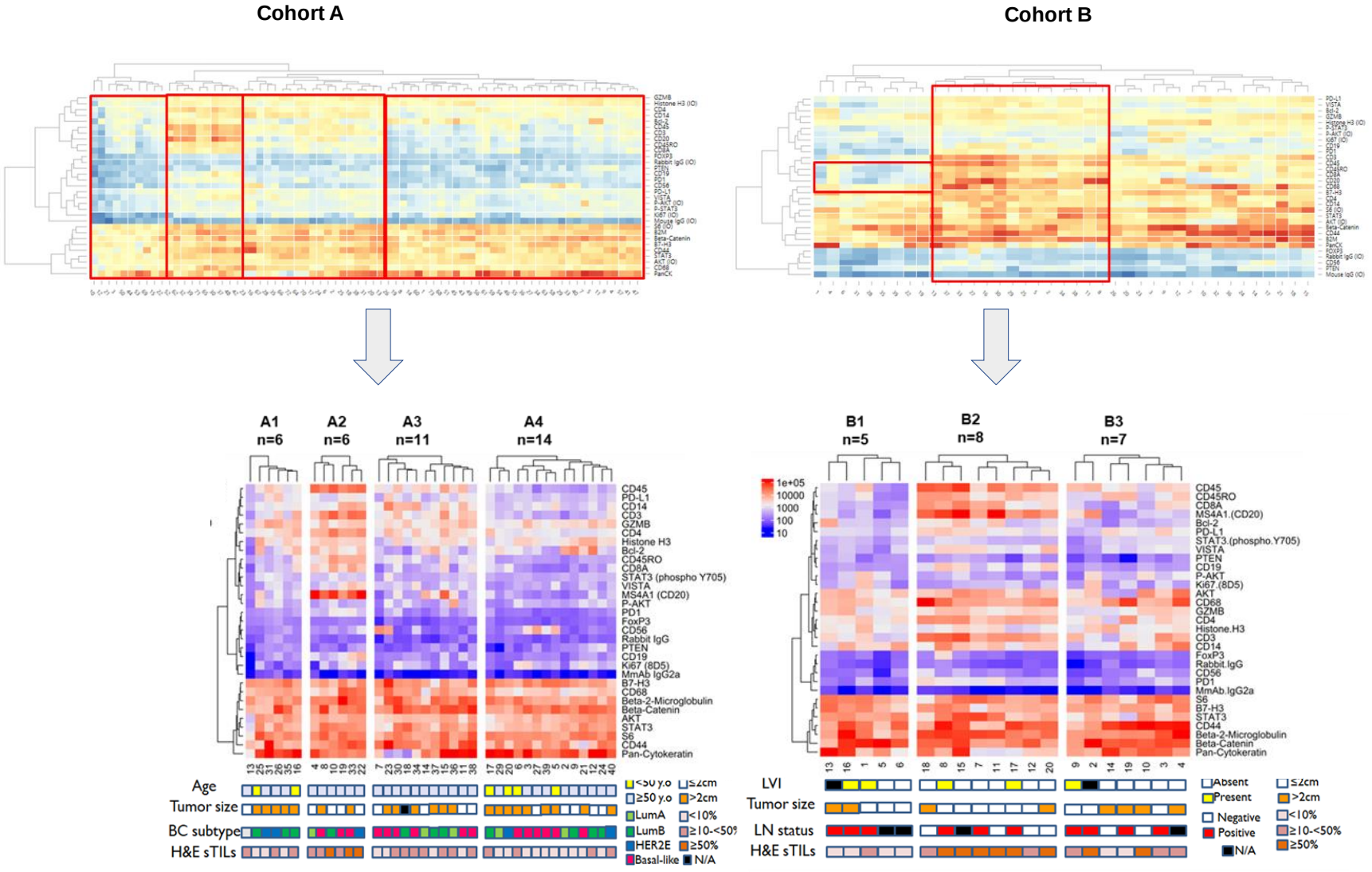
Cohort A
Cohort B
A1
n=6
A2
n=6
A3
n=11
A4
n=14
B1
n=5
B2
n=8
B3
n=7
CD45
PD-L1
CD14
CD3
GZMB
CD4
Histone H3
Bcl-2
CD45RO
CD8A
STAT3 (phospho Y705)
VISTA
MS4A1 (CD20)
P-AKT
PD1
FoxP3
CD56
Rabbit IgG
PTEN
CD19
Ki67 (8D5)
MmAb IgG2a
B7-H3
CD68
Beta-2-Microglobulin
Beta-Catenin
AKT
STAT3
S6
CD44
Pan-Cytokeratin
Age
Tumor size
BC subtype
H&E sTILs
LVI
LN status
Absent
Present
Negative
Positive
N/A
LumA
LumB
HER2E
Basal-like
<10%
≥10-<50%
≥50%
>2cm

Figure 4.6 Unsupervised hierarchical clustering of patients in Cohort A and B based on biomarker expression counts analyzed by DSP.
Top, heatmaps generated based on DSP technical control-normalized counts for each region of interest (or tissue microarray core) in each cohort. **Bottom,** DSP counts for regions of interest representing duplicated tissue microarray cores were averaged and a heatmap representing DSP counts per patient was generated for each cohort. Bottom of each heat map shows the clinico-pathological parameter associated with each patient. Color bar in the middle of the 2 heatmaps denotes the biomarkers counts.
H&E sTILs: Hematoxylin and eosin-stained stromal tumor-infiltrating lymphocytes; *LVI*: Lymphovascular invasion; *LN*: Lymph node status

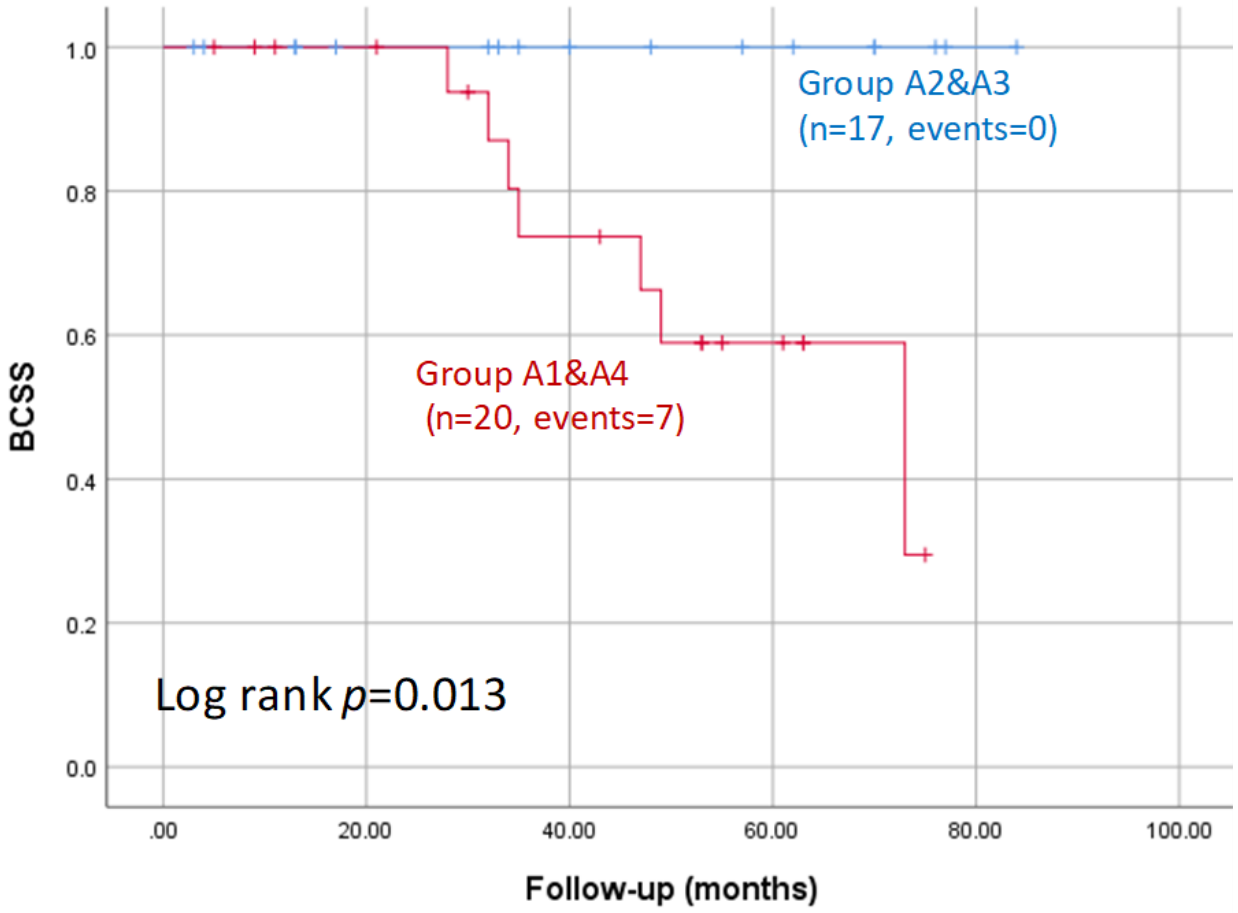

Figure 4.7 Prognostic value of DSP immune profiles in breast cancer patients from Cohort A.
Kaplan Meier curves of breast cancer-specific survival (BCSS) among patients with interpretable DSP counts (n=37/39) stratified by DSP clusters. The median follow-up time was 43 months. Number of events for each curve and the log rank *p* value of the Kaplan Meier are displayed.

Table 4.1 Cohort description

Cohort A	
Parameters	**N**
Age (yrs)	
<50	6
≥50	33 (85%)
Tumor size (cm)	
≤2	15
>2	33 (61%)
Tumor Grade	
Grade 1 or 2	12
Grade 3	27 (69%)
PAM50 subtypes	
Luminal A	6
Luminal B	12
HER2E	5
Basal-like	**15 (40%)**

Cohort B	
Parameters	**N**
Age (yrs)	
<40	4
≥40-47	16 (80%)
Tumor size (cm)	
≤2	10
>2	8 (44%)
Tumor Grade	
Grade 1 or 2	0
Grade 3	19 (100 %)
Lymph node status	
Negative	6
Positive	10 (63%)
Lymphovascular invasion	
Absent	13
Present	5 (28%)

Table 4.2 Cohort A DSP immune expression profile associations with clinicopathological parameters*

Cluster:	A1 (n=6)	A2 (n=6)	A3 (n=11)	A4 (n=14)	*p***
Age (yrs)					0.10
<50	2 (33%)	0	0	4 (29%)	
≥50	4 (67%)	6 (100%)	11 (100%)	10 (71%)	
Tumor size (cm)					0.35
≤2	1 (17%)	4 (67%)	4 (40%)	5 (36%)	
>2	5 (83%)	2 (33%)	6 (60%)	9 (64%)	
Tumor Grade					0.86
Grade 1 or 2	2 (33%)	2(33%)	4 (36%)	3 (21%)	
Grade 3	4 (67%)	4(67%)	7 (64%)	11 (79%)	
PAM50 subtypes					0.40
Luminal A	0	1 (17%)	2 (18%)	2 (14%)	
Luminal B	3 (60%)	1 (17%)	3 (27%)	4(29%)	
HER2E	2 (40%)	1 (17%)	0	2(14%)	
Basal-like	0	**3 (50%)**	**6 (55%)**	6 (43%)	
H&E sTILs level					0.001
Low (<10%)	3 (50%)	0	4(36%)	10 (71%)	
Intermediate (≥10-<50%)	3 (50%)	3 (50%)	7 (64%)	4 (29%)	
High or LPBC (≥50%)	0	3 (50%)	0	0	

LPBC: Lymphocyte-Predominant Breast Cancer

* Lymphovascular invasion and nodal status information were not available for the analysis.**Chi-square test

Table 4.3 Cohort B DSP immune expression profile associations with clinicopathological parameters

Cluster:	B1 (n=5)	B2 (n=8)	B3 (n=7)	*p**
Age				*n/a*
<50	5	8	7	
≥50	0	0	0	
Tumor grade				*n/a*
Grade 1 or 2	5	8	7	
Grade 3	0	0	0	
Tumor size (cm)				0.67
≤2	3 (60%)	4 (67%)	3 (43%)	
>2	2 (40%)	2 (33%)	4 (57%)	
Lymphovascular invasion				0.5
absent	2 (50%)	6 (75%)	5 (83%)	
present	2 (50%)	2 (25%)	1 (17%)	
Lymph node status				0.22
negative	0	4 (57%)	2 (33%)	
positive	3(100%)	3 (43%)	4 (67%)	
H&E sTILs level				0.02
Low (<10%)	4 (80%)	0	2 (29%)	
Intermediate (≥10-<50%)	1(20%)	2 (25%)	3 (43%)	
High or LPBC (≥50%)	0	6 (75%)	2 (28%)	

n/a: Not applicable
LPBC: Lymphocyte-Predominant Breast Cancer

*Chi-square test

Table 4.4 Identification of key biomarkers in breast tumors stratified by H&E sTILs levels from Cohort A and B.

Cohort A						
Biomarker	**F value**	**p**	**Post-hoc multiple comparison among H&E sTILs levels**		**LOG2 mean difference (95%CI)**	**p**
1. CD20	22.186	<0.001	LPBC	intermediate	4.78 (2.04-7.52)	<0.001
				Low	7.07 (4.33-9.81)	<0.001
			Intermediate	Low	2.29 (0.79-3.79)	0.002
2. CD45RO	21.220	<0.001	LPBC	intermediate	2.89 (1.41-4.36)	0.001
				Low	3.85 (2.38-5.33)	<0.001
			Intermediate	Low	0.96 (0.16-1.77)	0.02
3. CD3	20.144	<0.001	LPBC	intermediate	3.46 (1.58-5.34)	<0.001
				Low	4.74 (2.86-6.62)	<0.001
			Intermediate	Low	1.28 (0.25-2.31)	0.01
4. PD1	18.824	<0.001	LPBC	intermediate	1.97 (0.81-3.14)	0.001
				Low	2.81 (1.64-3.98)	<0.001
			Intermediate	Low	0.84 (0.20-1.48)	0.008
5. CD4	15.746	<0.001	LPBC	intermediate	2.29 (1.091-3.50)	<0.001
				Low	2.76 (1.55-3.96)	<0.001
			Intermediate	Low	0.46 (-0.198-1.12)	0.22
6. CD45	15.679	<0.001	LPBC	intermediate	3.46 (1.36-5.56)	0.001
				Low	4.69 (2.60-6.79)	<0.001
			Intermediate	Low	1.23 (0.08-2.38)	0.03
7. CD8A	14.466	<0.001	LPBC	intermediate	2.90 (1.09-4.71)	0.001
				Low	3.90 (2.09-5.71)	<0.001
			Intermediate	Low	0.99 (0.001-1.98)	0.05
8. CD19	13.091	<0.001	LPBC	intermediate	2.98 (1.38-4.59)	<0.001
				Low	3.34 (1.74-4.95)	<0.001
			Intermediate	Low	0.36 (-0.52-1.24)	0.58
Cohort B						
Biomarker	**F value**	**p**	**Post-hoc multiple comparison among H&E sTILs levels**		**LOG2 mean difference (95%CI)**	**p**
1. PD1	16.757	<0.001	LPBC	intermediate	0.60 (-0.46-1.65)	0.34
				Low	2.34 (1.28-3.39)	<0.001
			Intermediate	Low	1.74 (0.61-2.87)	0.003
2. CD20	14.777	<0.001	LPBC	intermediate	2.38 (-0.3-5.02)	0.08
				Low	5.60 (2.96-8.24)	<0.001
			Intermediate	Low	3.22 (0.40-6.05)	0.02
3. CD3	10.913	0.001	LPBC	intermediate	0.07 (-1.62-1.77)	0.99
				Low	2.82 (1.13-4.52)	0.001
			Intermediate	Low	2.75 (0.93-4.56)	0.003
4. CD45	1.455	0.001	LPBC	intermediate	0.51 (-1.53-2.56)	0.80
				Low	3.48 (1.43-5.52)	0.001
			Intermediate	Low	2.97 (0.78-5.15)	0.008

LPBC: Lymphocyte-Predominant Breast Cancer

Table 4.5 Assessment of the 4-biomarker signature for detecting immune-enriched breast tumors

	AUC (95% CI)	Hazard ratio for breast cancer-specific survival (95%CI), p value
4-biomarker signature in Cohort A	0.828 (0.697-0.962)	0.65 (0.39-1.09), p=0.10
4-biomarker signature in Cohort B	1.00	N/A

Predictive model: 4.051+ (0.035*[CD3 DSP counts]) + (1.412*[PD1 DSP counts])-(0.079*[CD45 DSP counts])+(0.055*[CD20 DSP counts])
AUC: Area under the receiver operating characteristics curve
N/A: No outcome data was available to compute hazard ratios in Cohort B

Table 4.6 List of biomarkers in the commercially available DSP immuno-oncology panel that will be used for the study on MA.5 clinical trial

Biomarker module	Biomarker list
Immune cell profiling core (20 markers)	Beta-2-microglobulin, CD11c, CD20, CD3, CD4, CD45, CD56, CD68, CD8, CTLA4, GZMB, Histone H3, Ki-67, PD1, PD-L1, Pan-cytokeratin, HLA-DR, SMA, Fibronectin, TGF-B
Immuno-oncology drug target module (11 markers)	4-1BB, B7-H4, LAG-3, OX40L, TIM-3, VISTA, ARG1, B7-H3, GITR, IDO-1, STING
Immune activation status module (10 markers)	CD127, CD25, CD80, CD86, ICOS, PD-L2, CD40, CD40L, CD27, CD44
Immune cell typing module (8 markers)	CD45RO, FOXP3, CD34, CD66b, gamma delta TCR, CD14, FAPalpha, CD163
Pan-tumor module (7 markers)	MART1, NY-ESO-1, S100B, Bcl-2, EpCAM, Her2/ERBB2, PTEN

Chapter 5: Overall conclusions and future directions

5.1 Summary of findings

Although breast cancer has not been generally viewed as an immunogenic cancer, the body of work presented in this thesis and accumulating evidence from others illustrates that this view is only applicable to a portion of breast cancers. Out of 3,992 breast cancer pathology specimens profiled in this thesis, hormone receptor negative breast cancers (specifically HER2+ and basal-like breast cancer subtypes) were frequently enriched in immune infiltrates. The immune populations evaluated in **Chapter 2** (LAG-3) and **Chapter 3** (TIM-3) express immunotherapy targets for agents currently in early phase clinical trials, guided by the remarkable results reported from agents targeting the PD-1/PD-L1 pathway in multiple cancer types. Thus, this work provides important pre-clinical data on the selection of breast cancer patients amenable to testing such new immunotherapy agents.

Although **Chapter 2** and **Chapter 3** are quite similar, there were some differences in statistical analyses presented in each chapter such as conducting an interaction test between LAG-3 and breast cancer intrinsic subtypes for predicting survival in **Chapter 2** and prognostic analyses of TIM-3 (**Chapter 3**) using overall survival as an endpoint. The different statistical analyses were provided to address reviewers' comments for each publication.

Predictive biomarkers for cancer immunotherapy are still being investigated and results from immune checkpoint clinical trials point to multiple candidates rather than a single biomarker. In **Chapter 4**, I profiled the immune expression of 57 breast cancers in a discovery-based study using breast cancer tissue microarrays to test a new multiplex technology called digital spatial profiling by Nanostring. This technology simultaneously and quantitatively assessed the expression of 31 biomarkers, representing predominantly an immuno-oncology

panel. I identified a signature of 4 biomarkers highly expressed in immune-enriched breast cancers. In addition, I present, at the end of **Chapter 4**, a proposal to apply the digital spatial profiling technology onto breast cancer clinical trial specimens to validate the prognostic aspect of this signature and to assess the predictive value of the 4-biomarker signature for response to anthracyclines, a type of chemotherapy drug with immune-modulating effects. Results from the proposed study will serve as a framework for evaluating the predictive value of immune biomarkers for response to immune checkpoint inhibitors in breast cancer immunotherapy clinical trials.

5.1.1 Perspectives for LAG-3-targeted agents

In **Chapter 2**, I investigated the presence of a newly recognized targetable immune checkpoint called LAG-3 in a large cohort of breast cancer patients. LAG-3 expression on tumor-infiltrating lymphocytes was enriched in basal-like breast cancers, highly associated with breast cancers positive for PD-L1 expression and was an independent favorable prognostic factor. This work constitutes the largest evaluation of the expression of LAG-3, PD-1, and PD-L1 at the protein level in breast cancer excision specimens.

A recent single-cell sequencing study of breast cancer excision specimens identified *LAG3* gene expression as one of the characteristic markers for tissue resident memory T cells, cells that are thought to be the key players in mediating the effects of immune checkpoint inhibitors[275]. LAG-3 can also be secreted in a soluble form with activating or inhibitory function on various immune populations but its cell surface expression on effector T cells leads to exhaustion[134,276] . This apparent contradiction may be partly due to the variety of LAG-3 ligands[276]. There is an ongoing Phase II clinical trial evaluating the efficacy of a LAG-3 agonist (IMP321) in hormone receptor-positive breast cancer patients which reported (as interim-results)

that no dose limiting toxicities in the 15 patients enrolled were observed[277] (NCT02614833). At the time of this writing, there were few anti-LAG-3 antagonistic agents being evaluated in clinical trials. An early report from a phase I/II clinical trial evaluated an anti-LAG3 agent (LAG525) alone or in combination with an anti-PD1 agent in advanced malignancies, and found that the combination was well tolerated with promising signs of response in triple negative breast cancer patients[278] .

The enthusiasm for finding new immune checkpoint targets for cancer immunotherapy and early results from LAG3 clinical trials point to LAG3 as a promising new candidate in breast cancer immunotherapy. Furthermore, results presented in **Chapter 2** can help guide combination strategies with other immune checkpoint targets.

5.1.2 Perspectives for TIM-3-targeted agents

In **Chapter 3**, I evaluated the expression of TIM-3, an emerging immunotherapy target, on tumor-infiltrating lymphocytes in our large cohort of 3,992 breast cancer patients. I found that in contrast to LAG-3, breast cancers infiltrated with TIM-3+ tumor-infiltrating lymphocytes were not particularly associated with the presence of a specific immune checkpoint biomarker but rather were strongly associated with all of them (PD-1, LAG-3, PD-L1). Moreover, TIM-3 remained an independent favorable prognostic factor in a multivariate analysis that included H&E sTILs as a covariate.

Some properties that contribute to make TIM-3 unique include its expression on several immune populations (resident memory T cells, macrophages and dendritic cells) and having multiple ligands (Galectin-9, CEACAM-1, Phosphatidyl serine)[234,275]. The significance of TIM-3 as an immune checkpoint was again put in evidence in a recent study that identified rare germline mutations in *HAVCR2* (TIM-3 coding gene) associated with TIM-3 deficiency that lead

to hematological malignancies in humans[279]. Results from early phase clinical trials of various anti-TIM-3 agents are yet to be published.

5.1.3 Digital Spatial profiling

Chapter 4 is quite distinct from the other chapters as it describes the application of a new technology, called digital spatial profiling, that I tested on two distinct, smaller tissue microarray cohorts. As the immuno-oncology field continues to expand and a variety of clinically relevant immune biomarkers are discovered, it is becoming important to have the tools to identify and ideally quantify multiple markers within formalin-fixed, paraffin-embedded patient tumor tissues removed at biopsy or surgery.

Immunohistochemistry is the workhorse in research or clinical pathology and although it is a simple methodology as an *in situ* detection system, conventional multiplex immunohistochemistry is restricted to antibody species that can work together sequentially as primary and secondary antibodies[260]. In contrast, the latest fluorescent multiplex immunohistochemistry systems (such as the Opal system) circumvent the restriction of antibody species by employing sequential antibody-directed attachment of fluorophores to the target epitopes[253]. However, this necessitates repeated antibody stripping and sequential hybridization steps that are unwieldy to run at scale; the most elaborate Opal detection system can measure up to six target biomarkers and thus would serve best as a validation tool for short lists of key biomarkers discovered by more highly multiplexed methods such as Nanostring-based digital spatial profiling. To measure multiple biomarkers quantitatively while preserving their spatial distribution in tumor tissue, conventional or fluorescent multiplex immunohistochemistry offers more highly resolved spatial distribution, but not such precise quantitative measurement.

Mass spectrometry imaging such as mass cytometry is another *in situ* multiplex detection system that offers quantitative measurement. It uses antibodies labeled with elemental isotopes thereby bypassing the requirement for different species' primary antibodies and fluorophore emission spectra when assaying multiple biomarkers and has recently been used to evaluate immune infiltrates in breast cancer tissue microarrays[254] but the technology requires the building of algorithms for multispectral imaging.

The digital spatial profiling technology allowed me to generate immune profiles of 57 breast cancer patients by analyzing the expression of 31 biomarkers using tissue microarray cores. Although there were only 4 out of 31 biomarkers that significantly distinguished immune-enriched from immune-desert breast tumors in the initial data sets, there were interesting trends observed with additional biomarkers such as beta-catenin and B7-H3 which show the value of assessing multiple biomarkers at once. As outlined in the proposal study at the end of **Chapter 4**, the clinical value of the 4-biomarker signature is intended, in future studies, to be evaluated using clinical trials specimens from breast cancer patients that received immune-modulating therapies including immune checkpoint inhibitors.

5.2 Significance of the research and perspectives for the future of breast cancer immunotherapy

Immunotherapy for breast cancer is just at its beginning and results from therapeutic agents being evaluated in ongoing clinical trials will provide more insights into factors enabling or preventing breast tumor responses to immunotherapies. This body of work brings a significant contribution into guiding the selection of breast cancer patients for clinical evaluation of emerging targets in immunotherapy. Furthermore, **Chapter 4** provides a framework and tools for

efficiently and quantitatively profiling immune expression in breast cancers by simultaneously screening multiple biomarkers using only a tiny fraction of tissue in precious tumor samples. As I demonstrate in this thesis, current strategies for immune restoration appear most applicable to a fraction of immunogenic breast tumors. Most breast cancers have low immunogenicity (i.e., hormone receptor positive breast cancers) and will likely require different or a variation of current therapeutic strategies such as immune-modulating combination treatments. An example of that approach includes cyclin-dependent kinase 4/6 inhibitors that have shown impressive results in breast cancer clinical trials and have now been approved by health authorities[280]. A recent study showed that in addition to inhibiting breast cancer growth, abemaciclib, a cyclin-dependent kinase 4/6 inhibitor, provoked anti-tumor innate and adaptive immune responses in mice and thus provides pre-clinical evidence that supports combining CDK4/6 inhibition with anti-PD-L1 agents[281]. This strategy is being evaluated in early phase I/II clinical trials (NCT01676753; NCT02778685; NCT02779751; NCT03294694; NCT03573648) with promising preliminary results already reported in conference proceedings[280]. Additional immune-modulating combination treatments strategies can include radiotherapy and DNA-demethylating agents[282].

In conclusion, the body of work and studies presented in this thesis contributes to the rapidly-expanding field anti-tumor immunity in breast cancer and supports the clinical evaluation of immune checkpoint combination immunotherapy that includes LAG-3 and TIM-3-targeted agents. The variety of therapeutic strategies and targets in cancer immunotherapy will continue to broaden; all with the hope of achieving personalized immunotherapy options for breast cancer patients, likely facilitated by technologies such as DSP.

Bibliography

1. Perou, C.M., Sorlie, T., Eisen, M.B., van de Rijn, M., Jeffrey, S.S., Rees, C.A., Pollack, J.R., Ross, D.T., Johnsen, H., Akslen, L.A., Fluge, O., Pergamenschikov, A., Williams, C., Zhu, S.X., Lonning, P.E., Borresen-Dale, A.L., Brown, P.O. & Botstein, D. Molecular portraits of human breast tumours. *Nature* **406**, 747-752 (2000).
2. Curtis, C., Shah, S.P., Chin, S.F., Turashvili, G., Rueda, O.M., Dunning, M.J., Speed, D., Lynch, A.G., Samarajiwa, S., Yuan, Y., Graf, S., Ha, G., Haffari, G., Bashashati, A., Russell, R., McKinney, S., Group, M., Langerod, A., Green, A., Provenzano, E., Wishart, G., Pinder, S., Watson, P., Markowetz, F., Murphy, L., Ellis, I., Purushotham, A., Borresen-Dale, A.L., Brenton, J.D., Tavare, S., Caldas, C. & Aparicio, S. The genomic and transcriptomic architecture of 2,000 breast tumours reveals novel subgroups. *Nature* **486**, 346-352 (2012).
3. Goldhirsch, A., Winer, E.P., Coates, A.S., Gelber, R.D., Piccart-Gebhart, M., Thurlimann, B. & Senn, H.J. Personalizing the treatment of women with early breast cancer: highlights of the St Gallen International Expert Consensus on the Primary Therapy of Early Breast Cancer 2013. *Ann Oncol* **24**, 2206-2223 (2013).
4. Comprehensive molecular portraits of human breast tumours. *Nature* **490**, 61-70 (2012).
5. Enerly, E., Steinfeld, I., Kleivi, K., Leivonen, S.K., Aure, M.R., Russnes, H.G., Ronneberg, J.A., Johnsen, H., Navon, R., Rodland, E., Makela, R., Naume, B., Perala, M., Kallioniemi, O., Kristensen, V.N., Yakhini, Z. & Borresen-Dale, A.L. miRNA-mRNA integrated analysis reveals roles for miRNAs in primary breast tumors. *PLoS One* **6**, e16915 (2011).
6. Mertins, P., Mani, D.R., Ruggles, K.V., Gillette, M.A., Clauser, K.R., Wang, P., Wang, X., Qiao, J.W., Cao, S., Petralia, F., Kawaler, E., Mundt, F., Krug, K., Tu, Z., Lei, J.T., Gatza, M.L., Wilkerson, M., Perou, C.M., Yellapantula, V., Huang, K.L., Lin, C., McLellan, M.D., Yan, P., Davies, S.R., Townsend, R.R., Skates, S.J., Wang, J., Zhang, B., Kinsinger, C.R., Mesri, M., Rodriguez, H., Ding, L., Paulovich, A.G., Fenyo, D., Ellis, M.J. & Carr, S.A. Proteogenomics connects somatic mutations to signalling in breast cancer. *Nature* **534**, 55-62 (2016).
7. Sorlie, T., Perou, C.M., Tibshirani, R., Aas, T., Geisler, S., Johnsen, H., Hastie, T., Eisen, M.B., van de Rijn, M., Jeffrey, S.S., Thorsen, T., Quist, H., Matese, J.C., Brown, P.O., Botstein, D., Lonning, P.E. & Borresen-Dale, A.L. Gene expression patterns of breast carcinomas distinguish tumor subclasses with clinical implications. *Proc Natl Acad Sci U S A* **98**, 10869-10874 (2001).
8. Sorlie, T., Tibshirani, R., Parker, J., Hastie, T., Marron, J.S., Nobel, A., Deng, S., Johnsen, H., Pesich, R., Geisler, S., Demeter, J., Perou, C.M., Lonning, P.E., Brown, P.O., Borresen-Dale, A.L. & Botstein, D. Repeated observation of breast tumor subtypes in independent gene expression data sets. *Proc Natl Acad Sci U S A* **100**, 8418-8423 (2003).
9. Hu, Z., Fan, C., Oh, D.S., Marron, J.S., He, X., Qaqish, B.F., Livasy, C., Carey, L.A., Reynolds, E., Dressler, L., Nobel, A., Parker, J., Ewend, M.G., Sawyer, L.R., Wu, J., Liu, Y., Nanda, R., Tretiakova, M., Ruiz Orrico, A., Dreher, D., Palazzo, J.P., Perreard, L.,

Nelson, E., Mone, M., Hansen, H., Mullins, M., Quackenbush, J.F., Ellis, M.J., Olopade, O.I., Bernard, P.S. & Perou, C.M. The molecular portraits of breast tumors are conserved across microarray platforms. *BMC genomics* **7**, 96 (2006).

10. Prat, A., Pineda, E., Adamo, B., Galvan, P., Fernandez, A., Gaba, L., Diez, M., Viladot, M., Arance, A. & Munoz, M. Clinical implications of the intrinsic molecular subtypes of breast cancer. *Breast (Edinburgh, Scotland)* **24 Suppl 2**, S26-35 (2015).
11. Prat, A. & Perou, C.M. Deconstructing the molecular portraits of breast cancer. *Molecular oncology* **5**, 5-23 (2011).
12. Parker, J.S., Mullins, M., Cheang, M.C., Leung, S., Voduc, D., Vickery, T., Davies, S., Fauron, C., He, X., Hu, Z., Quackenbush, J.F., Stijleman, I.J., Palazzo, J., Marron, J.S., Nobel, A.B., Mardis, E., Nielsen, T.O., Ellis, M.J., Perou, C.M. & Bernard, P.S. Supervised risk predictor of breast cancer based on intrinsic subtypes. *J Clin Oncol* **27**, 1160-1167 (2009).
13. Rouzier, R., Perou, C.M., Symmans, W.F., Ibrahim, N., Cristofanilli, M., Anderson, K., Hess, K.R., Stec, J., Ayers, M., Wagner, P., Morandi, P., Fan, C., Rabiul, I., Ross, J.S., Hortobagyi, G.N. & Pusztai, L. Breast cancer molecular subtypes respond differently to preoperative chemotherapy. *Clin Cancer Res* **11**, 5678-5685 (2005).
14. Cheang, M.C., Voduc, K.D., Tu, D., Jiang, S., Leung, S., Chia, S.K., Shepherd, L.E., Levine, M.N., Pritchard, K.I., Davies, S., Stijleman, I.J., Davis, C., Ebbert, M.T., Parker, J.S., Ellis, M.J., Bernard, P.S., Perou, C.M. & Nielsen, T.O. Responsiveness of intrinsic subtypes to adjuvant anthracycline substitution in the NCIC.CTG MA.5 randomized trial. *Clin Cancer Res* **18**, 2402-2412 (2012).
15. Aure, M.R., Vitelli, V., Jernstrom, S., Kumar, S., Krohn, M., Due, E.U., Haukaas, T.H., Leivonen, S.K., Vollan, H.K., Luders, T., Rodland, E., Vaske, C.J., Zhao, W., Moller, E.K., Nord, S., Giskeodegard, G.F., Bathen, T.F., Caldas, C., Tramm, T., Alsner, J., Overgaard, J., Geisler, J., Bukholm, I.R., Naume, B., Schlichting, E., Sauer, T., Mills, G.B., Karesen, R., Maelandsmo, G.M., Lingjaerde, O.C., Frigessi, A., Kristensen, V.N., Borresen-Dale, A.L. & Sahlberg, K.K. Integrative clustering reveals a novel split in the luminal A subtype of breast cancer with impact on outcome. *Breast Cancer Res* **19**, 44 (2017).
16. Mukherjee, A., Russell, R., Chin, S.F., Liu, B., Rueda, O.M., Ali, H.R., Turashvili, G., Mahler-Araujo, B., Ellis, I.O., Aparicio, S., Caldas, C. & Provenzano, E. Associations between genomic stratification of breast cancer and centrally reviewed tumour pathology in the METABRIC cohort. *NPJ breast cancer* **4**, 5 (2018).
17. Hammond, M.E., Hayes, D.F., Dowsett, M., Allred, D.C., Hagerty, K.L., Badve, S., Fitzgibbons, P.L., Francis, G., Goldstein, N.S., Hayes, M., Hicks, D.G., Lester, S., Love, R., Mangu, P.B., McShane, L., Miller, K., Osborne, C.K., Paik, S., Perlmutter, J., Rhodes, A., Sasano, H., Schwartz, J.N., Sweep, F.C., Taube, S., Torlakovic, E.E., Valenstein, P., Viale, G., Visscher, D., Wheeler, T., Williams, R.B., Wittliff, J.L. & Wolff, A.C. American Society of Clinical Oncology/College of American Pathologists guideline recommendations for immunohistochemical testing of estrogen and progesterone receptors in breast cancer (unabridged version). *Archives of pathology & laboratory medicine* **134**, e48-72 (2010).
18. Wolff, A.C., Hammond, M.E., Hicks, D.G., Dowsett, M., McShane, L.M., Allison, K.H., Allred, D.C., Bartlett, J.M., Bilous, M., Fitzgibbons, P., Hanna, W., Jenkins, R.B.,

Mangu, P.B., Paik, S., Perez, E.A., Press, M.F., Spears, P.A., Vance, G.H., Viale, G. & Hayes, D.F. Recommendations for human epidermal growth factor receptor 2 testing in breast cancer: American Society of Clinical Oncology/College of American Pathologists clinical practice guideline update. *J Clin Oncol* **31**, 3997-4013 (2013).
19. Goldhirsch, A., Wood, W.C., Coates, A.S., Gelber, R.D., Thurlimann, B. & Senn, H.J. Strategies for subtypes--dealing with the diversity of breast cancer: highlights of the St. Gallen International Expert Consensus on the Primary Therapy of Early Breast Cancer 2011. *Ann Oncol* **22**, 1736-1747 (2011).
20. Nielsen, T.O., Hsu, F.D., Jensen, K., Cheang, M., Karaca, G., Hu, Z., Hernandez-Boussard, T., Livasy, C., Cowan, D., Dressler, L., Akslen, L.A., Ragaz, J., Gown, A.M., Gilks, C.B., van de Rijn, M. & Perou, C.M. Immunohistochemical and clinical characterization of the basal-like subtype of invasive breast carcinoma. *Clin Cancer Res* **10**, 5367-5374 (2004).
21. Perou, C.M. Molecular stratification of triple-negative breast cancers. *The oncologist* **15 Suppl 5**, 39-48 (2010).
22. Lehmann, B.D., Jovanovic, B., Chen, X., Estrada, M.V., Johnson, K.N., Shyr, Y., Moses, H.L., Sanders, M.E. & Pietenpol, J.A. Refinement of Triple-Negative Breast Cancer Molecular Subtypes: Implications for Neoadjuvant Chemotherapy Selection. *PLoS One* **11**, e0157368 (2016).
23. Burstein, M.D., Tsimelzon, A., Poage, G.M., Covington, K.R., Contreras, A., Fuqua, S.A., Savage, M.I., Osborne, C.K., Hilsenbeck, S.G., Chang, J.C., Mills, G.B., Lau, C.C. & Brown, P.H. Comprehensive genomic analysis identifies novel subtypes and targets of triple-negative breast cancer. *Clin Cancer Res* **21**, 1688-1698 (2015).
24. Garrido-Castro, A.C., Lin, N.U. & Polyak, K. Insights into Molecular Classifications of Triple-Negative Breast Cancer: Improving Patient Selection for Treatment. *Cancer discovery* (2019).
25. Anampa, J., Makower, D. & Sparano, J.A. Progress in adjuvant chemotherapy for breast cancer: an overview. *BMC Med* **13**, 195 (2015).
26. Waks, A.G. & Winer, E.P. Breast Cancer Treatment: A Review. *Jama* **321**, 288-300 (2019).
27. Nielsen, T.O., Jensen, M.B., Burugu, S., Gao, D., Jorgensen, C.L., Balslev, E. & Ejlertsen, B. High-Risk Premenopausal Luminal A Breast Cancer Patients Derive no Benefit from Adjuvant Cyclophosphamide-based Chemotherapy: Results from the DBCG77B Clinical Trial. *Clin Cancer Res* **23**, 946-953 (2017).
28. Munzone, E., Curigliano, G., Burstein, H.J., Winer, E.P. & Goldhirsch, A. CMF revisited in the 21st century. *Ann Oncol* **23**, 305-311 (2012).
29. Pritchard, K.I., Messersmith, H., Elavathil, L., Trudeau, M., O'Malley, F. & Dhesy-Thind, B. HER-2 and topoisomerase II as predictors of response to chemotherapy. *J Clin Oncol* **26**, 736-744 (2008).
30. Nielsen, K.V., Muller, S., Moller, S., Schonau, A., Balslev, E., Knoop, A.S. & Ejlertsen, B. Aberrations of ERBB2 and TOP2A genes in breast cancer. *Molecular oncology* **4**, 161-168 (2010).
31. Di Leo, A., Desmedt, C., Bartlett, J.M., Piette, F., Ejlertsen, B., Pritchard, K.I., Larsimont, D., Poole, C., Isola, J., Earl, H., Mouridsen, H., O'Malley, F.P., Cardoso, F., Tanner, M., Munro, A., Twelves, C.J., Sotiriou, C., Shepherd, L., Cameron, D., Piccart,

M.J., Buyse, M. & Group, H.T.A.M.-a.S. HER2 and TOP2A as predictive markers for anthracycline-containing chemotherapy regimens as adjuvant treatment of breast cancer: a meta-analysis of individual patient data. *The Lancet. Oncology* **12**, 1134-1142 (2011).
32. Asleh, K., Lyck Carstensen, S., Tykjaer Jorgensen, C.L., Burugu, S., Gao, D., Won, J.R., Jensen, M.B., Balslev, E., Laenkholm, A.V., Nielsen, D.L., Ejlertsen, B. & Nielsen, T.O. Basal biomarkers nestin and INPP4B predict gemcitabine benefit in metastatic breast cancer: Samples from the phase III SBG0102 clinical trial. *International journal of cancer* (2018).
33. Fujii, T., Le Du, F., Xiao, L., Kogawa, T., Barcenas, C.H., Alvarez, R.H., Valero, V., Shen, Y. & Ueno, N.T. Effectiveness of an Adjuvant Chemotherapy Regimen for Early-Stage Breast Cancer: A Systematic Review and Network Meta-analysis. *JAMA Oncol* **1**, 1311-1318 (2015).
34. Nasrazadani, A., Thomas, R.A., Oesterreich, S. & Lee, A.V. Precision Medicine in Hormone Receptor-Positive Breast Cancer. *Front Oncol* **8**, 144 (2018).
35. Costa, R.B., Kurra, G., Greenberg, L. & Geyer, C.E. Efficacy and cardiac safety of adjuvant trastuzumab-based chemotherapy regimens for HER2-positive early breast cancer. *Ann Oncol* **21**, 2153-2160 (2010).
36. Lehmann, B.D., Bauer, J.A., Chen, X., Sanders, M.E., Chakravarthy, A.B., Shyr, Y. & Pietenpol, J.A. Identification of human triple-negative breast cancer subtypes and preclinical models for selection of targeted therapies. *J Clin Invest* **121**, 2750-2767 (2011).
37. Sharma, P., Klemp, J.R., Kimler, B.F., Mahnken, J.D., Geier, L.J., Khan, Q.J., Elia, M., Connor, C.S., McGinness, M.K., Mammen, J.M., Wagner, J.L., Ward, C., Ranallo, L., Knight, C.J., Stecklein, S.R., Jensen, R.A., Fabian, C.J. & Godwin, A.K. Germline BRCA mutation evaluation in a prospective triple-negative breast cancer registry: implications for hereditary breast and/or ovarian cancer syndrome testing. *Breast Cancer Res Treat* **145**, 707-714 (2014).
38. Lee, A. & Djamgoz, M.B.A. Triple negative breast cancer: Emerging therapeutic modalities and novel combination therapies. *Cancer treatment reviews* **62**, 110-122 (2018).
39. Geenen, J.J.J., Linn, S.C., Beijnen, J.H. & Schellens, J.H.M. PARP Inhibitors in the Treatment of Triple-Negative Breast Cancer. *Clinical pharmacokinetics* **57**, 427-437 (2018).
40. Ribatti, D. The concept of immune surveillance against tumors. The first theories. *Oncotarget* **8**, 7175-7180 (2017).
41. Hanahan, D. & Weinberg, R.A. Hallmarks of cancer: the next generation. *Cell* **144**, 646-674 (2011).
42. Heinrich, E.L., Walser, T.C., Krysan, K., Liclican, E.L., Grant, J.L., Rodriguez, N.L. & Dubinett, S.M. The inflammatory tumor microenvironment, epithelial mesenchymal transition and lung carcinogenesis. *Cancer Microenviron* **5**, 5-18 (2012).
43. Pardoll, D.M. Immunology beats cancer: a blueprint for successful translation. *Nat Immunol* **13**, 1129-1132 (2012).
44. Kelderman, S. & Kvistborg, P. Tumor antigens in human cancer control. *Biochimica et biophysica acta* **1865**, 83-89 (2016).

45. Angelova, M., Mlecnik, B., Vasaturo, A., Bindea, G., Fredriksen, T., Lafontaine, L., Buttard, B., Morgand, E., Bruni, D., Jouret-Mourin, A., Hubert, C., Kartheuser, A., Humblet, Y., Ceccarelli, M., Syed, N., Marincola, F.M., Bedognetti, D., Van den Eynde, M. & Galon, J. Evolution of Metastases in Space and Time under Immune Selection. *Cell* **175**, 751-765 e716 (2018).
46. Beatty, G.L. & Gladney, W.L. Immune escape mechanisms as a guide for cancer immunotherapy. *Clin Cancer Res* **21**, 687-692 (2015).
47. Alexandrov, L.B., Nik-Zainal, S., Wedge, D.C., Aparicio, S.A., Behjati, S., Biankin, A.V., Bignell, G.R., Bolli, N., Borg, A., Borresen-Dale, A.L., Boyault, S., Burkhardt, B., Butler, A.P., Caldas, C., Davies, H.R., Desmedt, C., Eils, R., Eyfjord, J.E., Foekens, J.A., Greaves, M., Hosoda, F., Hutter, B., Ilicic, T., Imbeaud, S., Imielinski, M., Jager, N., Jones, D.T., Jones, D., Knappskog, S., Kool, M., Lakhani, S.R., Lopez-Otin, C., Martin, S., Munshi, N.C., Nakamura, H., Northcott, P.A., Pajic, M., Papaemmanuil, E., Paradiso, A., Pearson, J.V., Puente, X.S., Raine, K., Ramakrishna, M., Richardson, A.L., Richter, J., Rosenstiel, P., Schlesner, M., Schumacher, T.N., Span, P.N., Teague, J.W., Totoki, Y., Tutt, A.N., Valdes-Mas, R., van Buuren, M.M., van 't Veer, L., Vincent-Salomon, A., Waddell, N., Yates, L.R., Australian Pancreatic Cancer Genome, I., Consortium, I.B.C., Consortium, I.M.-S., PedBrain, I., Zucman-Rossi, J., Futreal, P.A., McDermott, U., Lichter, P., Meyerson, M., Grimmond, S.M., Siebert, R., Campo, E., Shibata, T., Pfister, S.M., Campbell, P.J. & Stratton, M.R. Signatures of mutational processes in human cancer. *Nature* **500**, 415-421 (2013).
48. Vogelstein, B., Papadopoulos, N., Velculescu, V.E., Zhou, S., Diaz, L.A., Jr. & Kinzler, K.W. Cancer genome landscapes. *Science* **339**, 1546-1558 (2013).
49. Shalapour, S., Font-Burgada, J., Di Caro, G., Zhong, Z., Sanchez-Lopez, E., Dhar, D., Willimsky, G., Ammirante, M., Strasner, A., Hansel, D.E., Jamieson, C., Kane, C.J., Klatte, T., Birner, P., Kenner, L. & Karin, M. Immunosuppressive plasma cells impede T-cell-dependent immunogenic chemotherapy. *Nature* **521**, 94-98 (2015).
50. Pereira, B., Chin, S.F., Rueda, O.M., Vollan, H.K., Provenzano, E., Bardwell, H.A., Pugh, M., Jones, L., Russell, R., Sammut, S.J., Tsui, D.W., Liu, B., Dawson, S.J., Abraham, J., Northen, H., Peden, J.F., Mukherjee, A., Turashvili, G., Green, A.R., McKinney, S., Oloumi, A., Shah, S., Rosenfeld, N., Murphy, L., Bentley, D.R., Ellis, I.O., Purushotham, A., Pinder, S.E., Borresen-Dale, A.L., Earl, H.M., Pharoah, P.D., Ross, M.T., Aparicio, S. & Caldas, C. The somatic mutation profiles of 2,433 breast cancers refines their genomic and transcriptomic landscapes. *Nat Commun* **7**, 11479 (2016).
51. Ruffell, B., Au, A., Rugo, H.S., Esserman, L.J., Hwang, E.S. & Coussens, L.M. Leukocyte composition of human breast cancer. *Proc Natl Acad Sci U S A* **109**, 2796-2801 (2012).
52. Woo, S.R., Corrales, L. & Gajewski, T.F. Innate immune recognition of cancer. *Annu Rev Immunol* **33**, 445-474 (2015).
53. Gregory, A.D. & Houghton, A.M. Tumor-associated neutrophils: new targets for cancer therapy. *Cancer Res* **71**, 2411-2416 (2011).
54. Casbon, A.J., Reynaud, D., Park, C., Khuc, E., Gan, D.D., Schepers, K., Passegue, E. & Werb, Z. Invasive breast cancer reprograms early myeloid differentiation in the bone

marrow to generate immunosuppressive neutrophils. *Proc Natl Acad Sci U S A* **112**, E566-575 (2015).
55. Eruslanov, E.B., Bhojnagarwala, P.S., Quatromoni, J.G., Stephen, T.L., Ranganathan, A., Deshpande, C., Akimova, T., Vachani, A., Litzky, L., Hancock, W.W., Conejo-Garcia, J.R., Feldman, M., Albelda, S.M. & Singhal, S. Tumor-associated neutrophils stimulate T cell responses in early-stage human lung cancer. *J Clin Invest* **124**, 5466-5480 (2014).
56. Weber, R., Fleming, V., Hu, X., Nagibin, V., Groth, C., Altevogt, P., Utikal, J. & Umansky, V. Myeloid-Derived Suppressor Cells Hinder the Anti-Cancer Activity of Immune Checkpoint Inhibitors. *Front Immunol* **9**, 1310 (2018).
57. Budhwar, S., Verma, P., Verma, R., Rai, S. & Singh, K. The Yin and Yang of Myeloid Derived Suppressor Cells. *Front Immunol* **9**, 2776 (2018).
58. Chafe, S.C., Lou, Y., Sceneay, J., Vallejo, M., Hamilton, M.J., McDonald, P.C., Bennewith, K.L., Moller, A. & Dedhar, S. Carbonic anhydrase IX promotes myeloid-derived suppressor cell mobilization and establishment of a metastatic niche by stimulating G-CSF production. *Cancer Res* **75**, 996-1008 (2015).
59. Vincent, J., Mignot, G., Chalmin, F., Ladoire, S., Bruchard, M., Chevriaux, A., Martin, F., Apetoh, L., Rebe, C. & Ghiringhelli, F. 5-Fluorouracil selectively kills tumor-associated myeloid-derived suppressor cells resulting in enhanced T cell-dependent antitumor immunity. *Cancer Res* **70**, 3052-3061 (2010).
60. Yu, J., Du, W., Yan, F., Wang, Y., Li, H., Cao, S., Yu, W., Shen, C., Liu, J. & Ren, X. Myeloid-derived suppressor cells suppress antitumor immune responses through IDO expression and correlate with lymph node metastasis in patients with breast cancer. *J Immunol* **190**, 3783-3797 (2013).
61. Markowitz, J., Wesolowski, R., Papenfuss, T., Brooks, T.R. & Carson, W.E., 3rd. Myeloid-derived suppressor cells in breast cancer. *Breast Cancer Res Treat* **140**, 13-21 (2013).
62. Tang, X. Tumor-associated macrophages as potential diagnostic and prognostic biomarkers in breast cancer. *Cancer Lett* **332**, 3-10 (2013).
63. Medrek, C., Ponten, F., Jirstrom, K. & Leandersson, K. The presence of tumor associated macrophages in tumor stroma as a prognostic marker for breast cancer patients. *BMC Cancer* **12**, 306 (2012).
64. Mahmoud, S.M., Lee, A.H., Paish, E.C., Macmillan, R.D., Ellis, I.O. & Green, A.R. Tumour-infiltrating macrophages and clinical outcome in breast cancer. *J Clin Pathol* **65**, 159-163 (2012).
65. Raphael, J., Gong, I.Y., Nofech-Mozes, S., Bartlett, J., Nafisi, H. & Verma, S. Tumour infiltrating lymphocytes and stromal CD68 in early stage HER2 positive breast cancer. *J Clin Pathol* (2016).
66. Tiainen, S., Tumelius, R., Rilla, K., Hamalainen, K., Tammi, M., Tammi, R., Kosma, V.M., Oikari, S. & Auvinen, P. High numbers of macrophages, especially M2-like (CD163-positive), correlate with hyaluronan accumulation and poor outcome in breast cancer. *Histopathology* **66**, 873-883 (2015).
67. Hollmen, M., Roudnicky, F., Karaman, S. & Detmar, M. Characterization of macrophage--cancer cell crosstalk in estrogen receptor positive and triple-negative breast cancer. *Sci Rep* **5**, 9188 (2015).

68. Sznol, M. & Chen, L. Antagonist antibodies to PD-1 and B7-H1 (PD-L1) in the treatment of advanced human cancer. *Clin Cancer Res* **19**, 1021-1034 (2013).
69. Spranger, S., Spaapen, R.M., Zha, Y., Williams, J., Meng, Y., Ha, T.T. & Gajewski, T.F. Up-regulation of PD-L1, IDO, and T(regs) in the melanoma tumor microenvironment is driven by CD8(+) T cells. *Sci Transl Med* **5**, 200ra116 (2013).
70. Stanton, S.E., Adams, S. & Disis, M.L. Variation in the Incidence and Magnitude of Tumor-Infiltrating Lymphocytes in Breast Cancer Subtypes: A Systematic Review. *JAMA Oncol* **2**, 1354-1360 (2016).
71. Denkert, C., Loibl, S., Noske, A., Roller, M., Muller, B.M., Komor, M., Budczies, J., Darb-Esfahani, S., Kronenwett, R., Hanusch, C., von Torne, C., Weichert, W., Engels, K., Solbach, C., Schrader, I., Dietel, M. & von Minckwitz, G. Tumor-associated lymphocytes as an independent predictor of response to neoadjuvant chemotherapy in breast cancer. *J Clin Oncol* **28**, 105-113 (2010).
72. Figenschau, S.L., Fismen, S., Fenton, K.A., Fenton, C. & Mortensen, E.S. Tertiary lymphoid structures are associated with higher tumor grade in primary operable breast cancer patients. *BMC Cancer* **15**, 101 (2015).
73. Kroemer, G., Senovilla, L., Galluzzi, L., Andre, F. & Zitvogel, L. Natural and therapy-induced immunosurveillance in breast cancer. *Nat Med* **21**, 1128-1138 (2015).
74. Salgado, R., Denkert, C., Demaria, S., Sirtaine, N., Klauschen, F., Pruneri, G., Wienert, S., Van den Eynden, G., Baehner, F.L., Penault-Llorca, F., Perez, E.A., Thompson, E.A., Symmans, W.F., Richardson, A.L., Brock, J., Criscitiello, C., Bailey, H., Ignatiadis, M., Floris, G., Sparano, J., Kos, Z., Nielsen, T., Rimm, D.L., Allison, K.H., Reis-Filho, J.S., Loibl, S., Sotiriou, C., Viale, G., Badve, S., Adams, S., Willard-Gallo, K., Loi, S. & International, T.W.G. The evaluation of tumor-infiltrating lymphocytes (TILs) in breast cancer: recommendations by an International TILs Working Group 2014. *Ann Oncol* **26**, 259-271 (2015).
75. Aaltomaa, S., Lipponen, P., Eskelinen, M., Kosma, V.M., Marin, S., Alhava, E. & Syrjanen, K. Lymphocyte infiltrates as a prognostic variable in female breast cancer. *Eur J Cancer* **28A**, 859-864 (1992).
76. Shaveta Vinayak, R.J.G., Sylvia Adams, Kristin C. Jensen, Judith Manola, Anosheh Afghahi, Lori J. Goldstein, James M. Ford, Sunil S. Badve, Melinda L. Telli. Association of increased tumor-infiltrating lymphocytes (TILs) with immunomodulatory (IM) triple-negative breast cancer (TNBC) subtype and response to neoadjuvant platinum-based therapy in PrECOG0105. *J Clin Oncol 32:5s, 2014 (suppl; abstr 1000^)* (2014).
77. Loi, S., Drubay, D., Adams, S., Pruneri, G., Francis, P.A., Lacroix-Triki, M., Joensuu, H., Dieci, M.V., Badve, S., Demaria, S., Gray, R., Munzone, E., Lemonnier, J., Sotiriou, C., Piccart, M.J., Kellokumpu-Lehtinen, P.L., Vingiani, A., Gray, K., Andre, F., Denkert, C., Salgado, R. & Michiels, S. Tumor-Infiltrating Lymphocytes and Prognosis: A Pooled Individual Patient Analysis of Early-Stage Triple-Negative Breast Cancers. *J Clin Oncol*, JCO1801010 (2019).
78. Denkert, C., von Minckwitz, G., Darb-Esfahani, S., Lederer, B., Heppner, B.I., Weber, K.E., Budczies, J., Huober, J., Klauschen, F., Furlanetto, J., Schmitt, W.D., Blohmer, J.U., Karn, T., Pfitzner, B.M., Kummel, S., Engels, K., Schneeweiss, A., Hartmann, A., Noske, A., Fasching, P.A., Jackisch, C., van Mackelenbergh, M., Sinn, P., Schem, C., Hanusch, C., Untch, M. & Loibl, S. Tumour-infiltrating lymphocytes and prognosis in

different subtypes of breast cancer: a pooled analysis of 3771 patients treated with neoadjuvant therapy. *The Lancet. Oncology* **19**, 40-50 (2018).
79. Adams, S., Gray, R.J., Demaria, S., Goldstein, L., Perez, E.A., Shulman, L.N., Martino, S., Wang, M., Jones, V.E., Saphner, T.J., Wolff, A.C., Wood, W.C., Davidson, N.E., Sledge, G.W., Sparano, J.A. & Badve, S.S. Prognostic value of tumor-infiltrating lymphocytes in triple-negative breast cancers from two phase III randomized adjuvant breast cancer trials: ECOG 2197 and ECOG 1199. *J Clin Oncol* **32**, 2959-2966 (2014).
80. Loi, S., Michiels, S., Salgado, R., Sirtaine, N., Jose, V., Fumagalli, D., Kellokumpu-Lehtinen, P.L., Bono, P., Kataja, V., Desmedt, C., Piccart, M.J., Loibl, S., Denkert, C., Smyth, M.J., Joensuu, H. & Sotiriou, C. Tumor infiltrating lymphocytes are prognostic in triple negative breast cancer and predictive for trastuzumab benefit in early breast cancer: results from the FinHER trial. *Ann Oncol* **25**, 1544-1550 (2014).
81. Loi, S., Sirtaine, N., Piette, F., Salgado, R., Viale, G., Van Eenoo, F., Rouas, G., Francis, P., Crown, J.P., Hitre, E., de Azambuja, E., Quinaux, E., Di Leo, A., Michiels, S., Piccart, M.J. & Sotiriou, C. Prognostic and predictive value of tumor-infiltrating lymphocytes in a phase III randomized adjuvant breast cancer trial in node-positive breast cancer comparing the addition of docetaxel to doxorubicin with doxorubicin-based chemotherapy: BIG 02-98. *J Clin Oncol* **31**, 860-867 (2013).
82. Perez, E.A., Ballman, K.V., Tenner, K.S., Thompson, E.A., Badve, S.S., Bailey, H. & Baehner, F.L. Association of Stromal Tumor-Infiltrating Lymphocytes With Recurrence-Free Survival in the N9831 Adjuvant Trial in Patients With Early-Stage HER2-Positive Breast Cancer. *JAMA Oncol* **2**, 56-64 (2016).
83. Dieci, M.V., Mathieu, M.C., Guarneri, V., Conte, P., Delaloge, S., Andre, F. & Goubar, A. Prognostic and predictive value of tumor-infiltrating lymphocytes in two phase III randomized adjuvant breast cancer trials. *Ann Oncol* **26**, 1698-1704 (2015).
84. Loi S., M.S., Salgado R., Sirtaine N., Jose V., Fumagalli D et al. Tumor infiltrating lymphocytes (TILs) indicate trastuzumab benefit in early-stage HER2-positive breast cancer[abstract]. *Cancer Res* **abstract nr S1-05**(2013).
85. Nelson, B.H. CD20+ B cells: the other tumor-infiltrating lymphocytes. *J Immunol* **185**, 4977-4982 (2010).
86. Mahmoud, S.M., Lee, A.H., Paish, E.C., Macmillan, R.D., Ellis, I.O. & Green, A.R. The prognostic significance of B lymphocytes in invasive carcinoma of the breast. *Breast Cancer Res Treat* **132**, 545-553 (2012).
87. Mohammed, Z.M., Going, J.J., Edwards, J., Elsberger, B. & McMillan, D.C. The relationship between lymphocyte subsets and clinico-pathological determinants of survival in patients with primary operable invasive ductal breast cancer. *Br J Cancer* **109**, 1676-1684 (2013).
88. Wouters, M.C.A. & Nelson, B.H. Prognostic Significance of Tumor-Infiltrating B Cells and Plasma Cells in Human Cancer. *Clin Cancer Res* **24**, 6125-6135 (2018).
89. Shen, M., Wang, J. & Ren, X. New Insights into Tumor-Infiltrating B Lymphocytes in Breast Cancer: Clinical Impacts and Regulatory Mechanisms. *Front Immunol* **9**, 470 (2018).
90. Mohammed, Z.M., Going, J.J., Edwards, J., Elsberger, B., Doughty, J.C. & McMillan, D.C. The relationship between components of tumour inflammatory cell infiltrate and

clinicopathological factors and survival in patients with primary operable invasive ductal breast cancer. *Br J Cancer* **107**, 864-873 (2012).
91. Chen, Z., Gerhold-Ay, A., Gebhard, S., Boehm, D., Solbach, C., Lebrecht, A., Battista, M., Sicking, I., Cotarelo, C., Cadenas, C., Marchan, R., Stewart, J.D., Gehrmann, M., Koelbl, H., Hengstler, J.G. & Schmidt, M. Immunoglobulin kappa C predicts overall survival in node-negative breast cancer. *PLoS One* **7**, e44741 (2012).
92. Schmidt, M., Hellwig, B., Hammad, S., Othman, A., Lohr, M., Chen, Z., Boehm, D., Gebhard, S., Petry, I., Lebrecht, A., Cadenas, C., Marchan, R., Stewart, J.D., Solbach, C., Holmberg, L., Edlund, K., Kultima, H.G., Rody, A., Berglund, A., Lambe, M., Isaksson, A., Botling, J., Karn, T., Muller, V., Gerhold-Ay, A., Cotarelo, C., Sebastian, M., Kronenwett, R., Bojar, H., Lehr, H.A., Sahin, U., Koelbl, H., Gehrmann, M., Micke, P., Rahnenfuhrer, J. & Hengstler, J.G. A comprehensive analysis of human gene expression profiles identifies stromal immunoglobulin kappa C as a compatible prognostic marker in human solid tumors. *Clin Cancer Res* **18**, 2695-2703 (2012).
93. Olkhanud, P.B., Damdinsuren, B., Bodogai, M., Gress, R.E., Sen, R., Wejksza, K., Malchinkhuu, E., Wersto, R.P. & Biragyn, A. Tumor-evoked regulatory B cells promote breast cancer metastasis by converting resting CD4(+) T cells to T-regulatory cells. *Cancer Res* **71**, 3505-3515 (2011).
94. Iglesia, M.D., Vincent, B.G., Parker, J.S., Hoadley, K.A., Carey, L.A., Perou, C.M. & Serody, J.S. Prognostic B-cell signatures using mRNA-seq in patients with subtype-specific breast and ovarian cancer. *Clin Cancer Res* **20**, 3818-3829 (2014).
95. Mahmoud, S.M., Paish, E.C., Powe, D.G., Macmillan, R.D., Grainge, M.J., Lee, A.H., Ellis, I.O. & Green, A.R. Tumor-infiltrating CD8+ lymphocytes predict clinical outcome in breast cancer. *J Clin Oncol* **29**, 1949-1955 (2011).
96. Liu, S., Lachapelle, J., Leung, S., Gao, D., Foulkes, W.D. & Nielsen, T.O. CD8+ lymphocyte infiltration is an independent favorable prognostic indicator in basal-like breast cancer. *Breast Cancer Res* **14**, R48 (2012).
97. Ali, H.R., Provenzano, E., Dawson, S.J., Blows, F.M., Liu, B., Shah, M., Earl, H.M., Poole, C.J., Hiller, L., Dunn, J.A., Bowden, S.J., Twelves, C., Bartlett, J.M., Mahmoud, S.M., Rakha, E., Ellis, I.O., Liu, S., Gao, D., Nielsen, T.O., Pharoah, P.D. & Caldas, C. Association between CD8+ T-cell infiltration and breast cancer survival in 12,439 patients. *Ann Oncol* **25**, 1536-1543 (2014).
98. Dookeran, K.A., Dignam, J.J., Ferrer, K., Sekosan, M., McCaskill-Stevens, W. & Gehlert, S. p53 as a marker of prognosis in African-American women with breast cancer. *Annals of surgical oncology* **17**, 1398-1405 (2010).
99. Winslow, S., Leandersson, K., Edsjo, A. & Larsson, C. Prognostic stromal gene signatures in breast cancer. *Breast Cancer Res* **17**, 23 (2015).
100. West, N.R., Milne, K., Truong, P.T., Macpherson, N., Nelson, B.H. & Watson, P.H. Tumor-infiltrating lymphocytes predict response to anthracycline-based chemotherapy in estrogen receptor-negative breast cancer. *Breast Cancer Res* **13**, R126 (2011).
101. Liu, S., Chen, B., Burugu, S., Leung, S., Gao, D., Virk, S., Kos, Z., Parulekar, W.R., Shepherd, L., Gelmon, K.A. & Nielsen, T.O. Role of Cytotoxic Tumor-Infiltrating Lymphocytes in Predicting Outcomes in Metastatic HER2-Positive Breast Cancer: A Secondary Analysis of a Randomized Clinical Trial. *JAMA Oncol* **3**, e172085 (2017).

102. Lee, H.J., Seo, J.Y., Ahn, J.H., Ahn, S.H. & Gong, G. Tumor-associated lymphocytes predict response to neoadjuvant chemotherapy in breast cancer patients. *J Breast Cancer* **16**, 32-39 (2013).
103. Oda, N., Shimazu, K., Naoi, Y., Morimoto, K., Shimomura, A., Shimoda, M., Kagara, N., Maruyama, N., Kim, S.J. & Noguchi, S. Intratumoral regulatory T cells as an independent predictive factor for pathological complete response to neoadjuvant paclitaxel followed by 5-FU/epirubicin/cyclophosphamide in breast cancer patients. *Breast Cancer Res Treat* **136**, 107-116 (2012).
104. Seo, A.N., Lee, H.J., Kim, E.J., Kim, H.J., Jang, M.H., Lee, H.E., Kim, Y.J., Kim, J.H. & Park, S.Y. Tumour-infiltrating CD8+ lymphocytes as an independent predictive factor for pathological complete response to primary systemic therapy in breast cancer. *Br J Cancer* **109**, 2705-2713 (2013).
105. Zhu, J., Yamane, H. & Paul, W.E. Differentiation of effector CD4 T cell populations (*). *Annu Rev Immunol* **28**, 445-489 (2010).
106. Gu-Trantien, C., Loi, S., Garaud, S., Equeter, C., Libin, M., de Wind, A., Ravoet, M., Le Buanec, H., Sibille, C., Manfouo-Foutsop, G., Veys, I., Haibe-Kains, B., Singhal, S.K., Michiels, S., Rothe, F., Salgado, R., Duvillier, H., Ignatiadis, M., Desmedt, C., Bron, D., Larsimont, D., Piccart, M., Sotiriou, C. & Willard-Gallo, K. CD4(+) follicular helper T cell infiltration predicts breast cancer survival. *J Clin Invest* **123**, 2873-2892 (2013).
107. Liu, S., Foulkes, W.D., Leung, S., Gao, D., Lau, S., Kos, Z. & Nielsen, T.O. Prognostic significance of FOXP3+ tumor-infiltrating lymphocytes in breast cancer depends on estrogen receptor and human epidermal growth factor receptor-2 expression status and concurrent cytotoxic T-cell infiltration. *Breast Cancer Res* **16**, 432 (2014).
108. Droeser, R., Zlobec, I., Kilic, E., Guth, U., Heberer, M., Spagnoli, G., Oertli, D. & Tapia, C. Differential pattern and prognostic significance of CD4+, FOXP3+ and IL-17+ tumor infiltrating lymphocytes in ductal and lobular breast cancers. *BMC Cancer* **12**, 134 (2012).
109. Lee, S., Cho, E.Y., Park, Y.H., Ahn, J.S. & Im, Y.H. Prognostic impact of FOXP3 expression in triple-negative breast cancer. *Acta oncologica (Stockholm, Sweden)* **52**, 73-81 (2013).
110. West, N.R., Kost, S.E., Martin, S.D., Milne, K., Deleeuw, R.J., Nelson, B.H. & Watson, P.H. Tumour-infiltrating FOXP3(+) lymphocytes are associated with cytotoxic immune responses and good clinical outcome in oestrogen receptor-negative breast cancer. *Br J Cancer* **108**, 155-162 (2013).
111. Kim, S.T., Jeong, H., Woo, O.H., Seo, J.H., Kim, A., Lee, E.S., Shin, S.W., Kim, Y.H., Kim, J.S. & Park, K.H. Tumor-infiltrating lymphocytes, tumor characteristics, and recurrence in patients with early breast cancer. *Am J Clin Oncol* **36**, 224-231 (2013).
112. Bindea, G., Mlecnik, B., Tosolini, M., Kirilovsky, A., Waldner, M., Obenauf, A.C., Angell, H., Fredriksen, T., Lafontaine, L., Berger, A., Bruneval, P., Fridman, W.H., Becker, C., Pages, F., Speicher, M.R., Trajanoski, Z. & Galon, J. Spatiotemporal dynamics of intratumoral immune cells reveal the immune landscape in human cancer. *Immunity* **39**, 782-795 (2013).
113. Ma, C.S., Deenick, E.K., Batten, M. & Tangye, S.G. The origins, function, and regulation of T follicular helper cells. *J Exp Med* **209**, 1241-1253 (2012).

114. Santos, P.M. & Butterfield, L.H. Dendritic Cell-Based Cancer Vaccines. *J Immunol* **200**, 443-449 (2018).
115. Butterfield, L.H. Cancer vaccines. *BMJ (Clinical research ed.)* **350**, h988 (2015).
116. Kantoff, P.W., Higano, C.S., Shore, N.D., Berger, E.R., Small, E.J., Penson, D.F., Redfern, C.H., Ferrari, A.C., Dreicer, R., Sims, R.B., Xu, Y., Frohlich, M.W. & Schellhammer, P.F. Sipuleucel-T immunotherapy for castration-resistant prostate cancer. *N Engl J Med* **363**, 411-422 (2010).
117. Benedetti, R., Dell'Aversana, C., Giorgio, C., Astorri, R. & Altucci, L. Breast Cancer Vaccines: New Insights. *Frontiers in endocrinology* **8**, 270 (2017).
118. Yang, J.C. & Rosenberg, S.A. Adoptive T-Cell Therapy for Cancer. *Advances in immunology* **130**, 279-294 (2016).
119. Newick, K., O'Brien, S., Moon, E. & Albelda, S.M. CAR T Cell Therapy for Solid Tumors. *Annual review of medicine* **68**, 139-152 (2017).
120. Savas, P., Salgado, R., Denkert, C., Sotiriou, C., Darcy, P.K., Smyth, M.J. & Loi, S. Clinical relevance of host immunity in breast cancer: from TILs to the clinic. *Nat Rev Clin Oncol* (2015).
121. Zacharakis, N., Chinnasamy, H., Black, M., Xu, H., Lu, Y.C., Zheng, Z., Pasetto, A., Langhan, M., Shelton, T., Prickett, T., Gartner, J., Jia, L., Trebska-McGowan, K., Somerville, R.P., Robbins, P.F., Rosenberg, S.A., Goff, S.L. & Feldman, S.A. Immune recognition of somatic mutations leading to complete durable regression in metastatic breast cancer. *Nat Med* **24**, 724-730 (2018).
122. Kroemer, G., Galluzzi, L., Kepp, O. & Zitvogel, L. Immunogenic cell death in cancer therapy. *Annu Rev Immunol* **31**, 51-72 (2013).
123. Minn, A.J. Interferons and the Immunogenic Effects of Cancer Therapy. *Trends in immunology* **36**, 725-737 (2015).
124. Alizadeh, D. & Larmonier, N. Chemotherapeutic targeting of cancer-induced immunosuppressive cells. *Cancer Res* **74**, 2663-2668 (2014).
125. Brix, N., Tiefenthaller, A., Anders, H., Belka, C. & Lauber, K. Abscopal, immunological effects of radiotherapy: Narrowing the gap between clinical and preclinical experiences. *Immunological reviews* **280**, 249-279 (2017).
126. Derer, A., Deloch, L., Rubner, Y., Fietkau, R., Frey, B. & Gaipl, U.S. Radio-Immunotherapy-Induced Immunogenic Cancer Cells as Basis for Induction of Systemic Anti-Tumor Immune Responses - Pre-Clinical Evidence and Ongoing Clinical Applications. *Front Immunol* **6**, 505 (2015).
127. Reynders, K., Illidge, T., Siva, S., Chang, J.Y. & De Ruysscher, D. The abscopal effect of local radiotherapy: using immunotherapy to make a rare event clinically relevant. *Cancer treatment reviews* **41**, 503-510 (2015).
128. Bang, Y.J., Giaccone, G., Im, S.A., Oh, D.Y., Bauer, T.M., Nordstrom, J.L., Li, H., Chichili, G.R., Moore, P.A., Hong, S., Stewart, S.J., Baughman, J.E., Lechleider, R.J. & Burris, H.A. First-in-human phase 1 study of margetuximab (MGAH22), an Fc-modified chimeric monoclonal antibody, in patients with HER2-positive advanced solid tumors. *Ann Oncol* **28**, 855-861 (2017).
129. Musolino, A., Naldi, N., Bortesi, B., Pezzuolo, D., Capelletti, M., Missale, G., Laccabue, D., Zerbini, A., Camisa, R., Bisagni, G., Neri, T.M. & Ardizzoni, A. Immunoglobulin G fragment C receptor polymorphisms and clinical efficacy of trastuzumab-based therapy in

patients with HER-2/neu-positive metastatic breast cancer. *J Clin Oncol* **26**, 1789-1796 (2008).
130. Shi, Y., Fan, X., Deng, H., Brezski, R.J., Rycyzyn, M., Jordan, R.E., Strohl, W.R., Zou, Q., Zhang, N. & An, Z. Trastuzumab triggers phagocytic killing of high HER2 cancer cells in vitro and in vivo by interaction with Fcgamma receptors on macrophages. *J Immunol* **194**, 4379-4386 (2015).
131. Ferris, R.L., Jaffee, E.M. & Ferrone, S. Tumor antigen-targeted, monoclonal antibody-based immunotherapy: clinical response, cellular immunity, and immunoescape. *J Clin Oncol* **28**, 4390-4399 (2010).
132. Weiner, G.J. Building better monoclonal antibody-based therapeutics. *Nat Rev Cancer* **15**, 361-370 (2015).
133. Gul, N. & van Egmond, M. Antibody-Dependent Phagocytosis of Tumor Cells by Macrophages: A Potent Effector Mechanism of Monoclonal Antibody Therapy of Cancer. *Cancer Res* **75**, 5008-5013 (2015).
134. Nguyen, L.T. & Ohashi, P.S. Clinical blockade of PD1 and LAG3--potential mechanisms of action. *Nat Rev Immunol* **15**, 45-56 (2015).
135. Weber, J. Immune checkpoint proteins: a new therapeutic paradigm for cancer--preclinical background: CTLA-4 and PD-1 blockade. *Seminars in oncology* **37**, 430-439 (2010).
136. Gargi D Basu, A.G., Randal Vader, Sandeep Reddy, Karen Anderson, Ann McCullough, and Barbara Pockaj Expression of novel immunotherapeutic targets in luminal breast cancer patients [abstract]. *Cancer Res* **Abstract nr P5-04-08**(2015).
137. Schmidt M, v.d.S.L., Heimes A, Battista M, Lebrecht A, Almstedt K, Hoffmann G, Rahnenführer J, Hengstler JG Prognostic significance of immune checkpoint receptors in node-negative breast cancer[abstract]. *Cancer res* **Abstract nr P2-08-07**(2015).
138. Larkin, J., Chiarion-Sileni, V., Gonzalez, R., Grob, J.J., Cowey, C.L., Lao, C.D., Schadendorf, D., Dummer, R., Smylie, M., Rutkowski, P., Ferrucci, P.F., Hill, A., Wagstaff, J., Carlino, M.S., Haanen, J.B., Maio, M., Marquez-Rodas, I., McArthur, G.A., Ascierto, P.A., Long, G.V., Callahan, M.K., Postow, M.A., Grossmann, K., Sznol, M., Dreno, B., Bastholt, L., Yang, A., Rollin, L.M., Horak, C., Hodi, F.S. & Wolchok, J.D. Combined Nivolumab and Ipilimumab or Monotherapy in Untreated Melanoma. *N Engl J Med* **373**, 23-34 (2015).
139. Robert, C., Thomas, L., Bondarenko, I., O'Day, S., Weber, J., Garbe, C., Lebbe, C., Baurain, J.F., Testori, A., Grob, J.J., Davidson, N., Richards, J., Maio, M., Hauschild, A., Miller, W.H., Jr., Gascon, P., Lotem, M., Harmankaya, K., Ibrahim, R., Francis, S., Chen, T.T., Humphrey, R., Hoos, A. & Wolchok, J.D. Ipilimumab plus dacarbazine for previously untreated metastatic melanoma. *N Engl J Med* **364**, 2517-2526 (2011).
140. Schadendorf, D., Hodi, F.S., Robert, C., Weber, J.S., Margolin, K., Hamid, O., Patt, D., Chen, T.T., Berman, D.M. & Wolchok, J.D. Pooled Analysis of Long-Term Survival Data From Phase II and Phase III Trials of Ipilimumab in Unresectable or Metastatic Melanoma. *J Clin Oncol* **33**, 1889-1894 (2015).
141. Robert, C., Long, G.V., Brady, B., Dutriaux, C., Maio, M., Mortier, L., Hassel, J.C., Rutkowski, P., McNeil, C., Kalinka-Warzocha, E., Savage, K.J., Hernberg, M.M., Lebbe, C., Charles, J., Mihalcioiu, C., Chiarion-Sileni, V., Mauch, C., Cognetti, F., Arance, A., Schmidt, H., Schadendorf, D., Gogas, H., Lundgren-Eriksson, L., Horak, C., Sharkey, B.,

Waxman, I.M., Atkinson, V. & Ascierto, P.A. Nivolumab in previously untreated melanoma without BRAF mutation. *N Engl J Med* **372**, 320-330 (2015).
142. Vonderheide, R.H., LoRusso, P.M., Khalil, M., Gartner, E.M., Khaira, D., Soulieres, D., Dorazio, P., Trosko, J.A., Ruter, J., Mariani, G.L., Usari, T. & Domchek, S.M. Tremelimumab in combination with exemestane in patients with advanced breast cancer and treatment-associated modulation of inducible costimulator expression on patient T cells. *Clin Cancer Res* **16**, 3485-3494 (2010).
143. Freeman, G.J., Long, A.J., Iwai, Y., Bourque, K., Chernova, T., Nishimura, H., Fitz, L.J., Malenkovich, N., Okazaki, T., Byrne, M.C., Horton, H.F., Fouser, L., Carter, L., Ling, V., Bowman, M.R., Carreno, B.M., Collins, M., Wood, C.R. & Honjo, T. Engagement of the PD-1 immunoinhibitory receptor by a novel B7 family member leads to negative regulation of lymphocyte activation. *J Exp Med* **192**, 1027-1034 (2000).
144. Keir, M.E., Butte, M.J., Freeman, G.J. & Sharpe, A.H. PD-1 and its ligands in tolerance and immunity. *Annu Rev Immunol* **26**, 677-704 (2008).
145. Hui, E., Cheung, J., Zhu, J., Su, X., Taylor, M.J., Wallweber, H.A., Sasmal, D.K., Huang, J., Kim, J.M., Mellman, I. & Vale, R.D. T cell costimulatory receptor CD28 is a primary target for PD-1-mediated inhibition. *Science* **355**, 1428-1433 (2017).
146. Gong, J., Chehrazi-Raffle, A., Reddi, S. & Salgia, R. Development of PD-1 and PD-L1 inhibitors as a form of cancer immunotherapy: a comprehensive review of registration trials and future considerations. *J Immunother Cancer* **6**, 8 (2018).
147. Wein, L., Luen, S.J., Savas, P., Salgado, R. & Loi, S. Checkpoint blockade in the treatment of breast cancer: current status and future directions. *Br J Cancer* **119**, 4-11 (2018).
148. Schmid, P., Adams, S., Rugo, H.S., Schneeweiss, A., Barrios, C.H., Iwata, H., Dieras, V., Hegg, R., Im, S.A., Shaw Wright, G., Henschel, V., Molinero, L., Chui, S.Y., Funke, R., Husain, A., Winer, E.P., Loi, S. & Emens, L.A. Atezolizumab and Nab-Paclitaxel in Advanced Triple-Negative Breast Cancer. *N Engl J Med* **379**, 2108-2121 (2018).
149. Rugo, H.S., Delord, J.P., Im, S.A., Ott, P.A., Piha-Paul, S.A., Bedard, P.L., Sachdev, J., Tourneau, C.L., van Brummelen, E.M.J., Varga, A., Salgado, R., Loi, S., Saraf, S., Pietrangelo, D., Karantza, V. & Tan, A.R. Safety and Antitumor Activity of Pembrolizumab in Patients with Estrogen Receptor-Positive/Human Epidermal Growth Factor Receptor 2-Negative Advanced Breast Cancer. *Clin Cancer Res* **24**, 2804-2811 (2018).
150. Vikas, P., Borcherding, N. & Zhang, W. The clinical promise of immunotherapy in triple-negative breast cancer. *Cancer management and research* **10**, 6823-6833 (2018).
151. Adams, S., Schmid, P., Rugo, H.S., Winer, E.P., Loirat, D., Awada, A., Cescon, D.W., Iwata, H., Campone, M., Nanda, R., Hui, R., Curigliano, G., Toppmeyer, D., O'Shaughnessy, J., Loi, S., Paluch-Shimon, S., Tan, A.R., Card, D., Zhao, J., Karantza, V. & Cortes, J. Pembrolizumab Monotherapy for Previously Treated Metastatic Triple-Negative Breast Cancer: Cohort A of the Phase 2 KEYNOTE-086 Study. *Ann Oncol* (2018).
152. Adams, S., Loi, S., Toppmeyer, D., Cescon, D.W., De Laurentiis, M., Nanda, R., Winer, E.P., Mukai, H., Tamura, K., Armstrong, A., Liu, M.C., Iwata, H., Ryvo, L., Wimberger, P., Rugo, H.S., Tan, A.R., Jia, L., Ding, Y., Karantza, V. & Schmid, P. Title: Pembrolizumab Monotherapy for Previously Untreated, PD-L1-Positive, Metastatic

Triple-Negative Breast Cancer: Cohort B of the Phase 2 KEYNOTE-086 Study. *Ann Oncol* (2018).
153. Ribas, A. & Hu-Lieskovan, S. What does PD-L1 positive or negative mean? *J Exp Med* **213**, 2835-2840 (2016).
154. Page DB, Y.J., Diab A, Dong Z, Ginsberg A, Wong P et al. Integrated immunologic assessment of tumor infiltrating lymphocytes (TILs) and peripheral blood to assess synergy of cryoablation (cryo) plus ipilimumab (ipi) in early stage breast cancer (ESBC) patients[abstract]. *Cancer Res* **abstract nr P2-15-01**(2015).
155. Burugu, S., Dancsok, A.R. & Nielsen, T.O. Emerging targets in cancer immunotherapy. *Seminars in cancer biology* (2017).
156. Anderson, A.C., Joller, N. & Kuchroo, V.K. Lag-3, Tim-3, and TIGIT: Co-inhibitory Receptors with Specialized Functions in Immune Regulation. *Immunity* **44**, 989-1004 (2016).
157. Scurr, M., Ladell, K., Besneux, M., Christian, A., Hockey, T., Smart, K., Bridgeman, H., Hargest, R., Phillips, S., Davies, M., Price, D., Gallimore, A. & Godkin, A. Highly prevalent colorectal cancer-infiltrating LAP(+) Foxp3(-) T cells exhibit more potent immunosuppressive activity than Foxp3(+) regulatory T cells. *Mucosal Immunol* **7**, 428-439 (2014).
158. Bettini, M., Szymczak-Workman, A.L., Forbes, K., Castellaw, A.H., Selby, M., Pan, X., Drake, C.G., Korman, A.J. & Vignali, D.A. Cutting edge: accelerated autoimmune diabetes in the absence of LAG-3. *J Immunol* **187**, 3493-3498 (2011).
159. Williams, J.B., Horton, B.L., Zheng, Y., Duan, Y., Powell, J.D. & Gajewski, T.F. The EGR2 targets LAG-3 and 4-1BB describe and regulate dysfunctional antigen-specific CD8+ T cells in the tumor microenvironment. *J Exp Med* **214**, 381-400 (2017).
160. Casati, C., Camisaschi, C., Rini, F., Arienti, F., Rivoltini, L., Triebel, F., Parmiani, G. & Castelli, C. Soluble human LAG-3 molecule amplifies the in vitro generation of type 1 tumor-specific immunity. *Cancer Res* **66**, 4450-4460 (2006).
161. Shapiro, M., Herishanu, Y., Katz, B.Z., Dezorella, N., Sun, C., Kay, S., Polliack, A., Avivi, I., Wiestner, A. & Perry, C. Lymphocyte activation gene 3: a novel therapeutic target in chronic lymphocytic leukemia. *Haematologica* **102**, 874-882 (2017).
162. Tassi, E., Grazia, G., Vegetti, C., Bersani, I., Bertolini, G., Molla, A., Baldassari, P., Andriani, F., Roz, L., Sozzi, G., Pastorino, U., Mortarini, R. & Anichini, A. Early Effector T Lymphocytes Coexpress Multiple Inhibitory Receptors in Primary Non-Small Cell Lung Cancer. *Cancer Res* **77**, 851-861 (2017).
163. Bottai, G., Raschioni, C., Losurdo, A., Di Tommaso, L., Tinterri, C., Torrisi, R., Reis-Filho, J.S., Roncalli, M., Sotiriou, C., Santoro, A., Mantovani, A., Loi, S. & Santarpia, L. An immune stratification reveals a subset of PD-1/LAG-3 double-positive triple-negative breast cancers. *Breast cancer research : BCR* **18**, 121 (2016).
164. Deng, W.W., Mao, L., Yu, G.T., Bu, L.L., Ma, S.R., Liu, B., Gutkind, J.S., Kulkarni, A.B., Zhang, W.F. & Sun, Z.J. LAG-3 confers poor prognosis and its blockade reshapes antitumor response in head and neck squamous cell carcinoma. *Oncoimmunology* **5**, e1239005 (2016).
165. Llosa, N.J., Cruise, M., Tam, A., Wicks, E.C., Hechenbleikner, E.M., Taube, J.M., Blosser, R.L., Fan, H., Wang, H., Luber, B.S., Zhang, M., Papadopoulos, N., Kinzler, K.W., Vogelstein, B., Sears, C.L., Anders, R.A., Pardoll, D.M. & Housseau, F. The

vigorous immune microenvironment of microsatellite instable colon cancer is balanced by multiple counter-inhibitory checkpoints. *Cancer discovery* **5**, 43-51 (2015).
166. Meng, Q., Liu, Z., Rangelova, E., Poiret, T., Ambati, A., Rane, L., Xie, S., Verbeke, C., Dodoo, E., Del Chiaro, M., Lohr, M., Segersvard, R. & Maeurer, M.J. Expansion of Tumor-reactive T Cells From Patients With Pancreatic Cancer. *Journal of immunotherapy (Hagerstown, Md. : 1997)* **39**, 81-89 (2016).
167. Demeure, C.E., Wolfers, J., Martin-Garcia, N., Gaulard, P. & Triebel, F. T Lymphocytes infiltrating various tumour types express the MHC class II ligand lymphocyte activation gene-3 (LAG-3): role of LAG-3/MHC class II interactions in cell-cell contacts. *Eur J Cancer* **37**, 1709-1718 (2001).
168. Woo, S.R., Turnis, M.E., Goldberg, M.V., Bankoti, J., Selby, M., Nirschl, C.J., Bettini, M.L., Gravano, D.M., Vogel, P., Liu, C.L., Tangsombatvisit, S., Grosso, J.F., Netto, G., Smeltzer, M.P., Chaux, A., Utz, P.J., Workman, C.J., Pardoll, D.M., Korman, A.J., Drake, C.G. & Vignali, D.A. Immune inhibitory molecules LAG-3 and PD-1 synergistically regulate T-cell function to promote tumoral immune escape. *Cancer research* **72**, 917-927 (2012).
169. Huang, R.Y., Eppolito, C., Lele, S., Shrikant, P., Matsuzaki, J. & Odunsi, K. LAG3 and PD1 co-inhibitory molecules collaborate to limit CD8+ T cell signaling and dampen antitumor immunity in a murine ovarian cancer model. *Oncotarget* **6**, 27359-27377 (2015).
170. Huang, R.Y., Francois, A., McGray, A.R., Miliotto, A. & Odunsi, K. Compensatory upregulation of PD-1, LAG-3, and CTLA-4 limits the efficacy of single-agent checkpoint blockade in metastatic ovarian cancer. *Oncoimmunology* **6**, e1249561 (2017).
171. Brignone, C., Escudier, B., Grygar, C., Marcu, M. & Triebel, F. A phase I pharmacokinetic and biological correlative study of IMP321, a novel MHC class II agonist, in patients with advanced renal cell carcinoma. *Clin Cancer Res* **15**, 6225-6231 (2009).
172. Monney, L., Sabatos, C.A., Gaglia, J.L., Ryu, A., Waldner, H., Chernova, T., Manning, S., Greenfield, E.A., Coyle, A.J., Sobel, R.A., Freeman, G.J. & Kuchroo, V.K. Th1-specific cell surface protein Tim-3 regulates macrophage activation and severity of an autoimmune disease. *Nature* **415**, 536-541 (2002).
173. Hastings, W.D., Anderson, D.E., Kassam, N., Koguchi, K., Greenfield, E.A., Kent, S.C., Zheng, X.X., Strom, T.B., Hafler, D.A. & Kuchroo, V.K. TIM-3 is expressed on activated human CD4+ T cells and regulates Th1 and Th17 cytokines. *European journal of immunology* **39**, 2492-2501 (2009).
174. Gao, X., Zhu, Y., Li, G., Huang, H., Zhang, G., Wang, F., Sun, J., Yang, Q., Zhang, X. & Lu, B. TIM-3 expression characterizes regulatory T cells in tumor tissues and is associated with lung cancer progression. *PLoS One* **7**, e30676 (2012).
175. Yan, J., Zhang, Y., Zhang, J.P., Liang, J., Li, L. & Zheng, L. Tim-3 expression defines regulatory T cells in human tumors. *PLoS One* **8**, e58006 (2013).
176. Gleason, M.K., Lenvik, T.R., McCullar, V., Felices, M., O'Brien, M.S., Cooley, S.A., Verneris, M.R., Cichocki, F., Holman, C.J., Panoskaltsis-Mortari, A., Niki, T., Hirashima, M., Blazar, B.R. & Miller, J.S. Tim-3 is an inducible human natural killer cell receptor that enhances interferon gamma production in response to galectin-9. *Blood* **119**, 3064-3072 (2012).

177. Ndhlovu, L.C., Lopez-Verges, S., Barbour, J.D., Jones, R.B., Jha, A.R., Long, B.R., Schoeffler, E.C., Fujita, T., Nixon, D.F. & Lanier, L.L. Tim-3 marks human natural killer cell maturation and suppresses cell-mediated cytotoxicity. *Blood* **119**, 3734-3743 (2012).
178. Anderson, A.C., Anderson, D.E., Bregoli, L., Hastings, W.D., Kassam, N., Lei, C., Chandwaskar, R., Karman, J., Su, E.W., Hirashima, M., Bruce, J.N., Kane, L.P., Kuchroo, V.K. & Hafler, D.A. Promotion of tissue inflammation by the immune receptor Tim-3 expressed on innate immune cells. *Science* **318**, 1141-1143 (2007).
179. Wada, J. & Kanwar, Y.S. Identification and characterization of galectin-9, a novel beta-galactoside-binding mammalian lectin. *J Biol Chem* **272**, 6078-6086 (1997).
180. Zhu, C., Anderson, A.C., Schubart, A., Xiong, H., Imitola, J., Khoury, S.J., Zheng, X.X., Strom, T.B. & Kuchroo, V.K. The Tim-3 ligand galectin-9 negatively regulates T helper type 1 immunity. *Nat Immunol* **6**, 1245-1252 (2005).
181. Sabatos, C.A., Chakravarti, S., Cha, E., Schubart, A., Sanchez-Fueyo, A., Zheng, X.X., Coyle, A.J., Strom, T.B., Freeman, G.J. & Kuchroo, V.K. Interaction of Tim-3 and Tim-3 ligand regulates T helper type 1 responses and induction of peripheral tolerance. *Nat Immunol* **4**, 1102-1110 (2003).
182. Sanchez-Fueyo, A., Tian, J., Picarella, D., Domenig, C., Zheng, X.X., Sabatos, C.A., Manlongat, N., Bender, O., Kamradt, T., Kuchroo, V.K., Gutierrez-Ramos, J.C., Coyle, A.J. & Strom, T.B. Tim-3 inhibits T helper type 1-mediated auto- and alloimmune responses and promotes immunological tolerance. *Nat Immunol* **4**, 1093-1101 (2003).
183. Jones, R.B., Ndhlovu, L.C., Barbour, J.D., Sheth, P.M., Jha, A.R., Long, B.R., Wong, J.C., Satkunarajah, M., Schweneker, M., Chapman, J.M., Gyenes, G., Vali, B., Hyrcza, M.D., Yue, F.Y., Kovacs, C., Sassi, A., Loutfy, M., Halpenny, R., Persad, D., Spotts, G., Hecht, F.M., Chun, T.W., McCune, J.M., Kaul, R., Rini, J.M., Nixon, D.F. & Ostrowski, M.A. Tim-3 expression defines a novel population of dysfunctional T cells with highly elevated frequencies in progressive HIV-1 infection. *J Exp Med* **205**, 2763-2779 (2008).
184. Hafler, D.A. & Kuchroo, V. TIMs: central regulators of immune responses. *J Exp Med* **205**, 2699-2701 (2008).
185. Golden-Mason, L., Palmer, B.E., Kassam, N., Townshend-Bulson, L., Livingston, S., McMahon, B.J., Castelblanco, N., Kuchroo, V., Gretch, D.R. & Rosen, H.R. Negative immune regulator Tim-3 is overexpressed on T cells in hepatitis C virus infection and its blockade rescues dysfunctional CD4+ and CD8+ T cells. *Journal of virology* **83**, 9122-9130 (2009).
186. Takamura, S., Tsuji-Kawahara, S., Yagita, H., Akiba, H., Sakamoto, M., Chikaishi, T., Kato, M. & Miyazawa, M. Premature terminal exhaustion of Friend virus-specific effector CD8+ T cells by rapid induction of multiple inhibitory receptors. *J Immunol* **184**, 4696-4707 (2010).
187. Jin, H.T., Anderson, A.C., Tan, W.G., West, E.E., Ha, S.J., Araki, K., Freeman, G.J., Kuchroo, V.K. & Ahmed, R. Cooperation of Tim-3 and PD-1 in CD8 T-cell exhaustion during chronic viral infection. *Proc Natl Acad Sci U S A* **107**, 14733-14738 (2010).
188. Fourcade, J., Sun, Z., Benallaoua, M., Guillaume, P., Luescher, I.F., Sander, C., Kirkwood, J.M., Kuchroo, V. & Zarour, H.M. Upregulation of Tim-3 and PD-1 expression is associated with tumor antigen-specific CD8+ T cell dysfunction in melanoma patients. *J Exp Med* **207**, 2175-2186 (2010).

189. Baitsch, L., Baumgaertner, P., Devevre, E., Raghav, S.K., Legat, A., Barba, L., Wieckowski, S., Bouzourene, H., Deplancke, B., Romero, P., Rufer, N. & Speiser, D.E. Exhaustion of tumor-specific CD8(+) T cells in metastases from melanoma patients. *J Clin Invest* **121**, 2350-2360 (2011).
190. Yang, Z.Z., Grote, D.M., Ziesmer, S.C., Niki, T., Hirashima, M., Novak, A.J., Witzig, T.E. & Ansell, S.M. IL-12 upregulates TIM-3 expression and induces T cell exhaustion in patients with follicular B cell non-Hodgkin lymphoma. *J Clin Invest* **122**, 1271-1282 (2012).
191. Lu, X., Yang, L., Yao, D., Wu, X., Li, J., Liu, X., Deng, L., Huang, C., Wang, Y., Li, D. & Liu, J. Tumor antigen-specific CD8(+) T cells are negatively regulated by PD-1 and Tim-3 in human gastric cancer. *Cellular immunology* **313**, 43-51 (2017).
192. Linedale, R., Schmidt, C., King, B.T., Ganko, A.G., Simpson, F., Panizza, B.J. & Leggatt, G.R. Elevated frequencies of CD8 T cells expressing PD-1, CTLA-4 and Tim-3 within tumour from perineural squamous cell carcinoma patients. *PLoS One* **12**, e0175755 (2017).
193. Ceresoli, G.L. & Mantovani, A. Immune checkpoint inhibitors in malignant pleural mesothelioma. *The Lancet. Oncology* **18**, 559-561 (2017).
194. Shayan, G., Srivastava, R., Li, J., Schmitt, N., Kane, L.P. & Ferris, R.L. Adaptive resistance to anti-PD1 therapy by Tim-3 upregulation is mediated by the PI3K-Akt pathway in head and neck cancer. *Oncoimmunology* **6**, e1261779 (2017).
195. Li, Z., Liu, X., Guo, R. & Wang, P. TIM-3 plays a more important role than PD-1 in the functional impairments of cytotoxic T cells of malignant Schwannomas. *Tumour Biol* **39**, 1010428317698352 (2017).
196. Sakuishi, K., Apetoh, L., Sullivan, J.M., Blazar, B.R., Kuchroo, V.K. & Anderson, A.C. Targeting Tim-3 and PD-1 pathways to reverse T cell exhaustion and restore anti-tumor immunity. *J Exp Med* **207**, 2187-2194 (2010).
197. Zhou, Q., Munger, M.E., Veenstra, R.G., Weigel, B.J., Hirashima, M., Munn, D.H., Murphy, W.J., Azuma, M., Anderson, A.C., Kuchroo, V.K. & Blazar, B.R. Coexpression of Tim-3 and PD-1 identifies a CD8+ T-cell exhaustion phenotype in mice with disseminated acute myelogenous leukemia. *Blood* **117**, 4501-4510 (2011).
198. Gautron, A.S., Dominguez-Villar, M., de Marcken, M. & Hafler, D.A. Enhanced suppressor function of TIM-3+ FoxP3+ regulatory T cells. *European journal of immunology* **44**, 2703-2711 (2014).
199. Gupta, S., Thornley, T.B., Gao, W., Larocca, R., Turka, L.A., Kuchroo, V.K. & Strom, T.B. Allograft rejection is restrained by short-lived TIM-3+PD-1+Foxp3+ Tregs. *J Clin Invest* **122**, 2395-2404 (2012).
200. da Silva, I.P., Gallois, A., Jimenez-Baranda, S., Khan, S., Anderson, A.C., Kuchroo, V.K., Osman, I. & Bhardwaj, N. Reversal of NK-cell exhaustion in advanced melanoma by Tim-3 blockade. *Cancer Immunol Res* **2**, 410-422 (2014).
201. Kang, C.W., Dutta, A., Chang, L.Y., Mahalingam, J., Lin, Y.C., Chiang, J.M., Hsu, C.Y., Huang, C.T., Su, W.T., Chu, Y.Y. & Lin, C.Y. Apoptosis of tumor infiltrating effector TIM-3+CD8+ T cells in colon cancer. *Sci Rep* **5**, 15659 (2015).
202. Ngiow, S.F., von Scheidt, B., Akiba, H., Yagita, H., Teng, M.W. & Smyth, M.J. Anti-TIM3 antibody promotes T cell IFN-gamma-mediated antitumor immunity and suppresses established tumors. *Cancer research* **71**, 3540-3551 (2011).

203. Koyama, S., Akbay, E.A., Li, Y.Y., Herter-Sprie, G.S., Buczkowski, K.A., Richards, W.G., Gandhi, L., Redig, A.J., Rodig, S.J., Asahina, H., Jones, R.E., Kulkarni, M.M., Kuraguchi, M., Palakurthi, S., Fecci, P.E., Johnson, B.E., Janne, P.A., Engelman, J.A., Gangadharan, S.P., Costa, D.B., Freeman, G.J., Bueno, R., Hodi, F.S., Dranoff, G., Wong, K.K. & Hammerman, P.S. Adaptive resistance to therapeutic PD-1 blockade is associated with upregulation of alternative immune checkpoints. *Nat Commun* **7**, 10501 (2016).
204. Herbst, R.S., Baas, P., Kim, D.W., Felip, E., Pérez-Gracia, J.L., Han, J.Y., Molina, J., Kim, J.H., Arvis, C.D., Ahn, M.J., Majem, M., Fidler, M.J., de Castro, G., Garrido, M., Lubiniecki, G.M., Shentu, Y., Im, E., Dolled-Filhart, M. & Garon, E.B. Pembrolizumab versus docetaxel for previously treated, PD-L1-positive, advanced non-small-cell lung cancer (KEYNOTE-010): a randomised controlled trial. *Lancet* **387**, 1540-1550 (2016).
205. Nanda, R., Chow, L.Q., Dees, E.C., Berger, R., Gupta, S., Geva, R., Pusztai, L., Pathiraja, K., Aktan, G., Cheng, J.D., Karantza, V. & Buisseret, L. Pembrolizumab in Patients With Advanced Triple-Negative Breast Cancer: Phase Ib KEYNOTE-012 Study. *J Clin Oncol* **34**, 2460-2467 (2016).
206. Bortnik, S., Choutka, C., Horlings, H.M., Leung, S., Baker, J.H., Lebovitz, C., Dragowska, W.H., Go, N.E., Bally, M.B., Minchinton, A.I., Gelmon, K.A. & Gorski, S.M. Identification of breast cancer cell subtypes sensitive to ATG4B inhibition. *Oncotarget* **7**, 66970-66988 (2016).
207. Cheang, M.C., Treaba, D.O., Speers, C.H., Olivotto, I.A., Bajdik, C.D., Chia, S.K., Goldstein, L.C., Gelmon, K.A., Huntsman, D., Gilks, C.B., Nielsen, T.O. & Gown, A.M. Immunohistochemical detection using the new rabbit monoclonal antibody SP1 of estrogen receptor in breast cancer is superior to mouse monoclonal antibody 1D5 in predicting survival. *J Clin Oncol* **24**, 5637-5644 (2006).
208. Cheang, M.C., Chia, S.K., Voduc, D., Gao, D., Leung, S., Snider, J., Watson, M., Davies, S., Bernard, P.S., Parker, J.S., Perou, C.M., Ellis, M.J. & Nielsen, T.O. Ki67 index, HER2 status, and prognosis of patients with luminal B breast cancer. *J Natl Cancer Inst* **101**, 736-750 (2009).
209. Altman, D.G., McShane, L.M., Sauerbrei, W. & Taube, S.E. Reporting Recommendations for Tumor Marker Prognostic Studies (REMARK): explanation and elaboration. *PLoS Med* **9**, e1001216 (2012).
210. McDermott, D.F., Sosman, J.A., Sznol, M., Massard, C., Gordon, M.S., Hamid, O., Powderly, J.D., Infante, J.R., Fasso, M., Wang, Y.V., Zou, W., Hegde, P.S., Fine, G.D. & Powles, T. Atezolizumab, an Anti-Programmed Death-Ligand 1 Antibody, in Metastatic Renal Cell Carcinoma: Long-Term Safety, Clinical Activity, and Immune Correlates From a Phase Ia Study. *J Clin Oncol* **34**, 833-842 (2016).
211. Triebel, F., Hacene, K. & Pichon, M.F. A soluble lymphocyte activation gene-3 (sLAG-3) protein as a prognostic factor in human breast cancer expressing estrogen or progesterone receptors. *Cancer Lett* **235**, 147-153 (2006).
212. Chen, D.S. & Mellman, I. Elements of cancer immunity and the cancer-immune set point. *Nature* **541**, 321-330 (2017).
213. Ingold Heppner, B., Untch, M., Denkert, C., Pfitzner, B.M., Lederer, B., Schmitt, W., Eidtmann, H., Fasching, P.A., Tesch, H., Solbach, C., Rezai, M., Zahm, D.M., Holms, F., Glados, M., Krabisch, P., Heck, E., Ober, A., Lorenz, P., Diebold, K., Habeck, J.O. &

Loibl, S. Tumor-Infiltrating Lymphocytes: A Predictive and Prognostic Biomarker in Neoadjuvant-Treated HER2-Positive Breast Cancer. *Clin Cancer Res* **22**, 5747-5754 (2016).
214. Hamid, O., Schmidt, H., Nissan, A., Ridolfi, L., Aamdal, S., Hansson, J., Guida, M., Hyams, D.M., Gomez, H., Bastholt, L., Chasalow, S.D. & Berman, D. A prospective phase II trial exploring the association between tumor microenvironment biomarkers and clinical activity of ipilimumab in advanced melanoma. *J Transl Med* **9**, 204 (2011).
215. Tumeh, P.C., Harview, C.L., Yearley, J.H., Shintaku, I.P., Taylor, E.J., Robert, L., Chmielowski, B., Spasic, M., Henry, G., Ciobanu, V., West, A.N., Carmona, M., Kivork, C., Seja, E., Cherry, G., Gutierrez, A.J., Grogan, T.R., Mateus, C., Tomasic, G., Glaspy, J.A., Emerson, R.O., Robins, H., Pierce, R.H., Elashoff, D.A., Robert, C. & Ribas, A. PD-1 blockade induces responses by inhibiting adaptive immune resistance. *Nature* **515**, 568-571 (2014).
216. Schmid P, C.C., Braiteh FS et al. Atezolizumab in metastatic TNBC (mTNBC): Long-term clinical outcomes and biomarker analyses [abstract]. in *AACR Annual Meeting* Abstract nr 2986 (Washington, DC, 2017).
217. Dirix LY Y, T.I., Nikolinakos P et al. Avelumab (MSB0010718C), an anti-PD-L1 antibody, in patients with locally advanced or metastatic breast cancer: A phase
Ib JAVELIN solid tumor trial[abstract]. in *San Antonio Breast Cancer Symposium* Abstract nr S1-04 (San Antonio, Texas, USA, 2015).
218. Salama, A.K. & Moschos, S.J. Next Steps in Immuno-Oncology: Enhancing Antitumor Effects Through Appropriate Patient Selection and Rationally Designed Combination Strategies. *Ann Oncol* (2016).
219. Krishnamurti, U., Wetherilt, C.S., Yang, J., Peng, L. & Li, X. Tumor-infiltrating lymphocytes are significantly associated with better overall survival and disease-free survival in triple-negative but not estrogen receptor-positive breast cancers. *Human pathology* **64**, 7-12 (2017).
220. Heindl, A., Sestak, I., Naidoo, K., Cuzick, J., Dowsett, M. & Yuan, Y. Relevance of Spatial Heterogeneity of Immune Infiltration for Predicting Risk of Recurrence After Endocrine Therapy of ER+ Breast Cancer. *J Natl Cancer Inst* **110**(2018).
221. Herbst, R.S., Baas, P., Kim, D.W., Felip, E., Perez-Gracia, J.L., Han, J.Y., Molina, J., Kim, J.H., Arvis, C.D., Ahn, M.J., Majem, M., Fidler, M.J., de Castro, G., Jr., Garrido, M., Lubiniecki, G.M., Shentu, Y., Im, E., Dolled-Filhart, M. & Garon, E.B. Pembrolizumab versus docetaxel for previously treated, PD-L1-positive, advanced non-small-cell lung cancer (KEYNOTE-010): a randomised controlled trial. *Lancet* **387**, 1540-1550 (2016).
222. Dirix, L.Y., Takacs, I., Jerusalem, G., Nikolinakos, P., Arkenau, H.T., Forero-Torres, A., Boccia, R., Lippman, M.E., Somer, R., Smakal, M., Emens, L.A., Hrinczenko, B., Edenfield, W., Gurtler, J., von Heydebreck, A., Grote, H.J., Chin, K. & Hamilton, E.P. Avelumab, an anti-PD-L1 antibody, in patients with locally advanced or metastatic breast cancer: a phase 1b JAVELIN Solid Tumor study. *Breast Cancer Res Treat* **167**, 671-686 (2018).
223. McArthur, H.L., Diab, A., Page, D.B., Yuan, J., Solomon, S.B., Sacchini, V., Comstock, C., Durack, J.C., Maybody, M., Sung, J., Ginsberg, A., Wong, P., Barlas, A., Dong, Z., Zhao, C., Blum, B., Patil, S., Neville, D., Comen, E.A., Morris, E.A., Kotin, A., Brogi,

E., Wen, Y.H., Morrow, M., Lacouture, M.E., Sharma, P., Allison, J.P., Hudis, C.A., Wolchok, J.D. & Norton, L. A Pilot Study of Preoperative Single-Dose Ipilimumab and/or Cryoablation in Women with Early-Stage Breast Cancer with Comprehensive Immune Profiling. *Clin Cancer Res* **22**, 5729-5737 (2016).

224. Emens, L.A. Breast Cancer Immunotherapy: Facts and Hopes. *Clin Cancer Res* **24**, 511-520 (2018).
225. Kwa, M.J. & Adams, S. Checkpoint inhibitors in triple-negative breast cancer (TNBC): Where to go from here. *Cancer* (2018).
226. Bellmunt, J., de Wit, R., Vaughn, D.J., Fradet, Y., Lee, J.L., Fong, L., Vogelzang, N.J., Climent, M.A., Petrylak, D.P., Choueiri, T.K., Necchi, A., Gerritsen, W., Gurney, H., Quinn, D.I., Culine, S., Sternberg, C.N., Mai, Y., Poehlein, C.H., Perini, R.F., Bajorin, D.F. & Investigators, K.-. Pembrolizumab as Second-Line Therapy for Advanced Urothelial Carcinoma. *N Engl J Med* **376**, 1015-1026 (2017).
227. Balar, A.V., Galsky, M.D., Rosenberg, J.E., Powles, T., Petrylak, D.P., Bellmunt, J., Loriot, Y., Necchi, A., Hoffman-Censits, J., Perez-Gracia, J.L., Dawson, N.A., van der Heijden, M.S., Dreicer, R., Srinivas, S., Retz, M.M., Joseph, R.W., Drakaki, A., Vaishampayan, U.N., Sridhar, S.S., Quinn, D.I., Duran, I., Shaffer, D.R., Eigl, B.J., Grivas, P.D., Yu, E.Y., Li, S., Kadel, E.E., 3rd, Boyd, Z., Bourgon, R., Hegde, P.S., Mariathasan, S., Thastrom, A., Abidoye, O.O., Fine, G.D., Bajorin, D.F. & Group, I.M.S. Atezolizumab as first-line treatment in cisplatin-ineligible patients with locally advanced and metastatic urothelial carcinoma: a single-arm, multicentre, phase 2 trial. *Lancet* **389**, 67-76 (2017).
228. Balar, A.V., Castellano, D., O'Donnell, P.H., Grivas, P., Vuky, J., Powles, T., Plimack, E.R., Hahn, N.M., de Wit, R., Pang, L., Savage, M.J., Perini, R.F., Keefe, S.M., Bajorin, D. & Bellmunt, J. First-line pembrolizumab in cisplatin-ineligible patients with locally advanced and unresectable or metastatic urothelial cancer (KEYNOTE-052): a multicentre, single-arm, phase 2 study. *The Lancet. Oncology* **18**, 1483-1492 (2017).
229. Rittmeyer, A., Barlesi, F., Waterkamp, D., Park, K., Ciardiello, F., von Pawel, J., Gadgeel, S.M., Hida, T., Kowalski, D.M., Dols, M.C., Cortinovis, D.L., Leach, J., Polikoff, J., Barrios, C., Kabbinavar, F., Frontera, O.A., De Marinis, F., Turna, H., Lee, J.S., Ballinger, M., Kowanetz, M., He, P., Chen, D.S., Sandler, A., Gandara, D.R. & Group, O.A.K.S. Atezolizumab versus docetaxel in patients with previously treated non-small-cell lung cancer (OAK): a phase 3, open-label, multicentre randomised controlled trial. *Lancet* **389**, 255-265 (2017).
230. Antonia, S.J., Villegas, A., Daniel, D., Vicente, D., Murakami, S., Hui, R., Yokoi, T., Chiappori, A., Lee, K.H., de Wit, M., Cho, B.C., Bourhaba, M., Quantin, X., Tokito, T., Mekhail, T., Planchard, D., Kim, Y.C., Karapetis, C.S., Hiret, S., Ostoros, G., Kubota, K., Gray, J.E., Paz-Ares, L., de Castro Carpeno, J., Wadsworth, C., Melillo, G., Jiang, H., Huang, Y., Dennis, P.A., Ozguroglu, M. & Investigators, P. Durvalumab after Chemoradiotherapy in Stage III Non-Small-Cell Lung Cancer. *N Engl J Med* **377**, 1919-1929 (2017).
231. de Mingo Pulido, A., Gardner, A., Hiebler, S., Soliman, H., Rugo, H.S., Krummel, M.F., Coussens, L.M. & Ruffell, B. TIM-3 Regulates CD103(+) Dendritic Cell Function and Response to Chemotherapy in Breast Cancer. *Cancer Cell* **33**, 60-74 e66 (2018).

232. Yan, W., Liu, X., Ma, H., Zhang, H., Song, X., Gao, L., Liang, X. & Ma, C. Tim-3 fosters HCC development by enhancing TGF-beta-mediated alternative activation of macrophages. *Gut* **64**, 1593-1604 (2015).
233. Sabatos-Peyton, C.A., Nevin, J., Brock, A., Venable, J.D., Tan, D.J., Kassam, N., Xu, F., Taraszka, J., Wesemann, L., Pertel, T., Acharya, N., Klapholz, M., Etminan, Y., Jiang, X., Huang, Y.H., Blumberg, R.S., Kuchroo, V.K. & Anderson, A.C. Blockade of Tim-3 binding to phosphatidylserine and CEACAM1 is a shared feature of anti-Tim-3 antibodies that have functional efficacy. *Oncoimmunology* **7**, e1385690 (2018).
234. Das, M., Zhu, C. & Kuchroo, V.K. Tim-3 and its role in regulating anti-tumor immunity. *Immunological reviews* **276**, 97-111 (2017).
235. Granier, C., Dariane, C., Combe, P., Verkarre, V., Urien, S., Badoual, C., Roussel, H., Mandavit, M., Ravel, P., Sibony, M., Biard, L., Radulescu, C., Vinatier, E., Benhamouda, N., Peyromaure, M., Oudard, S., Mejean, A., Timsit, M.O., Gey, A. & Tartour, E. Tim-3 Expression on Tumor-Infiltrating PD-1(+)CD8(+) T Cells Correlates with Poor Clinical Outcome in Renal Cell Carcinoma. *Cancer Res* **77**, 1075-1082 (2017).
236. Li, H., Wu, K., Tao, K., Chen, L., Zheng, Q., Lu, X., Liu, J., Shi, L., Liu, C., Wang, G. & Zou, W. Tim-3/galectin-9 signaling pathway mediates T-cell dysfunction and predicts poor prognosis in patients with hepatitis B virus-associated hepatocellular carcinoma. *Hepatology* **56**, 1342-1351 (2012).
237. Japp, A.S., Kursunel, M.A., Meier, S., Malzer, J.N., Li, X., Rahman, N.A., Jekabsons, W., Krause, H., Magheli, A., Klopf, C., Thiel, A. & Frentsch, M. Dysfunction of PSA-specific CD8+ T cells in prostate cancer patients correlates with CD38 and Tim-3 expression. *Cancer immunology, immunotherapy : CII* **64**, 1487-1494 (2015).
238. Liu, Z., Meng, Q., Bartek, J., Jr., Poiret, T., Persson, O., Rane, L., Rangelova, E., Illies, C., Peredo, I.H., Luo, X., Rao, M.V., Robertson, R.A., Dodoo, E. & Maeurer, M. Tumor-infiltrating lymphocytes (TILs) from patients with glioma. *Oncoimmunology* **6**, e1252894 (2017).
239. Solinas, C., Garaud, S., De Silva, P., Boisson, A., Van den Eynden, G., de Wind, A., Risso, P., Rodrigues Vitoria, J., Richard, F., Migliori, E., Noel, G., Duvillier, H., Craciun, L., Veys, I., Awada, A., Detours, V., Larsimont, D., Piccart-Gebhart, M. & Willard-Gallo, K. Immune Checkpoint Molecules on Tumor-Infiltrating Lymphocytes and Their Association with Tertiary Lymphoid Structures in Human Breast Cancer. *Front Immunol* **8**, 1412 (2017).
240. Zhang, H., Xiang, R., Wu, B., Li, J. & Luo, G. T-cell immunoglobulin mucin-3 expression in invasive ductal breast carcinoma: Clinicopathological correlations and association with tumor infiltration by cytotoxic lymphocytes. *Mol Clin Oncol* **7**, 557-563 (2017).
241. Cheang, M.C., Voduc, D., Bajdik, C., Leung, S., McKinney, S., Chia, S.K., Perou, C.M. & Nielsen, T.O. Basal-like breast cancer defined by five biomarkers has superior prognostic value than triple-negative phenotype. *Clin Cancer Res* **14**, 1368-1376 (2008).
242. Burugu, S., Gao, D., Leung, S., Chia, S.K. & Nielsen, T.O. LAG-3+ tumor infiltrating lymphocytes in breast cancer: clinical correlates and association with PD-1/PD-L1+ tumors. *Ann Oncol* **28**, 2977-2984 (2017).
243. Chen, T.C., Chen, C.H., Wang, C.P., Lin, P.H., Yang, T.L., Lou, P.J., Ko, J.Y., Wu, C.T. & Chang, Y.L. The immunologic advantage of recurrent nasopharyngeal carcinoma from

the viewpoint of Galectin-9/Tim-3-related changes in the tumour microenvironment. *Sci Rep* **7**, 10349 (2017).
244. Liu, J.F., Ma, S.R., Mao, L., Bu, L.L., Yu, G.T., Li, Y.C., Huang, C.F., Deng, W.W., Kulkarni, A.B., Zhang, W.F. & Sun, Z.J. T-cell immunoglobulin mucin 3 blockade drives an antitumor immune response in head and neck cancer. *Molecular oncology* **11**, 235-247 (2017).
245. Gao, J., Ward, J.F., Pettaway, C.A., Shi, L.Z., Subudhi, S.K., Vence, L.M., Zhao, H., Chen, J., Chen, H., Efstathiou, E., Troncoso, P., Allison, J.P., Logothetis, C.J., Wistuba, II, Sepulveda, M.A., Sun, J., Wargo, J., Blando, J. & Sharma, P. VISTA is an inhibitory immune checkpoint that is increased after ipilimumab therapy in patients with prostate cancer. *Nature medicine* **23**, 551-555 (2017).
246. Zhang, Y., Cai, P., Liang, T., Wang, L. & Hu, L. TIM-3 is a potential prognostic marker for patients with solid tumors: A systematic review and meta-analysis. *Oncotarget* **8**, 31705-31713 (2017).
247. Le, D.T., Uram, J.N., Wang, H., Bartlett, B.R., Kemberling, H., Eyring, A.D., Skora, A.D., Luber, B.S., Azad, N.S., Laheru, D., Biedrzycki, B., Donehower, R.C., Zaheer, A., Fisher, G.A., Crocenzi, T.S., Lee, J.J., Duffy, S.M., Goldberg, R.M., de la Chapelle, A., Koshiji, M., Bhaijee, F., Huebner, T., Hruban, R.H., Wood, L.D., Cuka, N., Pardoll, D.M., Papadopoulos, N., Kinzler, K.W., Zhou, S., Cornish, T.C., Taube, J.M., Anders, R.A., Eshleman, J.R., Vogelstein, B. & Diaz, L.A., Jr. PD-1 Blockade in Tumors with Mismatch-Repair Deficiency. *N Engl J Med* **372**, 2509-2520 (2015).
248. Rizvi, N.A., Hellmann, M.D., Snyder, A., Kvistborg, P., Makarov, V., Havel, J.J., Lee, W., Yuan, J., Wong, P., Ho, T.S., Miller, M.L., Rekhtman, N., Moreira, A.L., Ibrahim, F., Bruggeman, C., Gasmi, B., Zappasodi, R., Maeda, Y., Sander, C., Garon, E.B., Merghoub, T., Wolchok, J.D., Schumacher, T.N. & Chan, T.A. Cancer immunology. Mutational landscape determines sensitivity to PD-1 blockade in non-small cell lung cancer. *Science* **348**, 124-128 (2015).
249. Davoli, T., Uno, H., Wooten, E.C. & Elledge, S.J. Tumor aneuploidy correlates with markers of immune evasion and with reduced response to immunotherapy. *Science* **355**(2017).
250. Le, D.T., Durham, J.N., Smith, K.N., Wang, H., Bartlett, B.R., Aulakh, L.K., Lu, S., Kemberling, H., Wilt, C., Luber, B.S., Wong, F., Azad, N.S., Rucki, A.A., Laheru, D., Donehower, R., Zaheer, A., Fisher, G.A., Crocenzi, T.S., Lee, J.J., Greten, T.F., Duffy, A.G., Ciombor, K.K., Eyring, A.D., Lam, B.H., Joe, A., Kang, S.P., Holdhoff, M., Danilova, L., Cope, L., Meyer, C., Zhou, S., Goldberg, R.M., Armstrong, D.K., Bever, K.M., Fader, A.N., Taube, J., Housseau, F., Spetzler, D., Xiao, N., Pardoll, D.M., Papadopoulos, N., Kinzler, K.W., Eshleman, J.R., Vogelstein, B., Anders, R.A. & Diaz, L.A., Jr. Mismatch repair deficiency predicts response of solid tumors to PD-1 blockade. *Science* **357**, 409-413 (2017).
251. Herbst, R.S., Soria, J.C., Kowanetz, M., Fine, G.D., Hamid, O., Gordon, M.S., Sosman, J.A., McDermott, D.F., Powderly, J.D., Gettinger, S.N., Kohrt, H.E., Horn, L., Lawrence, D.P., Rost, S., Leabman, M., Xiao, Y., Mokatrin, A., Koeppen, H., Hegde, P.S., Mellman, I., Chen, D.S. & Hodi, F.S. Predictive correlates of response to the anti-PD-L1 antibody MPDL3280A in cancer patients. *Nature* **515**, 563-567 (2014).

252. Allard, B., Aspeslagh, S., Garaud, S., Dupont, F.A., Solinas, C., Kok, M., Routy, B., Sotiriou, C., Stagg, J. & Buisseret, L. Immuno-oncology-101: overview of major concepts and translational perspectives. *Seminars in cancer biology* **52**, 1-11 (2018).
253. Halse, H., Colebatch, A.J., Petrone, P., Henderson, M.A., Mills, J.K., Snow, H., Westwood, J.A., Sandhu, S., Raleigh, J.M., Behren, A., Cebon, J., Darcy, P.K., Kershaw, M.H., McArthur, G.A., Gyorki, D.E. & Neeson, P.J. Multiplex immunohistochemistry accurately defines the immune context of metastatic melanoma. *Sci Rep* **8**, 11158 (2018).
254. Keren, L., Bosse, M., Marquez, D., Angoshtari, R., Jain, S., Varma, S., Yang, S.R., Kurian, A., Van Valen, D., West, R., Bendall, S.C. & Angelo, M. A Structured Tumor-Immune Microenvironment in Triple Negative Breast Cancer Revealed by Multiplexed Ion Beam Imaging. *Cell* **174**, 1373-1387 e1319 (2018).
255. Asleh-Aburaya, K., Sheffield, B.S., Kos, Z., Won, J.R., Wang, X.Q., Gao, D., Wolber, R., Gilks, C.B., Bernard, P.S., Chia, S.K. & Nielsen, T.O. Basal biomarkers nestin and INPP4b identify intrinsic subtypes accurately in breast cancers that are weakly positive for oestrogen receptor. *Histopathology* **70**, 185-194 (2017).
256. Amaria, R.N., Reddy, S.M., Tawbi, H.A., Davies, M.A., Ross, M.I., Glitza, I.C., Cormier, J.N., Lewis, C., Hwu, W.J., Hanna, E., Diab, A., Wong, M.K., Royal, R., Gross, N., Weber, R., Lai, S.Y., Ehlers, R., Blando, J., Milton, D.R., Woodman, S., Kageyama, R., Wells, D.K., Hwu, P., Patel, S.P., Lucci, A., Hessel, A., Lee, J.E., Gershenwald, J., Simpson, L., Burton, E.M., Posada, L., Haydu, L., Wang, L., Zhang, S., Lazar, A.J., Hudgens, C.W., Gopalakrishnan, V., Reuben, A., Andrews, M.C., Spencer, C.N., Prieto, V., Sharma, P., Allison, J., Tetzlaff, M.T. & Wargo, J.A. Neoadjuvant immune checkpoint blockade in high-risk resectable melanoma. *Nat Med* **24**, 1649-1654 (2018).
257. Blank, C.U., Rozeman, E.A., Fanchi, L.F., Sikorska, K., van de Wiel, B., Kvistborg, P., Krijgsman, O., van den Braber, M., Philips, D., Broeks, A., van Thienen, J.V., Mallo, H.A., Adriaansz, S., Ter Meulen, S., Pronk, L.M., Grijpink-Ongering, L.G., Bruining, A., Gittelman, R.M., Warren, S., van Tinteren, H., Peeper, D.S., Haanen, J., van Akkooi, A.C.J. & Schumacher, T.N. Neoadjuvant versus adjuvant ipilimumab plus nivolumab in macroscopic stage III melanoma. *Nat Med* **24**, 1655-1661 (2018).
258. Dieci, M.V., Radosevic-Robin, N., Fineberg, S., van den Eynden, G., Ternes, N., Penault-Llorca, F., Pruneri, G., D'Alfonso, T.M., Demaria, S., Castaneda, C., Sanchez, J., Badve, S., Michiels, S., Bossuyt, V., Rojo, F., Singh, B., Nielsen, T., Viale, G., Kim, S.R., Hewitt, S., Wienert, S., Loibl, S., Rimm, D., Symmans, F., Denkert, C., Adams, S., Loi, S., Salgado, R. & International Immuno-Oncology Biomarker Working Group on Breast, C. Update on tumor-infiltrating lymphocytes (TILs) in breast cancer, including recommendations to assess TILs in residual disease after neoadjuvant therapy and in carcinoma in situ: A report of the International Immuno-Oncology Biomarker Working Group on Breast Cancer. *Seminars in cancer biology* **52**, 16-25 (2018).
259. Picarda, E., Ohaegbulam, K.C. & Zang, X. Molecular Pathways: Targeting B7-H3 (CD276) for Human Cancer Immunotherapy. *Clin Cancer Res* **22**, 3425-3431 (2016).
260. Parra, E.R. Novel Platforms of Multiplexed Immunofluorescence for Study of Paraffin Tumor Tissues. *Journal of Cancer treatment and diagnosis* **2**, 43-53 (2018).
261. Parra, E.R., Uraoka, N., Jiang, M., Cook, P., Gibbons, D., Forget, M.A., Bernatchez, C., Haymaker, C., Wistuba, II & Rodriguez-Canales, J. Validation of multiplex

immunofluorescence panels using multispectral microscopy for immune-profiling of formalin-fixed and paraffin-embedded human tumor tissues. *Sci Rep* **7**, 13380 (2017).
262. Gorris, M.A.J., Halilovic, A., Rabold, K., van Duffelen, A., Wickramasinghe, I.N., Verweij, D., Wortel, I.M.N., Textor, J.C., de Vries, I.J.M. & Figdor, C.G. Eight-Color Multiplex Immunohistochemistry for Simultaneous Detection of Multiple Immune Checkpoint Molecules within the Tumor Microenvironment. *J Immunol* **200**, 347-354 (2018).
263. Stack, E.C., Foukas, P.G. & Lee, P.P. Multiplexed tissue biomarker imaging. *J Immunother Cancer* **4**, 9 (2016).
264. Decalf, J., Albert, M.L. & Ziai, J. New tools for pathology: a user's review of a highly multiplexed method for in situ analysis of protein and RNA expression in tissue. *The Journal of pathology* (2018).
265. Ayers, M., Lunceford, J., Nebozhyn, M., Murphy, E., Loboda, A., Kaufman, D.R., Albright, A., Cheng, J.D., Kang, S.P., Shankaran, V., Piha-Paul, S.A., Yearley, J., Seiwert, T.Y., Ribas, A. & McClanahan, T.K. IFN-gamma-related mRNA profile predicts clinical response to PD-1 blockade. *J Clin Invest* **127**, 2930-2940 (2017).
266. Gibney, G.T., Weiner, L.M. & Atkins, M.B. Predictive biomarkers for checkpoint inhibitor-based immunotherapy. *The Lancet. Oncology* **17**, e542-e551 (2016).
267. Spranger, S., Sivan, A., Corrales, L. & Gajewski, T.F. Tumor and Host Factors Controlling Antitumor Immunity and Efficacy of Cancer Immunotherapy. *Advances in immunology* **130**, 75-93 (2016).
268. Teng, M.W., Ngiow, S.F., Ribas, A. & Smyth, M.J. Classifying Cancers Based on T-cell Infiltration and PD-L1. *Cancer Res* **75**, 2139-2145 (2015).
269. Bruno, T.C., Ebner, P.J., Moore, B.L., Squalls, O.G., Waugh, K.A., Eruslanov, E.B., Singhal, S., Mitchell, J.D., Franklin, W.A., Merrick, D.T., McCarter, M.D., Palmer, B.E., Kern, J.A. & Slansky, J.E. Antigen-Presenting Intratumoral B Cells Affect CD4(+) TIL Phenotypes in Non-Small Cell Lung Cancer Patients. *Cancer Immunol Res* **5**, 898-907 (2017).
270. Coulie, P.G., Van den Eynde, B.J., van der Bruggen, P. & Boon, T. Tumour antigens recognized by T lymphocytes: at the core of cancer immunotherapy. *Nat Rev Cancer* **14**, 135-146 (2014).
271. Cristescu, R., Mogg, R., Ayers, M., Albright, A., Murphy, E., Yearley, J., Sher, X., Liu, X.Q., Lu, H., Nebozhyn, M., Zhang, C., Lunceford, J.K., Joe, A., Cheng, J., Webber, A.L., Ibrahim, N., Plimack, E.R., Ott, P.A., Seiwert, T.Y., Ribas, A., McClanahan, T.K., Tomassini, J.E., Loboda, A. & Kaufman, D. Pan-tumor genomic biomarkers for PD-1 checkpoint blockade-based immunotherapy. *Science* **362**(2018).
272. Galluzzi, L., Buque, A., Kepp, O., Zitvogel, L. & Kroemer, G. Immunological Effects of Conventional Chemotherapy and Targeted Anticancer Agents. *Cancer Cell* **28**, 690-714 (2015).
273. Alizadeh, D., Trad, M., Hanke, N.T., Larmonier, C.B., Janikashvili, N., Bonnotte, B., Katsanis, E. & Larmonier, N. Doxorubicin eliminates myeloid-derived suppressor cells and enhances the efficacy of adoptive T-cell transfer in breast cancer. *Cancer Res* **74**, 104-118 (2014).
274. Levine, M.N., Pritchard, K.I., Bramwell, V.H., Shepherd, L.E., Tu, D., Paul, N. & National Cancer Institute of Canada Clinical Trials, G. Randomized trial comparing

cyclophosphamide, epirubicin, and fluorouracil with cyclophosphamide, methotrexate, and fluorouracil in premenopausal women with node-positive breast cancer: update of National Cancer Institute of Canada Clinical Trials Group Trial MA5. *J Clin Oncol* **23**, 5166-5170 (2005).

275. Savas, P., Virassamy, B., Ye, C., Salim, A., Mintoff, C.P., Caramia, F., Salgado, R., Byrne, D.J., Teo, Z.L., Dushyanthen, S., Byrne, A., Wein, L., Luen, S.J., Poliness, C., Nightingale, S.S., Skandarajah, A.S., Gyorki, D.E., Thornton, C.M., Beavis, P.A., Fox, S.B., Darcy, P.K., Speed, T.P., Mackay, L.K., Neeson, P.J. & Loi, S. Single-cell profiling of breast cancer T cells reveals a tissue-resident memory subset associated with improved prognosis. *Nat Med* **24**, 986-993 (2018).
276. Andrews, L.P., Marciscano, A.E., Drake, C.G. & Vignali, D.A. LAG3 (CD223) as a cancer immunotherapy target. *Immunological reviews* **276**, 80-96 (2017).
277. Duhoux, F.P., Jager, A., Dirix, L., Huizing, M.T., Jerusalem, G.H.M., Vuylsteke, P., Cuypere, E.D., Breiner, D., Mueller, C., Brignone, C. & Triebel, F. Combination of paclitaxel and LAG3-Ig (IMP321), a novel MHC class II agonist, as a first-line chemoimmunotherapy in patients with metastatic breast carcinoma (MBC): Interim results from the run-in phase of a placebo controlled randomized phase II. *Journal of Clinical Oncology* **35**, 1062-1062 (2017).
278. Hong, D.S., Schoffski, P., Calvo, A., Sarantopoulos, J., Olza, M.O.D., Carvajal, R.D., Prawira, A., Kyi, C., Esaki, T., Akerley, W.L., Braud, F.G.D., Hui, R., Zhang, T., Soo, R.A., Maur, M., Weickhardt, A.J., Chowdhury, N.R., Sabatos-Peyton, C., Kwak, E.L. & Tan, D.S.-W. Phase I/II study of LAG525 ± spartalizumab (PDR001) in patients (pts) with advanced malignancies. *Journal of Clinical Oncology* **36**, 3012-3012 (2018).
279. Gayden, T., Sepulveda, F.E., Khuong-Quang, D.A., Pratt, J., Valera, E.T., Garrigue, A., Kelso, S., Sicheri, F., Mikael, L.G., Hamel, N., Bajic, A., Dali, R., Deshmukh, S., Dervovic, D., Schramek, D., Guerin, F., Taipale, M., Nikbakht, H., Majewski, J., Moshous, D., Charlebois, J., Abish, S., Bole-Feysot, C., Nitschke, P., Bader-Meunier, B., Mitchell, D., Thieblemont, C., Battistella, M., Gravel, S., Nguyen, V.H., Conyers, R., Diana, J.S., McCormack, C., Prince, H.M., Besnard, M., Blanche, S., Ekert, P.G., Fraitag, S., Foulkes, W.D., Fischer, A., Neven, B., Michonneau, D., de Saint Basile, G. & Jabado, N. Germline HAVCR2 mutations altering TIM-3 characterize subcutaneous panniculitis-like T cell lymphomas with hemophagocytic lymphohistiocytic syndrome. *Nature genetics* **50**, 1650-1657 (2018).
280. Pernas, S., Tolaney, S.M., Winer, E.P. & Goel, S. CDK4/6 inhibition in breast cancer: current practice and future directions. *Therapeutic advances in medical oncology* **10**, 1758835918786451 (2018).
281. Goel, S., DeCristo, M.J., Watt, A.C., BrinJones, H., Sceneay, J., Li, B.B., Khan, N., Ubellacker, J.M., Xie, S., Metzger-Filho, O., Hoog, J., Ellis, M.J., Ma, C.X., Ramm, S., Krop, I.E., Winer, E.P., Roberts, T.M., Kim, H.J., McAllister, S.S. & Zhao, J.J. CDK4/6 inhibition triggers anti-tumour immunity. *Nature* **548**, 471-475 (2017).
282. Roulois, D., Yau, H.L. & De Carvalho, D.D. Pharmacological DNA demethylation: Implications for cancer immunotherapy. *Oncoimmunology* **5**, e1090077 (2016).

Appendix A

Supplemental information on LAG-3 assay

Antibody: LAG-3

Clone: 17B4

Reactivity: Human

Sensitivity and Specificity

LAG-3 mouse clone 17B4 (Abcam) recognizes amino acids 70-99 of human LAG-3 protein. Clone 17B4 was tested by Western blot by the supplier using recombinant human LAG-3 protein. Other tested applications of LAG-3 clone 17B4, including flow cytometry and immunohistochemistry on formalin-fixed paraffin-embedded tissues, were reported in previous publications [PMID: 21441454; 25358689, 27301722, and 27912781].

Full protocol on Ventana

LAG-3 immunostains on tissue microarrays were performed on the Ventana Discovery Ultra (Ventana Medical Systems, Tucson, AZ, USA) semi-automated immunostainer. Slides underwent antigen retrieval with Standard Cell Conditioning 1 (Ventana Medical Systems) followed by 120 minutes of primary antibody incubation with no heat and detected using chromoMap DAB Detection Kit (Ventana Medical Systems). LAG-3 antibody (clone 17B4, Abcam, ab40466) was applied at dilution of 1:100. Membranous staining on activated lymphocytes localized in normal tonsil tissue served as a positive control.

Analytical validity

To assess the reproducibility of LAG-3 scoring, a second observer independently scored 145 cases from the training set (duplicate 0.6 mm diameter tissue microarray cores, stained by immunohistochemistry per the above protocol). As in **Chapter 2**, IHC-positive lymphocytes

were counted, and cases were categorized as positive if any (>0) were identified. There was a substantial inter-observer agreement between LAG-3 dichotomized scores for both the primary biomarker assessment in the **Chapter 2** intraepithelial tumor infiltrating lymphocytes = iTILs (Cohen's kappa = 0.69 ((95% CI 0.49-0.84) and for the alternative assessment of stromal tumor infiltrating lymphocytes, sTILs= 0.65 (0.46-0.81).

Appendix B

Pre-specified statistical plan for <u>Chapter 2</u> presented at the BC Cancer Agency Breast Outcome Unit

List of hypotheses generated on the half of the validation cohort (n= 2,003) and to be tested on the other half (n=1,989):

1) Breast tumors with LAG3+TILs are associated with improved relapse-free survival among ER–.

2) Breast tumors with PD1+TILs are associated with shorter relapse-free survival among ER+ patients.

3) Breast tumors with LAG3+TILs and/or PD-1+TILs or PD-L1 are associated with shorter disease-specific survival in cases that lack CD8+ iTILs and improved outcome in cases with CD8+iTILs among ER– patients.

Appendix C

Pre-specified statistical plan for <u>Chapter 3</u> presented at the BC Cancer Agency Breast Outcome Unit

List of hypotheses generated on the half of the validation cohort (n= 2,003) and to be tested on the other half (n=1,989):

1) ER- breast tumors (specifically the basal-like subtype) with H&E sTILs (≥10%) are significantly associated with improved relapse-free survival.

2) Breast tumors with H&E sTILs (≥10%) or with TIM-3+iTILs (≥1) are highly associated with the presence of LAG-3+iTILs, PD-1+iTILs and PD-L1+ tumors.

3) The improved survival of basal-like breast cancer patients with H&E sTILs (≥10%) is dependent on co-infiltration with FOXP3+iTILs.

Appendix D

Appendix Table D.1 DSP technical control-normalized counts by cohort

Cohort A

CaseID	Beta-Catenin	CD8A	B7-H3	CD4	FoxP3	MmAb IgG2a	CD68	PTEN	Rabbit IgG	CD14	S6	GZMB	Ki67 (8D5)	B2M	Histone H3	AKT	CD3	VISTA	PD1	pSTAT3	CD44	STAT3	CD56	PD-L1	CD45	P-AKT	CD19	CD20	PanCK	CD45RO	Bcl-2
2	14379.170	87.840	13647.300	571.215	63.265	19.390	782.810	158.265	54.370	468.475	4415.310	1667.045	78.380	2716.695	1390.590	3954.365	109.250	157.125	76.145	362.715	12352.625	6165.880	94.580	384.080	252.560	213.255	62.820	77.470	36080.790	114.505	5457.080
3	24076.700	182.310	14242.655	1279.680	74.030	23.600	2192.345	83.115	74.165	585.935	8084.240	3753.260	1928.570	7068.230	2324.620	2402.075	663.795	254.305	122.335	355.935	11352.590	3195.420	1593.510	579.365	503.135	378.470	181.665	142.700	68023.420	336.825	483.205
4	5238.365	1962.370	3147.055	3012.130	108.550	58.495	1147.160	75.235	116.690	741.050	6781.670	969.270	30.780	8253.065	1427.140	3043.625	2007.125	290.735	411.170	414.085	3965.615	2950.920	185.655	835.030	13206.060	192.185	661.760	36642.470	26044.265	710.005	2955.700
5	25301.750	102.280	16300.010	1079.755	91.820	32.305	3941.785	123.015	109.535	1857.195	5344.670	1605.095	388.090	4556.720	963.210	2987.030	322.075	938.365	76.730	283.890	5391.675	3198.610	3640.410	763.800	286.850	303.785	168.080	118.685	14633.850	211.000	206.345
6	8511.985	218.940	3937.415	734.710	85.690	35.170	1038.130	50.605	81.070	809.535	9027.705	1246.020	1479.035	17424.240	2305.240	4037.110	302.460	355.900	123.335	327.060	8981.845	3855.420	227.890	566.615	301.940	889.415	87.830	246.510	15288.340	323.335	1102.095
7	5683.360	117.880	7631.610	964.200	42.540	11.790	5452.740	112.960	38.290	1156.420	2813.100	1312.220	121.050	1947.820	367.070	1609.310	980.720	565.290	118.160	224.170	12408.020	1580.260	8313.220	320.030	1487.890	148.860	157.330	102.110	2538.380	579.130	591.460
8	28408.005	1153.065	5491.535	3433.485	109.450	22.440	2300.100	150.010	75.110	797.450	16430.360	3003.890	527.725	6988.840	2217.800	4441.760	6358.415	674.505	322.915	398.495	5059.075	12362.890	140.730	473.275	7136.085	368.775	248.385	14144.690	10621.425	1577.345	1238.780
9	8568.230	245.660	7151.940	722.445	75.430	22.505	1405.845	161.005	100.900	374.380	13431.540	1939.925	575.760	7039.690	2173.540	5963.685	327.175	199.230	68.275	229.855	1851.445	3903.315	59.230	339.690	180.470	308.830	131.215	151.380	41628.800	182.430	9901.320
10	3187.950	3928.470	2414.235	10182.060	111.465	17.645	1541.195	123.115	66.460	906.355	5471.615	1042.330	158.690	8349.335	2251.190	2684.895	15672.900	494.010	1058.915	816.180	7429.320	8351.110	278.585	464.585	16720.065	692.955	439.495	30143.300	6709.235	5503.470	2235.990
11	18591.585	807.035	3028.345	1736.500	155.495	49.715	4007.385	71.520	222.280	3668.625	6414.330	4173.500	137.025	22351.650	1098.565	1443.645	3080.625	965.410	309.305	692.745	23913.120	3079.210	91.775	1459.040	3535.045	428.075	709.955	251.555	39732.980	1071.410	265.660
12	20683.430	298.280	7342.895	718.895	108.575	36.120	2132.130	583.720	101.225	904.070	13650.555	3857.140	683.990	9175.730	4570.535	10107.985	611.005	392.725	150.775	449.505	2892.490	6366.580	177.335	670.045	598.605	491.865	317.965	870.225	149468.975	322.360	13085.040
13	1273.050	25.110	2620.100	280.220	51.920	8.050	968.380	12.110	22.680	153.480	475.210	151.040	6.430	2822.400	47.050	168.920	62.490	55.170	60.860	53.550	1202.360	250.160	38.920	122.610	121.790	38.920	6.430	51.920	406.970	81.980	29.990
14	14388.940	462.565	4560.970	1189.595	62.730	13.605	869.040	190.150	53.945	693.945	4635.285	1236.845	344.605	1776.125	1541.645	2786.435	1524.565	273.355	120.425	330.675	3864.620	3979.500	116.910	346.470	2436.750	252.110	188.260	3941.125	12746.630	427.505	2243.185
15	24201.230	1989.515	7099.425	4106.760	134.035	35.575	8090.570	166.680	93.180	2837.200	16348.265	2612.760	853.870	11227.145	1894.565	5445.130	7066.335	1027.810	489.585	538.720	17274.435	8046.425	169.390	981.930	5222.200	623.105	724.000	17596.405	42547.660	1913.710	1009.745
16	1308.635	625.650	1712.530	1443.615	45.760	16.940	1484.360	65.580	49.605	443.005	2700.300	1138.950	51.305	3716.885	547.885	1433.090	1594.945	188.280	109.040	123.880	1449.325	1134.105	52.620	361.205	431.955	126.625	88.950	284.985	19753.310	504.080	1203.760
17	5401.610	779.400	17365.690	3133.785	135.870	45.945	5984.420	29.950	96.315	749.575	13121.500	977.325	112.150	17503.630	498.300	1016.380	925.000	183.255	312.320	338.515	2984.145	1279.535	126.190	777.545	1127.290	152.740	114.390	775.250	190165.195	797.325	1129.080
18	16779.010	241.065	6098.210	1067.215	80.190	21.485	5083.830	80.745	75.375	3642.925	7565.165	2814.410	555.480	8380.150	738.525	3767.285	1150.845	492.605	147.160	290.260	11403.450	17318.580	110.680	504.370	913.495	907.865	297.090	281.490	175.145	533.750	135.820
19	10617.030	1489.355	8201.840	4182.665	153.480	42.860	18310.745	59.745	117.205	3483.925	13692.035	1681.385	629.325	39190.170	1544.615	2543.185	4753.195	1227.995	887.160	441.255	12636.935	6457.760	157.620	1095.640	6961.160	222.810	786.935	5451.170	9584.190	3176.895	1103.245
20	3516.845	1153.375	5925.540	858.490	78.580	40.120	1832.040	125.160	118.680	438.495	8013.790	1135.255	61.740	6448.680	858.035	2690.230	563.755	207.370	112.250	233.170	2208.790	3359.760	190.850	463.810	1013.430	191.125	97.095	414.095	120189.145	219.500	959.800
21	26861.605	111.310	4354.520	756.815	96.350	16.245	1557.620	280.695	54.615	560.805	17096.170	1551.785	1471.730	5534.615	4616.070	6871.340	269.625	564.875	96.870	464.355	601.035	12629.290	98.005	388.435	150.890	808.635	264.485	151.450	4982.605	348.250	2155.345
22	12807.305	2129.030	7536.480	6691.620	135.785	22.415	9611.250	287.935	89.260	3158.540	8622.360	2310.460	271.960	11421.595	1814.070	4989.590	10684.860	1549.590	435.035	429.100	15325.960	5179.475	733.890	797.425	12647.295	338.425	3241.065	42358.680	8471.295	3384.935	2366.160
23	7442.640	368.940	36147.320	3600.240	182.105	62.835	15471.870	76.250	163.455	9832.310	7009.910	1844.185	189.230	21113.465	683.280	2196.490	1464.460	492.895	402.055	1388.165	127829.855	1239.370	5126.285	2532.405	937.055	1149.155	195.355	318.215	267.410	937.950	278.055
24	18569.600	184.005	6605.380	948.180	79.370	21.580	3436.945	831.255	72.095	378.100	7384.410	1931.025	295.525	2373.475	1513.360	6172.860	552.465	158.860	124.270	351.425	15802.005	5214.335	123.060	397.710	250.450	835.260	121.485	225.860	60184.975	274.060	704.375
25	961.765	218.660	2221.625	444.900	56.040	19.935	1431.275	61.115	28.890	358.595	9596.475	715.815	170.695	1199.330	1737.405	2777.120	252.995	69.380	72.110	262.505	721.295	3388.085	36.930	162.405	476.920	677.325	39.590	776.750	12094.805	168.850	1372.575
26	14382.315	212.595	2891.215	677.120	101.235	45.975	1747.770	64.690	119.190	409.560	2082.595	1657.760	17.950	3615.270	307.700	1218.270	874.120	321.785	116.415	274.920	2236.045	3474.870	74.825	966.540	594.105	306.625	155.970	381.565	9437.020	205.875	249.905
27	11982.890	101.000	7007.860	837.190	72.105	13.265	2275.475	253.450	46.005	1151.160	9571.670	1615.000	407.110	4457.155	1623.740	6566.750	232.895	340.150	63.875	222.545	2225.025	4528.715	5984.325	340.985	103.845	367.065	159.870	111.065	24590.780	221.675	734.115
29	5621.860	449.275	8556.685	1139.925	65.575	17.380	1776.155	19.250	79.875	400.110	10042.835	852.625	63.130	9803.700	992.480	2519.950	413.115	132.095	85.650	230.390	12814.115	1758.730	83.280	304.795	596.510	119.265	70.590	161.415	55182.265	195.770	1803.330
30	32039.210	1123.595	7166.000	2096.095	122.930	39.425	5454.805	101.910	75.445	3269.795	12094.375	1404.505	1306.750	28485.830	2488.620	2833.200	3210.565	808.080	767.635	433.080	13238.010	11029.645	81.910	909.260	2962.465	391.315	185.135	1371.100	456.340	1365.250	351.675
31	1051.510	120.670	1933.340	377.700	74.520	24.110	1660.780	77.580	84.630	287.900	3624.470	2023.600	40.250	1039.770	575.030	1757.970	291.480	262.620	86.270	382.000	18161.450	759.390	61.720	574.580	989.090	216.090	80.320	125.900	51494.670	121.260	108.500
33	8917.215	4419.210	2510.455	4284.415	143.540	32.395	13491.585	199.355	80.720	4151.850	7937.145	2167.865	1196.785	14209.455	1692.640	4962.125	12597.165	2487.710	1107.880	535.545	22324.180	6444.295	293.215	1208.490	10354.545	322.010	1794.025	17611.485	6418.000	3401.620	954.315
34	11158.325	298.085	7812.080	2818.570	98.375	30.840	7158.670	156.455	132.065	4989.140	4156.380	1236.890	577.895	4782.110	1349.135	3162.205	752.390	1590.845	202.815	359.745	10497.310	5716.545	705.180	1012.945	1895.535	381.310	341.215	333.925	1755.640	1112.200	540.030
35	6498.190	166.320	5674.980	757.040	50.895	11.560	2319.255	94.850	50.080	324.460	3783.225	887.555	62.350	1817.655	879.560	2927.775	178.475	108.745	69.090	166.200	1098.945	1388.770	113.535	301.550	261.030	92.515	54.750	125.545	13401.995	108.485	536.850
36	25430.530	169.975	2953.925	1835.415	121.655	40.330	3934.095	291.440	120.215	1158.150	4795.225	2121.730	159.095	6586.075	2000.455	5060.365	1283.155	522.455	180.900	429.290	4203.185	6191.695	137.375	602.645	1848.405	5144.255	155.605	1595.955	116257.940	588.710	618.780
37	8418.235	640.340	1014.090	1273.745	85.605	33.860	4313.065	337.760	46.440	1299.370	6551.705	1835.990	155.225	16442.440	1041.945	3059.790	1462.130	338.840	197.505	322.910	7168.585	1783.610	92.965	573.650	1120.950	222.750	142.685	1391.850	6020.480	337.315	4034.890
38	36975.750	1492.010	14488.990	1207.155	121.950	34.965	2454.540	279.340	82.785	1385.885	21148.355	2991.855	655.355	16794.785	2056.520	6241.435	2423.595	549.235	592.330	572.280	30438.030	8982.390	253.865	1028.720	650.190	605.120	272.440	699.930	61955.570	806.795	701.565
39	9440.790	89.805	17001.945	954.000	48.795	21.845	2395.445	76.040	56.905	775.690	8423.040	1032.445	268.045	5192.375	830.195	2456.770	316.865	222.350	86.060	219.655	8037.580	2468.075	918.675	461.400	337.430	244.930	146.140	189.795	12577.300	232.940	256.455
40	11224.535	862.900	2124.585	1089.205	109.325	19.465	2628.460	177.250	78.545	1361.405	19019.590	2829.920	450.690	8184.480	1839.530	7934.215	1449.670	476.415	199.315	410.655	11590.560	8115.580	101.740	615.490	443.555	394.670	251.295	552.250	26310.815	303.770	457.585

Cohort B

CaseID	Beta-Catenin	CD8A	B7-H3	CD4	FoxP3	MmAb IgG2	CD68	PTEN	Rabbit IgG	CD14	S6	GZMB	Ki67 (8D5)	B2M	Histone H3	AKT	CD3	VISTA	PD1	p-STAT3	CD44	STAT3	CD56	PD-L1	CD45	P-AKT	CD19	CD20	PanCK	CD45RO	Bcl-2
1	26200.285	430.670	6987.325	2015.145	144.750	45.980	2146.190	98.850	63.410	1316.395	7821.135	607.055	2081.535	8784.280	2547.680	1374.915	1545.540	284.320	415.005	350.300	8132.210	3213.525	150.935	582.665	2182.680	1964.740	193.355	493.065	1843.775	1020.765	505.975
2	77482.975	371.395	8218.300	2683.800	137.530	37.445	2825.665	247.780	72.200	1351.265	18290.545	1086.225	3859.965	10726.035	3488.300	3869.680	1336.510	340.010	393.565	427.615	8807.185	6137.020	95.570	754.465	5502.695	2437.740	498.205	11462.565	5136.460	1017.570	544.430
3	38861.460	2989.260	2608.225	3517.260	251.790	86.105	5894.840	171.905	197.875	5057.635	28464.355	3861.295	1086.670	33445.490	1721.235	3206.755	10928.195	1593.435	1102.225	1088.895	59027.730	3160.320	337.260	3368.385	3242.705	704.435	344.885	1067.700	26170.825	1377.160	649.190
4	32793.980	2382.340	14527.860	2148.750	161.570	52.780	35716.065	375.510	148.630	18681.415	13070.035	2702.325	382.315	65487.465	2260.915	19358.785	4998.390	1189.770	482.700	1115.465	61780.170	6601.690	273.460	1587.100	2488.030	1511.125	391.245	699.480	9089.905	3581.230	899.920
5	29615.690	178.810	2738.690	759.805	41.265	21.145	1050.770	188.030	38.400	1333.440	4017.855	709.510	448.230	1478.100	881.265	850.495	414.570	123.965	89.855	177.185	2058.950	3529.295	30.460	310.695	206.710	740.435	214.560	81.325	5599.645	144.885	281.250
6	14995.310	196.310	1352.975	1398.305	97.785	31.260	888.185	218.650	105.220	4010.350	2092.650	1151.530	113.230	4633.300	674.930	2063.440	537.850	578.830	121.505	383.780	12224.775	6702.185	212.045	717.750	140.745	201.710	202.825	279.360	919.190	128.980	375.385
7	5970.905	4811.985	1059.045	2630.030	136.860	32.010	6084.835	352.080	87.875	2191.595	19136.515	1927.925	556.555	31313.425	1688.395	6740.830	4743.010	2104.740	960.350	668.375	2836.405	31211.330	186.910	2054.395	2097.310	329.640	485.765	6222.435	963.810	1419.590	1019.910
8	18898.025	5164.415	12637.330	8225.530	1919.450	59.290	17126.305	326.655	247.130	10012.485	6627.585	3449.680	268.465	36950.825	1370.205	3431.540	18664.730	2398.460	1510.270	945.150	46515.570	11833.255	257.240	3095.345	19726.330	445.530	3143.995	34437.965	4456.615	7587.715	1649.700
9	8497.905	996.500	7424.805	1622.680	63.725	13.180	2627.335	85.300	36.500	541.165	4478.645	971.795	361.780	8747.525	1166.810	2038.335	5070.370	239.430	120.385	199.390	3645.650	1713.465	82.695	498.195	4257.010	157.325	246.960	2377.380	7492.380	938.650	853.340
10	26200.140	499.365	8040.920	1341.865	189.275	40.595	4606.995	307.500	114.745	1678.745	14959.895	3508.180	250.405	11948.175	1598.410	11464.655	1443.900	1225.165	427.690	1098.585	91209.150	11924.365	1235.855	1211.040	868.430	2248.665	582.985	831.340	30091.190	672.630	448.655
11	5619.890	6652.755	3896.460	4148.500	158.245	25.130	4373.100	235.645	72.320	3566.920	10666.150	1361.510	555.545	28890.015	2158.415	5177.985	7894.115	1086.915	1816.245	440.400	3209.950	14167.630	255.445	1142.635	14700.855	380.255	1324.730	69850.755	877.835	2259.930	3078.325
12	24794.840	1082.630	5360.050	5023.355	106.425	32.655	7135.630	353.080	115.380	2597.255	5163.380	2692.190	255.050	8838.140	833.035	5222.680	6911.010	1319.005	455.285	400.000	18793.740	3486.340	113.000	815.065	8889.165	418.945	1353.745	13212.760	2662.680	2418.500	653.260
13	2330.440	591.140	10426.705	1004.820	117.400	62.690	2264.620	294.325	119.430	501.925	9381.315	2192.765	259.300	3826.615	1068.760	2457.085	1459.445	259.035	138.000	358.400	3193.605	4888.810	99.915	629.725	729.785	220.670	204.670	658.590	84449.635	609.590	3442.050
14	27888.995	235.220	4111.290	765.750	162.810	77.805	10828.030	103.935	261.355	1447.670	6339.565	1088.340	280.025	9450.865	5978.755	446.020	495.325	1212.500	206.975	1022.450	43192.170	2329.045	195.485	2776.555	1568.175	567.925	323.270	184.500	52102.965	4862.870	196.675
15	34597.390	12137.670	8466.270	9222.035	250.070	49.985	5859.320	492.165	143.670	3438.210	16281.600	3698.225	487.480	32004.400	2343.775	9520.985	27479.785	2292.295	1070.780	863.885	25319.460	28370.380	555.930	2109.470	36582.370	908.025	2015.540	55170.340	43086.575	5262.495	3651.650
16	22803.910	305.180	4930.570	1185.285	91.840	16.690	2798.040	411.810	76.690	3084.640	6960.765	3038.670	476.640	28513.400	827.260	3197.465	753.480	451.985	93.025	452.975	17919.710	5909.400	104.085	639.225	475.115	505.955	280.735	223.470	22319.730	471.560	489.190
17	11125.220	1261.480	4106.005	6139.570	90.260	35.680	4205.220	63.330	68.525	1027.010	4576.650	1743.500	790.000	12043.870	590.655	1865.145	8853.875	819.400	420.970	472.575	34275.505	2351.125	181.630	1497.745	5181.985	174.350	339.020	6727.175	1023.000	4859.650	505.200
18	18934.935	8255.025	7103.930	9502.465	204.495	65.880	52437.960	197.660	174.565	1294.525	1355.965	1638.920	253.900	30796.615	895.065	2561.740	15137.405	1117.660	2125.985	570.975	5289.850	1743.935	995.060	2325.125	23331.505	325.100	888.350	19135.700	15119.965	7675.760	1537.350
19	32886.620	1123.005	8103.615	10772.050	124.900	50.650	45537.770	38.440	92.570	7552.740	2157.180	1504.710	1019.415	12705.530	1334.725	361.295	2184.270	732.465	346.225	823.845	58100.835	732.065	224.315	1760.470	2358.895	527.660	245.580	294.345	15285.710	5101.770	707.545
20	5707.080	1929.160	4376.830	3723.090	104.390	25.940	9546.850	215.380	92.860	2700.700	10646.320	2231.910	704.900	17803.090	1220.320	3319.370	3627.700	3920.810	512.580	454.390	18875.190	6489.000	154.110	1695.300	5970.450	227.780	2711.450	6648.620	2845.660	1992.310	915.980

Appendix Table D.2 DSP signal to noise ratios values in each cohort for each biomarker

Cohort A

CoreID	Beta-Catenin	CD8A	B7-H3	CD4	FoxP3	MmAb IgG	CD68	PTEN	Rabbit IgG	CD14	S6	GZMB	Ki67 (8D5)	B2M	Histone H	AKT	CD3	VISTA	PD1	p-STAT3	CD44	STAT3	CD56	PD-L1	CD45	P-AKT	CD19	CD20	PanCK	CD45RO	Bcl-2
2	442.8588	2.7054	420.3182	17.5926	1.9485	0.5972	24.1095	4.8743	1.6745	14.4284	135.9855	51.3427	2.4140	83.6705	42.8283	121.7890	3.3648	4.8392	2.3452	11.1711	380.4440	189.9007	2.9129	11.8291	7.7785	6.5680	1.9348	2.3860	1111.2390	3.5266	168.0706
3	575.4949	4.3577	340.4360	30.5876	1.7695	0.5641	52.4027	1.9867	1.7727	14.0053	193.2341	89.7125	46.0978	168.9488	55.5644	57.4158	15.8664	6.0785	2.9241	8.5078	271.3560	76.3787	38.0890	13.8483	12.0262	9.0464	4.3423	3.4109	1625.9342	8.0510	11.5498
4	63.4044	23.7522	38.0915	36.4584	1.3139	0.7080	13.8851	0.9106	1.4124	8.9696	82.0844	11.7319	0.3726	99.8939	17.2739	36.8396	24.2940	3.5190	4.9767	5.0120	47.9992	35.7175	2.2471	10.1071	159.8443	2.3262	8.0098	443.5152	315.2361	8.5938	35.7754
5	425.3429	1.7194	274.0164	18.1516	1.5436	0.5431	66.2646	2.0680	1.8414	31.2210	89.8482	26.9829	6.5241	76.6022	16.1923	50.2144	5.4143	15.7747	1.2899	4.7724	90.6384	53.7712	61.1982	12.8401	4.8222	5.1069	2.8256	1.9952	246.0069	3.5471	3.4688
6	159.4096	4.1002	73.7386	13.7594	1.6048	0.6587	19.4418	0.9477	1.5183	15.1607	169.0679	23.3351	27.6989	326.3154	43.1718	75.6057	5.6644	6.6652	2.3098	6.1251	168.2090	72.2030	4.2678	10.6114	5.6546	16.6567	1.6449	4.6166	286.3150	6.0553	20.6397
7	267.4888	5.5481	359.1837	45.3803	2.0022	0.5549	256.6346	5.3165	1.8021	54.4272	132.3993	61.7600	5.6972	91.6746	17.2762	75.7426	46.1578	26.6055	5.5612	10.5506	583.9866	74.3753	391.2638	15.0623	70.0279	7.0061	7.4048	4.8058	119.4695	27.2569	27.8372
8	691.9591	28.0862	133.7622	83.6325	2.6660	0.5466	56.0256	3.6539	1.8295	19.4242	400.2089	73.1684	12.8543	170.2334	54.0209	108.1919	154.8776	16.4295	7.8655	9.7065	123.2284	301.1339	3.4279	11.5280	173.8200	8.9826	6.0501	344.5348	258.7155	38.4208	30.1741
9	179.8068	5.1552	150.0855	15.1607	1.5829	0.4723	29.5021	3.3787	2.1174	7.8565	281.8647	40.7099	12.0825	147.7299	45.6124	125.1496	6.8659	4.1809	1.4328	4.8236	38.8531	81.9122	1.2430	7.1285	3.7872	6.4809	2.7536	3.1768	873.5923	3.8283	207.7820
10	93.0937	114.7182	70.4999	297.3341	3.2550	0.5153	45.0056	3.5952	1.9407	26.4672	159.7808	30.4379	4.6340	243.8153	65.7387	78.4037	457.6762	14.4260	30.9222	23.8339	216.9492	243.8671	8.1352	13.5667	488.2553	20.2355	12.8340	880.2374	195.9215	160.7110	65.2948
11	176.8571	7.6771	28.8079	16.5189	1.4792	0.4729	38.1213	0.6804	2.1145	34.8987	61.0179	39.7015	1.3035	212.6257	10.4504	13.7330	29.3052	9.1837	2.9423	6.5899	227.4795	29.2918	0.8730	13.8795	33.6280	4.0722	6.7536	2.3930	377.9699	10.1921	2.5272
12	342.0620	4.9329	121.4366	11.8891	1.7956	0.5974	35.2611	9.6535	1.6741	14.9515	225.7525	63.7893	11.3118	151.7480	75.5874	167.1656	10.1048	6.4949	2.4935	7.4339	47.8359	105.2903	2.9328	11.0812	9.8997	8.1344	5.2585	14.3918	2471.9136	5.3312	216.4000
13	94.2163	1.8583	193.9092	20.7386	3.8425	0.5958	71.6682	0.8962	1.6785	11.3588	35.1695	11.1782	0.4759	208.8811	3.4821	12.5015	4.6248	4.0830	4.5041	3.9631	88.9846	18.5139	2.8804	9.0742	9.0135	2.8804	0.4759	3.8425	30.1192	6.0672	2.2195
14	531.1338	17.0745	168.3575	43.9111	2.3155	0.5022	32.0786	7.0189	1.9913	25.6153	171.1006	45.6552	12.7203	65.5615	56.9062	102.8547	56.2757	10.0903	4.4452	12.2061	142.6533	146.8939	4.3155	12.7891	89.9469	9.3060	6.9492	145.4773	470.5118	15.7803	82.8019
15	420.3428	34.5552	123.3075	71.3289	2.3280	0.6179	140.5223	2.8950	1.6184	49.2783	283.9474	45.3801	14.8306	195.0004	32.9060	94.5746	122.7327	17.8517	8.5034	9.3568	300.0337	139.7556	2.9421	17.0548	90.7026	10.8225	12.5749	305.6259	738.9956	33.2386	17.5379
16	45.1439	21.5830	59.0770	49.8003	1.5786	0.5844	51.2059	2.2623	1.7112	15.2823	93.1521	39.2903	1.7699	128.2212	18.9004	49.4372	55.0207	6.4951	3.7615	4.2735	49.9973	39.1232	1.8152	12.4605	14.9011	4.3682	3.0685	9.8311	681.4287	17.3892	41.5260
17	81.2002	11.7164	261.0514	47.1089	2.0425	0.6907	89.9614	0.4502	1.4479	11.2681	197.2502	14.6917	1.6859	263.1250	7.4907	15.2788	13.9051	2.7548	4.6950	5.0888	44.8594	19.2347	1.8970	11.6885	16.9461	2.2961	1.7196	11.6540	2858.6760	11.9859	16.9730
18	416.9510	5.9904	151.5378	26.5198	1.9927	0.5339	126.3309	2.0065	1.8730	90.5251	187.9910	69.9368	13.8034	208.2430	18.3520	93.6154	28.5980	12.2410	3.6569	7.2128	283.3707	430.3590	2.7503	12.5334	22.6999	22.5600	7.3826	6.9949	4.3523	13.2635	3.3751
19	149.7973	21.0135	115.7210	59.0138	2.1655	0.6047	258.3490	0.8430	1.6537	49.1552	193.1830	23.7229	8.8792	552.9400	21.7932	35.8822	67.0635	17.3260	12.5171	6.2257	178.2964	91.1135	2.2239	15.4585	98.2160	3.1437	11.1030	76.9114	135.2248	44.8233	15.5658
20	50.9664	16.7148	85.8734	12.4413	1.1388	0.5814	26.5501	1.8138	1.7199	6.3547	116.1365	16.4522	0.8947	93.4548	12.4347	38.9870	8.1700	3.0052	1.6267	3.3791	32.0100	48.6899	2.7658	6.7216	14.6867	2.7698	1.4071	6.0011	1741.7909	3.1810	13.9095
21	901.8123	3.7370	146.1923	25.4082	3.2347	0.5454	52.2933	9.4236	1.8336	18.8276	573.9618	52.0974	49.4097	185.8111	154.9732	230.6883	9.0520	18.9643	3.2522	15.5896	20.1783	423.9973	3.2903	13.0407	5.0658	27.1479	8.8794	5.0846	167.2787	11.6916	72.3604
22	286.3254	47.5975	168.4887	149.6006	3.0357	0.5011	214.8731	6.4372	1.9955	70.6136	192.7651	51.6536	6.0801	255.3459	40.5561	111.5494	238.8752	34.6433	9.7258	9.5931	342.6335	115.7945	16.4072	17.8276	282.7482	7.5660	72.4586	946.9883	189.3878	75.6750	52.8989
23	73.4391	3.6405	356.6779	35.5248	1.7969	0.6200	152.6662	0.7524	1.6129	97.0187	69.1692	18.1972	1.8672	208.3337	6.7422	21.6735	14.4503	4.8636	3.9672	13.6975	1261.3406	12.2293	50.5828	24.9881	9.2462	11.3391	1.9276	3.1399	2.6386	9.2551	2.7437
24	470.7868	4.6650	167.4632	24.0388	2.0122	0.5471	87.1353	21.0744	1.8278	9.5858	187.2136	48.9564	7.4923	60.1737	38.3675	156.4978	14.0064	4.0275	3.1506	8.9095	400.6212	132.1967	3.1199	10.0830	6.3495	21.1760	3.0800	5.7261	1525.8428	6.9481	17.8577
25	40.0763	9.1114	92.5740	18.5388	2.3352	0.8307	59.6405	2.5466	1.2038	14.9425	399.8801	29.8276	7.1128	49.9755	72.3968	115.7212	10.5422	2.8910	3.0048	10.9384	30.0560	141.1797	1.5389	6.7673	19.8730	28.2238	1.6497	32.3668	503.9843	7.0359	57.1945
26	194.2889	2.8719	39.0571	9.1471	1.3676	0.6211	23.6104	0.8739	1.6101	5.5327	28.1335	22.3945	0.2425	48.8382	4.1567	16.4575	11.8084	4.3470	1.5726	3.7139	30.2065	46.9416	1.0108	13.0569	8.0257	4.1422	2.1070	5.1545	127.4835	2.7811	3.3759
27	485.0711	4.0885	283.6804	33.8897	2.9188	0.5370	92.1119	10.2597	1.8623	46.5993	387.4642	65.3757	16.4799	180.4270	65.7295	265.8241	9.4277	13.7694	2.5857	9.0087	90.0697	183.3238	242.2473	13.8032	4.2037	14.8589	6.4716	4.4959	995.4425	8.9735	29.7172
29	150.8863	12.0582	229.6546	30.5947	1.7600	0.4665	47.6706	0.5167	2.1438	10.7386	269.5417	22.8838	1.6944	263.1235	26.6374	67.6335	11.0877	3.5453	2.2988	6.1835	343.9207	47.2029	2.2352	8.1805	16.0099	3.2010	1.8946	4.3323	1481.0482	5.2543	48.3999
30	587.4633	20.6020	131.3941	38.4335	2.2540	0.7229	100.0180	1.8686	1.3833	59.9542	221.7596	25.7527	23.9603	522.3093	45.6307	51.9489	58.8681	14.8168	14.0752	7.9409	242.7290	202.2369	1.5019	16.6720	54.3190	7.1751	3.3946	25.1402	8.3673	25.0329	6.4482
31	23.2784	2.6714	42.8004	8.3615	1.6497	0.5337	36.7664	1.7175	1.8735	6.3735	80.2387	44.7985	0.8911	23.0185	12.7300	38.9180	6.4528	5.8139	1.9098	8.4567	402.0590	16.8114	1.3664	12.7201	21.8965	4.7838	1.7781	2.7872	1139.9912	2.6845	2.4020
33	174.3812	86.4202	49.0934	83.7842	2.8070	0.6335	263.8356	3.8985	1.5785	81.1918	155.2154	42.3938	23.4038	277.8740	33.1005	97.0372	246.3447	48.6486	21.6652	10.4729	436.5620	126.0218	5.7340	23.6327	202.4890	6.2971	35.0832	344.4026	125.5076	66.5206	18.6622
34	174.8429	4.6708	122.4096	44.1650	1.5415	0.4832	112.1712	2.4515	2.0694	78.1762	65.1275	19.3812	9.0552	74.9322	21.1400	49.5495	11.7894	24.9274	3.1780	5.6369	164.4853	89.5741	11.0497	15.8721	29.7017	5.9749	5.3466	5.2324	27.5096	17.4274	8.4619
35	270.0731	6.9125	235.8594	31.4636	2.1153	0.4804	96.3912	3.9421	2.0814	13.4850	157.2357	36.8879	2.5913	75.5441	36.5556	121.6821	7.4176	4.5196	2.8715	6.9075	45.6736	57.7191	4.7187	12.5328	10.8487	3.8450	2.2755	5.2178	557.0041	4.5088	22.3122
36	365.2262	2.4411	42.4235	26.3597	1.7472	0.5792	56.5004	4.1856	1.7265	16.6330	68.8677	30.4717	2.2849	94.5874	28.7300	72.6756	18.4283	7.5034	2.5980	6.1653	60.3650	88.9234	1.9729	8.6550	26.5463	73.8804	2.2348	22.9207	1669.6644	8.4549	8.8867
37	212.2909	16.1481	25.5733	32.1213	2.1588	0.8539	108.7668	8.5176	1.1711	32.7675	165.2208	46.3000	3.9145	414.6452	26.2758	77.1617	36.8720	8.5449	4.9807	8.1431	180.7773	44.9791	2.3444	14.4663	28.2681	5.6173	3.5982	35.0997	151.8244	8.5064	101.7518
38	687.2653	27.7319	269.3057	22.4373	2.2667	0.6499	45.6223	5.1921	1.5387	25.7593	393.0828	55.6094	12.1810	312.1633	38.2244	116.0090	45.0472	10.2086	11.0096	10.6369	565.7492	166.9550	4.7186	19.1207	12.0850	11.2473	5.0638	13.0095	1151.5632	14.9958	13.0399
39	267.7670	2.5471	482.2224	27.0581	1.3840	0.6196	67.9415	2.1567	1.6140	22.0007	238.9008	29.2830	7.6025	147.2702	23.5466	69.6808	8.9872	6.3065	2.4409	6.2300	227.9681	70.0015	26.0562	13.0866	9.5705	6.9469	4.1449	5.3831	356.7272	6.6068	7.2738
40	287.0661	22.0686	54.3360	27.8563	2.7960	0.4978	67.2225	4.5331	2.0088	34.8178	486.4236	72.3749	11.5263	209.3171	47.0458	202.9166	37.0751	12.1843	5.0975	10.5025	296.4271	207.5549	2.6020	15.7411	11.3439	10.0936	6.4268	14.1237	672.8958	7.7689	11.7027

Cohort B

CoreID	Beta-Catenin	CD8A	B7-H3	CD4	FoxP3	MmAb IgG	CD68	PTEN	Rabbit IgG	CD14	S6	GZMB	Ki67 (8D5)	B2M	Histone H	AKT	CD3	VISTA	PD1	p-STAT3	CD44	STAT3	CD56	PD-L1	CD45	P-AKT	CD19	CD20	PanCK	CD45RO	Bcl-2
1	485.2244265	7.975929	129.404	37.32011	2.680743	0.851541	39.74704	1.830684	1.174341	24.37939	144.846	11.24255	38.54964	162.6832	47.18256	25.46317	28.62311	5.265554	7.685816	6.487491	150.607	59.51389	2.795288	10.79085	40.42283	36.38662	3.580899	9.131472	34.14637	18.90438	9.370563
2	1490.187002	7.142834	158.058	51.61603	2.645038	0.720159	54.34444	4.765415	1.388582	25.98813	351.7719	20.89076	74.23656	206.2879	67.08854	74.42341	25.70435	6.539223	7.569217	8.224082	169.3837	118.0299	1.838045	14.51021	105.8303	46.8837	9.5817	220.4531	98.78668	19.57036	10.47072
3	297.720996	22.90098	19.98184	26.94603	1.928985	0.659658	45.16088	1.316979	1.515937	38.74698	218.0679	29.58171	8.325073	256.2288	13.18653	24.56723	83.72184	12.20744	8.444241	8.342118	452.2165	24.21148	2.583778	25.80549	24.84264	5.396737	2.642194	8.179742	200.4969	10.55054	4.973501
4	370.2594875	26.89774	164.0264	24.2604	1.824201	0.595911	403.2512	4.239685	1.678103	210.922	147.5669	30.51052	4.316517	739.3843	25.5268	218.5698	56.43418	13.43306	5.44991	12.59413	697.5272	74.53619	3.087492	17.91911	28.09103	17.06131	4.41734	7.897459	102.6293	40.43377	10.16052
5	1039.327452	6.275124	96.11107	26.66445	1.448146	0.742059	36.87552	6.598689	1.347602	46.79549	141.0018	24.89941	15.7301	51.87216	30.92695	29.84711	14.54884	4.350404	3.153354	6.218097	72.2564	123.8564	1.068958	10.90347	7.254242	25.98469	7.529728	2.854004	196.5129	5.084567	9.870135
6	261.463947	3.422936	23.59099	24.38138	1.705017	0.545061	15.48673	3.812465	1.834656	69.92599	36.48824	20.07852	1.974321	80.78799	11.76834	35.97893	9.378158	10.0927	2.118608	6.691735	213.1558	116.8619	3.697298	12.51496	2.454084	3.517093	3.536534	4.871028	16.02735	2.248944	6.545356
7	112.5808842	90.72955	19.9682	49.58898	2.580483	0.603546	114.729	6.638437	1.656875	41.32233	360.8173	36.35085	10.4938	590.4119	31.83454	127.0978	89.42903	39.68469	18.10731	12.60215	53.48016	588.4869	3.524171	38.73544	39.54459	6.215333	9.159056	117.3235	18.17255	26.76624	19.23031
8	156.1215878	42.6646	104.4003	67.95328	15.85708	0.48981	141.4849	2.698583	2.041606	82.71579	54.75223	28.49872	2.21786	305.2605	11.31963	28.34886	154.1943	19.81431	12.47674	7.808134	384.2774	97.75765	2.125128	25.57146	162.9644	3.680641	25.97338	284.5011	36.81728	62.68412	13.62861
9	387.4429246	45.43318	338.5173	73.98246	2.905398	0.600913	119.7874	3.889062	1.664136	24.6732	204.1938	44.30681	16.49455	398.8238	53.19809	92.93331	231.1722	10.91627	5.488684	9.09074	166.2152	78.12159	3.770293	22.71408	194.0888	7.172881	11.25959	108.3913	341.5983	42.79564	38.90612
10	383.8843912	7.316695	117.8155	19.661	2.773257	0.594798	67.50168	4.505489	1.681243	24.59697	219.1923	51.40185	3.668933	175.0646	23.4199	167.9801	21.15602	17.95111	6.266513	16.09646	1336.396	174.7158	18.10774	17.74416	12.72423	32.94743	8.541895	12.18079	440.896	9.855373	6.573692
11	131.8263908	156.0544	91.3997	97.31183	3.711971	0.589477	102.5803	5.527551	1.696418	83.66964	250.1971	31.93709	13.03148	677.6763	50.63018	121.4606	185.1731	25.49589	42.60386	10.33051	75.29616	332.3317	5.992002	26.80292	344.8396	8.919684	31.07434	1638.497	20.59147	53.01143	72.20862
12	403.9440345	17.63762	87.32302	81.83776	1.733818	0.531997	116.2498	5.752187	1.879708	42.31306	84.11898	43.85969	4.155136	143.9862	13.57135	85.08506	112.5904	21.48851	7.417255	6.516582	306.1774	56.79755	1.840934	13.2786	144.8174	6.825224	22.05448	215.2551	43.37893	39.40089	10.64256
13	26.93283528	6.83179	120.5012	11.61268	1.356789	0.724507	26.17216	3.401506	1.380249	5.800734	108.4196	25.34173	2.996723	44.22409	12.35163	28.39647	16.86677	2.993661	1.594862	4.14202	36.90841	56.49985	1.154715	7.277716	8.434107	2.550278	2.365366	7.611308	975.9823	7.045016	39.77968
14	195.5751646	1.649511	28.83095	5.36992	1.141726	0.545618	75.93295	0.728858	1.832786	10.15197	44.45701	7.632124	1.963711	66.27541	41.92679	3.127773	3.47353	8.502812	1.451439	7.170062	302.8906	16.33273	1.370864	19.47095	10.99703	3.982647	2.266972	1.29383	365.3787	34.1015	1.379209
15	408.2633954	143.2295	99.90546	108.8238	2.950929	0.589844	69.14238	5.807749	1.695365	40.57229	192.1296	43.64057	5.752464	377.665	27.65751	112.3515	324.2727	27.05002	12.63564	10.1942	298.78	334.7821	6.560202	24.89261	431.687	10.71507	23.7842	651.0326	508.4393	62.0996	43.09097
16	637.3995919	8.530187	137.816	33.13029	2.56705	0.466508	78.20894	11.51064	2.143587	86.21979	194.5626	84.93487	13.32272	796.9874	23.12302	89.3734	21.06077	12.63358	2.600172	12.66125	500.8797	165.1756	2.909314	17.86719	13.2801	14.14211	7.846916	6.246284	623.8661	13.18073	13.67351
17	224.9943762	25.51194	83.03908	124.1655	1.825401	0.721586	85.04559	1.280774	1.385837	20.77006	92.55732	35.26022	15.97681	243.573	11.9453	37.72034	179.0591	16.57139	8.513619	9.557269	693.1814	47.54871	3.673251	30.29012	104.7995	3.526022	6.856277	136.0491	20.68896	98.28066	10.21707
18	176.5665523	76.97736	66.2435	88.60962	1.906897	0.614325	488.9792	1.843162	1.627803	12.07133	12.64425	15.28278	2.367594	287.1756	8.3464	23.88799	141.1549	10.42208	19.82462	5.32429	49.32737	16.26204	9.278844	21.68158	217.5642	3.031528	8.283783	178.4387	140.9923	71.57577	14.33565
19	480.2798689	16.40049	118.3461	157.3162	1.824054	0.739698	665.0387	0.561382	1.351903	110.3011	31.5037	21.97495	14.88765	185.553	19.49247	5.276393	31.89932	10.697	5.056309	12.03152	848.5111	10.69116	3.275921	25.7101	34.44957	7.706006	3.586478	4.298647	223.2342	74.50682	10.33307
20	116.2825735	39.30691	89.17854	75.85849	2.126961	0.528531	194.5184	4.388398	1.892036	55.02715	216.9203	45.47549	14.36244	362.7405	24.8642	67.63264	73.91491	79.88707	10.44389	9.258261	384.5847	132.2143	3.140013	34.54198	121.6488	4.64105	55.24618	135.4666	57.98073	40.5936	18.66322